PHYTOCHEMICAL ANALYSIS, BIOLOGICAL ACTIVITIES AND COMPUTATIONAL STUDY OF COMPOUNDS ISOLATED FROM SELECTED MEDICINAL PLANTS OF ETHIOPIA

By

MATHEWOS ANZA ALEMU

A DISSERTATION SUBMITTED TO DEPARTMENT OF APPLIED CHEMISTRY, SCHOOL OF APPLIED NATURAL SCIENCE IN PARTIAL FULFILMENT FOR THE DEGREE OF DOCTOR OF PHILOSOPHY IN APPLIED CHEMISTRY (NATURAL PRODUCT CHEMISTRY).

OCTOBER, 2021

ADAMA, ETHIOPIA

Phytochemical Analysis, Biological Activities and Computational Study of Compounds Isolated from Selected Medicinal Plants of Ethiopia

By

Mathewos Anza Alemu

Supervisors

Prof. Mª Luz Cardona Prósper (Department of Chemistry, University of Valencia, Spain).

Prof. Diego Miguel Cortes (Department of Pharmacology, University of Valencia, Spain).

Dr. Milkyas Endale Annisa (Department of Applied Chemistry, Adama Science and Technology University, Ethiopia).

A Dissertation Submitted to Department of Applied Chemistry School of Applied Natural Science, in Partial Fulfilment for the Degree of Doctor of Philosophy in Applied Chemistry (Natural Product Chemistry).

Office of Graduate Studies

Adama Science and Technology University

October, 2021

Adama, Ethiopia

DECLARATION

I hereby declare that this Dissertation entitled "Phytochemical Analysis, Biological Activities and Computational Study of Compounds Isolated from Selected Medicinal Plants of Ethiopia" is my original work. That is, it has not been submitted for the award of any academic degree, diploma or certificate in any other university. All sources of materials used for this thesis have been duly acknowledged through appropriate citations.

Name: Mathewos Anza Signature:  Date : 14/09/21

SUPERVISOR'S APPROVAL SHEET

This is to certify that the dissertation entitled "Phytochemical Analysis, Biological Activities and Computational Study of Compounds Isolated from Selected Medicinal Plants of Ethiopia" prepared under our guidance by Mathewos Anza Alemu Id. No GSR/017/10 submitted in partial fulfillment of the requirements for the degree of Doctor of Philosophy in Applied Chemistry (Natural Product Chemistry), the Graduate Program of the Department of Applied Chemistry. Therefore, we recommend that the student has fulfilled the requirements, and hence hereby, he can submit the dissertation to the department.

Prof. Luz Cardona		14/09/21
Name of major supervisor	Signature	Date
Prof. Diego Cortes		14/09/21
Name of Co-supervisor	Signature	Date
Dr. Milkyas Endale		14/09/21
Name of Co-supervisor	Signature	Date

ACKNOWLEDGEMENT

First of all, I express my deep sense of gratitude to my supervisors: Prof Mª Luz Cardona, Dr. Milkyas Endale and Prof Diego Cortes for their invaluable guidance, support and endless kindness throughout my study. I also express my gratitude to Prof Maria Trelis and Prof Marius V. Fuentes Pharmaceutical and Pharmaceutical Technology and Parasitology Department, Faculty of Pharmacy, University of Valencia, Spain, for supporting larvicidal activity study. I thank Inés Domingo-Ortí, Drug Discovery Unit, IIS La Fe, Valencia, Spain and Martina Palomino-Schätzlein, NMR Facility, Principe Felipe Research Center, Valencia, Spain, for their support during cytotoxicity study. I also express my gratitude to Prof Hortensia Rico and Prof Jesus Zueco, Department of Microbiology and Ecology, Faculty of Pharmacy, University of Valencia, Spain for support given during antimicrobial activity analysis. Many thanks goes to Prof Belen Abarca, Dr. Nuria Cabedo and Prof Rafa Ballesteros, Faculty of Pharmacy, University of Valencia, Spain, for material support and encouragement during my research visit to University of Valencia, Spain.

I also want to express my gratitude to Dr. Rajalakshmanan Eswaramoorthy, Department of Chemistry, Adama Science and Technology University, for technical support during computational study of the isolated compounds.

I am also thankful to Dean of Applied Natural Science and head of Applied Chemistry Department of ASTU for their support and encouragement. I express my sincere thanks to all academic staffs of Applied of Chemistry Department, especially Dr. Fedlu Kedir, Dr. Yadessa Melaku and Prof Aman Dekebo for their friendly care, encouragement and moral support to accomplish my study. Mr. Shambel Alemu a taxonomist at Addis Ababa University is also thanked for identifying the plants. I acknowledge and recognize Adama Science and Technology University for giving PhD study opportunity and Wolaita Sodo University for granting the study leave of absence.

I am deeply indebted to my family at large for their patience, love, encouragement and support.

Above all, I praise and thank ‘God Almighty’ for everything forever.

DEDICATION

This PhD dissertation is dedicated to my family, especially to my wife, Ejigayehu Daniel, my sons Yilkal Mathewos and Enku Mathewos.

You are always indeed my best.

LIST OF CONTENTS

SCHEMES

TABLE OF FIGURES

LIST OF TABLES

LIST OF APPENDIXES

ABBREVIATIONS

1D	1-Dimensional
2D	2-Dimensional
ATCC	American Type Culture Collection
COSY	Correlation Spectroscopy
DEPT	Distortionless Enhancement by Polarization Transfer
DMSO	Dimethyl Sulfoxide
DNA	Deoxyribonucleic acid
d	Doublet
dd	Doublet of a doublet
DMEM/F 12	Dulbecco's modified eagel medium/nutrient mixture F12
DPBS	Dulbecco's phosphate buffered saline medium
GC	Gas Chromatography
ELISA	enzyme-linked immunosorbent assay
ESI-MS	Electronic Spray Ionization-Mass Spectrometry
FBS	Fetal bovine serum
HMBC	Heteronuclear Multiple Bond Coherence
HSQC	Heteronuclear Single Quantum Coherence
HREIMS	High Resolution Electron Impact Mass Spectrometry
IC_{50}	50% Inhibitory Concentration
J	Coupling constant
IR	Infra-Red
LCMS	Liquid chromatography–mass spectrometry
MCF-7	Michigan Cancer Foundation-7
MDA-MB-23	M.D. Anderson-Metastasis Breast Cancer
MHz	Megahertz
MIC	Minimum Inhibitory Concentration
MTT	3-(4,5-Dimethylthiazol-2-Yl)-2,5-Diphenyltetrazolium Bromide
MTS	(3-(4,5-dimethylthiazol-2-yl)-5-(3-carboxymethoxyphenyl)-2-(4-sulfophenyl)-2H-tetrazolium)
NAHIDIC	National animal health diagnostic and investigation center
NMR	Nuclear Magnetic Resonance
RPMIM-1640	Roswell Park Memorial Institute Medium
TLC	Thin-Layer Chromatography
WHO	World Health Organization
s	Singlet
t	Triplet
UV	Ultraviolet
VERO	kidney normal cell line of monkey

LIST OF PUBLISHED ARTICLES

1. Mathewos Anza, Milkyas Endale, Luz Cardona, Diego Cortes, Rajalakshmanan Eswaramoorthy, Nuria Cabedo, Belen Abarca, Jesus Zueco, Hortensia Rico, Inés Domingo-Ortí, Martina Palomino-Schätzlein (2021). Cytotoxicity, Antimicrobial Activity, Molecular Docking, Drug likeness and DFT Analysis of Benzo[c]phenanthridine Alkaloids from Roots of *Zanthoxylum chalybeum*, *Biointerface Research in Applied Chemistry,* Volume 12(2): 1569 – 1586.

   https://doi.org/10.33263/BRIAC122.15691586

2. Mathewos Anza, Milkyas Endale, Luz Cardona, Diego Cortes, Rajalakshmanan Eswaramoorthy, Jesus Zueco, Hortensia Rico, Maria Trelis , Belen Abarca (2021). Antimicrobial Activity, *In Silico* Molecular Docking, ADMET and DFT Analysis of secondary metabolites from Roots of Three Ethiopian Medicinal Plants. *Advances and Applications in Bioinformatics and Chemistry,* 14: 1–16.

   https://doi.org/10.2147/AABC.S323657

3. Mathewos Anza, Milkyas Endale, Luz Cardona, Diego Cortés, Nuria Cabedo, Maria Trelis, Màrius V. Fuentes, Belén Abarca, (2021). Chemical Composition, Cytotoxicity and Larvicidal Activity of Essential Oils of Three Medicinal Plants of Ethiopian Flora against *Anisakis* L_3 Larvae. *Research journal of Pharmacognocy,* 8(4): 1-8. https://doi.org/10.22127/RJP.2021.291618.1719

4. Mathewos Anza, Milkyas Endale, Luz Cardona, Diego Cortes, Nuria Cabedo, Rajalakshmanan Eswaramoorthy, Belen Abarca, Inés Domingo-Ortí, Martina Palomino-Schätzlein (2021). Cytotoxicity, Molecular Docking, ADMET and DFT Analysis of Alkaloids from Roots and Fruit of *Vepris dainelli. Current Bioactive Compounds*, in press.

ABSTRACT

Background

Breast cancer is a significant public health problem worldwide and the second leading cause of cancer-related death among women. Several risk factors, including environmental and genetic aspects, have been claimed to be responsible as a cause of breast cancer. Most active treatment strategies and combinations adversely affect the patient's quality of life through severe side effects. On the other hand, infectious diseases are also public health problems and a major cause of death worldwide. Increasing cases of drug resistance, unwanted side effects of existing antibiotics, and the reappearance of earlier known infections have demanded the need for new, safe and effective antimicrobial agents. In Ethiopia, over 70% of the people depend on traditional medicines in one way or another for their healthcare, including cancer and infectious diseases. More than 95% of the preparations are made from plant origin. Traditionally, *Vepris dainelli* (Rutaceae), *Zanthoxylum chalybeu*m (Rutaceae), *Uvaria scheffleri* (Annonaceae), *Clematis burgensis* (Ranunculaceae), and *Euphorbia schimperiana* (Euphorbiaceae) are medicinal plants used for the treatment of abdominal cramps, intestinal worms, skin diseases, malaria, tuberculosis, intestinal problems, pneumonia cough, tuberculosis, asthma sore throat, and fever, and breast cancer in Ethiopia.

Objectives: This study aimed to identify anticancer and antimicrobial lead compounds from selected medicinal plants of Ethiopian flora.

Methods: Acid-base extraction was used to extract alkaloids from the roots of *V. dainelli* and *Z. chalybeum*. Extraction by maceration technique was used to extract the fruits of *V. dainelli* and the roots of *U. scheffleri*, *C. burgensis* and *E. schimperiana*. Essential oils were extracted by hydrodistillation. Silica gel column chromatographic technique was used to isolate compounds. Spectroscopic techniques (IR, 1D (^{1}H, ^{13}C, and DEPT-135) and 2D (COSY, HSQC, and HMBC) NMR, ESI-MS, HRMS, GC-MS, and LC-MS were used to elucidate structures of isolated compounds. The cytotoxicity effects of alkaloids were evaluated *in vitro* against MCF-7 and MDA-MB-231 human breast cancer cell lines by using MTS assay. Antimicrobial activity of isolated compounds and extracts were evaluated against *S. aureus*, *E.coli* and *C. albicans* via broth dilution techniques. The larvicidal activity of essential oils was determined by marinade solution, and their cytotoxicity was studied on VERO cells using an MTT assay.

Results: Silica gel flash column chromatographic separation of the extracts of five selected medicinal plants gave a total of 26 compounds, of which two compounds, uvarindole-F (**248**) and G (**249**), are new natural products. The cytotoxicity assay displayed alkaloids (**13**, **17**, **55**, **67**, and **245**) induced a significant reduction of cell growth of both breast cancer cell lines in a dose-dependent manner of which chelerythrine (**55**) and evodiamine (**245**) showed the highest potency against the aggressive and metastatic MDA-MB-231 cell line (IC_{50}= 1.73 ± 0.48 and 3.616 ± 0.51 µM), respectively, with respect to standard doxorubicin (0.23 µM). In addition, the alkaloids (**55** and **245**) showed the influence in the cell cycle in the MDA-MB-231 cell line by arresting some cells in the G_2/M phase, preventing cells with damaged DNA from entering mitosis. On the other hand, alkaloids (**13**, **17** and **67**) showed moderate activity against the MDA-MB-231 cell line (IC_{50}= 69.30 ± 5.34, 55.99 ± 12.17 and 24.14±5.24 µM), respectively. Arborinine (**13**) and evoxanthine (**17**) exhibited higher cytotoxicity against MCF-7 than MDA-MB-231 and showed influence the cell cycle in both cell lines by arresting some cells in the G2/M phase, preventing cells with damaged DNA from entering mitosis. Antimicrobial assay of Chelerythrine (**55**) isolated from *Z. chaleybeum*, dichloromethane extract and isolated Uvarindole-F **(248)** from roots of *U. scheffleri* displayed potential antibacterial activity against *S. aureus* (MIC =12.5, 6.25 and 12.5 µg/mL), respectively, compared with gentamicin (5 µg/mL against *S. aureus*). Chelreythrine (**55)** and uvarindole-F (**248)** showed an antifungal effect on *C. albicans* (50 µg/mL and 12.5), respectively, compared with fluconazole (8 µg/mL against *C. albicans*).

In silico molecular docking analysis of isolated compounds against *E. coli* DNA gyrase B and against human topoisomerase IIα revealed a promising scoring pose (lowest energy) with a value ranging from -7.5 to -5.5 Kcal/mol and -6.4 to -5.3 Kcal/mol, compared to ciprofloxacin (-7.2 Kcal/mol) and vosaroxin (-6.2 Kcal/mol). Among the studied compounds, chelerythrine (**55**, -6.4 Kcal/mol), 6-hydroxydihydrochelerythrine (**62**, -6.3 Kcal/mol), dihydrocherythrine (**67**, -6.3 Kcal/mol) and evodimaine (**245**, -6.3 Kcal/mol)) showed higher lowest binding energy, interactions with human topoisomerase IIα than vosaroxin (-6.2 Kcal/mol) whereas interactions with *E. coli* DNA gyrase B, chelerythrine (**55**,-7.4 Kcal/mol), dihydrocherythrine (**67**, -7.5 Kcal/mol) and uvarindole-F (**248**, -7.3 Kcal/mol) showed higher lowest binding energy with respect to ciprofloxacin (-7.2 Kcal/mol). In addition, ADMET studies showed the highest drug-likeness properties of the isolated compounds, except compound **250**, suggesting these

compounds can act as a drug and exhibit remarkable biological activities. DFT calculations indicated that studied compounds showed the lowest gap energy and were chemically reactive.

Essential oils of *U. scheffleri* roots, *Z. chalybeum* and *V. dainelli* fruits were extracted by hydrodistillation to afford 0.5, 2.0, and 2.7 % (v/w) yields, respectively. Gas Chromatography-Mass Spectrometry analysis of essential oils revealed a total of 58, 18 and 20 chemical compositions, representing 86.3, 99.6, and 98.8 % of the total oil contents, respectively. Tricyclo[5.3.0.0(3, 9)] decane was identified to be the principal constituent in essential oils of *Z. chalybeu*m (82.8%) and *V. dainelli* (69.8%), reported herein for the first time from both species and could be considered as a marker constituent for Ethiopian species. The larvicidal activity of the essential oils in marinated solutions was tested *in vitro* against *Anisakis* L_3 larvae isolated from blue whiting fish (*Micromesistius poutassou*) for the first time, achieving 100% mortality after 7 h at 0.5 and 1% essential oils concentrations of *U. scheffleri* and *Z. chalybeum*, and at 5% concentration after 5 and 3 h, respectively. Similarly, 100% mortality was observed after 7 and 5 h at 1 and 5% concentrations, respectively, for *V. dainelli*. The cytotoxicity study of essential oils on VERO cells displayed moderate toxicity with half-maximal inhibitory concentration values of 65.46 µg/mL, 83.88 µg/mL, and 96.82 µg/mL, respectively.

Conclusions: The results obtained from molecular docking, drug-likeness properties, ADMET, and DFT analysis are in good agreement with *in vitro* experimental results obtained for compounds. Hence, compounds **13**, **17**, **55**, **67** and **245** may serve as a lead molecules that could be developed into potent topoisomerase IIα inhibitors against human breast cancer whereas compounds **55** and **248** may serve as a lead molecules that could be developed into potent *E. coli* DNA gyrase B inhibitors.

The findings of this study support the traditional uses of the root decoction of *U. scheffleri* and *Z. calybeum* for the treatment of infectious diseases caused by gram-positive bacteria strains such as pneumonia and sore throat. The weak cytotoxicity of the essential oils at low concentrations increases the possibility of developing effective and safe botanical larvicides. However, these results should be further supported by *in vivo* studies.

Keywords: *Vepris dainelli, Zanthoxylum chalybeum, Uvaria scheffleri, Clematis burgensis, Euphorbia schimperiana*, Cytotoxicity, Antimicrobial, Computational studies.

CHAPTER ONE

1. INTRODUCTION

1.1. Background of the Study

Traditional medicine is defined by the World Health Organization (WHO) as ‘‘the sum of total knowledge, skill, and practices based on the theories, beliefs, and experiences indigenous to different cultures, whether explicable or not, used in the maintenance of health as well as in the prevention, diagnosis, improvement or treatment of physical and mental illness’’[1]. Herbal medicine has been used as a traditional medicine for many human and livestock ailments for thousands of years in Africa, Asia, and other parts of the developing world. Particularly for those living in rural areas of developing countries, it continues to be used as the primary source of medicine [2]. According to the world health organization (WHO), about 80% of the world’s populations living in developing countries have incorporated medicinal plants in their primary healthcare modality [3].

It was not until the 19th century that man began to use active principles of medicinal plants. One particular landmark was the discovery of quinine from *Cinchona* bark by the French scientists Caventou and Pelletier. Much less is known about the isolation and use of quinine before that [4]. Such discoveries led to an interest in plants from the new world, and expeditions scoured in search of new medicines. Before World War II, a series of natural products isolated from higher plants became clinical agents, and some are still in use today. For example, (Figure 1, **1**-**6**), morphine (**1**) and codeine (**2**) from the latex of the opium poppy, quinine (**3**) from *Cinchona* bark, digoxin (**4**) from *Digitalis purpurea* leaves, atropine (**5**) (derived from (-)-hyoscyamine and hyoscine (**6**) from species of the *Hyoscyamus niger* and *Atropa belladonna* continue to be in clinical use [5].

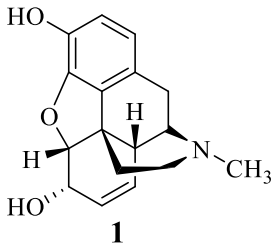

1

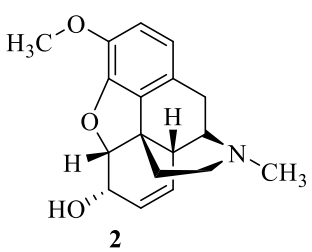

2

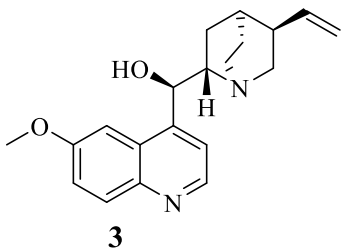

3

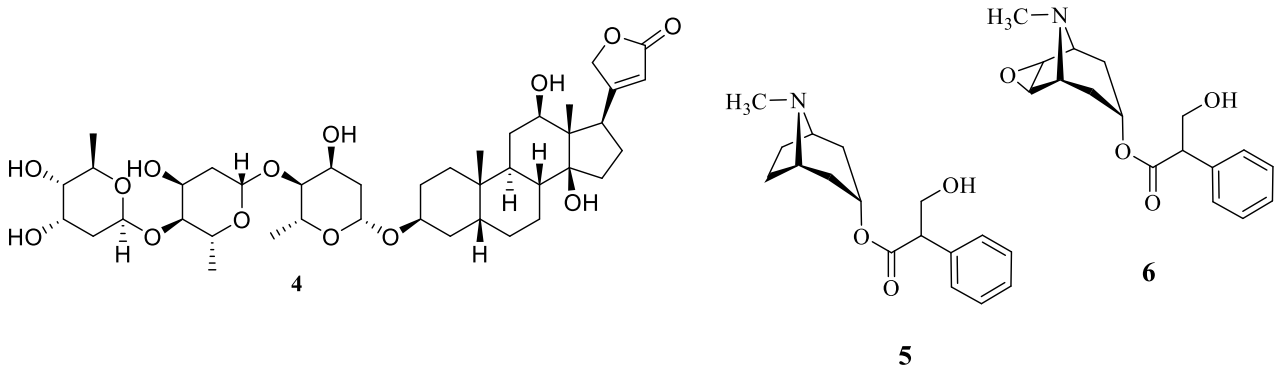

Figure 1: Some natural products isolated from higher plants as clinical agents

Nowadays, medicinal plants have played a pivotal role in primary health care and are rich in novel bioactive compounds. Studies revealed that drug development from natural sources has shown that natural products or natural product-derived drugs comprised about 28% of all new drugs entering the market [6]. Plants produce secondary metabolites due to a prominent function such as protection against predators and microbial pathogens, repellence to herbivores and microbes, defense against abiotic stress (e.g., UV-B exposure), for the communication of the plants with other organisms, and are insignificant for growth and developmental processes [7,8]. In recent years, medicinal plants have become popular for treating several diseases due to their efficacy and cost-effectiveness. Systematic studies involving pharmacological activities and the mechanism of action of bioactive molecules derived from herbal medicine provide the vital knowledge required to design new medications [9].

Cancer is a disease originated by an uncontrolled splitting up of abnormal cells in a fraction of the body. It is one of the significant public health burdens in both developed and developing countries [10]. Cancer cells typically attack as well as destroy normal cells. Worldwide, an estimated 19.3 million new cancer cases and almost 10.0 million cancer deaths occurred in 2020 [11]. Breast cancer is a significant public health problem worldwide and the second leading cause of cancer-related death among women [12]. Several risk factors, including environmental and genetic aspects, have been claimed to be responsible as a cause of breast cancer [13]. The recent challenge in oncology is the lack of homogeneity of the lesions where different cell components respond differently to a treatment. Most active treatment strategies and

combinations adversely affect the patient's quality of life through severe side effects [14]. There is growing consensus that monotherapies are insufficient to eradicate the disease, and there is an unmet need for more potent combinatorial treatments [15]. Consequently, plant extracts and their constituents are well known to have lower side effects and can be a better option against breast cancer. Therefore, screening bioactive constituents of medicinal plants and evaluating their efficacy against cancer cells received attention in drug discovery [16].

Infectious diseases are also public health problems and a major cause of death worldwide [17]. Infections due to pathogenic microorganisms cause a severe concern to human health. Increasing cases of drug resistance, unwanted side effects of existing antibiotics, and the reappearance of earlier known infections have demanded the need for new, safe and effective antimicrobial agents [18-20].

The consumption of raw seafood causes a wide range of health problems in humans. Among them, anisakiasis is one of the essential fish-borne zoonotic diseases. This parasitosis, caused by nematodes belonging to the genus *Anisakis*, can invade the stomach or the intestinal wall of humans [21]. The transmission is due to the consumption of certain raw or undercooked sea fish and cephalopods. The paratenic hosts of *Anisakis*, and infective third stage (L_3) larvae [21, 22], leading to gastrointestinal disorders and/or allergies in humans [23]. In some European countries, where the consumption of raw or undercooked sea products is increasing, human cases are increasingly reported [24].

The effective therapy is larval extirpation by endoscopy when the parasite is located in the digestive tract and is accessible by gastroscopy. Several authors have proposed antibiotics, anticholinergics and/or corticosteroids, and anthelmintic drugs to treat anisakiasis [25], but there is no clinically approved pharmacological treatment yet. Therefore, the response of *Anisakis* larvae to the most common food preservation techniques, such as salting, marinating, or mild thermal treatments, needs to be assessed. In recent years, the effects of natural products against *Anisakis* L_3 larvae have attracted a great deal of attention [26, 27], particularly essential oils from various plants [28].

Ethiopia has a tremendously rich flora in its diversity, with an estimated number between 6,500 to 7,000 species of higher plants, of which about 12 % are endemic [29]. Plants in the Aannonaceae, Rutaceae, Ranunculaceae, and Euphorbiaceae families are broadly known medicinal plants worldwide, including Ethiopia. *Vepris dainelli* (Pichi-serm) Kokwaro and *Zanthoxylum chalybeum*(Rutaceae), *Uvaria scheffleri* Diels (Annonaceae), *Clematis burgensis* Engl (Ranunculaceae), and *Euphorbia schimperiana* (Euphorbiaceae) are well known medicinal plants in Ethiopia, traditionally used for the treatment of various ailments, particularly, infectious and cancer-related diseases in human as well as livestock's [30].

1.2. Statement of the Problem

Cancer is a current major public health problem worldwide and cause of death [31]. According to WHO (2018) cancer country profile report, breast cancer is the leading among various types of cancer in Ethiopia, with a mortality rate of 22.9 per 100,000 population [32]. Most active chemoteraphy treatment strategies and combinations adversely affect the patient's quality of life through severe side effects [14]. Different traditional medicinal plants are being used in Ethiopia to treat a broad spectrum of diseases, including cancer [30]. Therefore, screening bioactive constituents of medicinal plants and evaluating their efficacy against cancer cells received attention in drug discovery [16].

The rapid development of a multidrug-resistant strain of bacteria and fungus increased bacterial and fungal infections that hampered treatment using conventional anti-microbial agents [33, 34]. In addition, rising cases of drug resistance, unwanted side effects of existing antibiotics, and the reappearance of earlier known infections have demanded the need for new, safe, and effective antimicrobial agents [18-20]. Due to this reason, scientists are always searching for novel infection-fighting strategies [33, 34]. Therefore, it is imperative to search for new antimicrobial agents from a natural source that could either overcome or avoid multi-drug resistance [35, 36].

In the recent years, the consumption of raw fish in Ethiopia highly experienced, however there was no studies carried out to know the prevalence of Anisakiasis cases, in any case it is not recommended that the consumption of raw or uncooked fishes/seafood's. The safe way is

cooking or marinating fishes/seafood's with essential oils before consume it. Therefore, it is important to search the effect of essential oils against ansakias L_3 in food safety industry.

Enhancing the knowledge of screening traditional medicinal plants for various biological activities and determining the structure of the active chemical constituents may help sustain natural products for drug discovery and development. In this regard, medicinal plants used to treat cancer and infectious diseases traditionally needs scientific support for their claimed traditional uses [8].

1.3. Justification of the Study

Medicinal plants played a pivotal role in treating and protecting breast cancer and infectious diseases in Africa [37]. In Ethiopia, *V. dainellii* (Rutaceae), *Z. chalybeu*m (Rutaceae), and *E. schimperiana* (Euphorbiaceae) used to treat cancer and related diseases [30, 38, 39 and 40]. Also, *Z. chalybeu*m (Rutaceae), *U. scheffleri* (Annonaceae), *C. burgensis* (Ranunculaceae), and *E. schimperiana* (Euphorbiaceae) are among medicinal plants used to treat infectious diseases [39-41]. Considering the broad spectrum of their ethnobotanical uses, bioactive compounds within the plants mentioned above have not been thoroughly identified. In addition, essential oils from the fruits of *V. dainelli*, *Z. chalybeum*, and roots of *U. scheffleri* have not been investigated. It is therefore inevitable to identify chemical constituents and screen for cytotoxicity, antimicrobial, and larvicidal activity. Thus, motivated by a broad spectrum of traditional uses of the plants mentioned above and lack of comprehensive prior phytochemical investigation, this study aimed to fill this gap and enrich the existing scientific knowledge on the aforementioned medicinal plants coupled with an attempt to search for new drug leads.

1.4. Objectives

1.4.1. General Objective

The overall objective of this study was to identify anticancer and antimicrobial lead compounds from selected medicinal plants of Ethiopian flora.

1.4.2. Specific Objectives

The specific objectives of the study were:

- To isolate secondary metabolites from roots of *V. dainelli, Z. chalybeum, U. sheffleri, C. burgensis* Engl, and *E. schimperiana,* and fruits *V. dainelli*.
- To extract essential oils from the roots of *U. sheffleri,* fruits of *Z. chalybeum,* and *V. dainelli*.
- To elucidate the chemical structures of isolated compounds based on spectroscopic techniques (IR and NMR) and MS, and comparing with literature data.
- To identify and quantify the chemical composition of essential oils by using GC and GC-MS techniques.
- To evaluate antibacterial activity of the isolated compounds and *U. scheffleri* extracts against *S. aureus* and *E. coli* via broth dilution method.
- To evaluate *in vitro* antifungal activity of isolated compounds and extracts against *C. albicans* via broth dilution method.
- To determine the cytotoxicity of isolated compounds using MTS assay against MDA-MB-231 and MCF-7 breast cancer cell lines.
- To test larvicidal activities of essential oils from root of *U. sheffleri* and fruits of *Z. chalybeum* and *V. dainelli.*
- To carry out *in silico* molecular docking, drug-likeness, ADMET, and DFT analysis of the isolated compounds.

1.5. Significance of the Study

This research is expected to:

- ❖ Provide information on the chemical constituents of various parts of the studied medicinal plants.
- ❖ Provide cytotoxicity information of isolated compounds against MDA-MB-231 and MCF-7 breast cancer cell lines to provide scientific support to traditional uses of the plants to treat cancer diseases.

- Provide antimicrobial activity information of the plant extracts and isolated compounds against selected microbial strains to provide scientific support to traditional uses of the plants to treat infectious diseases.
- Provide larvacidal activity information of essential oils from Ethiopian medicinal plants against Anisakias L_3 in marinade solution.
- Provide scientific data to have a better understanding of the molecular mechanisms of interaction between the compounds with protein domains of selected bacterial strains using computational analysis.
- Provide baseline information for future related scientific studies on the plants.

CHAPTER TWO

2. REVIEW OF LITERATURE

2.1. Botanical Description and Geographical Distribution

2.1.1. Rutaceae

Rutaceae family is a flowering plant that contains about 170 genera and about 2070 species. Members of this family are distributed throughout the world, mostly in warm temperate and tropical regions, where significant number of the species found in Africa and Australia, often in semi-arid woodlands. Species of the family generally have flowers that divide into four or five parts, usually with strong scents. They range in f orm and size from shrubs, trees, and sometimes perennial herbs [42].

2.1.2. Genus *Vepris*

Genus *Vepris* (Rutaceae) comprises about 83 species and grows mainly in tropical Africa, Madagascar, Zanzibar, the Mascarene Islands, and a lesser extent in Arabia and India. They contain evergreen shrubs and trees, predominantly of tropical lowland evergreen forest, but some species extend into submontane forests and some into drier forests and woodland [43].

2.1.2.1. *Vepris dainelli*

Vepris dainelli Pichi-serm Kokwaro (Figure 2), Chawula (Goffigna, Ethiopia) is a medium-sized, shade-tolerant afromontane tree and endemic to Ethiopia [44]. It typically grows as an understory tree mixed with other small tree and shrub species in forests, but it is sometimes seen growing at the margin of afromontane forest and open forest areas. The plant occurs in the altitudinal range of 1050-2500m above sea level. In Ethiopia, it is distributed in Kefa, Ilubabor, Wollega, Bale, Shewa, Sidamo, Gojam, Dawuro, Gamo and Gofa in Ethiopia [45].

Figure 2: Photo of *Vepris dainelli* (taken by Mathewos Anza in November 2018 from Geze Gofa, Ethiopia).

2.1.3. Genus *Zanthoxylum*

Genus *Zanthoxylum* belongs to the Rutaceae family, and it is the largest genus in the family. It comprises about 549 species and distributed worldwide, mainly in tropical and temperate regions. The different species demonstrate a very close similarity among them. They are identified as trees, erect shrubs or small trees, straggling or scandent shrubs, or as a forest liane, most of which are aromatic with spiny trunks and branches. A common feature of most of the species of this genus is the wonderful capacity to produce gums and volatile oils. It is economically significant because of its alimentary, industrial, and medicinal applications [46].

2.1.3.1. *Zanthoxylum chalybeum*

Zanthoxylum chalybeum Knob wood (English), Ga'da (Sidamigna, Ethiopia) (Figure 3) is a deciduous tree that grows in medium altitudes up to 1,500 m above sea level in dry woodland, bushland, or grassland. Bark pale grey; smooth dark with scales and prickles. The bole has characteristic large, conical, woody knobs with sharp prickles. The branches also bear scattered thorns with conspicuous dark scales. It often grows on termite mounds in eastern and southern Africa [47].

Figure 3: Photo of *Zanthoxylum chalybeum* (taken by Mathewos Anza in November 2018 from Yirgalem, Ethiopia).

2.1.4. Annonaceae

Annonaceae is a tropical and subtropical family that comprises about 135 genera and 2500 species. The family has considerable economic importance, mainly as a source of edible fruit. Among them, the prickly soursop (*Annona muricata* L.) is widely used in the production of pulp and juice, as well as the sugar apple (*Annona squamosa* L.), cherimoya (*Annona cherimola* Mill), and custard apple (*Annona reticulata* L.), which are consumed in nature [48, 49].

2.1.5. Genus *Uvaria*

The genus *Uvaria* (Annonaceae) is woody climbers and the scandent shrubs plant. It comprises more than 150 species commonly occurring in wet tropical forests of Africa, Madagascar, continental Asia, Malaysia, Northern Australia, and Melanesia [50]. The generic name *Uvaria* is derived from the Latin *Uva* meaning grape, likely because the edible fruit of some species in the genus resembles grapes [51]. The characteristics of *Uvaria* are stellate hairs, valvate sepals, partially or fully imbricate petals in two sub-equal whorls, monadal inaperturate pollen, and generally many-seeded apocarpous fruits [52].

2.1.5.1. *Uvaria scheffleri*

Uvaria scheffleri Diels (Figure 4) Boyyiniya (Wolaitigna, Ethiopia) is a medicinal plant widely distributed in East Africa, growing in the coastal evergreen and mountain forests [41]. The plant grows in the high land area of the southern part of Ethiopia, and its fruits are edible [53].

Figure 4: Photo of *Uvaria scheffleri* (taken by Mathewos Anza in October 2018, from Humbo carbon project forest, Wolaita, Ethiopia).

2.1.6. Ranunculaceae

The family Ranunculaceae possesses about 2,000 known species of flowering plants with 43 genera distributed worldwide. Ranunculaceae family are primarily herbaceous annuals or perennials, but some woody climbers or shrubs. Most members of the family have bisexual flowers, which can be showy or inconspicuous. Flowers may be solitary but are frequently found aggregated in cymes, panicles, or spikes. The sepals, petals, stamens, and carpels are generally free (unfused). The outer flower segments typically number four or five. In some genera in the family, the sepals are colorful and appear petal-like, and the petals can be inconspicuous or absent. The stems are unarmed. Most species have basal and cauline (stem) leaves, usually compound or lobed but simple. Many species, especially the perennials, form rhizomes that develop new roots each year. The fruits are most commonly free, unfused achenes (e.g., *Ranunculus*, *Clematis*) or follicles (e.g., *Helleborus*, *Eranthis*, *Nigella*), but a berry in *Actaea* [54].

2.1.7. Genus *Clematis*

Genus *Clematis* comprises about 350 species and is distributed from cool temperate to tropical regions in China, Europe, Australia, New Zealand, India, North America, Africa, Himalayas, and Japan. *Clematis* are charming climbers, bearing flowers profusely in spring or summer in a variety of colors. Some species can grow 7 to 10 meters in a single season; others reach a height of only 1.5 to 3.5 meters. Sepals make up the colorful portion of the flower. These may be thin, wide, pointed, rounded, crinkled, twisted, or even crimped [55].

2.1.7.1. *Clematis burgensis*

Clematis burgensis (Figure 5) (Fiiti, Oromiffa, Ethiopia) grows in open montane forest and forest borders, along roads, streams, on fences, and woodland associations. It is endemic and widely distributed in different parts of Ethiopia at an altitude of 1300-1500m.

Figure 5: Photo of *Clematis burgensis* Engl (taken by Mathewos Anza in September 2018 from Otana secondary school compound, Wolaita, Ethiopia).

2.1.8. Euphorbiaceae

Euphorbiaceae family is commonly known as the spurge family distributed in tropical, subtropical, and temperate climates. The family is quite large, with about 300 accepted genera and some 7500 species, predominantly occurring in the tropical region like tropics of Asia. Most

family members are herbs, but some, especially in tropical regions, are shrubs or trees. Some subfamilies are characterized by leaching a milky, sometimes poisonous, white latex and are a primary source of natural rubber in the world. Other plants from this family with economic uses include cassava, castor oil plant, barbados nut, and some medicinal species. Due to the large morphological variability in this family, only a few could be identified with certainty to genus and species level [56].

2.1.9. Genus *Euphorbia*

The genus *Euphorbia* is the largest in the plant family Euphorbiaceae, comprising about 2000 known species ranging from annuals to trees. All contain latex and have unique flower structures. A significant percentage, primarily those originating in Africa and Madagascar. The *Euphorbias* are named after the Greek surgeon Euphorbus. He was a physician of Juba II, a Romanized king of a North African kingdom, and is supposed to have used the species' milky latex as an ingredient in his medicine [57].

2.1.9.1. *Euphorbia schimperiana*

Euphorbia schimperiana (Figure 6) (Benjile, Sidamigna, Ethiopia) is a much-branched, annual, perennial plant growing up to 2 meters tall. The stems become more or less woody at the base.

Figure 6: *Euphorbia schimperiana* [picture taken by Mathewos Anza on Sep, 2018, Wolaita, Ethiopia].

2.2. Ethnobotanical Studies

2.2.1. Ethnobotanical Uses of the Genus *Vepris* and *V. dainelli*

Various species of *Vepris* are traditionally used for the treatment of a diverse range of ailments. The leaf of *V. ezcgeniifoliu* is used to treat pneumonia and lung diseases, a decoction of the roots is used to treat kidney disorders [58], a root decoction of *V. lanceolata* is used as an astringent and against amenorrhoea [59], and the dried powdered root bark is added to boiling water, and the eyes are exposed to the vapours to treat eye troubles [60]. A decoction of the roots of *V. glomerata* is used to treat malaria, and the bark is used to treat cardiac pain, epilepsy, stroke, and psychosis [61, 62]. The leaves of *V. undulata* are used to treat headache and infertility [63], and the leaves of *V. elliotii* are as an aphrodisiac and disinfectant activities [64]. In Africa folk medicine, *V. heterophylla* is used as a diuretic and antipyretic [65]. Also, its leaves are used to protect the crop as a diuretic, antipyretic, treat conjunctivitis, and reduce high blood pressure [66]. In addition, *V. verdoornianais* and *V. sclerophylla* are used to treat malaria, conjunctivitis, and tape-worm [67, 68].

Ethnobotanical Uses of *Vepris dainelli* (Pichi-Serm.) Kokwaro

According to Tesfaye & Sebsebe (2009) report, the seeds of *V. dainelli* are used to treat abdominal cramps, the bark and fruits are used to treat intestinal worms, skin diseases, and tooth pain [69]. In the southern part of Ethiopia, the seeds of *V. dainelli* are used as an additive coffee drink, also used to treat tumor and wound [38].

2.2.2. Ethnobotanical Studies of the Genus *Zanthoxylum* and *Zanthoxylum chalybeum*

Species of *Zanthoxylum* have been used to treat several diseases in humans and livestock worldwide, especially in Asia, Africa, and America [70, 71]. The bark of *Z. integrifoliolum* (Merr.) has been used in traditional medicine to remedy snakebite, dyspepsia, and an aromatic tonic in fever. In Sri Lanka, *Z. tetraspermum* (Sinhala-katukeena) is employed in folklore medicine to treat rheumatism and some forms of diarrhea. The bark of *Z. gilletii* is pungent, and sticks prepared from it prevent toothache [71]. The stem bark of *Z. liebmanniaum* (Engelm.) P. Wilson is used in Mexican traditional medicine to treat stomach aches, amebiasis, intestinal parasites, and local anesthetic agents [72].

Z. oxyphyllum fruits are sweetish bitter, hot and digestible, appetizer, anthelmintic and remove pain, tumors, useful in gastric problem, headache, body ache, fever, cough and also used for the purification of blood. The bark is considered as stomachic and digestive stimulant. It is also administered during fevers as a sudorific. The stem bark has been used to treat rheumatism, varicose ulcers, varicose veins, skin diseases, and leg pains. Moreover, it is used in relieving inflammation, fevers, and hypotension. Besides, it has stimulant, astringent and digestive properties and is also used in the treatment of dyspepsia and diarrhea [73].

As reviewed by Patiño et al. (2008), the major ethnobotanical uses attributed to *Zanthoxylum* species are relief of dental problems, treatment of malaria, gastrointestinal disorders, gonorrhea and lung diseases, antidiarrheal use in animals and humans, emmenagogue action, effective for rheumatism, anthelmintic use in animals and humans, aphrodisiac, analgesic, action against various skin diseases, febrifuge, antihemorrhagic, effective for genitourinary diseases, anticancer, diuretic, stomachic, anti-convulsive, tonic and stimulant. In addition to the medicinal properties, some species are also used as pesticides, building materials, and textile dyes [70].

Ethnobotanical Studies of *Zanthoxylum chalybeum*

Z. chalybeum is widely used in traditional medicine. Stem bark decoctions or root bark decoctions are widely taken to treat malaria, fevers, and headache, sickle cell disease, respiratory tract ailments including colds and tuberculosis, skin diseases including ulcers, urticaria, tumors and measles, intestinal problems including abdominal pain, diarrhea, intestinal worms, bilharzia, amoebas, colic, general body pain and vomiting [74]. A root infusion is drunk to treat bacterial muscle infections, female sterility, venereal diseases, uterine fibroids, and, together with chicken meat, as an aphrodisiac [39]. *Z. chalybeum* is also used throughout eastern and southern Africa for its aromatic leaves, shoots, and fruits, which are used to make various tea-like beverages and decoctions. In Ethiopia, root bark and stem bark are taken to treat toothache, and the leaves are taken to treat the breast cancer of livestock [40].

2.2.3. Ethnobotanical Uses of the Genus *Uvaria* and *Uvaria Scheffleri*

Various species of *Uvaria* are used as traditional medicine. A decoction of the root bark of *U. narum* is used to control fits in pregnant women at the time of delivery. It is also used for treating rheumatism, bowel complaints, and eczema [75]. The leaves of *U. narum* are recommended for jaundice, biliousness, and fevers. The roots of *U. chamae* are said to have purgative and febrifugal properties. A decoction of the root is drunk to ease severe abdominal pains and fever [75]. In Kenya, *U. lucida* Benth root has been used to remedy stomach and bowel troubles, especially for diarrhea and vomiting [76]. The roots of *U. acuminata* OLIV are used as remedies for menstrual pain, dysentery, snakebite, and chest diseases [77]. In Côte d'Ivoire, the roots of *U. afzelii* Scott Elliot are used in folk herbal medicine to treat fever, bronchitis, malaria, and jaundice [78].

Ethnobotanical Uses of *Uvaria scheffleri*

In Kenya, *U. scheffleri* Diels is used for the treatment of cough, tuberculosis, asthma, and sore throat [79]. In Tanzania, it is widely used for the treatment of fever, a symptom that may be associated with malaria or bacterial or even viral infection [41]. In Ethiopia, the fruit is edible [53].

2.2.4. Ethnobotanical Studies of the Genus *Clematis* and *Clematis bugensis*

As reviewed by Chawla *et al*. (2012), the aerial parts of various *Clematis* species are used as diuretic, antimalarial, antidote in snake bites, antidysentery, treatment of rheumatic pain, fever, eye infections, gonorrheal symptoms, bone illnesses, chronic skin disorders, gout, and varicosity [80]. In addition, in folk medicine, it is used to treat blisters, and as a poultice for festering wound sand ulcers, asthma, beriberi, urination and travail, antitumor, anti-inflammatory agents, reducing fever, inducing urination, stimulating menstrual discharge and promoting lactation, to ease headaches, coughs, chest ailments and abdominal upsets. Hot decoctions of the leaves, stems and roots are also used separately to relieve cold, malaria, common colds, sinus infections, and asthma, used for treating schistosomiasis, breast infection, and gonorrhea [80, 81].

The roots and rhizomes of *C. chinensis*, *C. mandshurica*, and *C. hexapetala* are all called weilingxian in the Chinese Pharmacopeia, which is prescribed for treatment of inflammation, rheumatoid arthritis, and tumor, used as an analgesic, abirritative, antibacterial, antiphlogistic, anticancer, and diuretic agent [82, 83]. *C. tangutica* (Maxim.) Korsh. is used to treat skin ulcers and indigestion [84].

Ethnobotanical Uses of *Clematis burgensis*

In Ethiopia, the leaves of *C. burgensis* are used to treat otorrhoea *(Dhukuba Gurra)* and eczema *(Chiifee, Abiyatoo)* [85].

2.2.5. Ethnobotanical Uses of the Genus *Euphorbia* and *Euphorbia schimperiana*

The genus *Euphorbia* has been used as medicinal plant for a long time [86, 87]. The roots of *E. ebracteolata* are used to treat pulmonary tuberculosis, chronic tracheitis, and psoriasis in Traditional Chinese Medicine (TCM) [88]. The roots of *E. ebracteolata* have been used to treat cancer, lymphatic tuberculosis, and ascites [89]. *E. sororia* is commonly used in traditional Uighur medicines to cure abdominal pain, abdominal distention, skin disease, and paralysis [90, 91]. The dried roots of *E. fischeriana* are used in traditional Chinese medicine to remedy edema, ascites, and cancer [92]. The latex of *E. pterococca* is used to treat Aures, a region of Algeria, against thorns and warts [93].

Ethnobotanical *Uses of Euphorbia schimperiana*

The latex *E. schimperiana* is used as ear drops to treat otitis and snakebite, the leaf paste in water, is taken to treat coughs and colds. Leaf powder is applied to impetigo and stubborn skin infections. A leaf and root decoction is taken as a purgative to treat venereal diseases, as an anthelmintic, and the fruits, crushed together with roots of *Cyathula polycephala* and then mixed with water, are taken to treat anthrax in cattle [94].

2.3. Chemical Constituents

2.3.1. Chemical Constituents of the Genus *Vepris and V.dainelli*

Vepris species are a rich source of various secondary metabolites such as acridones, furoquinolines, quinolones, azole, coumarins, flavonoids, indoloquinazolines, limonoids, lignans, phenolic compounds, and terpenoids [95].

Acridones, furoquinolines, and quinolones alkaloids were reported from the *Vepris* species (Figure 7, **7-25**). The leaves extract of *V. bilocularis* afforded 7-methoxyflindersine (**7**), 7-prenyloxyflindersine (**8**), N-methyl-7-prenyloxyflindersine (**9**), 6-methoxyflindersine (**10**), 3-prenyloxy acridone (**11)**, 1,2,3-trimethoxy-N-methylacridone (**12**), and arborinine (**13**) [96]. Rasoanaivo et al. (1999) reported four acridone alkaloids from stem bark of *V. sclerophylla* such as melicopicine (**14),** tecleanthine (**15)**, 6-methoxytecleanthine (**16)** and evoxanthine (**17**) (Figure 7) [66]. Two acridone alkaloids, verdoocridone A (**18)** and B (**19**), were also reported from roots and leaves of *V. verdoorniana* [95]. Phytochemical investigation on the roots of *V. uguenensis* afforded furoquinolines alkaloids, flindersiamine **(20**), and maculosidine **(21**) [97]. A related study revealed four furoquinoline alkaloids i.e. haplopine-3,3'-dimethylallyl ether (**22**), anhydroevoxine (**23**), evoxine (**24**), and skimmianine (**25**), from the aerial part of *V. glomerata* [98].

Flavanoids such as veprisinol (**26,** Figure 7) [98] and hesperetin (**27**, Figure 7) [99] have been reported from *V. glomerata* of which the former was showed antioxidant activity compared to ascorbic acid. Moreover, phenolic compounds such as prenylated cinnamaldehyde, glomeral (**28**), p-hydroxycinnamic acid (**29**), caffeic acid (**30**), methyl cinnamate (**31**), scoparone (**32**), syringaresinol (**33**) have been reported from the roots and stem bark of *V. glomerata* [97]. Recent studies also revealed limonoids such as limonin (**34**) and limonyl acetate (**35**) from the roots and stem bark of .*V glomerata* [97], and more limonoids (**36-41**) along with terpenoids (Figure 7, **42-50**) were reported from *V. punctate* [99,100].

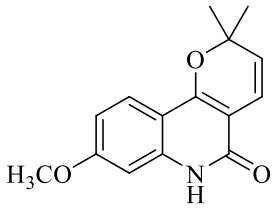

7

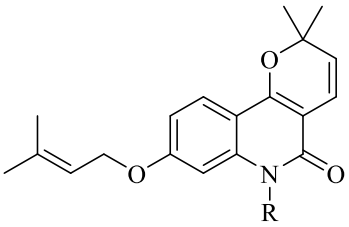

8 R=H
9 R=CH3

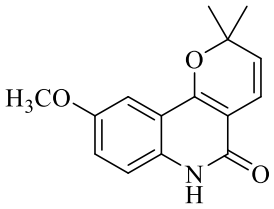

10

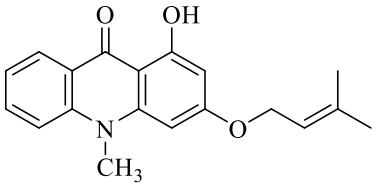

11

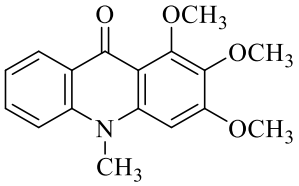

12

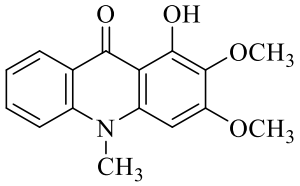

13

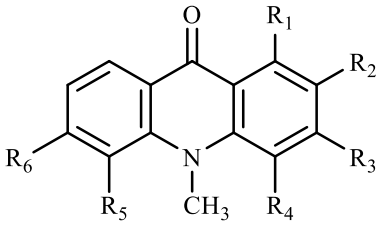

	R1	R2	R3	R4	R5	R6
14	OCH_3	OCH_3	OCH_3	OCH_3	H	H
15	OCH_3	OCH2O		H	OCH_3	H
16	OCH_3	OCH2O		H	OCH_3	OCH_3
17	OCH_3	OCH2O		H	H	H

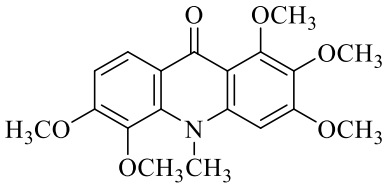

18

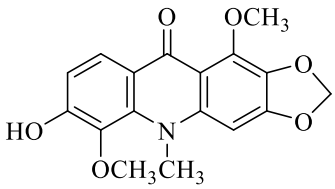

19

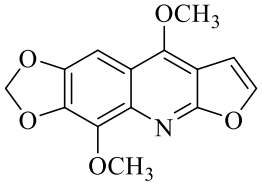

20

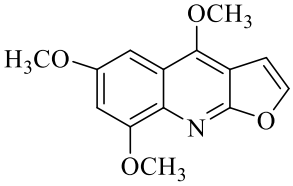

21

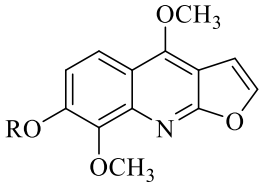

22

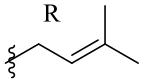

23

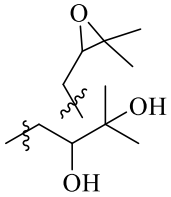

24

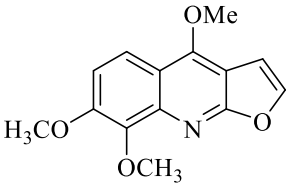

25

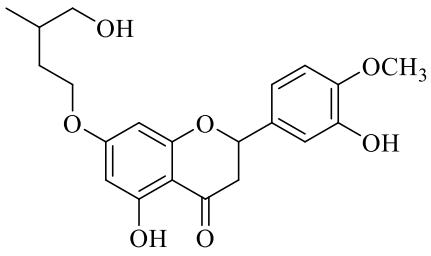

26

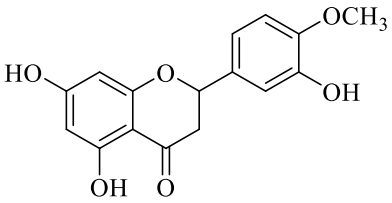

27

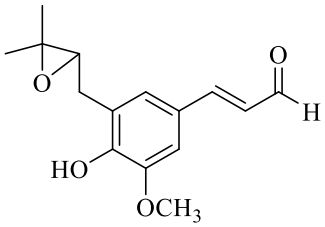

28

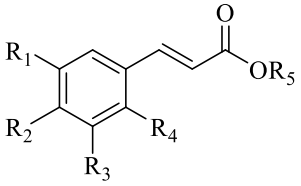

29. R1=H, R2=OH, R3=H, R4=H, R5=H
30. R1=R2=OH, R3=R4=R5=H
31. R1=R2=R3=R4= H, R5=CH_3

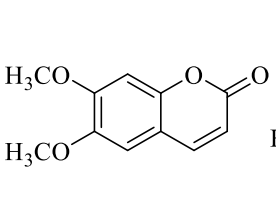

32

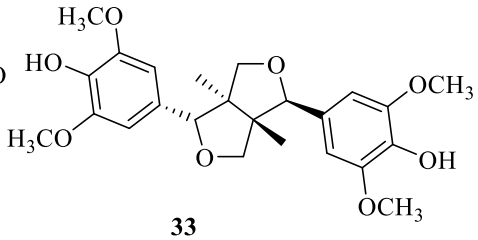

33

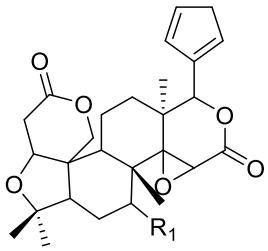

34 R1= O
35 R1= OAC

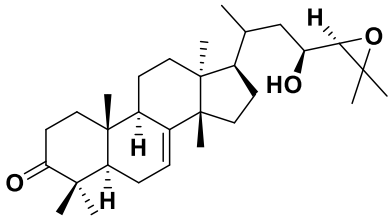

36

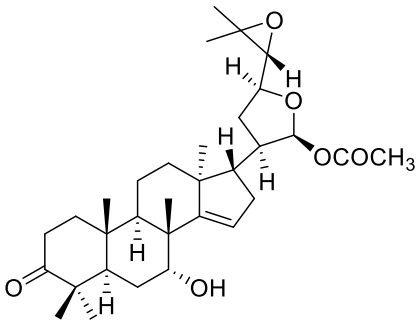

37

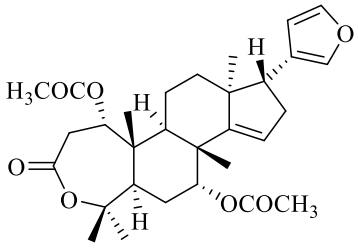

38

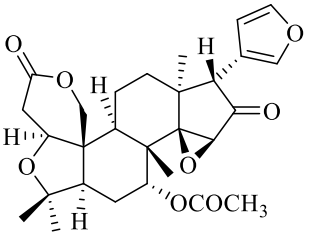

39

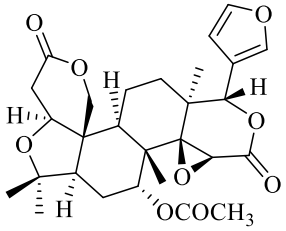

40

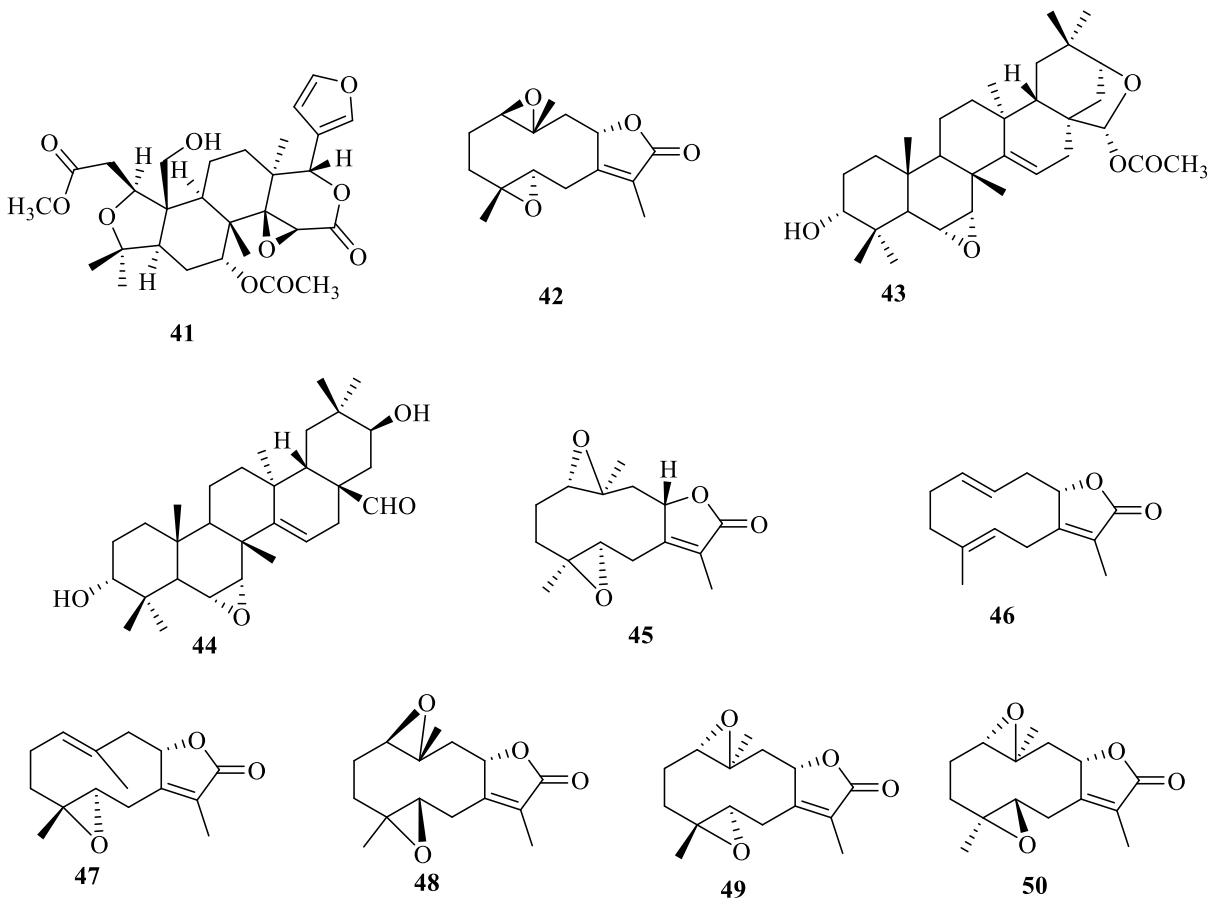

Figure 7: Compounds reported from the genus *Vepris*.

Chemical Constituents of *Vepris danielli*

There were limited scientific studies undertaken on the chemical compositions of this species. One of the prominent studies was the one conducted by Dagne et al (1988) which reported four alkaloidal constituents from leaves of *V. dainellii* such as kokusaginine (**51**), skimmianine (**25**), acridones xanthoxoline (**52**), and arborinine (Figure 8, **13**) [44].

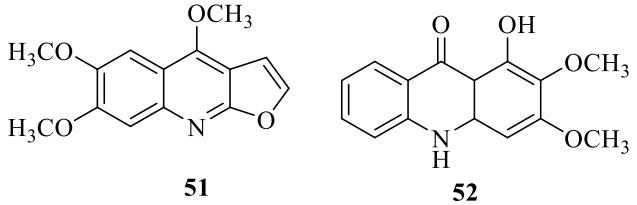

Figure 8: Compounds reported from leaves of *V. dainellii*.

2.3.2. Chemical Constituents of the Genus *Zanthoxylum and Zanthoxylum chalybeum*

Previous studies on chemical constituents of the genus *Zanthoxylum* revealed the genus is rich in sources of various classes of secondary metabolites such as alkaloids, lignans, coumarins, flavonoids, and terpenes [70].

Benzophenanthridines (Figure 9, **53-66**) are the most frequently reported type of alkaloids in the genus *Zanthoxylum* including fagaronine (**53**), nitidine (**54**), chelerythrine (**55**), sanguinarine (**56**), iwamide (**57**) and integriamide (**58**) from various species of the genus *Zanthoxylum* [70, 101]. Wang *et al* (2015) reported six benzophenanthridines such as norchelerythrine (**59**), decarine (**60**), 8-hydroxy-9-methoxy-2, 3-(methylenedioxy) benzophenanthridine (**61**), 6-hydroxydihydrochelerythrine (**62**), 6-methoxy-7-hydroxydihydrochelerythrine (**63**) and oxychelerythrine (**64**) from the stem barks of *Z. schinifolium* [102]. A related study on the root bark of *Z. simulans* reported 6-methyldihydochelerythrine (**65**) and 6-methylnorchelerythine (**66**) [103]. Dihydrochelerythrine (**67**) was also reported from stem bark Z. *parachanthum* [104].

Patiño *et al* (2010) reported benzylisoquinoline alkaloids (Figure 9, **68-71**) (*R*)-(+)-isotembetarine (**68**) and (*S*)-(-) xylopinidine (**69**) along with protoberberine alkaloids such as *N*-methyltetrahydrocolumbamine (**70**) and *N*-methyltetrahydropalmatine (**71**) from *Z. quinduense* [105]. A related study on *Z. monophyllum* reported berberine (Figure 9, **72**) [106]. Aporphine alkaloid such as *N*, *N*-dimethyllindicarpine (Figure 9, **73**) was reported from the root barks of *Z. zanthoxyloides* [107].

Pyranoquinoline alkaloids such as *N*-methylflindersine (**74**) and zanthobungeanine (**75**) were reported together with two furoquinolines dictamine (**76**) and skimmianine (**25**) from bark of *Z. budrunga* [108], and zhantosimulin (**77**) and huajiaosimulim (**78**) from the stem bark of *Z. simulans* [109].

Bishoderninyl terpene alkaloids (**80**, Figure 9) have been isolated from the leaves of *Z. integrifoliolum* [110]. Indolopyridoquinazoline alkaloids (**81-83**, Figure 9) 1-hydroxyrutaecarpine (**81**), rutaecarpine (**82**), and 1-methoxyrutaecarpine (**83**) have been reported

from the fruits of *Z. integrifoliolum* [111]. Canthin-6-one (**84,** Figure 9) and 5-methoxycanthin-6-one (**85**, Figure 9) were reported from *Z. rugosum* [112] and *Z. budrunga* [113], respectively.

Lignans reported from the *Zanthoxylum* species, such as syringaresinol (Figure 9, **86**) from *Z. monophyllum* [105], and (+)-sesamin (**87**) from *Z. quinduense* [106], *Z. budrunga* [108], and *Z. americanum* [114] and asarinin (**88**) from *Z. americanum* [114].

Coumarins (Figure 9, **89-92**) were reported from *Z. shinifolium* including larcinatin (**89)** [115]**,** auraptene (**90**) and collinine (**91**) [116], and psoralen (**92**) from berries of *Z. americanum* [117]. Four pyranocoumarins; dipetaline (**93**), alloxanthoxyletin (**94**), xanthoxyletin (**95**) and xanthyletin (**96**) were isolated from *Z. americanum* [114]. Polymethoxylated flavanoid such as 3, 5-diacetyltambuline (**97**) have been reported from fruits of *Z. integrifoliolum* [118]. Finally, lupeol (**98**) were isolated from *Z. parachanthum* [119]

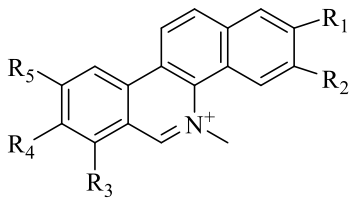

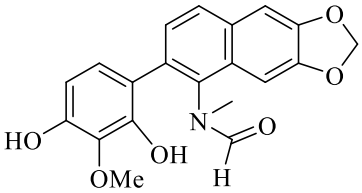

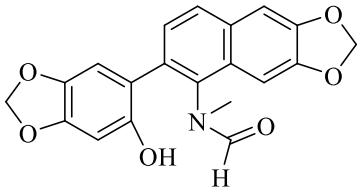

53 R_1=OH, R_3=H, R_2= R_4=R_5=OCH_3
54 R_1+R_2=OCH_2O, R_3=H, R_4=R_5=OCH_3
55 R_1+R_2=OCH_2O, R_3= R_4=OCH_3, R_5=H
56 R_1+R_2=OCH_2O, R_3 + R_4=OCH_2O, R_5=H

57

58

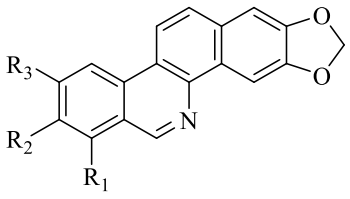

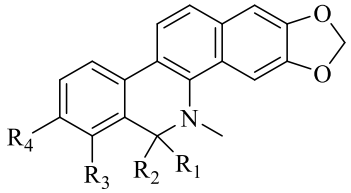

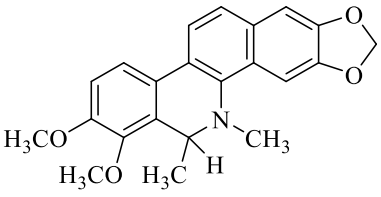

59 R_1=R_2=OCH_3, R_3=H
60 R_1=OCH_3,R_2=OH, R_3=H
61 R_1=H, R_2=OH, R_3=OCH_3

62 R_1=OH, R_2=H, R_3=R_4=OCH_3
63 R_1=R_4=OCH_3,R_2=H, R_3=OH
64 R_1+ R_2=O, R_3=R_4=OCH_3

65

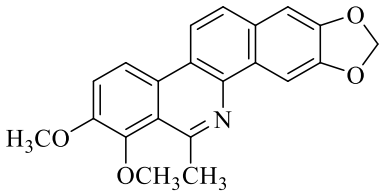

66

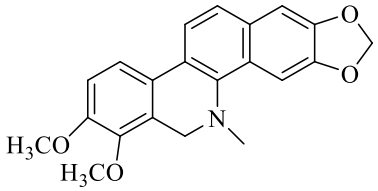

67

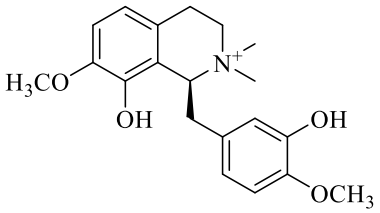

68

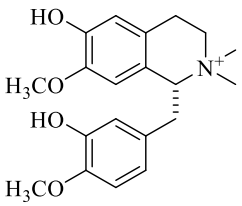

69

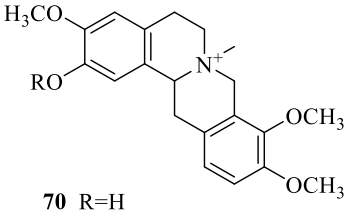

70 R=H
71 R=CH_3

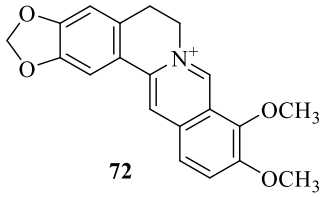

72

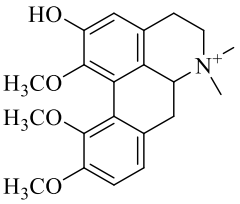

73

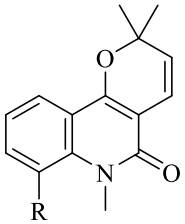

74 R=H
75 R=OCH_3

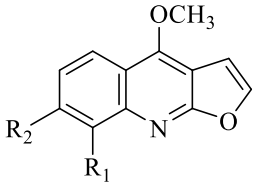

76 R_1=R_2=H
77 R_1=R_2=OCH_3

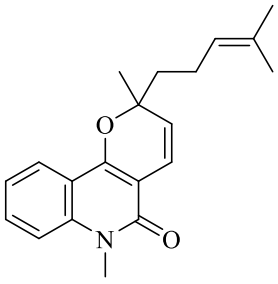

78

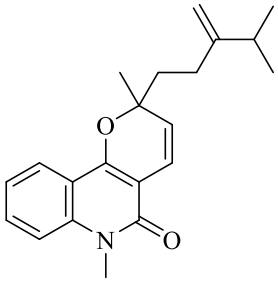

79

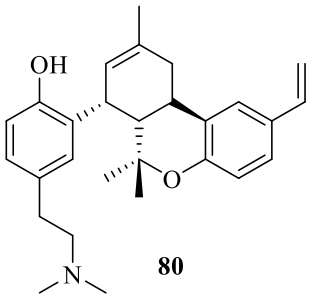

80

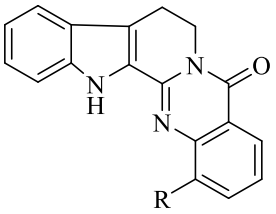

81 R=OH
82 R=H
83 R=OCH_3

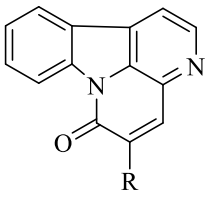

84 R=H
85 R=OCH_3

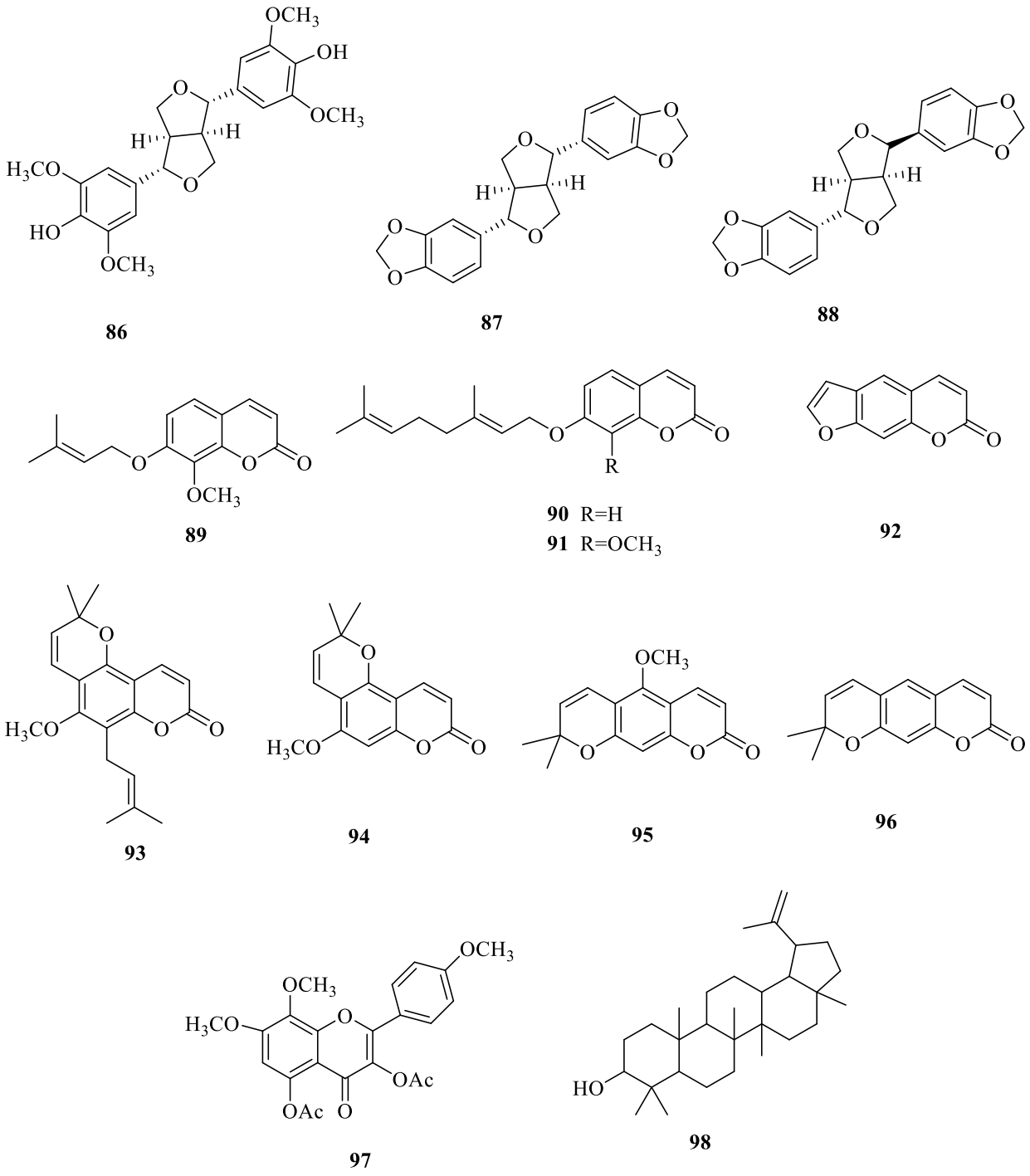

Figure 9: Compounds reported from the genus *Zanthoxylum.*

Chemical Constituents of *Zanthoxylum chalybeum*

There were limited phytochemical studies on this species, however, 2, 3-epoxy-6.7-ethylenedioxyconiferyl alcohol (Figure 10, **99**), dihydrochelerythrine (Figure 10, **67**) [120], and

chelerythrine [121] (Figure 10, **55**) were reported from the species. Recently, stem bark extract of *Z. chalybeum* yielded 4- (isoprenyloxy)-3-methoxy-3, 4-deoxymethylenedioxyfagaramide and fagaramide (Figure 10, **100**, **101**) [119]

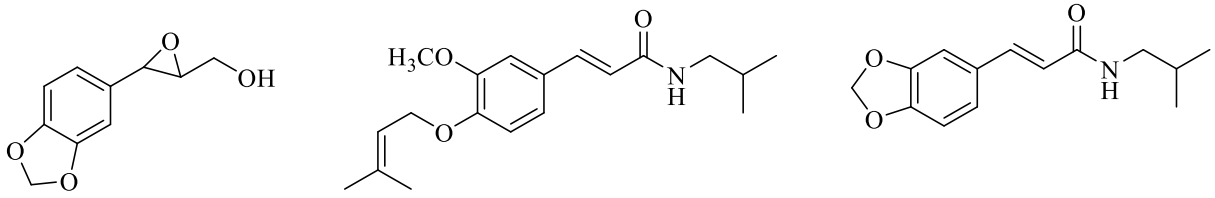

99 **100** **101**

Figure 10: Compounds reported from *Z.chalybeum*

2.3.3. Chemical Constituents of the Genus *Uvaria* and *Uvaria Scheffleri*

Uvaria species are rich in bioactive compounds such as acetogenins, alkaloids, dihydrochalcones, flavonoinds, polyhydroxycyclohexene, pyrenes, terpenes, xanthenes, and phenolics having wide spectrum of biological activities [122]. Sesquiterpenes (Figure 11, **102-106**) were reported from *Uvaria* species. Such as Tanzanene (**102**) was reported from root bark extract of *U. tanzaniae* [123] whereas lucidene (**103**) and uvariasesquiterpene (A-C) (**104-106**) were reported from *U. lucida* [124] and *U. angolensis* [125], respectively. Flavanones pinocembrin **(107**), pinostrobin (**108**), C-benzylated flavanones chamanetin (**109**), isochamanetin (**110**), dichamanetin (**111**) and C-benzylated dihydrochalcones uvaretin (**112**), isouvaretin (**113**), diuvaretin (**114**) and uvarinol (**115**) [126] were reported from *Uvaria chamae*. In a related study by Weenen et al. (1991), uvaretin (**112**), isouvaretin (**113**), diuvaretin (**114**), chamuvaretin (**1116**), and isotriuvaretin (**117**) were reported from *U. tanzaniae* and displayed anti-plasmodial activity against the multidrug-resistant K_1 strain of *Plasmodium falcipururn.* (Figure11, **112-114, 116-117**) [123].

Acetogenins (Figure 11, **118-122**) such as chamuvarinin (**118**), squamocin (**119**), desacetyluvaricin (**120**), and neoannonin (**121**) were reported from the roots of *U. chamae* [127]. In a related study, tonkinecin (**122**) has been isolated from the roots of *U. tonkinesis* [49]. Ankisetty et al., (2006) reported four aromatic compounds (Figure 11, **123-126**) such as grandiuvarone A (**123**) and grandiuvarins A-C (**124-126**) from *U. grandiflora* [128]. In a related study, 7-membered lactone (5-acetoxy-7-benzoyloxymethyl-7H-oxepin-2-one) (**127**) [129] and (-

) zeylenol (**128**) [130].were reported from the stems of *U. grandiflora* and *U. klaineana*, respectively. Four indol alkaloids, such as uvarindole A-D (Figure 11, **129-132**), were reported from the stem bark of *U. angolensis* [131, 132]. Recently, three pyrenes and two pyrenediones with one sesquiterpene (Figure 11, **133-138**) were isolated from the roots of *U. lucida* Benth [79].

Macabeo et al., (2017) reported highly oxygenated seco-cyclohexene derivative, valderepoxide (**139**) along with uvamalols D (**140**) and G (**141**), grandiuvarone (**142**), 2'-hydroxy- 3',4',6'-trimethoxychalcone (**143)**, valderramenol B (**144**) from *U. valderramensis* [133]. Moreover, three polyoxygenated cyclohexene derivatives named cherrevenisyls A (**145**) and B (**146**), along with ellipeiopsol E (**147**), were reported from the roots of *U cherrevensis* (Figure 11) [134]. In a related study on *U. alba*, two chlorine-containing polyoxygenated seco-cyclo- hexenes, albanols A (**148**) and B (**149**) along with oxepinone metabolite grandiuvarone (**150**), were reported (Figure 11) [135].

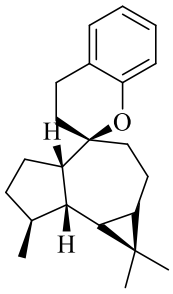

102

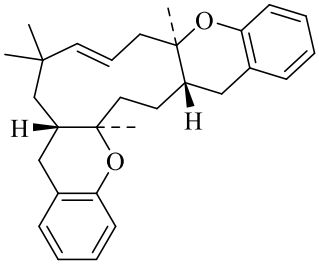

103

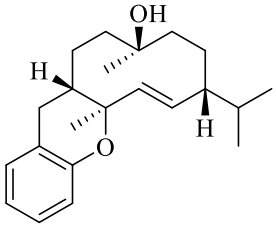

104

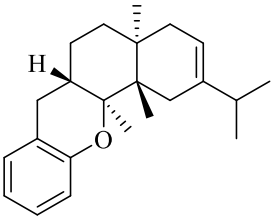

105

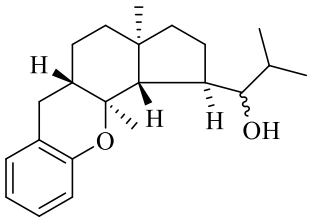

106

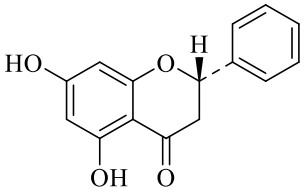

107

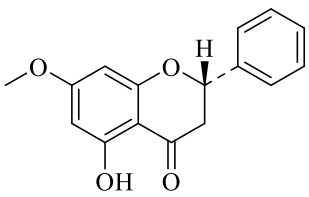

108

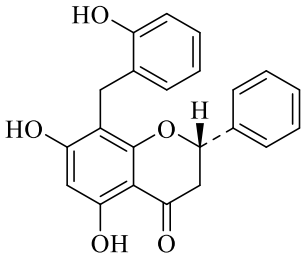

109

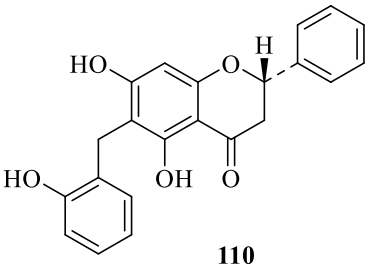

110

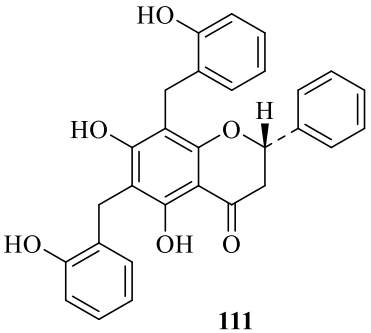

111

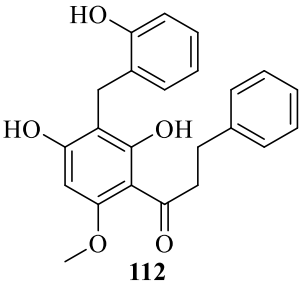

112

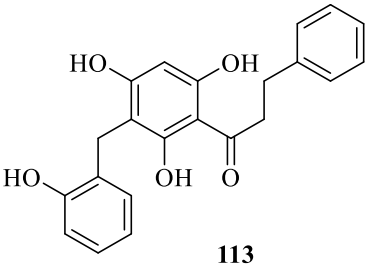

113

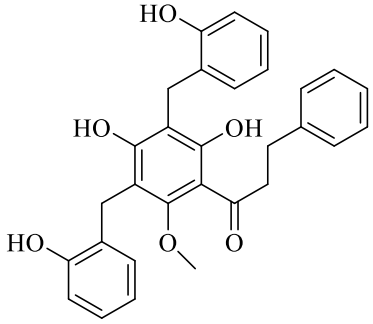

114

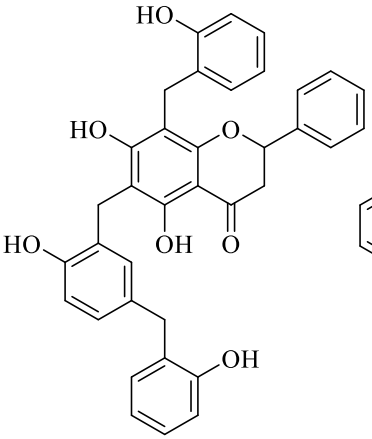

115

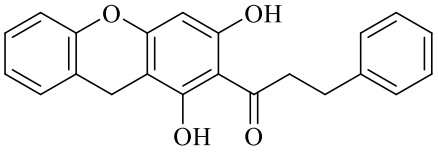

116

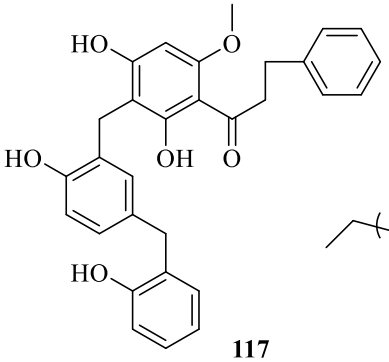

117

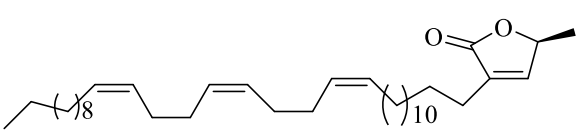

118

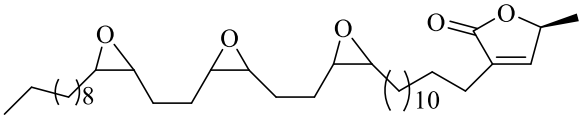

119

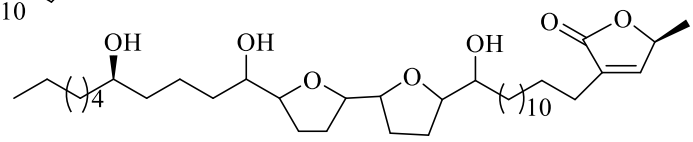

120

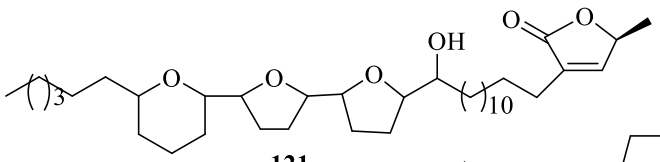

121

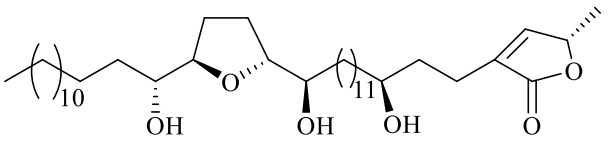

122

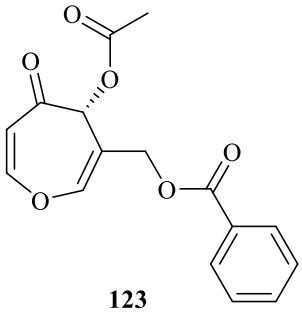

123

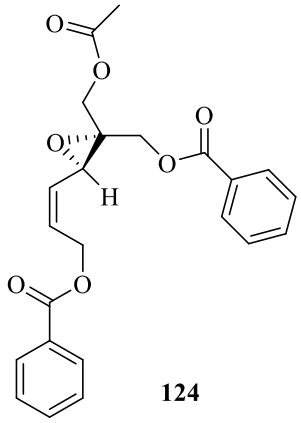

124

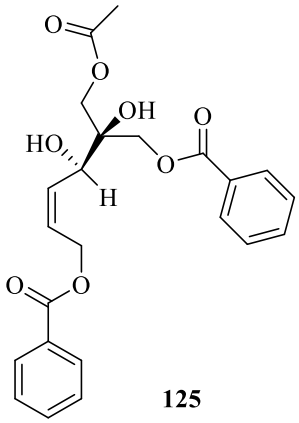

125

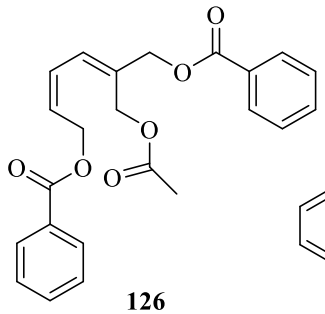

126

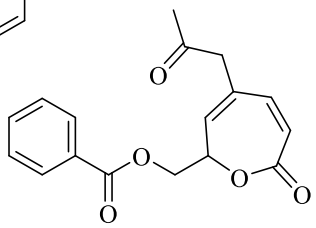

127

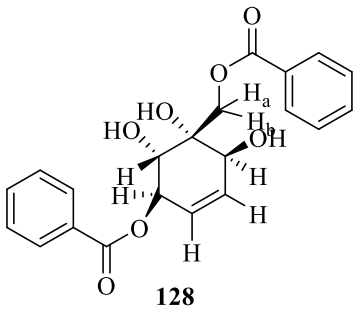

128

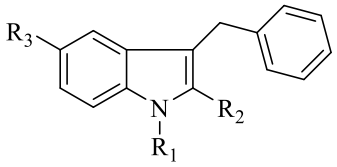

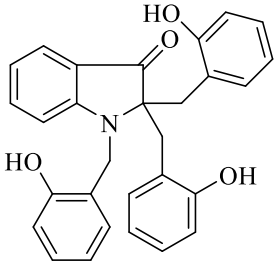

132

129 R1=R2= 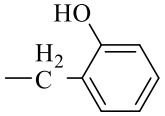 , R3=H

130 R1=R2=R3= 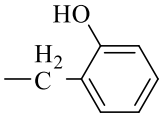

131 R1=R3=H, R2= 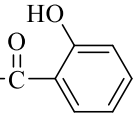

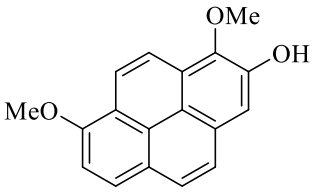

133

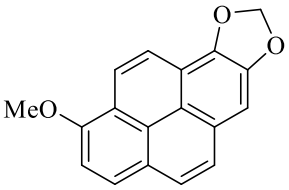

134

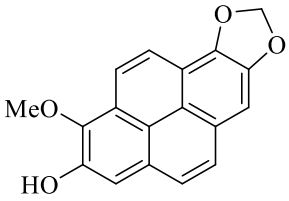

135

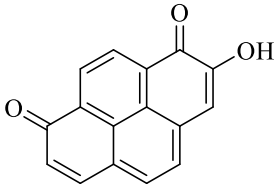

136

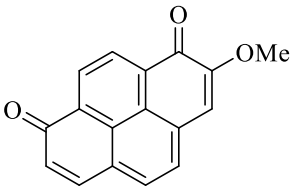

137

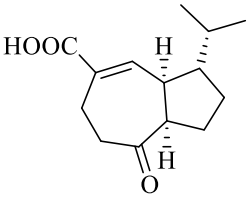

138

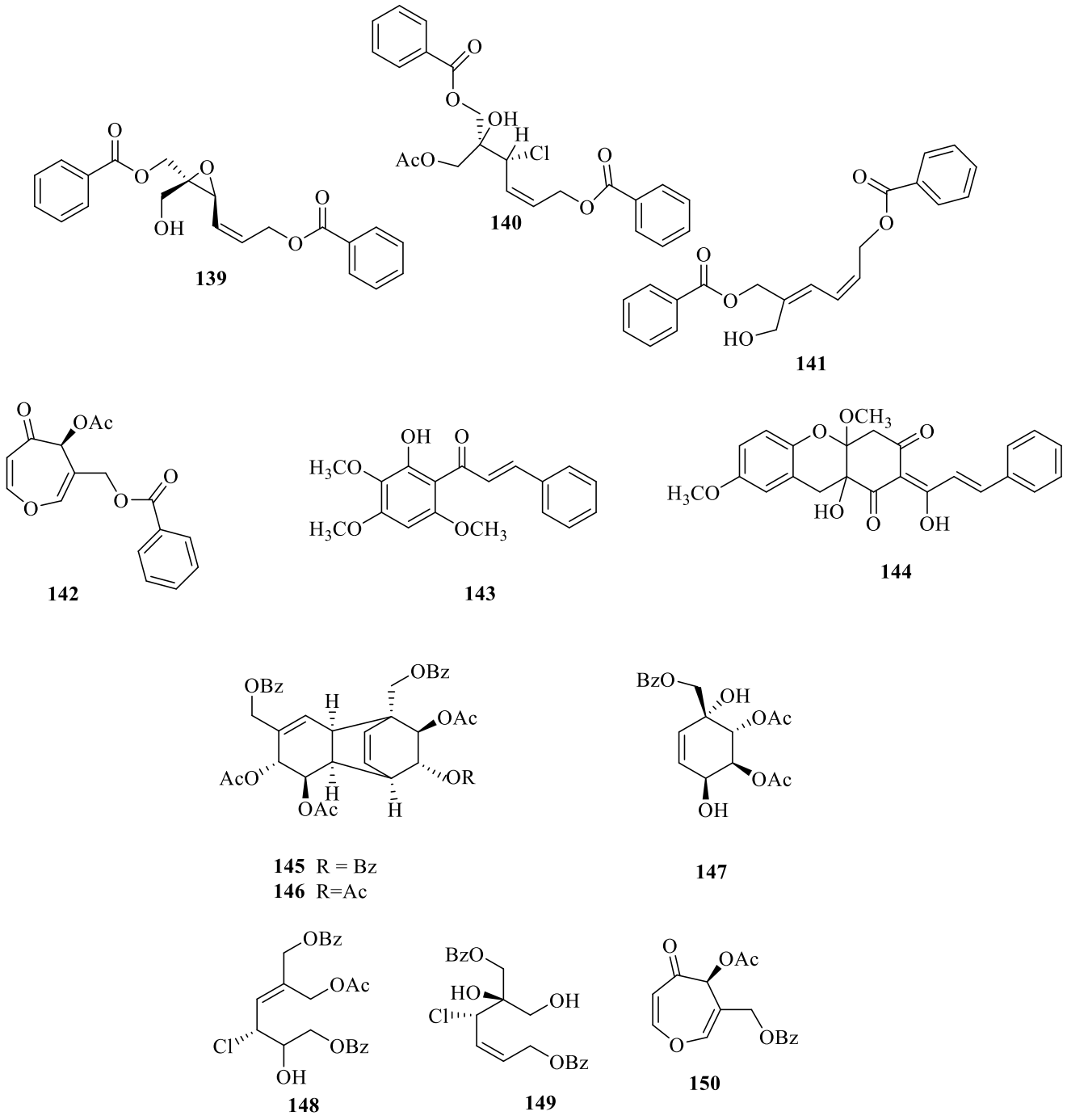

Figure 11: Compounds reported from the genus *Uvaria*.

Chemical Constituents of *Uvaria scheffleri*

There were limited phytochemical studies on this species of which some of the prominent ones reported stigmasterol (**151**), β-sitosterol (**152**), 3-farnesylindole (**153**), 2',6'-dihydroxy-3',4'-

dimethoxychalcone (**154**) (Figure 12, **151-154**) [41]. In a related study, Ichimaru *et al* (2010) were also reported scheffl erichalcone (**155**), espintanol (**156**), benzylbenzoate (**157**), 2',6'-dihydroxy-4'-methoxychalcone (**158**), 5,7-dihydroxyflavone (**159**), hydroxyespintanol (**160**), oxoxylopine (**161**), oxoanolobine (**162**), and (±)-schefflone (**163**) from the same species (Figure 12, **155-163**) [136].

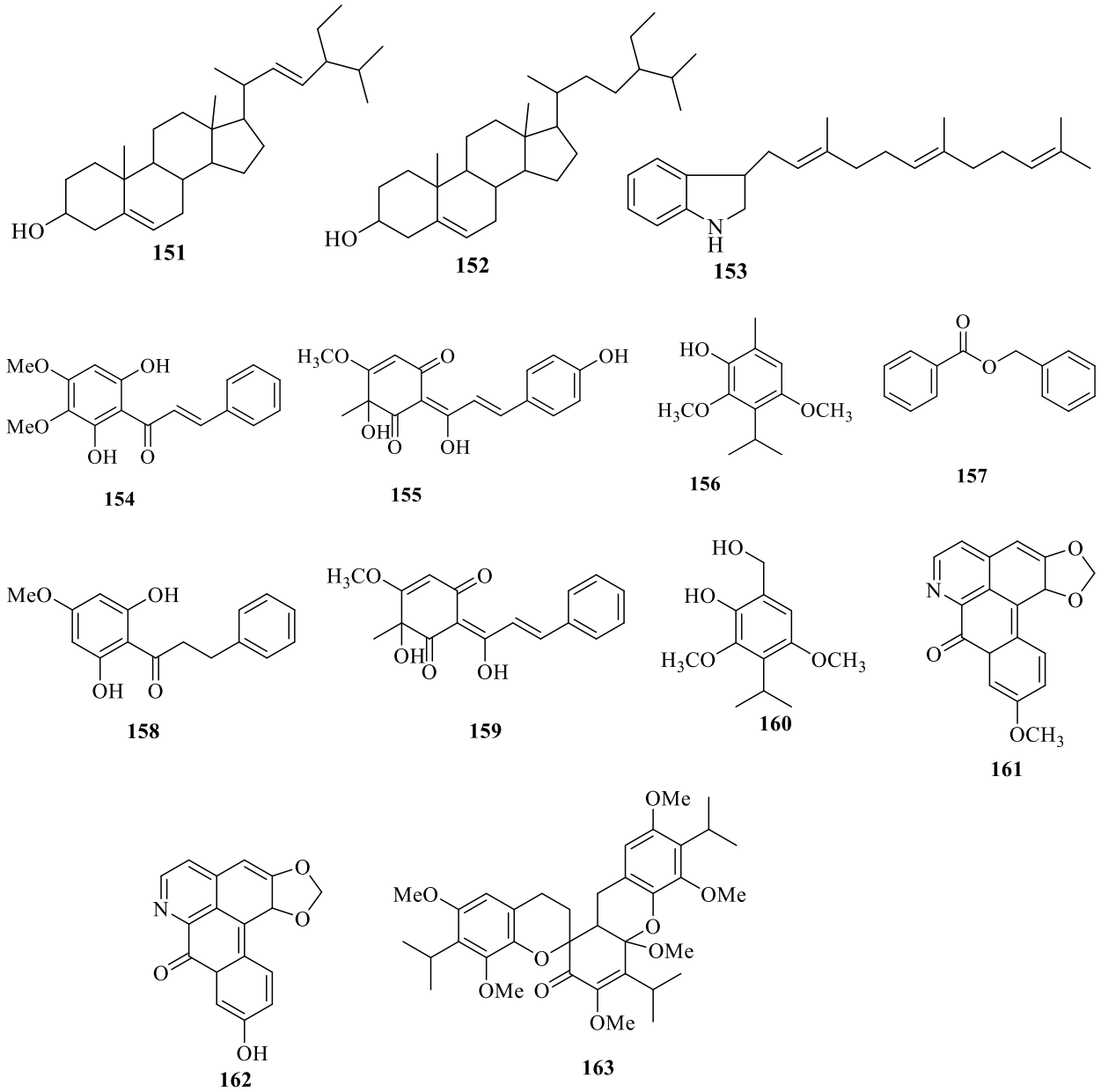

Figure 12: Reported compounds from *U. scheffleri*.

2.3.4. Chemical Constituents of the Genus *Clematis*

The *Clematis* species are a rich source of phenolic compounds and their derivatives. Lin et al.,(2012) reported seventeen phenolic compounds and their derivatives (Figure 13, **164-179**) from *C. connata* including 3,4-dihydroxyphenethyl-5-hydroxy-4-oxopentanoate (**164**), 3-(4-hydroxy-2,5-dimethoxyphenyl)-3-oxopropyl acetate (**165**), hydroxytyrosol (**166**), 2-(4'-O-b-D-glucopyranosyl-3'-hydroxyphenyl)-ethanol (**167**), 2-(3'-O-b-D-glucopyranosyl-4'-hydroxyphenyl)-ethanol (**168**), caffeic acid (**30**), isoferulic acid (**169**), ferulic acid (**170**), 3-hydroxy-4 methoxybenzoic acid (**171**), 4-hydroxybenzoic acid (**172**), 3,4-dihydroxybenzaldehyde (**173**), 3-hydroxy-4-methoxybenzaldehyde (**174**), 2-hydroxy-3-phenylpropionic acid (**175**) and (7*S*, 8*R)*-dihydrodehydrodiconiferyl alcohol (**176**); flavonoids, such as naringenin (**177**), genistein (**178**), and coumarin i.e. 6,7- dihydroxycoumarin (**179**) [137]. A related study revealed eight phenolic glycosides (Clematisides A to H, Figure 13, **180 −187**) isolated from aerial part of *C. tashiroi* [138].

Triterpene saponins are the dominant chemical constituents in the *Clematis* species [139]. Four triterpenoid saponins i.e clematochinenoside H–K (**188–191,** Figure 13) were reported from the roots and rhizomes of *C. chinensis* [140], whereas Mimaki et *al* (2004) identified five triterpene saponins (**192-196**) [141], from the roots of *C. chinensis*. Cheng et al., (2018) reported hederagenin saponin (**197**) from *C. ganpiniana* [142]. In a related study done on the same species by Ding et al., (2009) reported 3β-[(α-L-arabinopyranosyl)-oxy]olean-12-en-28-oic acid (**198**), hederagenin 3β-O-α-L-arabinopyranoside (**197**), 3β-O-α-lrhamnopyranosyl-(1→2)-α-L-arabinopyranosyl oleanolic acid (**199**), and α-hederin (**200**) [83], whereas Sun et al, (2007) reported triterpene saponnin (**201)** from this plant species [143] (Figure 13).

Alkaloids and their glucoside were also reported from *Clematis* species (Fig.13, **202-209**). β-magnoflorine (**202**) and α-magnoflorine (**203**) were reported from the aerial parts of *C. parviloba* [144]. In addition, four indole alkaloids (**204-207**) were reported from the roots of *C. manshurica* [145]. In a related study, indole alkaloidal glucoside (**208**), aurantiamide acetate (**209**), eleutheroside E (**210**) and 1-O-caffeoyl-b-D-glucopyranoside (**211**) were reported from ethanol extract of the aerial parts of *C. terniflora* DC [146].

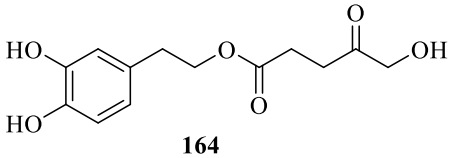

164

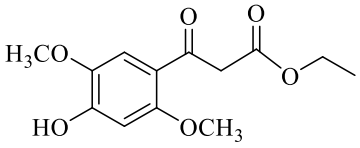

165

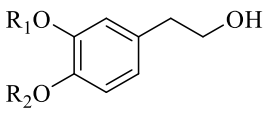

	R1	R2
166	H	H
167	glu	H
168	H	glu

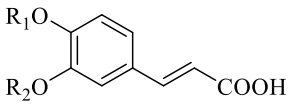

	R1	R2
169	CH3	H
170	H	CH3

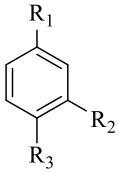

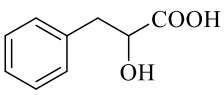

175

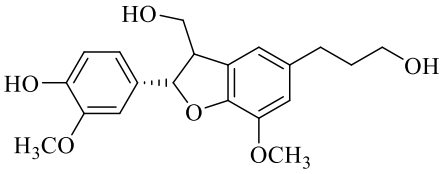

176

	R1	R2	R3
171	COOH	OH	OCH3
172	COOH	H	OH
173	CHO	OH	OH
174	CHO	OH	OCH3

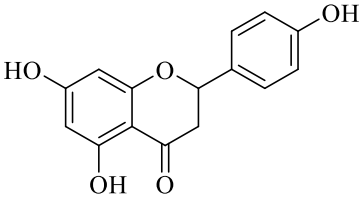

177

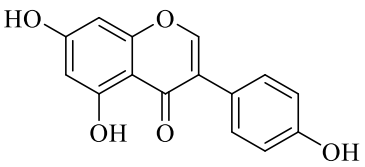

178

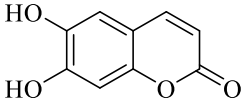

179

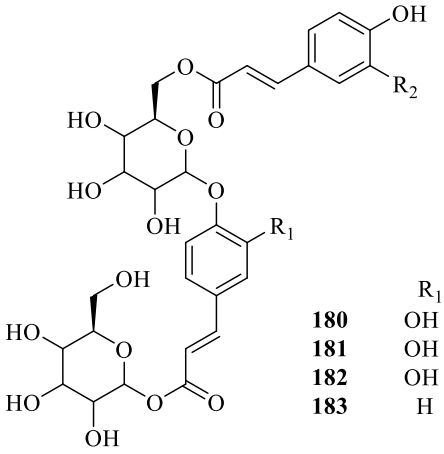

	R_1	R_2
180	OH	OH
181	OH	OCH3
182	OH	H
183	H	OH

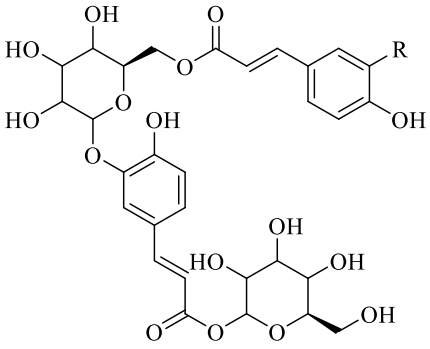

184 R= OH
185 R= H

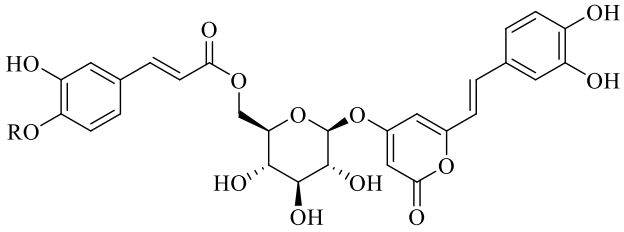

186 R=H

187 R=

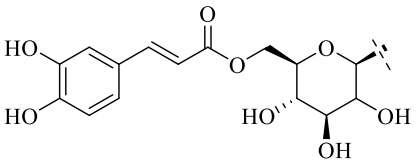

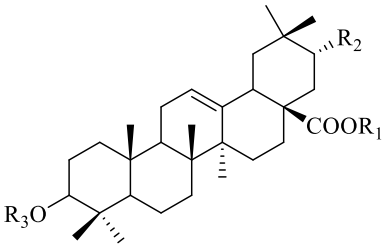

	R_1	R_2	R_3
188	H	OH	Glc(1 → 4)Glc (1→4)Rib(1→ 3) Rha(1 →2)Ara
189	H	OH	Rib(1→3)Rha (1 →2)Ara
190	H	OH	Rib 1→ 3)Rha (1→)Glc(1 → 4) Ara
191	Glc	H	Rib 1 → 3)Rha (1 →2)Glc(1 → 4) Ara

Ara= 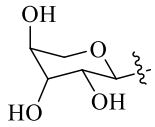

Rha= 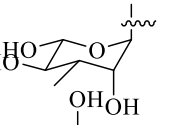

Rib = 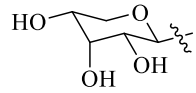

Glc= 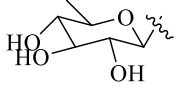

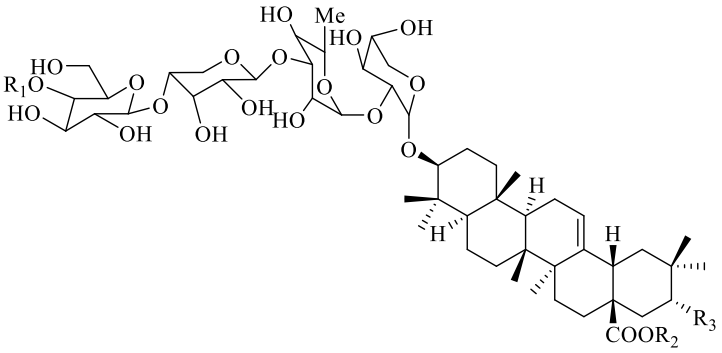

	R_1	R_2	R_3
192	S-1	H	H
193	S-1	H	S-2
194	H	H	S-2
195	S-1	OH	S-3
196	S-1	H	S-3

S-1= 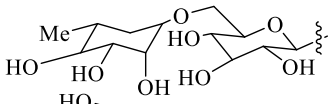

S-2= 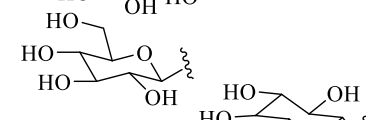

S-3 = 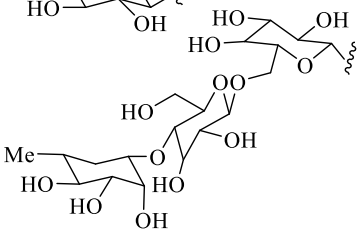

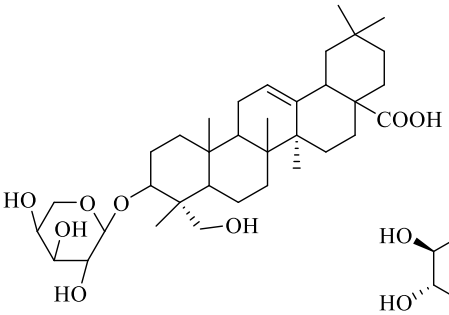

197

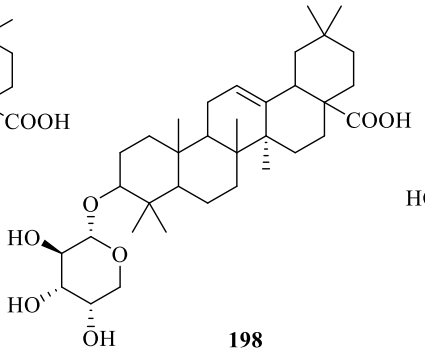

198

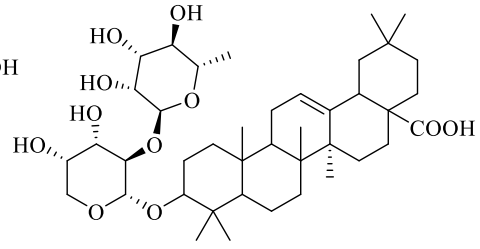

199

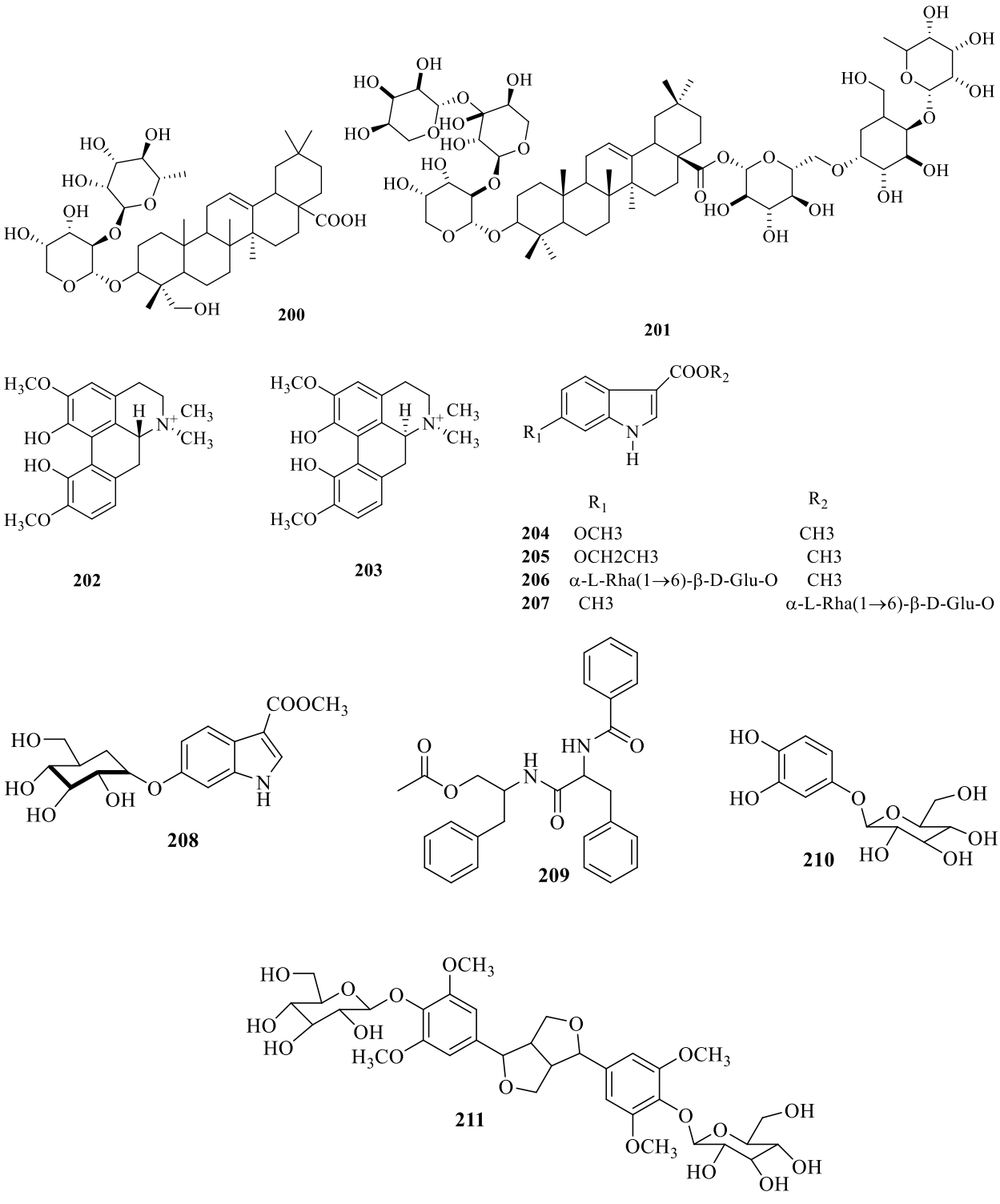

Figure 13: Compounds reported from the genus *Clematis*.

Chemical Constituents of *Clematis bugenisis*

Preliminary phytochemical screening of the extracts of this plant revealed the presence of Tannins, sapponins and flavonoids [85]. Nevertheless, to the best of our knowledge, there are not prior phytochemical reports on this species from Ethiopian flora.

2.3.5. Chemical Constituents of the Genus *Euphorbia* and *Euphorbia schimperiana*

Shi *et al* (2008) reviewed the chemical and pharmacological studies of genus *Euphorbia*, the diterpenoids such as jatrophane, lathyrane, tigliane, ingenane, *ent*-abietane, segetane, paraliane, pepluane, euphoractine, *ent*-atisnae, *ent*-kaurane, casbane,and myrsinol skeletons are among the most studied diterpenoids isolated from *Euphorbia* plants. Triterpenes, sesquiterpenoids, steroids, and flavonoids were also reported [147]. Euphane type triterpenes, 24,24-dimethoxy-25,26,27-trinoreuphan- 3β-ol (**212**), (24S)-24-hydroperoxyeupha-8,25-dien-3β-ol (**213**), and an ent-atisine diterpene (**214**), and ent-atisane-3α,16α,17-triol (**215**) were reported from an acetone extract of the stems of *E. antiquorum* together with diterpenes (**216** – **222**) (Figure 14, **212-222**) [148].

Ent-abietane diterpernoid, ebracteolata D (**223**) (Figure 14, **223**), and eleven analogues (**224-234**) were reported from the roots of *E. ebracteolata* [149]. In a related study, Kim et al., (2018) reported two diterpenoid glycosides kansuingol A (**235**) and kansuingol B (**236**) (Figure 14, **235-236** from the roots of *E. kansui* [150]. Two jatrophane diterpenoids, Heliojatrones A and B (Figure 14, **237** & **238**) with an unprecedented trans-bicyclo[8.3.0]tridecane core were reported from *E. helioscopia* [149]. As Sook et al., (2018) reported, highly oxidized ent-norabietane diterpenoid lathyrisol A from roots of *E. lathyris* L (Figure 14, **239**) [151].

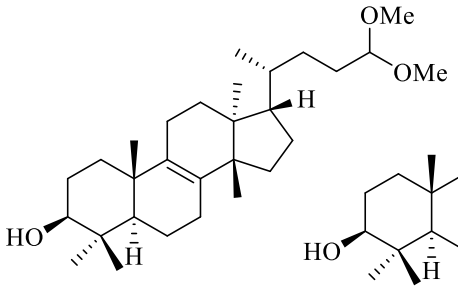

212

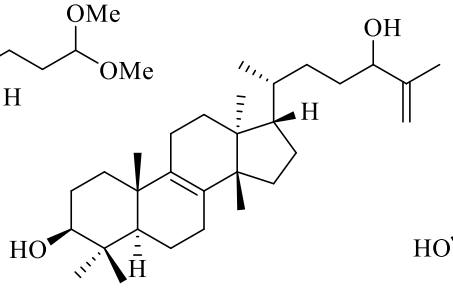

213

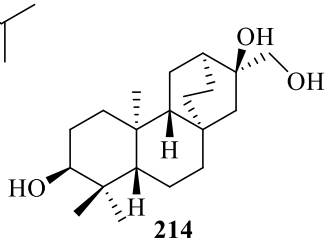

214

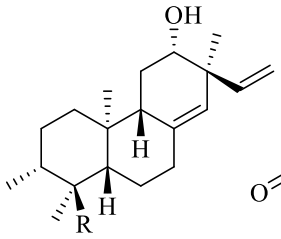

215 R=CHO
216 R=CH2OH

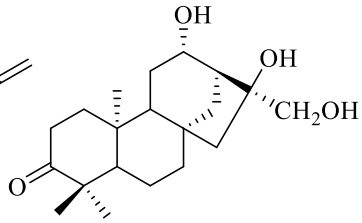

217

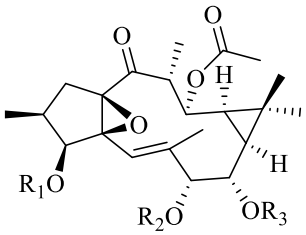

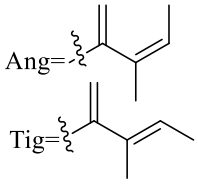

	R1	R2	R3
218	Ac	Bz	Me
219	Ac	Tig	Ac
220	Ac	Bz	Ac
221	H	Bz	Me
222	Ac	Ang	Me

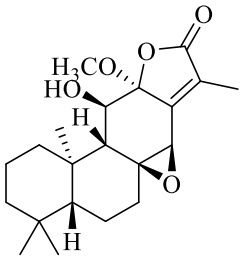

223

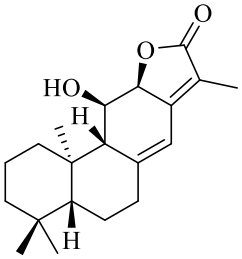

224

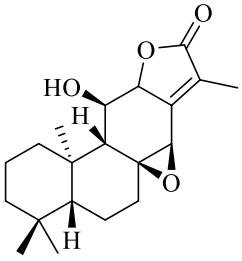

225

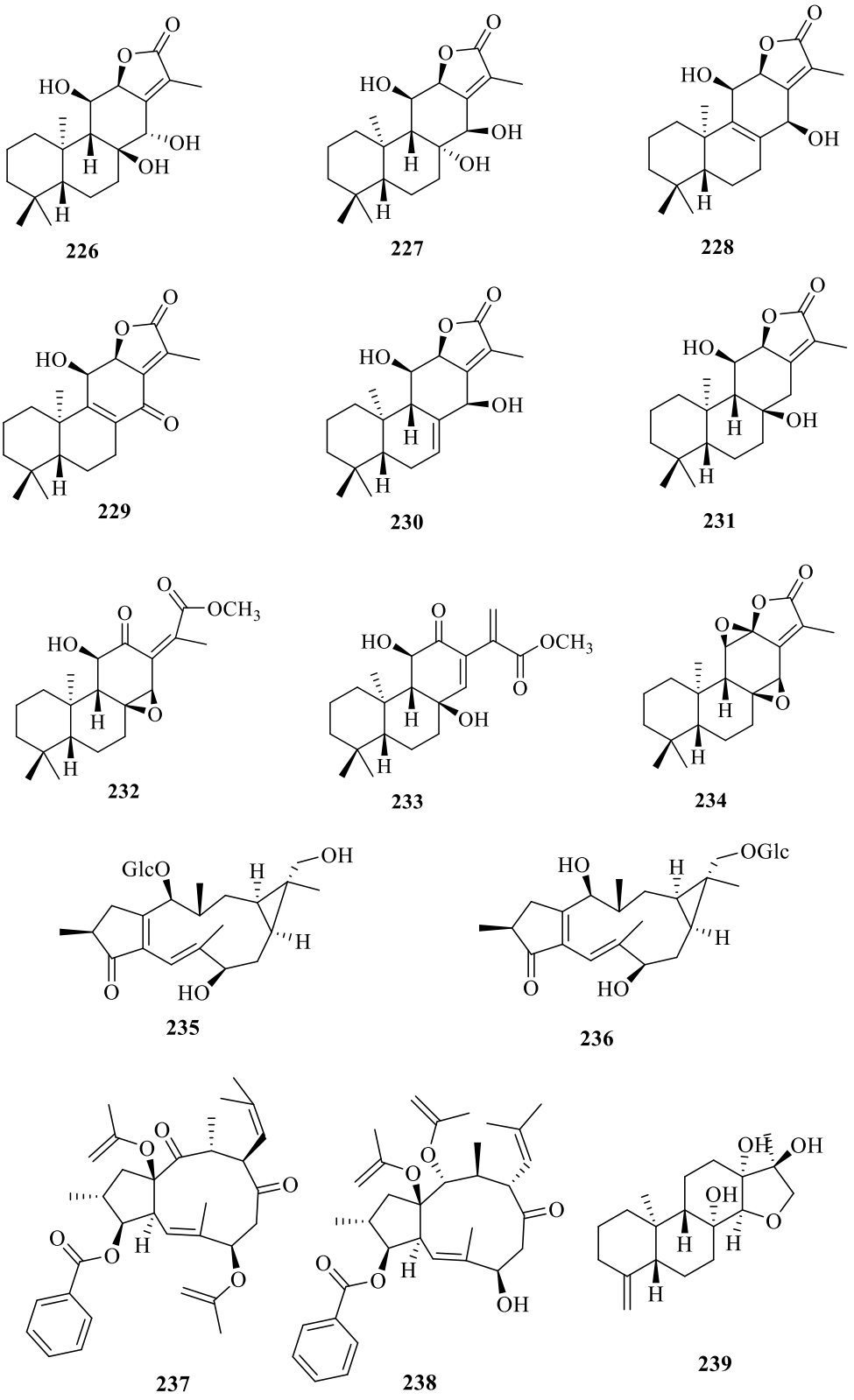

Figure 14: Compounds reported from the genus *Euphorbia*.

Chemical Constituents of *Euphrobia schimperiana*

3β-Cycloartenol (**240**) and three phenolic compounds chrysin (**241**), quercetin-7-O-β-D-glucoronside (**242**), and 3-methyl-quercetin-7-*O*-β-D-glucoronside (**243**) (Figure 15, **240**-**243**), were reported from the whole part of *E. schimperiana* [152]. There were no previous reports on the chemical constituents of this species from Ethiopian flora.

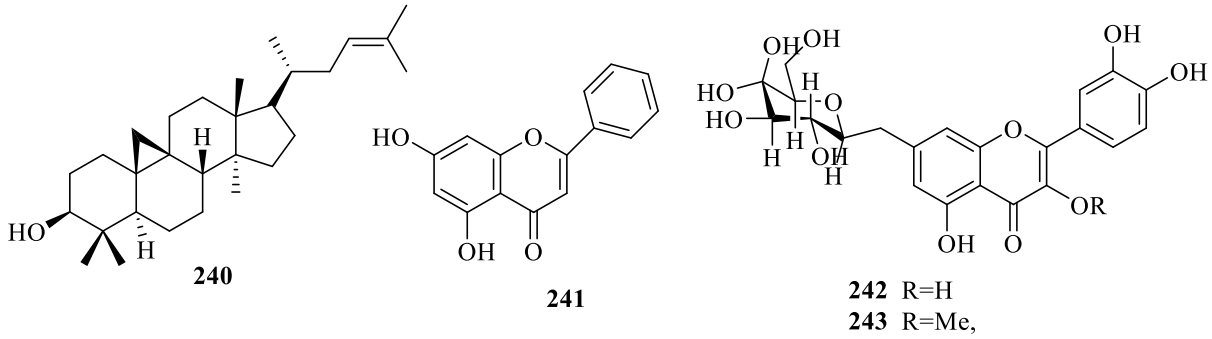

Figure 15: Compounds reported from *E. schimperiana*

2.4. Biological Activities Studies

2.4.1. Cytotoxicity Study

2.4.1.1. Cytotoxicity Studies of *Vepris* Species

Furo and pyranoquinolines alkaloids from *V. punctata* and *V. suaveolens* were examined for their potential cytotoxic effect against the A2780 cell line, and the results revealed IC_{50} values ranging 2.8-3.5 μg/mL [100]. A related study on the A549 cell line showed IC_{50} values ranged from 8.9-10 μM [153]. Furoquinoline 2′-(*R*)-acetylmontrifoline (**38**) and 2′-(*R*)-nkolbisine (**39**) from *T. nobilis* were tested against the KB cell line, and the result displayed low cytotoxicity with IC_{50} > 50 μg/mL [154]. Indolopyridoquinazoline alkaloids from *V. renieri* were examined on PC-3 cell line, and the result showed IC_{50} values ranging from 23.1-37.5 μM [155]. Acridone alkaloids isolated from *V. renieri* and *V. suaveolens* were tested against the HepG2, HT-29, PC-3, Ovcar-3, and MCF-7 cell lines, and the result revealed IC_{50} values 11.4, 13.6, 11.9 14.7 and 12.7 μM, respectively [156].

2.4.1.2. Cytotoxicity of *Zanthoxylum* Species

Berberine (**72**) reported from the bark of *Z. monophyllum* showed activity against HT- 29 (colorectal cancer), MCF-7 (breast cancer), HEp-2 (larynx cancer), and MKN-45 (gastric cancer)

cell lines with the IC_{50} Value 30.9±7.1, 28.7±3.2, 19.6±2.21, and 40.5±7.1 μM respectively [157, 158]. *In vitro* studies of compounds isolated from *Z. americanum* were showed cytotoxicity against human leukaemia (HL-60) with an IC_{50} of values of dipetaline (**93**) is 0.68 ppm, followed by alloxanthoxyletin (**94**) 1.31 ppm, sesamin (**87**) 2.71 ppm, asarinin (**88**) 4.12 ppm, xanthoxyletin (**95**) (3.48 ppm) and xanthylletin (**96**) 3.84 ppm [114]. Another study revealed compounds such as 4- (isoprenyloxy)-3-methoxy-3,4-deoxymethylenedioxyfagaramide (**100**), canthin-6-one (**84**), and sesamin (**87**) obtained from stem bark extract of *Z. parachanthum* displayed moderate cytotoxicity with IC_{50} values below 50 μM against the drug-sensitive CCRF-CEM and multidrug-resistant CEM/ADR5000 leukemia cell lines [106].

2.4.1.3. Cytotoxicity of *Uvaria* Species

Uvarinol (**102**) reported from ethanolic extracts of *U. chamae* displayed cytotoxicity (ED_{50}) against KB cell cultures at 5.9 μg/mL [126]. A related study revealed that chamuvarinin (**105**) reported from the roots of *U. chamae* displayed significant cytotoxicity toward the KB 3-1 cell line (IC_{50}) 8 x 10^{-10} M) [159]. Tonkinecin (**109**) reported from the roots of *U. tonkinesis* exhibited potent cytotoxicity especially against the HL-60 (human leukemia) (IC_{50}=0.51) BGC (IC_{50}=5.1 μM), HCT-8 (human colon adenocarcinoma) (IC_{50}=0.38 μM) and Bel 7402 (IC_{50}=1.5 μM) cancer cell lines [49].

2.4.1.4. Cytotoxicity of *Clematis* Species

The aromatic acids derivatives such as 3-(4-hydroxy-2, 5-dimethoxyphenyl)-3-oxopropyl acetate (**152**) and hydroxytyrosol (**153**) isolated from *C. connata* exhibited important potential cytotoxic activity against MDA-MB-231 and HepG2, respectively. Methanol root extract of *C. chinensis* exhibited a potent HL-60 cell growth inhibitory activity (98.6% inhibition at a sample concentration of 10 μg/mL; IC50 1.4 μg/mL) [141]. Cheng et al., (2018) reported hederagenin saponin (**184**) from *C. ganpiniana* showed a strong cytotoxic effect on MDA-MB-231 and MCF-7 breast cancer cells and can also cause apoptosis in breast cancer cells, significantly reducing mitochondrial Apaf-1 and Cyto C level and increased the activities of caspase-3 and -9 [142]. In a related study on the same species by Ding et al., (2009), triterpene derivatives (**185-187**) displayed cytotoxicity against both MCF-7 and MDA-MB-231 with IC_{50} value of 0.7–16.5μg/mL and significant apoptosis for MCF-7 and MDA-MB-231 [83]. Compounds such as

eleutheroside E (**210**) and 1-*O*-caffeoyl-b-D-glucopyranoside (**211**) reported from ethanol extract of the aerial parts of *C. terniflora* DC showed significant cytotoxicity against human ECA-109 with IC_{50} values of 1.85 and 3.26 μM/mL, respectively [146].

2.4.1.5. Cytotoxicity of *Euphorbia* Species

Kim *et al*., (2018) reported diterpenoid glycosides such as kansuingol A (**235**) and kansuingol B (**236**) from the roots of *E. kansui* with inhibitory activities in the production of IL-6 with IC_{50} values of 2.96, and 1.94 μM, respectively [150]. Furthermore, kansuingol A (**235**) is reduced mRNA expressions of TNF-α and IL-6. From *E. helioscopia* jatrophane-derive diterpenoid, heliojatrones B has been isolated and showed significant P-glycoprotein inhibitory activity with IC_{50} value 12.03 ± 4.14 μM compared with the positive control (cyclosporine A) [149].

2.4.2. Antimicrobial Study

2.4.2.1. Antimicrobial Activity of *Vepris* Species

Acridone alkaloid such as verdoocridone A (**18**) reported from the methanol extracts of *V. verdoorniana* was found to be active against human photogenic microorganism strains *S. aureus*, and fungi *M. meihei* and *C. albicans* with MIC values between 21.3 and 29.4 μM compared to gentamycin with 0.2 μM and nystatin with 5.2 μM against both fungi strains [95]. Flindersiamine (**20**) isolated from *V. punctata* showed anti-bacterial activity against *S. aureas* and *S. faecials* [43]. Kiplimo and Koorbanally (2012) reported hesperetin (**27**) known flavonoid constituent with good antibacterial properties against *S. aureus* and *S. dysentrieae* at low molar concentration (MIC=0.2 and 4.0 μg/mL) [98]. On the other hand, glomeral (**28**) reported from *V. glomerata*, inhibited the growth of *S. aureus* and *S. dysentrieae* at low concentrations (MIC of 2 mg/mL and 0.4 mg/mL), respectively [99].

2.4.2.2. Antimicrobial Activity of *Zanthoxylum* Species

Benzophenanthridine alkaloids are potent antimicrobials of Rutaceae and attractive lead compounds for drug development. Chelerythrine (**55**), *N*-methyltetrahydrocolumbamine (**70**), *N*-methyltetrahydropalmatine (**71**), and berberine (**72**), alkaloids isolated from *Z. quinduense* exhibited promising antibacterial activity against different Gram-positive and Gram-negative bacteria, where chelerythrine (**55**) was observed to be the most active compound comparable to

kanamycine, tetracycline and anthracycline standard drugs [105, 106]. Ethanolic extracts of root bark of *Z. fagara*, *Z. elephantiasis* and *Z. martinicense* were evaluated against *C. albicans, S. cerevisiae*, *A. niger*, *A. flavus*, *M. canis,* and *T. mentagrophytes*. All of the extracts assayed showed activity against common dermatophytes of domestic animals, of which the activity exhibited by the ethanolic extract of the bark of *Z. fagara* is the prominent one [160]. The essential oils of *Z. xanthoxyloides* and *Z. leprieurii*, two Cameroonian plants used as spices in local food, showed antibacterial and antifungal activity against *E. coli*, *S. aureus*, *K. pneumoniae*, *E. faecalis*, *C. glutamicum*, *B. cereus*, *B. subtilis* and *A. flavus* [161].

2.4.2.3. Antimicrobial Activity of *Uvaria* Species

Antimicrobial activity of *Uvaria* species has been evaluated mainly using human pathogenic microorganisms. Uvarinol (**115**) reported from *U. chamae* showed significant antimicrobial activity against *S. aureus, B. subtil*is, and *M. smegmatis* [126]. Angoluvarin (**117**) which is dihydrochalcone reported from *U. angolensis* showed antimicrobial activity with MIC values of 0.78, 1.56, and 3.12 µg/mL against *B. subtilis*, *S. aureus*, and *M. smegmatis*, respectively [162]. The hexane and ethyl acetate extracts of both *U. narum* and *U. hookeri* showed significant antibacterial and antifungal activities [163]. A 1:1 mixture of stigmasterol (**151**) and β-sitosterol (**152**) obtained from the leaves extract of *U. scheffleri* also showed shown antifungal activity against *C. albicans* [41].

2.4.2.4. Antimicrobial Activity of *Clematis* Species

Aromatic compounds (Figure 13, **164-179**) obtained from *C. connata* displayed weak activities against *S. aureus*, methicillin-resistant *S. aureus* and β-lactamase positive *S. aureus* at the concentration of 50 µg/disk [137]. Triterpene derivative (**200**) isolated from *C. ganpiniana* showed weak antibacterial activity [83]. Antimicrobial activity of ethanolic extract *C. montana* leaves showed a greater inhibition zone against gram-positive bacteria than gram-negative bacteria. [164]. The methanol and petroleum ether extracts of *C.burgnesis* showed antibacterial and antifungal activity with the MIC values 0.78 mg/mL on bacteria and 3.125 mg/mL on fungi for methanol extract and 1.56 mg/mL on both fungi and bacteria for petroleum ether extract [85].

2.5. Biosynthesis of Acridones and Benthophenanthridines Alkaloids

The biosynthetic pathway of acridone alkaloids is given below based on the shikimate pathway as a precursor is an anthranilic acid (Scheme 1) [165].

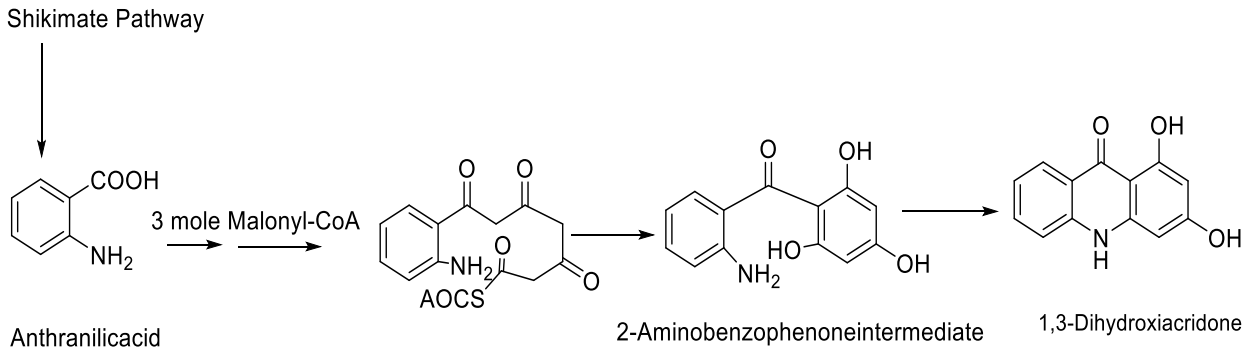

Scheme 1: Biosynthesis pathway of acridones alkaloids.

The biosynthetic pathway of benthophenanthridines alkaloids utilizes two units of L-tyrosine in which one tyrosine molecule is metabolized to dopamine that constitutes the isoquinoline part while the origin of the benzylic part is from tyramine that arises from decarboxylation of tyrosine [166]. The scheme below shows the biosynthesis of benthophenanthridines (Scheme2).

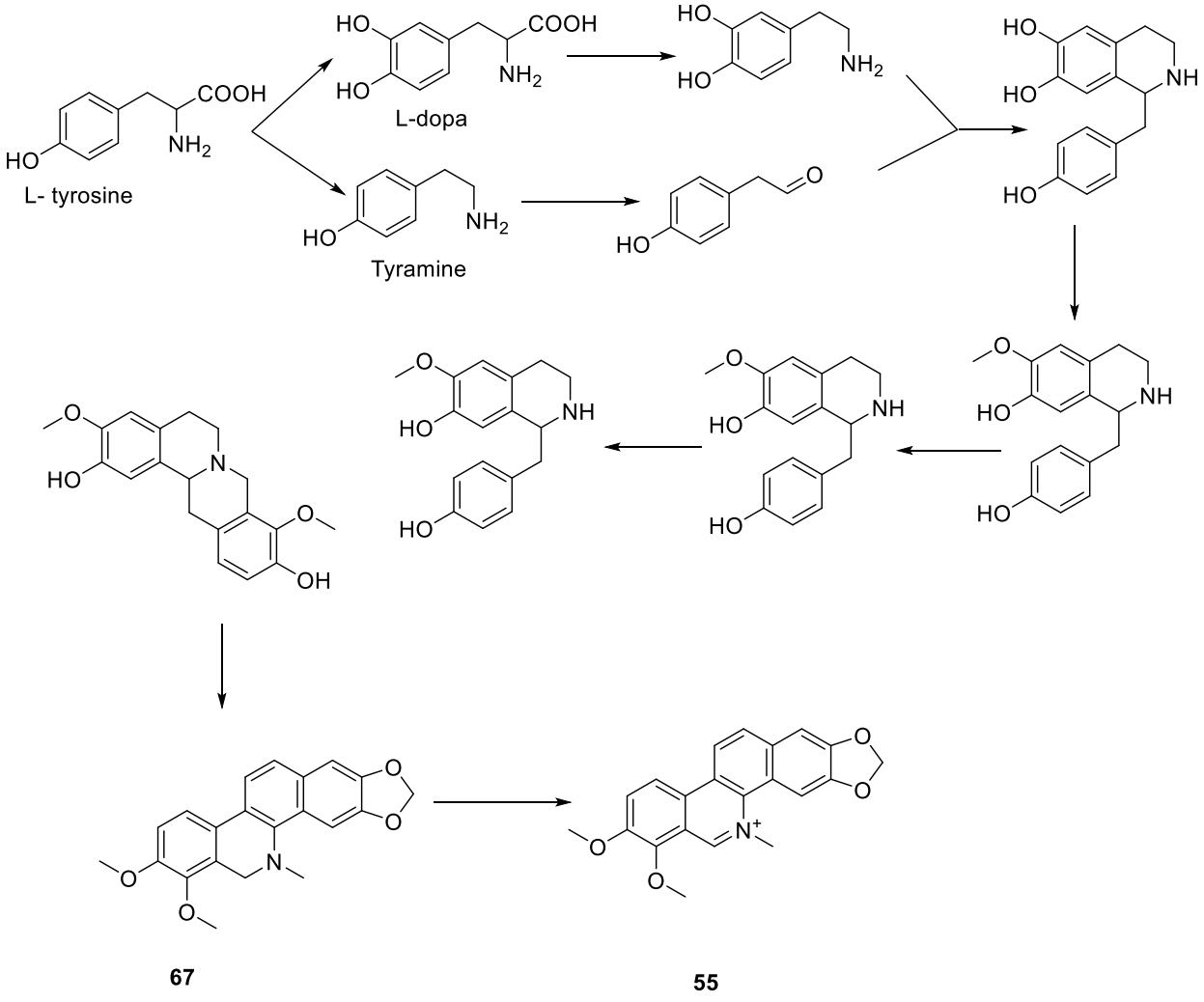

Scheme 2: Biosynthesis pathway of Benthophenanthridines alkaloids.

CHAPTER THREE

3. MATERIALS AND METHODS

3.1. General

The melting point was determined by a Cambridge microscopy instrument with a Reichart-Jung machine. IR spectrum was recorded by Cary 630 FTIR Spectrometer (USA). NMR spectral data were recorded on a Bruker Avance 300 MHz and Bruker DRX 500 MHz spectrometers. Mass spectra was recorded using VG Auto Spec Fisons spectrometer instrument (Fisons, Manchester, United Kingdom), and on a Shimadzu 8040 LC-MS/MS triple quadrupole with electrospray ionization (ESI) ion source (Shimadzu, Kyoto, Japan). Analytical TLC plates with silica gel 60 F_{254} TLC (Merck, Germany) were used to determine the TLC profile. The spots on TLC plates were visualized using a UV lamp (254 and 365 nm). Silica gel column chromatography was performed on silica gel (60-120 mesh). 96-well plates, CLARIOstar microplate reader, CytoFLEX Flow Cytometer, (ELISA reader, CLX800-BioRAD Instruments), light microscopy, incubator.

3.2. Chemical and Reagents

All chemicals, solvents, and reagents were analytical grade. The solvents were either Indian or France products.

3.3. Gas Chromatography-Mass Spectrometry

Gas Chromatography-Mass Spectrometry (GC-MS) analyses was carried out using GC (7890A, Agilent-Technologies, USA) coupled with MS (5977B, Network Agilent-Technologies). The GC with an HP-5MS column (30 m in length, 250 μm in diameter, 0.25 μm in film thickness) which was coated with 5 % phenyl and 95 % methylpolysiloxane as stationary phase. The carrier gas was helium flowing at a rate 1mL/min. The temperature of the injector was fixed at 230 °C and the injection mode with spilt mode with the ratio 10:1. The initial oven temperature 40 °C with 5 min hold time. It raised to 250 °C at 6 °C/min held at this temperature 20 min, the total run time was 6 min. The mass spectra were recorded in electron impact mode at 70 eV, with scanning from 40 to 500 m/z at 0.5 seconds. The mass spectrometer was equipped with a computer fed mass spectra data bank. The syringe was washed with 8 μL of chloroform, and then 2 μL of the

essential oil and fraction 12-15 of *E. schimperiana* extract solution in chloroform was injected through an auto sampler and analyzed with the HP-5MS column. The contents of phytochemicals present in the test samples were identified based on comparison of their retention time (min), peak area, and mass spectral patterns with those spectral database of authentic compounds stored in the National Institute of Standards and Technology (NIST) library.

3.4. Plant Collection, Identification and Preparation

Roots and fruits of *V. dainelli* and *Z. chalybeum* were collected from *Gofa* and Yirgalem, respectively. Roots of *U. scheffleri*, C. *burgensis* Eng l, and *E. schimperiana* were collected from Wolaita, Ethiopia, in November 2018. All plant species were identified by Botanist Mr. Shambel Alemu and the specimens deposited at the National Herbarium, Addis Ababa University, Ethiopia (Voucher codes: MAVd-003/11, MAZc-002/11, MAUs-001/11, MACb-004/11 and MAEs-005/11 respectively). The collected plant materials were air-dried and ground into a fine powder at room temperature.

3.4.1. Extraction and Isolation of *Vepris dainelli*

Acid-base extraction

Alkaloid constituents were selectively extracted with acid-base extraction approach as previously described by Satyajit *et al*., (2006) [167], with minor modification. Ground roots of *V. dainelli* (400 g) were extracted with CH_3OH (3 x 1.5 L) for 24 h at room temperature by maceration while shaking using electronic shaker at a speed of 230 rpm. The solution was filtered and concentrated using a vacuum rotary evaporator to yield 37 g (9.25 %) of a crude extract. The methanol extract was dissolved in chloroform (100 mL) and then extracted with aqueous H_2SO_4 5% to pH 3-4 (3 x 50 mL) in a separatory funnel to remove lipids acidic and neutral metabolites. The aqueous phases were combined and basified with NH_4OH 5 % to pH 11 and extracted with chloroform (3 x 100 mL). The chloroform phases were combined dried over anhydrous Na_2SO_4, filtered, and concentrated using a vacuum rotary evaporator to afford extract 1 (6.9 g, 1.72 %). Finally, the TLC profile of crude extract was checked and kept under refrigerator at 4 °C until further study.

Extraction by maceration

Friut powder of V. *dainelli* (400 g) were extracted with CH_3OH (3 x 1.5 L) for 24 h by maceration while shaking by electronic shaker at a speed of 230 rpm at room temperature. The solution was filtered and concentrated using a vacuum rotary evaporator to yield 41 g (10.3 %) brownish crude extract. The dichloromethane soluble portion of the methanol extract was separated and concentrated by a rotary evaporator to afford extract 2 (12.5 g, 3.125%). Finally, TLC profile of crude extract was checked and kept under refrigerator at 4 ℃ until further study.

Isolation of Compounds from *V. dainelli*

A 5 g portion of extract 1 was subjected to silica gel flash column chromatography (22 cm length and 2.5 cm diameter , 60 g silica gel) eluted with increasing gradient of methanol in dichloromethane while checking TLC profileA total of 21 fractions were collected (each 50 mL). Fraction 2 (eluted with 100 % dichloromethane) afforded compound (**244**) (6 mg) as colorless needles. Fraction 4 (eluted with 2 % methanol in dichloromethane afforded compound (**17**) (88 mg) as a yellow powder. Fractions 14-19 (eluted with 5-8 % methanol in dichloromethane were combined (147 mg) and further purified by silica gel column chromatography using ingredient solvent system of methanol (1-10 %) in dichloromethane. A total of 18 subfractions (each 50 mL) were collected. Subfraction 3-5 (eluted with 2-3 % methanol) afforded compound (**13**) (46 mg) as yellow powder.

Similarly, an 11 g portion of extract 2 was subjected to silica gel flash column chromatography (30 cm length and 3 cm diameter 80 g silica gel) and eluted with increasing the gradient of ethyl acetate in *n*-hexane. A total of 53 fractions (each 25 mL) were collected. Fraction 4, which was eluted with 5 % ethyl acetate in *n*-hexane, offered white amorphous crystalline (**246**) (18 mg). Fractions 20 - 24 (eluted with 20 % EtOAc in *n*-hexane) combined and rechromatographed by silica gel column eluted with increasing polarity ethyl acetate in *n*-hexane. A total of 32 subfractions (each 25 mL) were collected. Subfractions 10-16 (eluted with 15 % EtOAc in *n*-hexane) were combined and washed further with *n*-hexane to afford compound (**9**) (89 mg). Fractions 25-28 (eluted with 30 % EtOAc in *n*-hexane) were combined and washed with *n*-hexane

to offer compound (**245**) (60 mg). Fraction 28 (eluted with 50% of EtOAc) was afforded mixtures of compound (**25** and **51**) (12 mg).

3.4.2. Extraction and Isolation of *Zanthoxylum chalybeum*

Acid-base extraction

Root powder of *Z. chalybeum* (400 g) was extracted with 97 % ethanol (3 x 1.5 L) for 24 h at room temperature by maceration while shaking by electronic shaker at a speed of 230 rpm at room temperature. The solution was filtered and concentrated using a vacuum rotary evaporator to yield a crude extract. The crude extract was further dissolved in chloroform (100 mL) and then extracted with aqueous H_2SO_4 5% to pH 3-4 (3 x 50 mL) in a separatory funnel to remove lipids, acidic and neutral metabolites. The aqueous phases were combined and basified with NH_4OH 5% to pH 11 and extracted with chloroform (3 x 100 mL). The chloroform phases were combined, dehydrated with anhydrous Na_2SO_4, filtered, and concentrated using a rotary evaporator to afford an alkaloid extract of 8.9 g (2.23 %) (Extract 3). The test for alkaloids was performed by Dragondroff and Mayer's reagent. Finally, TLC profile of crude extract was checked and kept under refrigerator at 4 ^oC until further study.

Extraction by maceration

Root powder of *Z. chalybeum* (400 g) was extracted with DCM/MeOH (1:1) (3 x 1.5 L) for 24 h by maceration while shaking by electronic shaker at a speed of 230 rpm at room temperature. The solution was filtered and concentrated by a vacuum rotary evaporator at 40 ^0C to yielding the brown crude extracts (38.5 g, 9.6% (Extract 4). Finally, TLC profile of crude extract was checked and kept under refrigerator at 4 ℃ until further study.

Isolation of Compounds from *Zanthoxylum chalybeum*

Acid-base extract (5.6 g, extract 3) was subjected to silica gel flash column chromatography (22 cm length and 2.5 cm diameter, 60 g silica gel) eluting with gradient methanol in dichloromethane while checking TLC profile. A total of 22 fractions (each 50 mL) were collected. Fractions 3-5 (100% DCM as eluent) afforded compound **55** (60 mg) as pale yellow powder. Fractions 7-10 were combined (146 mg) and purified by silica gel column

chromatography (2-5 % MeOH in DCM as eluent) to afforded compound **62** (7.4 mg) as a pale yellow powder. Similarly, fractions 13-16 (122 mg) were combined and purified by silica gel column chromatography (1-12 % MeOH in DCM as eluent) to give compound **247** (11.7 mg).

Extract 4 (30 g) was subjected to silica gel flash column chromatography (35 cm length and 3 cm diameter, 120 g silica gel) and eluted with an increasing gradient of ethyl acetate in *n*-hexane while checking TLC profile. A total of 68 fractions (each 50 mL) were collected. Fractions 8-10 (15 % EtOAc in *n*-hexane as eluent) afforded compound **67** (81 mg).

3.4.3. Extraction and Isolation of *U. scheffleri*

In the same way, grounded roots of *U. scheffleri* (500 g) were extracted with (3 x 2.5 L) of dichloromethane for 24 h by maceration while shaking by an electronic shaker at a speed of 230 rpm at room temperature. The solution was filtered and concentrated using a vacuum rotary evaporator to yield 32 g (8%) brownish crude extract (Extract 5). Finally, the TLC profile of crude extract was checked and kept under refrigerator at 4 ℃ until further study.

Isolation of Compounds from *U. scheffleri*

The dried root extract of *U. scheffleri* (30 g, extract 5) was subjected to silica gel flash column chromatography (35 cm length and 3 cm diameter , 120 g silica gel) eluted with an increasing gradient of ethyl acetate in *n*-hexane. A total of 75 fractions were collected (each 50 mL). Fraction 17 (eluted with 35% ethyl acetate) afforded compound **248** (18 mg) as pale gray needles. Fraction 20 (eluted with 45% ethyl acetate in *n*-hexane) afforded compound **249** (12 mg) as a yellow powder. Fraction 22-25 (eluted with 50% ethyl acetate in *n*-hexane) were combined and subjected to silica gel column chromatography by eluting an increasing gradient of ethyl acetate in n-hexane. A total of 18 subfractions (50 mL each) were collected. Subfraction 10 (eluted with 25% ethyl acetate) afforded compound **112** (11.7mg).

3.4.4. Extraction and Isolation of *Clematis burgensis*

Roots powder of *C. burgensis* (800 g) were extracted with DCM/MeOH (1:1) (3 x 3 L) for 24 h by maceration while shaking by electronic shaker at a speed of 230 rpm at room temperature,

respectively. The solution was filtrated and concentrated by a vacuum rotary evaporator at 40 ℃ to afford brown crude extract 32.30 g (4.04 %) (Extract 6). Finally, the TLC profile of crude extract was checked and kept under refrigerator at 4 ℃ until further study.

Isolation of Compounds from *Clematis burgensis*

The dried roots extract of *C. burgensis* (28 g, extract 6) was subjected to silica gel column chromatography (30 cm length and 3 cm diameter, 120 g silica gel) eluted with an increasing gradient of ethyl acetate in petroleum ether, followed by increasing gradient methanol in dichloromethane. A total of 104 fractions (50 mL each) were collected. Fraction 5, eluted with 5 % ethyl acetate, afforded white amorphous powder compound **251** (11 mg). Fraction 20 and 21 eluted with 85 % ethyl acetate afford compound **250** (40 mg). Fraction 22-30 combined and further purified by silica gel column chromatography using increasing gradient of ethyl acetate in petroleum ether as eluent, totally 22 fractions (25 mL each) were collected. Subfraction 10, eluted with 25 % ethylacetate in petroleum ether afford compound **98** (45 mg) as a white powder.

3.4.5. Extraction and Isolation of *E. schimperiana*

Grounded roots of *E. schimperiana* (400 g) were extracted with 1.5 L of dichloromethane for 24 h by maceration while shaking by electronic shaker at speed of 230 rpm at room temperature. The solution was filtered and concentrated using a vacuum rotary evaporator to yield brownish crude extract 22 g (5.5 %) (Extract 7). Finally, the TLC profile of crude extract was checked and kept under refrigerator at 4 ℃ until further study.

Isolation compounds from *Euphorbia schimperiana*

The dried root extract of *E. schimperiana* (20 g, extract 7) was subjected to silica gel flash column chromatography (28 cm length and 3 cm diameter , 100 g silica gel)eluted with increasing gradient of ethyl acetate in *n*-hexane, then increasing gradient of methanol. A total of 62 fractions were collected (each 25 mL). Fraction 9 (eluted with 15% ethyl acetate) afforded compound (**252)** (12 mg) as yellowish amorphous powder. Fraction 42 eluted with 100 methanol offered compound **254**

(30mg). Fraction 12 - 15 (eluted with 30 and 35% ethyl acetate) were combined and subjected to GC/MS. Totally 8 compounds (**255**-**262**) were identified by GC/MS analysis.

3.4.6. Extraction of Essential oils

Powdered fruit parts of *V. dainelli* and *Z. chalybeum* and root parts of *U. sheffleri* (400g each) were separately soaked in 5L distilled water placed in a round bottom flask and subjected to hydrodistillation using a Clevenger apparatus for five hours. The condensate (mixture of essential oil and water) was collected in a 100 mL separator funnel. The essential oils were separated from the aqueous layer using a separatory funnel and dried by adding anhydrous magnesium sulphate ($MgSO_4$). Finally, purified essential oils were transferred into small vials and refrigerated (4 ^oC) until further analysis.

3.5. Biological Activity Study

3.5.1. Cytotoxicity Study

Cell lines and culture conditions

The MCF-7 and MDA-MB-231 cell lines were cultured in DMEM/F12 (Gibco, USA) with 10% (v/v) fetal bovine serum (FBS) (HyClone, USA). The cell lines were incubated at 37 °C in a 5% CO_2 atmosphere. Alkaloids were dissolved in DMSO (Sigma, USA) to prepare a stock solution at a concentration of 10 mM and stored in −20 °C before use. Then, the required amount of solution is added to the complete culture medium (DMEM/F12, 10% FBS) under sterile conditions to obtain freshly prepared solutions of the drugs at the desired concentrations.

3.5.2. Cell Viability Assay

The cells in complete medium (50 μL) were seeded into 96-well plates at a concentration of 5,000 cells per well and allowed to attach to the plate for 18 h. The cells were incubated with complete culture medium alone, containing 0.01-1.5% of DMSO (vehicle), or with solutions of the compounds at the desired concentrations (200-0.195 μg/mL by half-fold dilutions) for a further 72 h. Then, 10 μL of a freshly prepared mixture of 3-(4, 5-dimethylthiazol-2-yl)-5-(3-carboxymethoxyphenyl)-2-(4-sulfophenyl)-2H-tetrazolium (MTS) solution in Dulbecco's phosphate buffered saline medium (DPBS) (2 mg/mL) and phenazine methosulfate (PMS) as a

redox intermediary at 20:1 (v/v, PMS/ MTS ratio) was added to each well. The plates were incubated for an additional 2-3 h at 37ºC. Untreated cells were used as a negative control, and doxorubicin was taken as a positive control. The absorbance was measured at 490 nm in a CLARIOstar microplate reader. The cytotoxic activity of compounds was tested in both MCF-7 and MDA-MB-231 cells after 72 h by MTS assay [168]. The result was expressed as IC_{50} values (the compound concentration inhibiting the cell growth by 50%).

3.5.3. Cell Cycle Assay

Both cell lines were seeded in complete medium (600 µL) into 24-well plates at a concentration of 30,000 cells per well. After 18 h, the cells were treated with the compounds at the IC_{50} value for 72h. Then, the medium was removed, and the cells were washed with PBS and detached from the plate with trypsin. The cell suspension was centrifuged at 400 g for 5 minutes and the cell pellet was resuspended with 200 µL of hypotonic solution of propidium iodide (1mg/mL trisodium phosphate, 0.1% Triton X-100 (v/v), 5 µg/mL), 100 µg/mL RNasa) and incubated at 4ºC for 24 hours. Then, the DNA content of the cells was measured by flow cytometry (CytoFLEX Beckman-Coulter).

3.5.4. Antimicrobial Activity Assay

Microorganism strain

In vitro antimicrobial activity of isolated compounds (**13**, **17**, **55**, **67**, **98**, **245**, **248**, **249** and **252**) were evaluated against *Staphylococcus aureus* (CECT-59) and *Escherichia coli* (CECT- 434) whereas antifungal activity was examined only against *Candida albicans* (ATCC- 26555) strains.

Antimicrobial activity assay

The assays of compounds were determined by the broth dilution technique as previously described [169]. A microdilution method in 96-well plates, using Mueller-Hinton broth media, was performed to determine minimum inhibitory concentrations. Isolated compounds were dissolved in DMSO (Sigma, USA) to prepare stock solutions at a concentration of 100 µg/mL. Further half-fold serial dilutions were performed by the addition of culture broth to reach concentrations ranging from 100 to 1.56 µg/mL were distributed in 96-well plates and a sterility/negative control and growth control (containing culture broth plus DMSO, without

antimicrobial substance). Each test and growth control well was inoculated with 10 µL of a bacterial suspension giving a concentration of 10^5 CFU/mL in bacteria and 10^4 CFU/ml in the case of *C. albicans*. The medium without strain was used as a negative control, gentamicin, and fluconazole for bacterial and fungal strain as a positive control, respectively. All experiments were performed in triplicate, and the microdilution trays were incubated at 37 ºC for bacterial strains, at 28 ºC fungal strain for 24h. The microbial growth was detected by optical density measurement at 595 *nm* (ELISA reader, CLX800-BioRAD Instruments). MIC values were defined as the lowest concentration of each compounds, which completely inhibited microbial growth. The results were expressed in micrograms per milliliter [169].

3.5.5. *In vitro* larvicidal Activity of Essential Oils

In order to evaluate the *in vitro* larvicidal activity of the essential oils, *Anisakis* larvae were collected by dissecting specimens of the blue whiting (*Micromesis tiuspoutassou*), a much-consumed fish and frequently parasitized by nematodes of the genus *Anisakis* [170]. Fish specimens were bought 1 h before at a local market in Burjassot (València, Spain). The *in vitro* larvicidal activity analyses of the essential oils were carried out at the Faculty of Pharmacy, University of Valencia, Spain.

All larvae were collected alive from the viscera of the dissected fish, were morphologically identified as L_3 larvae of *Anisakis* type I. The worms were washed several times on a sterile solution of 0.9% NaCl and identified under a light microscope according to morphological features. Only those actively moving helminths, and without any injury, were placed in plastic Petri dishes with different concentrations of the test essential oils and then kept at room temperature.

The marinade solution usually used to marinate raw fish for consumption was prepared [28], consisting of water/vinegar at a 1:1 ratio, 3% NaCl, and 1% citric acid. Then, the obtained solutions were spiked with decreasing concentrations of essential oils: 5%, 1%, 0.5%, and 0.1%. Four larvae were placed on each plate. As control, larvae were assayed without test compounds under identical experimental conditions in the marinade solution. All experiments were carried out in duplicate, using a total of 104 larvae, 96 tested with essential oils, and 8 as controls.

Larvae were examined under a stereoscopic microscope at hourly intervals of 1 to 7 h and at 12 h and 24 h to test the anthelmintic effect of the essential oils. During the experimental treatments, at each fixed time interval, the viability was checked [27], assessing the subsequent score: 3 (viable), 2 (reduction of mobility), 1 (mobility only after stimulation), and 0 (death). Larvae were considered dead when no mobility was observed in saline solution (0.9% NaCl) under the stereoscopic microscope. The normalized mean viability was according to previously described by Giarratana *et al*., (2017) [171]. LT_{100} (lethal time required to kill 100% of nematodes) and LT_{50} (lethal time needed to kill 50% of nematodes) were calculated. For the *in vitro* larvicidal activity measurements, the results are presented as mean percentages of three independent experiments.

3.5.6. Cytotoxicity of Essential Oils by MTT Assay

Cell lines

In order to investigate the cytotoxic effect of essential oils, VERO cells (a normal cell line from kidney of monkey) were used. The VERO cells were obtained from the national animal health diagnostic and investigation center (NAHIDIC), Sebata, Ethiopia. Vero cells were maintained in RPMI-1640 medium supplemented with 10% FBS, glutamine (2 raM), penicillin (100 units/mL) and streptomycin (100 µg/mL). The cells were cultured at 37 °C in a humidified 5% CO_2 incubator.

MTT assay

In vitro cytotoxicity activity of essential oils was tested by using MTT assay as previously discussed by Kavitha *et al* (2017) [172]. In MTT cytotoxicity assay, the MTT reduction rate is an indicator of the functional integrity of the mitochondria and, hence, of cellular viability. The VERO cell line was seeded in a 96-well flat-bottom microtiter plate at a density of 2×10^4 cells/well and allowed to adhere for 24 hours at 37°C in a CO_2 incubator. After 24 hours of incubation, the culture medium was replaced with a fresh medium. Cells were then treated with the concentration of essential oils (100 to 0.78 half-fold serial dilution) for 24 hours at 37°C in a CO_2 incubator. After 24 hours of incubation, the culture medium was replaced with a fresh

medium. Then, subsequently, 10µL of MTT working solution (5 mg/mL in phosphate buffer solution) was added to each well, and the plate was incubated for 4 hours at 37°C in a CO_2 incubator. The medium was then aspirated, and the formed formazan crystals were solubilized by adding 50 µL of 5% DMSO per well for 30 min at 37°C in a CO_2 incubator. Finally, the dissolved formazan crystals (purple color) were quantified using the ELISA plate reader at 490 and 630nm, and the cell viability was expressed as the percent cytotoxicity (% cytotoxicity). The results were expressed as a mean of triplicate.

The calculation of % cytotoxicity follows the equation:

$$\%\ \text{cytotoxicity} = \left[\frac{Absorbance\ of\ treated}{absorbance\ of\ \ control}\right] x\ 100$$

The half maximal inhibitory concentration (IC_{50}) values were determined from a dose-response curve of the percentage of cell viability (Y-axis) versus log EOs concentration (µg/mL) (x-axis) by using GraphPad Prism Version 8.0.

3.6. Computational Study

3.6.1. Ligand Preparation

The chemical structures of the isolated compounds (**9**, **13**, **17**, **55**, **62**, **67**, **98**, **244**, **245**, **247**, **248-250,** and **252**) were drawn using the ChemOffice tool (Chem Draw 16.0) assigned with proper 2D orientation, and the energy of each molecule was minimized using ChemBio3D. Then the energy minimized ligand molecules were used as input for AutoDock Vina in order to carry out the docking simulation.

3.6.2. Protein Preparation

The crystal structure of receptor molecule *E. coli* DNA gyrase B (PDB ID: 6F86) and Human Topoisomerase II α (PDB ID: 3QX3) were downloaded from the protein data bank. The protein preparation was done using the reported standard protocol [173, 174], by removing the co-crystallized ligand, selected water molecules, and cofactors, the target protein file was prepared by leaving the associated residue with protein by using auto preparation of target protein file Auto Dock 4.2 (MGL tools 1.5.7).

3.6.3. Molecular Docking

The graphical user interface program was used to set the grid box for docking simulations. The grid was developed so that it surrounds the region of interest in the macromolecule. The docking algorithm provided with AutoDock Vina was used to search for the best-docked conformation between ligand and protein. AutoDock Vina with the standard protocol was used to dock the proteins (PDB ID: 6F86 and 3QX3) and isolated compounds into the active site of proteins [175]. During the docking process, a maximum of nine conformers were obtained for each ligand. The conformations with the most favorable (least) free binding energy were selected for analyzing the interactions between the target receptor and ligands by the discovery studio visualizer and PyMOL. The ligands are represented in a different color, H-bonds, and the interacting residues are represented in ball and stick model representation.

3.6.4. *In silico* Drug-likeness and Toxicity Predictions

Drug-likeness properties of isolated compounds (**9, 13, 17, 55, 62, 67, 98, 244, 245, 247, 248-250,** and **252**) were predicted based on an already established concept by Lipinski *et al* (1997) [176]. The structures of isolated compounds were converted to their canonical simplified molecular-input line-entry system (SMILE). Then submitted to SwissADME and PreADMET tool to estimate *in-silico* pharmacokinetic parameters such as the number of hydrogen donors, hydrogen acceptors, and rotatable bonds, and total polar surface area of a compound. The isolated compounds' organ toxicities and toxicological endpoints were predicted using PreADMET and OSIRIS Property [177]. The selection of compounds as drug candidates were determined by a parameter called drug score. The higher the drug score value, the higher the compound's chance of being considered a drug candidate [178].

3.6.5. Quantum Computational Studies

Density functional theory (DFT) is emerging as a very powerful technique to study biomolecular systems to know the reaction coordinates and the transition state of a reaction is fundamental for developing mechanism-based inhibitors that usually mimic the transition state [176]. In the present study, the DFT analysis of isolated compounds (**9, 13, 17, 55, 62, 67, 98, 244, 245, 247, 248-250,** and **252**) was performed using Gaussian 09 and visualized through Gauss view 6.0. The structural coordinates were optimized using B3LYP/6-31 G (d,p) level basis set without any

symmetrical constraints. The molecular electrostatic potential map and energies of the compounds were obtained from the optimized geometry. Koopman's approximation was used to estimate the highest occupied molecular orbital (HOMO), lowest unoccupied molecular orbital (LUMO), energy gap, and related reactive parameters (electronegativity, chemical potential, hardness, softness, electrophilicity) [179].

3.7. Statistical Analysis

The IC_{50} values of the compound and essential oils concentrations inhibiting the cell growth by 50% were determined from each dose-response curve by GraphPad Prism version 9 software (San Diego, CA. USA).

CHAPTER FOUR

4. RESULTS AND DISCUSSION

4.1. Phytochemical Analysis

From five selected medicinal plants species, a total of 26 compounds were isolated and fully characterized using IR, ^{1}H NMR, ^{13}C NMR, DEPT-135, 2D NMR (HSQC, COSY, and HMBC), HRMS, ESI-MS, and GC/ MS techniques, and comparing with the literature data. The detailed characterizations of these compounds are presented below.

4.1.1. Secondary Metabolites Isolated from *V. dainelli*

The roots and fruits extracts of *V. dainelli* after silica gel column chromatography gave eight compounds (**9**, **13**, **17**, **25**, **51**, **244**, **245**, and **246**) reported herein for the first time from the species, except compounds (**13, 25** and **51)**.

4.1.1.1. Acridone Alkaloids (13, 17 and 244)

Compound **244** was isolated as colorless needles, and a melting point is 203-206 ^{o}C. The ESI-MS showed the molecular ion peak m/z = 269. The ^{1}H NMR (Table 1, Appendix 1A) showed a singlet at δ 14.87 attributed to the hydroxyl group with peri effect to the carbonyl group. A downfield chemical shift value of aromatic proton at δ 8.49 (*dd*, *J* = 8.1, 1.7 Hz, 1H, H-8) agrees with the anisotropic effect of carbonyl at C-9. Four aromatic protons were observed at δ 7.73 (*dd*, *J*= 8.1, 1.7 Hz, 1H, H-7), 7.53 (*dd*, *J* = 8.7, 1.2 Hz, 1H, H-5), and 7.33 (*d*, *J* = 8.7, 1.2 Hz, 1H, H-6) and δ 6.50 (s, 1H, H-4). A singlet peak at δ 6.09 (s, 2H) is a characteristic of methylenedioxy group, supported by DEPT-135 (Appendix 1C) pointing down. A singlet peak at δ 3.86 (*s*, 3H) belongs to methyl attached to nitrogen.

Its ^{13}C NMR (Table 1, Appendix 1B) displayed seven quaternary carbons at δ 155.3 (C- 1), 145.4 (C-2), 141.8 (C- 3), 127.5 (C-4a), 141.0 (C -5a), 122.6 (C-8a) and 107.1 (C-9a), one carbonyl carbon at *δ* 181.0 (C-9), five methines at δ 85.4 (C-4), 114.6 (C-5), 133.6 (C-6), 121.6 (C-7), and 126.6 (C-8), methylenedioxy signals at δ 101.1 and methyl attached to nitrogen at δ 34.4. All assignments were supported by HSQC experiments (Appendix 1D). The above spectral features are in good agreement with acridone skeleton, and comparison with the ^{13}C spectra and ion peak in mass spectra of the literature [180, 181], compound **244** is identical to

norevoxanthine (**244,** Figure 16) previously reported from *Teclea grandifolia* [48], but report herein for the first time from *Vepris* species.

Table 1: ^{1}H NMR (300 MHz) and ^{13}C NMR (75 MHz), chemical shifts (ppm) in $CDCl_3$ of compound (**244**) and ^{13}C NMR (75 MHz) in $CDCl_3$ of [66].

No	**244**		**[66]**
	δ_H (in ppm), (*J* in Hz)	δ_C (in ppm)	δ_C (in ppm)
1	-	155.3	153.4
2	-	145.4	143.0
3	-	141.8	142.6
4	δ 6.50 (s)	86.4	89.7
4a	-	127.5	127.5
5	7.53 (*dd*, *J* = 8.7, 1.2)	114.6	114.1
5a	-	141.0	142.2
6	7.33 (dd, *J* =8.7, 1.2)	133.6	132.5
7	7.73 (d, *J* = 8.1, 1.7)	121.7	122.5
8	8.49 (d, *J* = 8.1, 1.7)	126.6	121.2
8a	-	122.6	123.8
9	-	180.0	176.7
9a	-	107.1	106.6
-OCH_2O	6.09 (s)	101.1	101.9
-OCH_3	-	-	60.9
-NCH_3	3.86 (s)	34.4	35.1
-O<u>H</u>	14.8	-	

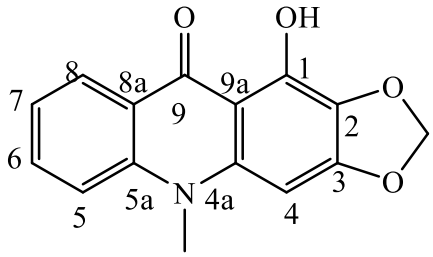

244

Figure 16: Norevoxanthine isolated from root extract of *V. dainelli*.

Compound **17** was obtained as yellow powder, and its melting point is 217-218℃. The ESI-MS [M]+ showed the molecular ion peak m/z = 283. The ^{1}H NMR (300 MHz, Chloroform-*d*/MeOD) (Table 2, Appendix 2A) displayed a one-proton signal at *δ* 6.64 (s,1H) was assigned to H-4, and three-proton signals at *δ* 7.59 (*m*, 1H), 7.38 (*d*, *J* = 8.7 Hz, 1H), and 7.20 (m,1H) corresponding to H-5, 6 and 7; and H-8 being deshielded by the carbonyl group, gives rise to a broadened doublet of doublet centered at δ 8.36 (*dd*, *J* = 8.1, 1.7 Hz, 1H). Two signals at *δ* 4.07 (*s*, 3H), 3.74 (*s*, 3H) were assigned to methoxyl and methylimino protons respectively.

The ^{13}C (300 MHz, Chloroform-*d*/MeOD) (Table 2, Appendix 2B) spectrum analyzed with the aid of DEPT-135, shown seven quaternary carbons including one carbonyl carbon at δ 177.1, 153.9, 142.9 142.2 141.1, 126.7and 123.0 are well resolved. And five methine carbon signals were observed at δ 89.3, 110.9, 114.2, 121.1, and 132.0. One methylenedioxy carbon signal was observed at δ 101.9 supported by Dept-135 pointed downward. And two signals at δ 34.8 and 60.1 corresponding to methyl group attached to nitrogen and methoxy respectively. Based on the spectroscopic evidence and comparison with the literature [63], compound (**17**) is identical to evoxanthine (**17**, Figure 17) previously isolated from *Vepris lecomteana* [182] but reported herein for the first time from this species.

Table 2: ^{1}H NMR (300 MHz) and ^{13}C NMR (75 MHz), chemical shifts (ppm) in $CDCl_3$/MeOD of compound (**17**) and ^{13}C NMR (75 MHz) in $CDCl_3$ [66].

No	**17**		[66]
	δ_H (in ppm), (*J* in Hz)	δ_C (in ppm)	δ_C (in ppm)
1	-	153.9	153.4
2	-	142.9	143.0
3	-	142.2	142.6
4	δ 6.64 (*s*)	89.3	89.7
4a	-	132.8	127.5
5	7.59 (*m*)	114.2	114.1
5a	-	141.1	142.2
6	7.38 (*d*, *J* = 8.7)	132.0	132.5
7	7.20 (*m*, 1H)	121.1	122.5
8	8.36 (*dd*, *J* = 8.1, 1.7)	126.7	121.2
8a	-	123.0	123.8
9	-	177.1	176.7
9a	-	110.9	106.6
$-OCH_2O$	5.98 (*s*)	101.9	101.9
$-OCH_3$	4.07 (*s*, 3H)	60.1	60.9
$-NCH_3$	3.74(*s*)	34.8	35.1

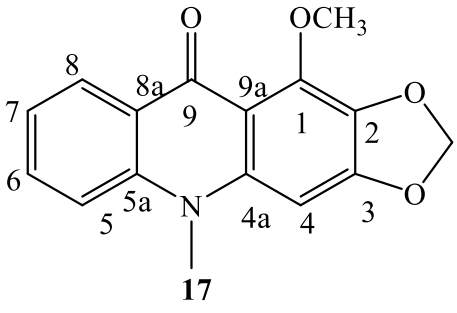

17

Figure 17: Evoxanthine isolated from root extract of *V. dainelli*.

Compound **13** was obtained as yellow powder with a melting point is 175-176 ℃. The ESI-MS showed the molecular ion peak m/z = 283. The ^{1}H NMR (300 MHz, Chloroform-*d*) (Table 3, Appendix 3A) spectrum showed downfield resonance signal at *δ* 14.75 (*s*, 1-OH), which disappeared on exchange with deuterium oxide, confirming C1-OH, showed peri effect to the carbonyl group. Aromatic protons at *δ* 7.71 (1H, *t*, *J* = 8.2 Hz, H-6), 7.51 (1H, *d*, *J* = 8.6 Hz, H-5), and 7.28 (1H, *t*, *J* = 8.0 Hz, H-7), which indicate that the ring A is unsubstituted, and C8-H, being deshielded by the carbonyl group, resonated as a broadened doublet of doublet centered at *δ* 8.44 (1H, *d*, *J* = 8.3 Hz, H-8) is characteristic of the C-8 proton in acridones. And one aromatic proton at *δ* 6.50 (1H, *s*, H-4). Three signals at *δ* 3.83 (*s*, 3H), 3.93 (s, 3H) and 4.02 (*s*, 3H) were assigned to methylimino, and two methoxyl protons respectively is in consistency of arborine [44].

^{13}C NMR (75 MHz, Chloroform-*d*) (Table 3, Appendix 3B) spectrum showed seven quaternary carbons at δ 159.3, 143.2, 142.8, 139.1, 130.1, 122.5, and 120.7 and one carbonyl carbon at δ 180.8. And five methine carbon signals were observed at δ 86.6, 114.2, 121.5, 126.6, and 133.6 in the aromatic system. Also three signals at δ 34.4, 55.4 and 60.8 corresponding to methyl group attached with heteroatom nitrogen and two methoxy respectively. Based on the above spectroscopic evidence and comparison with the literature [44, 66], compound **(13)**, is identical with arborinine (**13,** Figure 18) previously reported from the leaves of this plant [44]. However, herein reported for the first time from the roots of *V. dainelli.*

Table 3: ^{1}H NMR (300MHz) and ^{13}C NMR (75 MHz), chemical shifts (ppm) in $CDCl_3$/MeOD of compound (**13**) and ^{13}C NMR (75 MHz) in $CDCl_3$ [63].

No	**13**		[66]
	δ_H (in ppm), (*J* in Hz)	δ_C (in ppm)	δ_C (in ppm)
1		159.3	153.4
2		143.2	143.0
3		142.8	142.6
4	6.50 (1H, *s*)	86.6	89.7
4a	-	130.6	127.5

5	7.51 (1H, *d*, *J*=8.0)	114.2	114.1
5a	-	139.1	142.2
6	7.28 (1H, *t*, *J* = 8.0)	133.6	132.5
7	7.71 (1H, *t*, *J* = 8.2)	121.5	122.5
8	8.44 (1H, *dd*, *J* = 8.2, 1.7)	126.6	121.2
8a	-	120.7	123.8
9	-	180.8	176.7
9a	-	109.5	106.6
-OCH_2O	-	-	101.9
-OCH_3	4.02 (*s*, 3H)	60.8	60.9
-OCH_3	3.93 (*s*, 3H)	55.4	
-NCH_3	3.83 (*s*, 3H)	34.4	35.1
-O<u>H</u>	14.75		

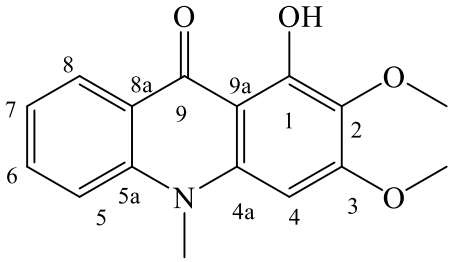

13

Figure 18: Arbronine isolated from root extract of *V. dainelli*.

4.1.1.2. Compound 245

Compound **245** was obtained as a white powder with a melting point value is 278-279 ℃. The ESI-MS showed the molecular ion peak m/z = 303. Its ^{1}H NMR (300 MHz, DMSO-d_6) (Table 4, Appendix 4A) showed signal at δ 11.07 (*s*, 1H) assigned for N-H, eight methine aromatic protons at δ 7.81 (*d*, *J* = 7.8 Hz, 1H, H-4), 7.49 (*m*, 2H, H-2,3), 7.37 (*d*, *J* = 8.1 Hz, 1H, H-1), 7.04 (*m*, 4H, H-9-12), and one sp^3 methine at δ 6.14 (*s*, 1H, H-14). The presence of methylene protons bonded to sp^2 quaternary carbon and hetroatom are observed at δ 2.72-2.85 (*m*, 2H, H-7), δ 4.62 (*dd*, *J* = 12.8, 1.6 Hz, 1H, H-7) and δ 3.25 (*m*, 1H, H-8). A singlet signal at δ 2.88 (3H, *s*)

belongs to methyl attached to nitrogen. Its ^{13}C NMR (100 MHz, DMSO-d_6) (Table 4, Appendix 4B) showed one carbonyl carbon at δ 164.7 (C-5), six sp^2 quaternary carbons at δ 149.8 (C-1a), 136.3 (C-12a), 127.8 (C-13a), 125.2 (C-4a), 111.9 (C-9a), and 110.8 (C-8a). Eight sp^2 methines at δ 136.3 (C-2), 127.2, (C-3) 121.8 (C-4), 121.6 (C-9), 122.4 (C-10), 120.4 (C-11), 118.7 (C-1) and 117.8 (C-12), one sp^3 methine at δ 68.7 (C-14), methyl group attached with nitrogen at δ 35.6. Two methylene signals at δ 39.2 (C-7), and 19.7 (C-8), supported by DEPT-135 (Appendix 4C). HSQC experiment (Appendix 4D) was showed a ^1J correlation between H-4 (7.81) → C-4 (121.8), H-2, 3 (7.49) → C-2, 3 (136.3, 127.2), H-1 (7.37) → C-1(118.7), H-9, 10,11,12 (7.04) → C-9,10,11,12 (1219, 122.4, 120.4, and 117.8 respectively), H-14 (6.14) → C-14(68.7), H-7 (2.72-2.85) → C-7 (39.2), H-8 (4.62 and 3.25) →C-8 (19.7) and N-C$\underline{H}_3$ (2.88) → N$\underline{C}H_3$ (35.6). The HMBC correlation showed the methyl group δ 35.6 directly correlated ^3J with C-1a (δ 149.8) and C-14 (δ 68.7) and the methylene protons at H-7 and H-8 showed ^3J and ^1J correlations with C-14 (δ 68.7) and C-8a (δ110.8) (Figure 20, Appendix 4G). Thus, based on the above spectral data, compound (**245**) was found to be identical with evodiamine (Figure 19, **245**) previously isolated from *Evodia rufaecarpa* Bentham [183] and *Z. budrunga* [184], but reported herein for the first time from *Vepris* species.

Table 4: ^1H (300 MHz) and ^{13}C NMR (75 MHz), chemical shifts (ppm) in DMSO-d_6 of evodiamine (**245**).

No	**(245)**		**[184]**	
	δ_H (in ppm), (*J* in Hz)	δ_C (in ppm)	δ_H (in ppm), (*J* in Hz)	δ_C (in ppm)
1	7.37 (1H, *d*, *J* = 8.1)	118.7	6.92-7.82 (8, *m*, Ar-H)	119.7
1a	-	149.8	-	150.1
2	7.81 (1H, *d*, *J* = 7.8)	136.3		133.4
3	7.49 (2H = *m*)	127.2		127.1
4		121.8		122.6
4a	-	125.2	-	129.2
5	-	164.7	-	164.9
7	4.64 (*dd*, *J* = 12.8, 1.6, 1H),	39.2	2.85 (*m*, 2H)	40.6

	3.25 (*m*, 1H)			
8	2.72-2.85 (*m*, 2H)	19.7	4.64 (*m*, 1H), 3.20 (*m*, 1H)	20.4
8a	-	110.8	-	112.2
9	7.04 (4H, *m*)	121.6	6.92-7.82 (8, *m*, Ar-H)	122.8
9a	-	111.9	-	112.8
10	7.04 (4H, *m*)	122.4	6.92-7.82 (8, *m*, Ar-H)	122.9
11		120.4		119.2
12		117.8.		117.9
12a	-	136.3		138.1
13a		127.8		130.2
-	11.7 (*s*, N-H)		-	-
14	6.14 (1H, *s*)	68.7	5.98 (*s*)	69.9
NCH_3	2.88 (3H, *s*)	35.6	2.88(*s*)	36.8

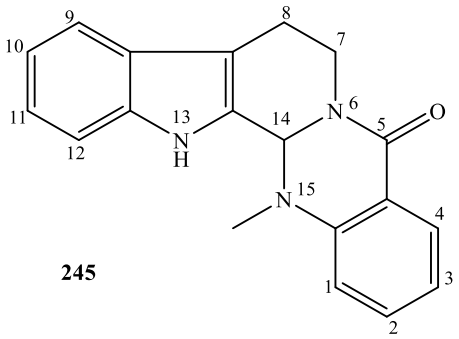

245

Figure 19: Evodiamine (**245**) isolated from fruit extract of *V. dainelli*.

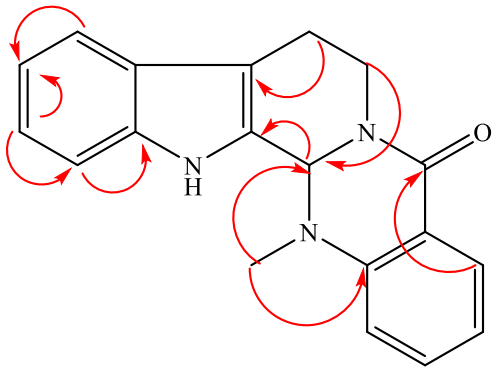

Figure 20: Important HMBC correlations of evodiamine (**245**)

4.1.1.3. Compound 9

Compound **9** was obtained as pale grey crystals with a melting point of 175-176 ℃. The ESI-MS showed the molecular ion peak m/z = 325. Its ^{1}H NMR (300 MHz, $CDCl_3$) (Table 5, Appendix 5A) displayed a peak at δ 3.64 (s, 3H) assigned to methyl attached to the nitrogen. The presence of prenyl moiety attached to oxygen was confirmed based on signals at δ 4.62 (*d*, 2H, *J* = 6.8 Hz, l"-OCH_2-), δ 5.53 (*t*, lH) and methyls at δ 1.82, 1.79 (*s*, 3H, 3"$(CH_3)_2$). Likewise, the presence of olefinic protons coupling to each other at δ 5.47 (1H, *d*, *J* = 9.9 Hz, 4'-H), 6.72 (1H, *d*, *J* = 9.9 Hz, 3'-H), along with singlet signals at δ 1.49 (*s*, 6H, 2'-$(CH_3)_2$) suggested the presence of pyran moiety. Aromatic protons with ABX spin patterns appeared at δ 6.78 (*d*, l H, *J* = 8.8 Hz, H-6), 6.82 (*dd*, lH, *J* = 8.8 and 2.3 Hz, H-7), 7.86 (*d*, l H, *J* = 8.8 Hz H-5). Its ^{13}C NMR (75 MHz, $CDCl_3$) (Table 5, Appendix 5B) showed one carbonyl carbon at δ 161.8 (C-2), six sp2 quaternary carbons at δ 161.7 (C-8), 155.9 (C-4), 141.9 (C-8a), 139.4 (C-3''), 110.2 (C-3), and 104.0 (C-4a). One sp3 quaternary carbon was observed at δ 78.6 (C-2'), three aromatic methine groups at δ 99.8 (C-5), 124.2 (C-7), and 118.4 (C-6), three olefinic carbons of pyran and prenyl moiety at δ 110.2 (C-3'), 125.7 (C-2"), and 119.4 (C-4'). The downfield chemical shift value of the prenyl methylene group at δ 66.5, supported by DEPT-135 (Appendix 5C), suggests that the prenyl is attached to oxygen. Three methyl signals were observed at δ 28.3 (C-5' 6'), 26.2 (C-4"), and 18.6 (C-5").

HSQC experiment (Appendix 5E) showed a ^{1}J correlation between H-5 (7.86) → C-5 (99.8), H-6 (6.78) → C-6 (118.4), H-7 (6.82) → C-7 (124.2), H-3' (6.72) → C3' (125.7), H-4'(5.49) → C-4' (119.4), H-5', 6' (1.49) → C-5', 6' (28.3), H-1" (4.62) →C-1" (66.5) H-1" (4.62) →C-1" (66.5), H-2" (5.53) →C-2" (110.2), H-4" (1.87) →C-4" (26.2), H-5" (1.79) →C-4" (18.8) and N-C$\underline{H}_3$ (3.64) → N$\underline{C}H_3$ (29.3).The higher intensity of the first one belonged to methyls of pyran moiety with identical signals, and the last two belong to methyl groups of the prenyl moiety, which was supported by the HSQC experiment. Its HMBC experiment (Figure 22, Appendix 5F) confirmed the quinone skeleton by N-CH_3 protons at δ 3.64 showing ^{3}J correlation with the carbonyl group C-2 at δ 161.8 and nitrogen attached quaternary carbon C-8a at δ 141.9. In addition the prenyl moiety attached with oxygen confirmed by ^{3}J correlation of methylene protons at δ 4.62 with oxygenated quaternary carbon C-8 at δ 161.7. And also the pyran moiety

was confirmed by the methyl protons δ 1.69 showed ^{2}J and ^{3}J correlation with sp^3 methine carbon C-2' at δ 78.6 and olefinic carbon C-3' at δ 125.7 respectively.

Based on the above spectroscopic evidence and comparison with the literature proton spectra data [185], compound (**9**) was found to be identical to N-methyl-8-(3",3"-dimethylallyloxy)-findersine (**9**, Figure 21), previously isolated from *Vepris stolsii* [185], but isolated herein for the first time from this species.

Table 5: ^{1}H (300 MHz) and ^{13}C (75 MHz) of N-methyl-8-(3", 3''-dimethylallyloxy)-findersine (**9**) in $CDCl_3$

No	**9**		[**185**]
	δ_H (in ppm), (*J* in Hz)	δ_C (in ppm)	δ_H (in ppm), (*J* in Hz)
2		161.8	
3		110.2	
4		155.9	
4a		104.0	
5	7.86 (*d*, *J* = 8.8)	99.8	7.87 (*dd*, lH, *J* = 9.0, 1.2)
6	6.78 (*d*, *J* = 8.8)	118.4	6.88 (*dd*, lH, *J* = 8.8 , 1.2)
7	6.82 (*dd*, *J* = 8.8, 1.3)	124.2	6.84 (*dd*, *J* = 8.8, 1.2)
8		161.7	
8a		141.9	
2'		78.6	
3'	6.72 (*d*, *J* = 9.9)	110.2	6.73 (*q*, *J* =10)
4'	5.49 (*d*, *J* = 9.9)	119.4	5.48 (*d*, *J* = 9.8)
5'	1.49 (*s*, 6H, 5', 6'-$(CH_3)_2$	28.3	1.50 (s, 6H, 5', 6'-$(CH_3)_2$
6'		28.3	
1''	4.62 (2H, *d*, *J* = 6.8)	66.5	4.64 (2H, d, *J* = 6.8)
2''	5.53 (*t*, lH, *J* =7.0, 2'-CH),	125.7	5.53 (t, lH, *J* =7, 2'-CH),
3''		139.4	
4''	1.82 (*s*)	26.2	1.80(*s*)

5''	1.79 (*s*)	18.8	1.83 (*s*)
NCH_3	3.64	29.3	3.74

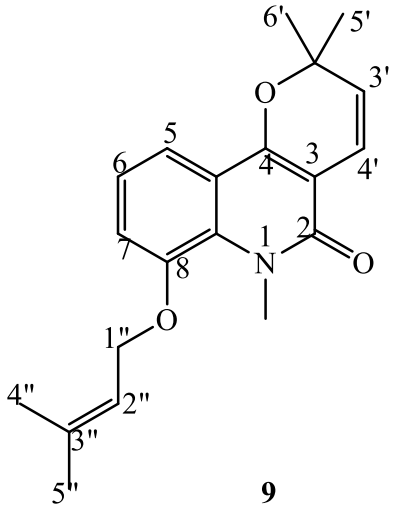

9

Figure 21: N-methyl-8-(3", 3"-dimethylallyloxy)-findersine (**9**) from fruit extract of *V. dainelli*

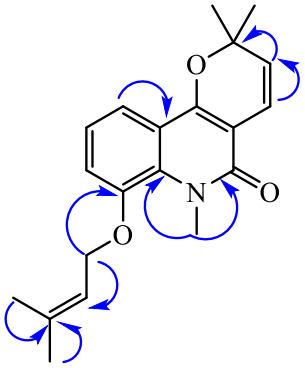

Figure 22: Important HMBC correlations of N-methyl-8-(3", 3"-dimethylallyloxy)-findersine (**9**).

4.1.1.4. Compound 25 and 51

Compound **51** and compound **25** were obtained as amorphous yellow mixtures. The two structures were identified after a detailed analysis of their spectra data in comparison with the literature. The NMR spectra of mixtures were showed two compounds in a different ratio based on their spectra intensity. Very intense peaks were belonged to kokusaginine [186, 187] and the less intense peaks skimmianine [186, 187] in this mixture. The ^{1}H NMR (300 MHz, $CDCl_3$) (Table 6, Appendix 6A) showed two doublet peaks at δ 7.48 (*d*, 1H, *J* = 2.8 Hz, H-2), 6.93 (*d*,

1H, *J* = 2.8 Hz, H-3) assigned for furan ring two protons. Two singlet Peaks at δ 7.36 (*s*, 1H, H-5) and 7.25 (*s*, 1H, H-8) clearly showed para-meta substituted AX aromatic system. Three singlets at δ 4.32 (*s*, 3H), 3.97 (s, 3H), and 3.95 (*s*, 3H) belonged to three methoxy groups.

^{13}C-NMR (300 MHz, $CDCl_3$) supported by DEPT-135 and 2D (COSY, HSQC, and HMBC) (Table 6, Appendix 6B-E) spectra displayed fifteen very intense carbon peaks. Four oxygenated quaternary carbon signals were observed at δ 162.9 (C-8b), 155.3 (C-4), 152.4 (C-6), and 147.5. Two aromatic methine peaks at δ 100.2 (C-5) and 106.4 (C-8). Three quaternary aromatic carbon peaks displayed at 114.6 (C-3a), 101.9 (C-4a), 142.7 (C-8a). Two furan ring methine carbons were observed at δ 142.1 (C-2) and 104.4 (C-3). In addition, three methoxy groups were displayed at δ 59.1 (4-OCH_3), 56.2 (6-OCH_3), 56.0 (7-OCH_3). Based on the above spectra information and comparison with the literature [186, 187], the major peak in the mixtures was kokusaginine (Figure 23, **51**), previously reported from the leaves of this plant by Dagne et al 1988 [40].

The spectra feature of skimmianine (Figure 23, **25**) is identical to kokusaginine. The major difference is the position of the methoxy group in the aromatic system. Which were confirmed by the ^{1}H NMR (300 MHz, $CDCl_3$), peeks at δ 7.89 (1H, *d*, *J* = 9.4 Hz, H-5), and 7.13 (1H, *d*, *J* = 9.4 Hz, H-6) clearly showed the Orth-para substituted aromatic system. Based on the spectra data (Table 6, Appendix 6A-E) and comparing with the literature [186, 187], the weak intense peak in the mixtures was skimmianine (Figure 23, **25**), previously reported from the leaves of this plant by Dagne *et al* 1988 [44].

Table 6: ^{1}H and ^{13}C of Kokusaginine (**51**) and skimmianine (**25**), (300 MHz for ^{1}H, 75 MHz for ^{13}C)

NO	**Kokusaginine**		**[186]**		**Skimmianine**		**[186]**	
	δ δ_H (in ppm), (*J* in Hz)	δ_C (in ppm)	δ_H (in ppm), (*J* in Hz)	δ_C (in ppm)	δ_H (in ppm), (*J* in Hz)	δ_C (in ppm)	δ_H (in ppm), (*J* in Hz)	δ_C (in ppm)
2	7.48 (*d*, 1H, *J* = 2.8)	142.1	7.56 (*d*, 1H, J = 3)	142.4	7.47 (1H, *d*, *J*= 2.8 , H-2)	142.8	7.56 (*d*, 1H, *J* = 3)	143.2
3	6.93 (*d*, 1H,	104.4	7.03 (*d*, 1H,	104.5	6.93 (1H, *d*,	104.4	7.02 (*d*, 1H,	104.6

	J = 2.8)		*J* = 3)		*J* = 2.8)		*J* = 3)	
3a		112.7		112.3		114.6		114.9
4		155.3		155.5		156.9		157.2
4a		101.9		102.1		101.7		102.0
5	7.36 (*s*)	100.2	7.46 (*s*)	100.1	7.89 (*d*, *J* = 9.4, 1H)	118.0	7.99 (*d*, 1H, *J* = 9)	118.1
6		152.4		152.6	7.13 (1H, *d*, *J* = 9.4)	111.7	7.21 (*d*, 1H, *J* = 9)	112.1
7		147.5		152.6		142.3		142.0
8	7.25 (*s*)	106.4	7.34 (*s*)	106.6		141.7		141.3
8a		142.7		143.8		151.9		152.2
8b		162.9		163.0		164.2		164.3
4-OCH_3	4.32 (*s*, 3H)	58.6	4.41 (*s*, 3H)	58.9	4.31 (3H, *s*)	58.7	4.41 (*s*, 3H)	58.8
6-OCH_3	3.97 (*s*, 3H)	55.9	4.01 (*s*, 3H)	55.9				
7-OCH_3	3.95 (*s*, 3H)	55.8	4.03 (*s*, 3H)	55.8	3.95 (3H, *s*)	56.5	4.09 (*s*, 3H)	55.8
8-OCH_3					4.06 (3H, *s*)	61.4	4.01 (*s*, 3H)	61.6

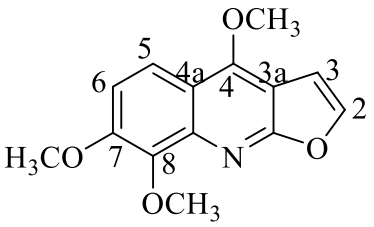

25

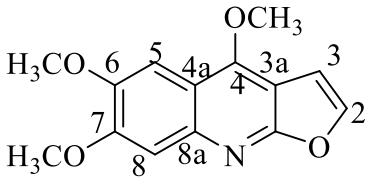

51

Figure 23: Skimmianine (**25**) and kokusaginine (**51**) isolated from fruit extract of *V. dainelli*

4.1.1.5. Compound 246

Compound (**246**) was obtained as an amorphous white crystal. A high-resolution mass spectrum experiment provided $[M]^+$*m/z* value 379.2362 (Appendix 7D), suggesting the molecular formula $C_{24}H_{42}O_3$. Its ^1H NMR (300 MHz, $CDCl_3$) (Table 7, Appendix 7A) shown a triplet peak at δ 0.87 (t, 3H) assigned for terminal methyl protons. Chemical shifts were observed at δ 1.27-1.32 (m, 16H), 1.55-1.61 *(m*, 4H), 2.00 (*t*, *J* = 8.5, and 6.7 Hz, 4H), 2.30 (*m*, 2H), and 5.19-5.31 (*m*, 4H, vinylic-H) are an indicator for the presence of long-chain unsaturated fatty acid. Protons at δ 4.12- 4.15 (*J* = 5.7 Hz, 2H) and 4.27-4.31(*dd*, *J* = 5.7 Hz, 2H) were assigned for methylene protons attached to the heteroatom oxygen. Deshielded sp^3 methine proton was observed at δ 4.12 (*m*, 1H, H-3'), suggesting methine attached to a heteroatom of tetrahydropyran moiety.

The ^{13}C NMR (75 MHz, $CDCl_3$) (Table 7, Appendix 6B) displayed twenty four carbon signals. The signal at δ 14.0 indicated the presence of terminal methyl carbon. Ester carbonyl was observed at δ 173.2. Four vinyl carbon peaks were observed at δ 129.6, 129.8, 129.9, and 130.0. The DEPT-135 experiment (Appendix 7C) showed two oxygenated methylene carbons at δ 66.0 and 62.2, and one deshielded methine carbon at 68.8. The remaining methylene carbons resonating at δ 22.5 to 34.2. Based on the spectroscopic data (Table 7, Appendix 7A-D) and literature spectral data [188], compound (**246**, Figure 24) is Tetrahydro-2H-pyran-2-ylmethyl octadeca-9, 12-dienoate, which is reported here for the first time from a plant source.

Table 7: ^{1}H (300 MHz) and ^{13}C (75MHz) of tetrahydropyranyl Octadeca-9, 12-dienoate (**246**) in $CDCl_3$.

Position	**246**		**[188]**	
	δ_H (in ppm), (*J* in Hz)	δ_C (in ppm)	δH (in ppm), (*J* in Hz)	δ_C (in ppm)
1		173.1		173.8
2	2.28	34.1	2.28	34.2
3	1.58	24.6	1.40-1.61	24.9
4-7	1.29-1.33	29-31	1.09-1.32	29-31
8	1.99-2.02	27.2	1.93-1.99	27.2
9	5.29-5.35 (*m*)	130.0	5.19-5.31 (*m*)	130.0
10	5.29-5.35 (*m*)	129.9	5.19-5.31 (*m*)	129.9
11	2.55	31.09	2.70	25.6
12	5.29-5.35 (*m*)	129.8	5.19-5.31 (*m*)	130.0
13	5.29-5.35 (*m*)	129.7	5.19-5.31 (*m*)	129.7
14	1.99-2.02	27.21	1.93-1.99	27.2
15	1.29-1.33	29.05	1.09-1.32	29.1
16	1.29-1.33	29.6	1.35	29.6
17	1.29-1.33	22.6	1.09-1.32	22.5
18	0.86	14.0	0.82	14.0
1’	4.16-4.31	66.0	3.88-4.06	68.4

2’	3.33 and 4.10	68.8	3.33 and 4.10	75.5
3’	1.55	29-31	1.55	29-31
4’	1.29	29-31	1.29	29-31
5;	1.29-1.33	29-31	1.29-1.33	29-31
6’	2.55	62.0	2.55	67.2

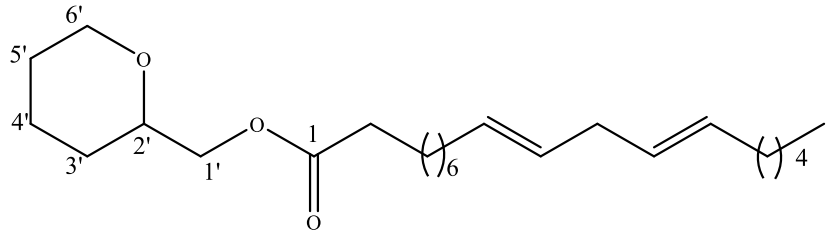

246

Figure 24: Tetrahydro-2H-pyranylmethyl octadeca-9, 12-dienoate (**246**) isolated from fruit extract of *V. dainelli*

4.1.2. Secondary Metabolites from *Zanthoxylum chalybeum*

The root extracts of *Z. chalybeum* after silica gel column chromatography furnished four benzophenanthridine alkaloids (**55, 62, 67,** and **247**), of which compounds (**62**) and (**247**) are reported herein for the first time from the species. The detailed characterization is presented here below.

4.1.2.1. Benzophenanthridine Alkaloids (55, 62, 67, and 247)

Compound (**55**) was obtained as yellow crystals with the melting point 203-207 ºC. The ESI-MS showed the molecular ion peak m/z = 348. Its ^{1}H NMR (400 MHz, DMSO-d_6) (Table 8, Appendix 8A) revealed a peak at δ 10.10 (*s*, 1H, H-6) due to through-space interactions with lone pairs of 7-OMe group [189]. A pair of *ortho* coupled aromatic protons appeared at δ 8.83 (1H, *d*, *J* = 9.6 Hz, H-10), 8.85 (1H, *d*, *J*= 9.6 Hz, H-9) and δ 8. 29 (1H, *d*, *J* = 9.7, H-12) and δ 8.31 (1H, *d*, *J*= 9.7 Hz, H-11) with AB spin pattern which suggest the presence of two tetra substituted aromatic rings. Two aromatic singlets were observed at δ 8.30 (1H, *s*, H-4) and 7.78 (1H, *s*, H-1). Singlet peaks were also observed at δ 6.35 (2H, *s*), δ 4.23 (3H, *s*), and 4.18 (3H, *s*)

belong to methylenedioxy group and two methoxy groups, respectively. The presence of methyl peak at δ 5.00 (3H, *s*), with a ^{1}J correlation to a peak at δ 52.7 in HSQC spectrum (Appendix 8D), suggests methyl protons attached to a quaternary nitrogen atom. Its ^{13}C NMR (75 MHz, DMSO-d_6) (Table 9, Appendix 8B) spectrum analyzed with the aid of DEPT-135 (Appendix 7C) revealed 21 carbons, of which seven sp^2 methines, four sp^2 oxygenated quaternary carbons, six sp^2 quaternary carbons, two methoxy, one methylenedioxy and one methyl attached to nitrogen. Based on the above spectroscopic evidence (Table, 8, 9, Appendix 8A-D) and comparison with the literature [189, 101], the compound was found to be identical to chelerythrine (**55**, Figure 25) previously reported from this plant [190] and a major chemical constituent to the Ethiopian species.

Compound (**62**) was identified as pale yellow needles with a melting point value of 201-204 °C. The ESI-MS showed the molecular ion peak m/z =365. Its ^{1}H NMR (300 MHz, $CDCl_3$) (Table 8, Appendix 9A) spectrum revealed two sp^2 methines at δ 7.17 (1H, *s*, H-1) and 7.93 (1H, *s*, H-4). A pair of ortho coupled doublet protons were observed at δ 7.69 (1H, *d*, *J*= 8.7 Hz, H-9), 7.46 (1H, *d*, *J*= 8.7 Hz, H-10) and δ 7.47 (1H, *d*, *J*= 8.5Hz, H-11), δ 6.85 (1H, *d*, *J*= 8.5 Hz, H-12). The presence of the methylenedioxy group was observed at δ 6.11 (2H, s), correlated to methylene at δ 101.1 pointing down in DEPT-135 spectrum (Appendix 9C). Singlet peak was observed at δ 5.30 (1H), correlated to sp^3 methine at δ 77.4, suggest the presence of hemiaminal sp^3 methine. Three singlet peaks were observed at δ 3.77 (*s*, 3H), δ 3.05 (*s*, 3H), and δ 2.41 (*s*, 3H) that belong to two methoxy groups and methyl attached to nitrogen, respectively. Its ^{13}C NMR (100 MHz, $CDCl_3$) (Table 9, Appendix 9B), with the aid of DEPT-135 (Appendix 9C), revealed a total of 21 carbons, of which six sp^2 methines, four sp^2 oxygenated quaternary carbons, six sp^2 quaternary carbon, two methoxy, one methylenedioxy, one methyl attached to nitrogen and one sp^3 oxygenated methine are evident. Based on the above spectroscopic evidence (Table 8, 9, Appendix 9A-D) and comparison with the literature [191, 192], the compound was found to be identical to 6-hydroxydihydrochelerythrine (**62**, Figure 25) previously reported from *Z. capense* [192] and *Z. nitidum* [193], but reported herein for the first time from this plant species.

The spectroscopic data of compound (**247**) (melting point 199-201 °C. The ESI-MS showed the molecular ion peak m/z = 379, is comparable to compound (**62**), except additional one methoxy signal at δ 3.46 (*s*, 3H) (Table 8, Appendix 10B) correlated to peak at δ 55.9 in HSQC spectrum (Appendix 10D) coupled with the absence of hemiaminal sp^3 methine peak is in agreement with the placement of the methoxy group at the C-6 position. Based on the spectroscopic evidence (Table 8, 9, Appendix 10A-E) and comparison with the literature [192, 194], compound (**247**) is identical with 6-methoxydihydrochelerythrine (**247**, Figure 25) previously reported from *Z. nitidum* [192], but reported herein for the first time this plant species.

The spectroscopic data of compound (**67**) (melting point 162-166 ^{o}C. The ESI-MS showed the molecular ion peak m/z = 349.13, Appendix 11D) is comparable to compound (**62**) except additional methylene peak at δ 4.29 (*s*, 2H) (Table 8, Appendix 11B) coupled with the absence of hemiaminal sp^3 methine peak is in agreement with the placement of the methylene attached to nitrogen at C-6 position. Thus, based on spectroscopic evidence (Table 8, 9, Appendix 11A-D) as well as comparison with the literature [101, 120], the structure of the isolated compound (**67**) was found to be identical to dihydrochelerythrine (**67**, Figure 25) previously reported from this plant [190] and a major chemical constituent to the Ethiopian species.

Table 8:^{1}H NMR (300MHz) chemical shifts (ppm) of benzo[c]phenanthridine alkaloids (**55**, **62**, **247** and **67**).

No	δ_H (in ppm), (*J* in Hz)			
	55	**62**	**247**	**67**
1	7.78 (*s*, 1H)	δ 7.17 (*s*, 1H)	7.46 (*s*, 1H)	7.11 (*s*, 1H)
4	8.30 (*s*, 1H)	7.93 (*s*, 1H)	7.62 (*s*, 1H)	7.67 (*s*, 1H)
6	10.10 (*s*, 1H)	5.30 (*s*, 1H)	5.30 (*s*, 1H)	4.29 (*s*, 2H)
9	8.85 (*d*, *J* = 9.6 Hz, 1H)	7.69 (*d*, *J* = 8.6 Hz, 1H)	7.46 (d, *J* = 8.7 Hz, 1H)	7.70 (*d*, *J* = 8.6 Hz, 1H)
10	8.83 (*d*, *J* = 9.6 Hz, 1H)	7.46 (*d*, *J* = 8.7 Hz, 1H)	7.70 (*d*, *J* = 8.7 Hz, 1H)	7.51 (*d*, *J* = 8.8 Hz, 2H)
11	8.31 (*d*, *J* = 9.7	7.47 (*d*, *J* = 8.5	7. 78 (*d*, *J* = 8.8	7.48 (*d*, *J* = 8.9 Hz,

	Hz, 2H)	Hz, 1H)	Hz, 1H)	2H)
12	8.29 (*d*, *J* = 9.7 Hz, 1H)	6.85 (*d*, *J* = 8.6 Hz, 1H)	7.66 (*d*, *J* = 8.7 Hz, 1H)	6.94 (*d*, *J* = 8.5 Hz, 1H)
-O$\underline{C}$H$_2$O-	6.35 (*s*, 2H)	6.11 (*s*, 2H)	6.06 (*s*, 2H)	6.05 (*s*, 2H)
6- O$\underline{C}$H$_3$	-	-	3.46 (*s*, 3H)	-
7-O$\underline{C}$H$_3$	4.23 (*s*, 3H)	3.77 (*s*, 3H)	3.96 (*s*, 3H)	3.93 (*s*, 3H)
8-O$\underline{C}$H$_3$	4.18 (*s*, 3H)	3.05 (*s*, 3H)	3.93 (*s*, 3H	3.88 (*s*, 3H)
-N$\underline{C}$H$_3$	5.00 (*s*, 3H)	2.41 (*s*, 3H)	2.77 (*s*, 3H)	2.60 (*s*, 3H)

Table 9: ^{13}C NMR (75 MHz) chemical shifts (ppm) of benzo[c]phenanthridine alkaloids (**55**, **62**, **247** and **67**) and ^{13}C NMR of [186].

No	δ_C (in ppm)							
	55	**[189]**	**62**	**[191]**	**247**	**[192]**	**67**	**[186]**
1	106.2	107.1	104.0	105.3	106.6	103.7	104.4	104.3
2	149.2	151.8	147.6	148.8	147.9	147.5	148.0	148.1
3	149.1	150.8	147.0	148.2	147.3	148.1	147.6	147.5
4	104.7	105.1	100.4	101.2	100.6	99.8	100.6	100.7
4a	120.6	121.9	111.8	128.2	127.6	126.5	130.9	130.9
4b	131.5	132.6	130.7	140.1	138.3	137.9	135.5	142.8
6	151.2	152.1	77.4	80.0	86.0	86.1	48.8	48.7
6a	119.8	119.9	119.3	124.3	118.9	126.9	119.9	118.7
7	145.0	147.6	145.9	146.9	149.3	146.5	146.6	146.2
8	151.0	151.8	151.0	150.6	150.2	152.0	152.4	152.3
9	126.5	127.5	126.4	129.1	126.7	113.2	124.3	124.2
10	119.9	121.0	118.2	118.3	112.9	118.6	118.8	118.7
10a	128.5	130.2	125.0	124.3	124.8	124.8	130.6	126.3
10b	125.7	127.2	125.7	129.1	125.7	122.4	130.0	126.4
11	119.7	119.5	122.8	120.1	123.4	119.4	120.0	123.8
12	132.1	132.7	122.5	121.0	120.0	123.3	111.5	110.9
12a	132.7	134.4	137.8	124.2	131.0	131.1	132.8	132.8

-O<u>C</u>H$_2$O-	103.2	104.3	101.1	102.0	104.6	101.1	103.2	101.0
6- O<u>C</u>H$_3$	-	-	-		55.9	-	-	-
7-O<u>C</u>H$_3$	62.7	62.8	59.9	62.2	61.6	60.5	61.1	61.1
8-O<u>C</u>H$_3$	57.5	57.6	55.2	-	53.9	55.7	55.8	55.8
-N<u>C</u>H$_3$	52.7	52.9	40.8	40.6	40.6	39.5	41.3	41.3

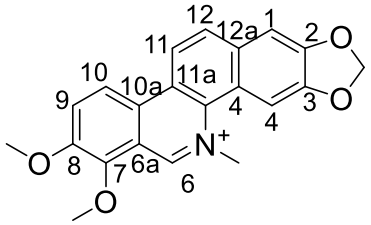

55

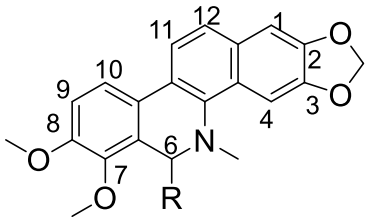

62. R= OH
247. R= OCH_3
67. R= H

Figure 25: Benzophenanthridine alkaloids isolated from the root extract of *Z. chalybeum*

4.1.3. Secondary Metabolites Isolated from *Uvaria. scheffleri*

The roots extract of *U. scheffleri* after silica gel column chromatography furnished two new uvarindoles such as uvarindole F (**248**) and G (**249)**, along with uvaretin **(112)**. The detailed characterizations of these compounds are presented here below.

4.1.3.1. Compound 248 and compound 249

Compound **248** was obtained as a pale gray needles and positive reaction to Dragendorff reagent indicative of alkaloid. The HRMS spectrum showed $[M]^+$ *m/z* = 451.1707 (calculated for the chemical formula $C_{29}H_{23}NO_4$ = 451.1784, Appendix 12A). The ^{1}H NMR (500 MHz, $CDCl_3$) spectrum (Table 10, Appendix 12B) displayed two methylene singlets at δ 4.33 (C-CH_2) and 4.17 (N-CH_2) together with three singlets at δ 11.33, 5.38, and 4.11 attributed to phenolic hydroxyl protons of which the downfield chemical shift of the former is due to peri effect to the carbonyl group of 2-acylindole. HSQC experiment (Appendix-12F) suggest protons at δ 4.16 correlated ^{1}J correlation with carbon at δ 68.2 in the replacement of N-H by hydoxybenzyl unit, which confirmed by HMBC experiment (Figure 27, Appendix-12G) with ^{3}J correlation with sp^2 quaternary carbons C-2 (δ 129.6) and C-7a (δ 137.0). Furthermore, protons at δ 4.33 ^{1}J

correlation with carbon at δ 27.9 in the placement of the placement of the benzyl at C-3 was also confirmed by HMBC correlations, in which methylene singlets at δ 4.33 (C-CH_2) showed ^{2}J correlation with sp^2 quaternary carbons C-3 (δ 119.6) and C-1‴ (δ 124.0), and comparison with NMR spectral data of uvarindole-C (**131**).

The ^{13}C NMR (125 MHz, $CDCl_3$) spectrum with the aid of DEPT-135 (Table 10, Appendix 12C, and D) displayed sixteen aromatic methines, two sp^3 methylenes at δ 27.9, and 68.2, assigned for C-CH_2 and N-CH_2, respectively. Three sp^2 downfield quaternary carbons were observed at δ 162.7, 155.2, and 140.5, of which the first two are connected to oxygen whereas the later connected to nitrogen. The Carbonyl group appeared at δ 192.3, in agreement with *α, β*-conjugated carbonyl, and a characteristic peak of a carbonyl group linked at C-2 in indole alkaloids. Furthermore, seven quaternary aromatic carbons were observed at δ 119.6 (C-3), 124.0 (C-1‴), 124.5 (C-1″), 126.6 (C-1′), 127.8 (C-3a), 129.6 (C-2) and 137.0 (C-7a). The NMR spectral data of compound (**248**) is consistent with that of Uvarindole-C (**131**) previously reported from *U. angolensis* [123, 195], except the observed additional one hydroxybenzyl unit attached to nitrogen in the case of compound (**248**). Thus, based on the above spectroscopic evidence (Table 10, Appendix 12A-G) and comparison with the literature of uvarindole-C (**131**) spectra [125, 195], the compound was identified to be uvarindole-F (**248**, Figure 26), reported herein for the first time.

Compound (**249**) was obtained as pale gray crystals and positive reaction to Dragendorffs reagent inductive to alkaloid. Its HRMS displayed $[M]^+$ *m/z* peak at 343.2953 (calculated 343.2972 for the chemical formula $C_{23}H_{21}NO_2$, Appendix 13A). The ^{1}H NMR spectrum **(**Table 10, Appendix 13B**)** showed two singlets at δ 4.44 and 4.61 (2 x C-CH_2, C-2a) attributed to methylene moiety. Methyl attached to nitrogen was observed at δ 2.66 (N-CH_3), showing a ^{1}J correlation with δ 36.5 peaks in the HSQC spectrum and a ^{3}J HMBC correlation with C-2 (140.7) and C-7a (δ 143.0) (Figure 27, and Appendix 13E and G). In addition, a signal at δ 5.89 and 3.42 showed broad singlet peaks attributed to phenolic hydroxyl proton. The remaining 12 protons were displayed in the aromatic region.

The ^{13}C NMR spectrum(Table 10, Appendix 13C) supported by Dept-135 and HSQC experiments (Appendix 13 D, F) showed twelve aromatic methines, two sp^3 methylene carbons at δ 42.8 (C-2a) and 40.8 (C-3a), two oxygenated sp^2 quaternary carbons at δ 158.9 and 151.2 along with six sp^2 quaternary carbons at δ 143.0, 140.7, 134.5, 132.9, 119.8 and 122.9. Placement of two 2-hydroxybenzyl substituents at C-2 and C-3 positions were done with the help of ^2J and ^3J HMBC correlations of methylene protons (Figure 27, Appendix 13G). Based on the above spectroscopic evidence and comparison with spectral data of uvarindole-C (**131**) [125, 195], compound (**249)** is found to be a new compound named Uvarindole G (Figure 26, **249**), reported herein for the first time.

Table 10: 1H and 13C NMR chemical shifts (ppm) of uvarindole-F and G (**248** and **249**) (500 MHz for 1H, 125 MHz for 13C in CDCl3).

Assignments	**Compound 248**		**Compound 249**		**[195]**
	δ_H (in ppm), (*J* in Hz)	δ_C (in ppm)	δ_H (in ppm), (*J* in Hz)	δ_C (in ppm)	δ_C (in ppm)
2	-	129.6	-	140.7	129.8
3	-	119.6	-	119.8	119.7
3a	-	127.8	-	122.9	127.9
4	8.15 (*d*, *J* = 9.4 , 1H)	118.8	8.10 (m, 1H)	118.6	118.7
5	8.48 (*d*, *J* = 9.4,1H)	121.8	7.86 (*d*, *J* = 8.2 Hz, 1H)	121.3	121.7
6	7.35 (*m*, 1H)	126.7	7.78 (*t*, *J* = 7.5 Hz, 1H)	129.2	126.7
7	7.70 (*m*, 1H)	111.8	8. 09 (*m*, 1H)	111.8	111.9
7a	-	137. 0	-	143.0	137. 1
N-CH_2	4.17 (*s*, 2H)	42.0	-NCH_3	36.5	--
1'	-	126.6	-	-	-
2'	-	155.2	-	-	-
3'	7.49 (*m*, 1H)	130.8	-	-	-
4'	7.13 (*m*, 1H)	128.1	-	-	-
5'	8.08 (*d*, *J* = 8.4) Hz,	125.7	-	-	-
6'	7.49 (*m*, 1H)	130.6	-	-	-
-CO-	-	192.3		43.1	192.4
1"	-	124.5		132.5	124.5

2"	-	162.7		158.9	162.8
3"	6.90 (*td*, *J* = 7.4, 1.3 Hz, 1H)	119.6	7.31 (*dd*, *J* = 8.2, 6.9 Hz, 1H)	122.0	119.3
4"	7.49 (*m*, 1H)	131.0	7.38 (*d*, *J* = 8.1 Hz, 1H)	130.1	131.2
5"	7.13 (*m*, 1H)	119.3	7.53 (*m*, 1H)	119.7	119.8
6"	7.59 – 7.61 (*m*, 1H)	136.6	8.10 (*m*, 1H)	137.3	136.1
C-CH_2	4.33 (*s*, 2H)	27.9		40.8	27.9
1'"	-	124.0	-	124.5	124.0
2'"	-	140.5	-	151.2	155.1
3'"	6.82 (*d*, *J* = 7.3 Hz, 1H)	116.4	7.67 (*d*, *J* = 8.6 Hz, 1H)	113.7	116.5
4'"	7.13 (*m*, 1H)	128.1	8.43 (*dd*, J = 7.9, 1.4 Hz, 1H)	128.9	128.2
5'"	8.26 (*d*, *J* = 9.2 Hz, 1H)	120.9	7.86 (*d*, *J* = 8.2 Hz, 1H)	122.8	120.9
6'"	7.88 (*d*, *J* = 9.0 Hz, 1H)	132.0	7.53 (*m*, 1H)	134.5	132.3

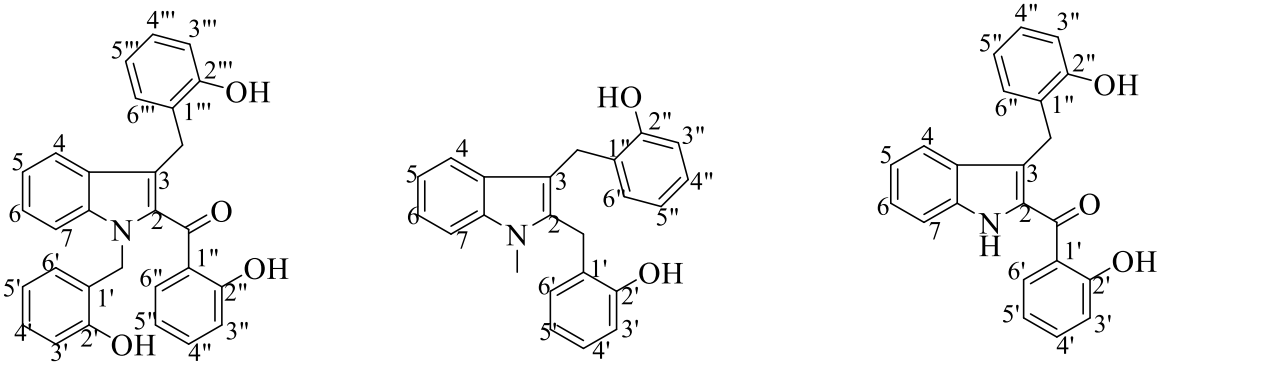

Figure 26: Structures of compounds **248** and **249** isolated from the roots extract of *U. scheffleri* and uvarindole-C (131) [195].

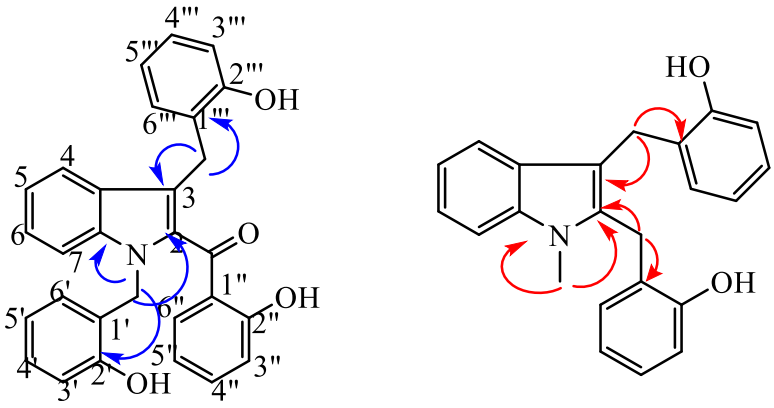

248 **249**

Figure 27: Important HMBC correlations of compounds **248** and **249**.

4.1.3.2. Compound 112

Compound **112** was obtained as deep gray needles. It's ESI-MS *m/z* showed 378. The ^{1}H NMR spectrum (Table, 11, Appendix 14A) displayed a singlet peak at δ 4.90 (2H, Ar-CH_2) attributed to methylene linked with two phenyl rings and two signals with A_2B_2 spin pattern observed at δ 2.85 and 3.15 suggesting a β-propiophenone moiety. Two singlets at δ 4.37 and δ 11.33 attributed to methoxy and hydroxyl group with peri effect to the carbonyl group, respectively. The presence on a mono substituted aromatic ring was clearly evident from peaks at δ 7.77 (*d*, *J* = 8.2, 1H, H-2), 7.81 (*dd*, *J* = 8.1, 1.7 Hz, 1H, H-3), 7.56 (*t*, 1H, H-4), 7.30 (*m*, 1H, H-5) and 7.49 (*dd*, *J* = 7.5, 1.7 Hz, 1H, H-6). This substitution pattern coupled with the apperance of a singlet aromatic proton at δ 7.23 (*s*, 1H) displayed by H-5' suggest a tetra substituted ring A and mono substituted ring B pattern of dihydrochalcone. The ^{13}C NMR spectrum supported by DEPT-135 (Table 11, Appendix 14 B and C) displayed 22 carbon signals. Ten sp^2 methines were observed at δ 112.1, 116.6, 119.5, 119.9, 126.8, 128.4, 128.5, 131.3, and 126.8. Four sp^2 oxygenated quaternary carbons and one carbonyl carbon were observed at δ 162.9 (C-2'), 155.4 (C-4'), 155.0 (C-6'), 154.0 (C-2") and δ 203.3, respectively. In addition, four sp^2 quaternary carbons were observed at δ 118.2 (C-1'), 121.2 (C-3'), 122.0 (C-1"), and 140.6 (C-1). Furthermore, three sp^3 methylenes were observed at δ 28.2 (C-3'a), 30.6 (α-CH_2) and 41.0 (β-CH_2). Thus, based on the above spectroscopic evidence and comparison with literature [21], compound **112** was identified as uvaretin (Figure 28, **112**) previously reported from various *Uvaria* species [125,195], reported herein for the first time from the species.

Table 11: ^{1}H (300MHz) and ^{13}C NMR (75 MHz), chemical shifts (ppm) of uvaretin (**112**) in $CDCl_3$ and litrature [195] in MeOD.

No	**Uvaretin (121)**		**[195]**	
	δ_H (in ppm), (*J* in Hz)	δ_C (in ppm)	δ_H (in ppm), (*J* in Hz)	δ_C (in ppm)
1		140.6		142.6
2	7.77 (*d*, *J* = 8.2, 1H, H-2)	128.6	7.21 (5H, *brs. m*)	127.2
3	7.81 (*dd*, *J* = 8.1, 1.7 Hz, 1H, H-3)	128.5		129.1
4	7.56 (*t*, 1H, H-4)	126.6		126.6
5	7.30 (*m*, 1H, H-5)	128.4		129.1
6	7.49 (*dd*, *J* = 7.5, 1.7 Hz, 1H, H-6)	127.8		127.2
α	3.15 (*m*, 2H)	30.6	2.95 (2H, *m*)	31.4
β	2.85 (*m*, 2H)	41.0	3.35 (2H, *m*)	46.3
C=O		203.4		205.4
1′		118.2		107.8
2′		162.9		163.1
3′		121.2		109.0
4′		155.4		165.2
5′	5.81 (*s*, 1H, H-5’)	112.1	6.73 (1H, *s*)	91.8
6′		155.0		162.6
3a	4.90 (*s*, 2H, H-3'a')	28.2	4.89(2H, *s*)	22.7
1″		122.0		126.6
2″		154.0		154.3
3″	6.97 (*m*, 1H, H-3")	116. 6	6.75-7.60 (*br. m.* 4H)	115.9
4″	6.91 (*m*, 1H, H-4")	119. 9		129.1
5″	6.82 (*dd*, *J* = 7.9, 1.3 Hz, 1H, H-5")	119.5		120.6
6″	7.12 (*d*, *J* = 8.2 Hz, 1H, H-6")	131.3		131.2
	4.37 (*s*, 3H, 6'-OCH_3)	56.1	3.61 (*s*, 3H)	56.0

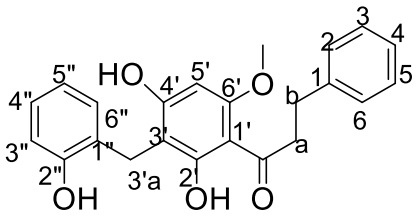

112

Figure 28: Structures of uvaretin (**112**) isolated from the roots extract of *U. scheffleri.*

4.1.4. Secondary Metabolites Isolated from *Clematis burgensis*

The roots extract of *C. burgensis* after silica gel column chromatography furnished three compounds (**98**, **250,** and **251**) for the first time from the species. The detailed characterizations of these compounds are presented here below.

4.1.4.1. Compound 250

Compound **250** was obtained from the root extract of *C. burgensis* as yellow amorphous crystals. Its HRMS displayed $[M+H]^+$ *m/z* at 419.3363 (calculated 419.3156 for the chemical formula $C_{26}H_{42}O_4$, Appendix 15A). Its ^1H NMR (300 MHz, $CDCl_3$) spectrum (Table 12, Appendix 15B) showed typical AA'BB' system at δ 7.64 (2H, dd, *J* = 8.8, 2.2 Hz, H-3, 6), and 7.46 (2H, dd, *J* = 8.8, 2.2 Hz, H-4, 5) which implied an ortho-substituted benzene ring [196]. Twelve methylene protons were observed at δ 4.21 (4H, *t*, CH_2-1, 1'), 1.65 (4H, *m*, CH_2-2, 2'), 1.25 (4H, *m*, CH_2-3, 3'), 1.29 (8H, *m*, CH_2-4, 4', 5, 5'), 1.31 (4H, *m*, CH_2 -6,6'), 1.40 (4H, *m*, CH_2 -8, 8'), along with four methyl groups at δ 0.90 (6H, *m*, CH_3 -9, 9') and 0.89 (6H, *m*, CH_3-7, 7'). The ^{13}C NMR (75 MHz, $CDCl_3$) (Table 12, Appendix 15C), assigned with the aid of DEPT-135, HSQC and HMBC spectra (Appendix 15D, E and F respectively), confirmed the presence of two symmetrical carbonyl carbons at δ 167.8, four sp^2 aromatic methines, four methyl groups, two *O*-bearing methylene moiety, at δ 68.1and six methylene groups at, δ 23.7, 30.3, 28.9, 29.7, and 22.9. The methyl groups appeared at δ 14.0 and 10.9 attributed to C-7', 7" and C-9', 9" terminal carbons, respectively. In addition, three peaks at δ 130.8, 128.8, and 38.7 were assigned to olefinic methines C-1, C-2 and C-6, respectively. Thus, based on the spectral evidence (Table 12, Appendix 13A - G) and comparison with literature [196, 197], the structure of compound **250**

was assigned to bis (2-ethylheptyl) phthalate (Figure 29, **250**) previously isolated from *Cynodon dactylon* [196], reported herein from the first time from the genus *Clematis*.

Table 12: ^{1}H and ^{13}C NMR chemical shifts (ppm) of bis (2-ethylheptyl) phthalate (**250**), (300 MHz for ^{1}H, 75 MHz for ^{13}C in $CDCl_3$).

Position	**250**		**[196, 197]**	
	δ_H (in ppm), (*J* in Hz)	δ_C (in ppm)	δ_H (in ppm), (*J* in Hz)	δ_C (in ppm)
1,8	-	167.8		167.8
2, 7	-	132.4		132.4
3, 6	7.70 (*dd*, 2H, *J* = 8.8, 2.2)	130.8	7.70 (*J* = 8.8, 2.2)	130.8
4, 5	7.53 (*dd*, 2H, *J* = 8.8, 2.2)	128.8	7.53 (*J* = 8.8, 2.2)	128.8
1', 1''	4.21 (6.2)	68.1	4.21 (6.2)	68.1
2', 2''	1.63 (*m*)	38.7	1.63 (*m*)	38.7
3', 3''	1.25 (*m*)	30.3	1.25 (*m*)	30.3
4', 4''	1.25 (*m*)	28.9	1.25 (*m*)	28.9
5', 5''	1.29 (*m*)	29.7	1.29 (*m*)	29.7
6', 6''	1.31 (*m*)	22.9	1.31 (*m*)	22.9
7',7''	0.90 (*m*)	14.0	0.90 (*m*)	14.0
8', 8''	1.40 (*m*)	23.7	1.40 (*m*)	23.1
9', 9''	0.89 (*m*)	10.9	0.89 (*m*)	10.9

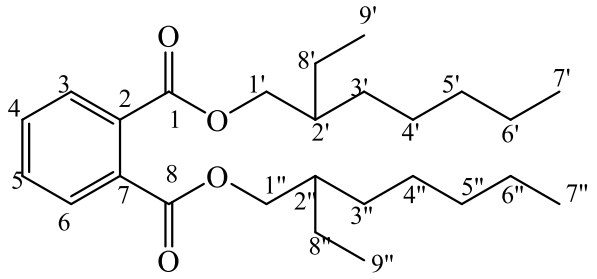

250

Figure 29: Bis (2-ethylheptyl) phthalate (**250**) isolated from root extract of C. *burgensis*.

4.1.4.2. Compound 98

Compound **98** was obtained as a white amorphous powder. Its IR spectrum (Appendix 16A) showed a broad absorption peak at 3346 cm^{-1} due to hydroxyl moiety, the absorption peak around 2990 cm^{-1} was due to olefinic C-H, peaks at 2936 cm^{-1} and 2865 cm^{-1}were assigned for sp^3 C-H stretch and an intense peak at 1010 cm^{-1} assigned for C-O stretch. The ^1H NMR (300 MHz, $CDCl_3$) spectra (Table 13, Appendix 16A) showed oxygenated sp^3 methine proton at δ 3.18 (*dd*, *J* = 10.9, 5.3 Hz, 1H, H-3) and seven methyl signals at *δ* 1.66, 1.05, 0.96, 0.85, 0.85, 0.83 and 0.78. Terminal sp^2 methylene protons were observed at δ 4.68 and 4.56 (*dd*, *J* = 2.6, 1.4 Hz, 2H, H-29a, 29b). Its ^{13}C NMR (75 MHz, $CDCl_3$) spectrum (Table 13, Appendix 16B) and DEPT-135 spectra (Appendix 16C) suggested a triterpenoid skeleton with characteristic peaks at δ 151.2 and 109.5 ppm attributed to C-20 and C-29 respectively, of which the former suggested a sp^2 quaternary carbon and the latter suggest terminal olefinic methylene, pointing downwards in DEPT-135 spectrum. Oxygenated sp3 methine carbon peak was observed at δ 79.2 (C-3). Thus, based on the above spectroscopic evidence and comparison with literature [197,198], the structure of compound **98** was found to be lupeol (Figure 30, **98**) reported herein for the first time from the genus *Clematis*.

Table 13: ^1H and ^{13}C NMR chemical shifts (ppm) of lupeol (**98**) (300 MHz for ^1H and 75 MHz for ^{13}C NMR in $CDCl_3$).

	98		**[198]**	
	δ_H (in ppm), (*J* in Hz)	δ_C (in ppm)	δ_H (in ppm), (*J* in Hz)	δ_C (in ppm)
1.	0.99 (*m*)	38.9	0.99 (*m*)	38.7
2.	1.85 (*m*)	27.6	1.85 (*m*)	27.4
3.	3.18 (*m*)	79.2	3.18 (*m*)	79.0
4.	-	39.8	-	38.9
5.	0.69 *t*	55.5	0.69 (*t*)	55.3
6.	1.39 (*m*)	18.5	1.39 (*m*)	18.3
7.	1.35 (*m*)	34.5	1.35 (*m*)	34.3
8.	-	41.0	-	410.8
9.	1.71 (*m*)	50.6	1.71 (*m*)	50.3
10.	-	37.4	-	37.1
11.	1.29 (*m*)	21.1	1.29 (*m*)	21.1
12.	1.38 (*m*)	25.3	1.38 (*m*)	25.3

13.	0.68 (*m*)	38.2	0.68 (*m*)	38.0
14.	-	43.0	-	42.8
15.	1.40 (*m*)	27.6	1.40 (*m*)	27.0
16.	1.34 (*m*)	35.8	1.34 (*m*)	35.0
17.	-	43.2	-	43.0
18.	1.79 (*m*)	48.5	1.79 (*m*)	48.0
19.	2.38 (*m*)	48.2	2.38 (*m*)	48.0
20.	-	151.2	-	150.9
21.	1.41 (*m*)	30.0	1.41(*m*)	30.0
22.	1.35 (*m*)	40.2	1.35 (*m*)	40.0
23.	0.78 (*s*)	28.2	0.76 (*s*)	28.0
24.	0.85 (*s*)	16.2	0.78 (*s*)	15.2
25.	0.85 (*s*)	16.3	0.82 (*s*)	16.1
26.	0.94 (*s*)	15.6	0.94 (s)	15.9
27.	0.96 (*s*)	14.7	0.96 (s)	14.5
28.	1.05 (*s*)	18.5	1.03 (*s*)	18.0
29.	4.69, 4.57(*dd*, 2.6, 1.4)	109.9	4.69, 4.57 (*dd*)	109.3
30.	1.66 (*s*)	19.5	1.68 (*s*)	19.3

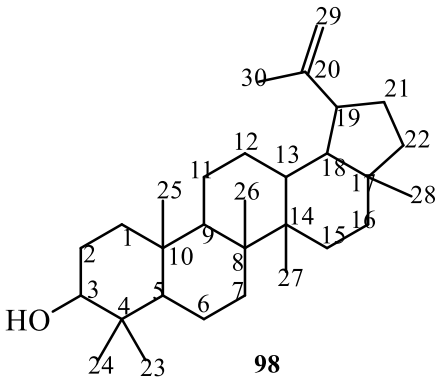

98

Figure 30: Lupeol (**98**) isolated from root extract of *C. burgensis*.

4.1.4.3. Compound 251

Compound **251** was isolated as a pale white solid with. Its ^{1}H NMR (300 MHz, $CDCl_3$) (Table 14, Appendix 17A) spectral data showed the corresponding up field unsaturated fatty acid signals below δ 3.0. Its ^{13}C-NMR (75 MHz, $CDCl_3$) (Table 14, Appendix 17B), aided with DEPT-135 (Appendix 17C), displayed carbonyl group (-CO-) of carboxylic acid at δ 180.2, twelve methylene carbon peaks were observed at δ 20-40 of which the most deshilded one at δ 34.1

suggests methylene next to carbonyl (C-2). The terminal methyl group appeared at δ 14.0. Thus, the above spectral data suggest that compound (**251**) is identical with stearic acid (**251**, Figure 31), in good agreement with literature spectra data [200].

Table 14: ^{1}H and ^{13}C NMR Linoleic acid fatty acid (**251**) (300 MHz for ^{1}H NMR and 75 MHz for ^{13}C NMR in $CDCl_3$).

Position	**251**		**[200]**	
	δ_H (in ppm), (*J* in Hz)	δ_C (in ppm)	δ_H (in ppm), (*J* in Hz)	δ_C (in ppm)
1		180.2		180.1
2	2.32	34.1	2.36	34.0
3	1.58	24.6	1.64	24.7
4-7	1.29-1.33	29-3		29-31
8	2.02	27.2	2.06	27.2
9	5.37(*m*)	30.0	5.37 (*m*)	30.0
10	5.37(*m*)	29.9	5.37 (*m*)	29.9
11	2.37	31.0	2.06	25.6
12	5.37 (*m*)	29.8	5.37 (*m*)	29.8
13	5.37 (*m*)	29.7	5.37 (*m*)	29.7
14	2.04	27.2		27.2
15	1.29-1.33	29.0	1.35	29.05
16	1.29-1.33	29.6	1.35	29.63
17	1.29-1.33	22.6	1.35	22.5
18	0.90	14.0	0.90	14.0

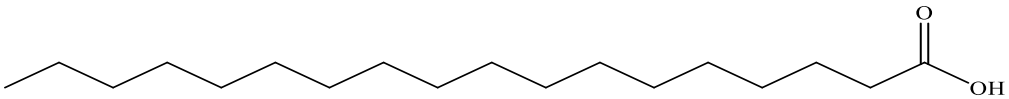

251

Figure 31: Stearic acid (**251**) isolated from root extract of from *C. burgensis*.

4.1.5. Secondary Metabolite Isolated from Root of *E. schimperiana*

The roots extract of *E. schimperiana* after silica gel column chromatography furnished ten compounds (**252, 254- 262**). Compounds **252** and **254** were isolated as a pure compounds. The remaining **255-262** were identified from the fractions by GC/MS analysis. The detailed characterizations of the compounds are presented here below.

4.1.5.1. Compound 252

Compound **252** was obtained as yellow needles. IR spectra analysis (Appendix 18A) showed absorption bond at 2940 cm^{-1} and 2886 cm^{-1} assigned for sp^3 C-H stretch and a sharp and intense peak at 1705 cm^{-1} assigned for carbonyl group. The absorption peak at 1015 cm^{-1} belongs to C-O stretch. Its ^1H NMR (300 MHz, $CDCl_3$) (Table 15, Appendix 18B) spectrum showed two doublets at δ 6.26 and 7.61 (*d, J* = 9.5 Hz) and two aromatic singlets at δ 6.84 (*s*, H-8) and 6.91 (s, H-5). The presence of a doublet methyl signals at δ 0.88 (*d, J* = 5.3 Hz, 6H) coupled with methine at 2.02 (1H, m) and methylene protons at δ 2.02 (*m*, 2H) and 2.31(*m*, 2H) suggested the presence of a reduced prenyl moiety. The singlet peak at δ 3.95 belong to methoxyl group. Its ^{13}C NMR (75 MHz, $CDCl_3$) spectra (Table 15, Appendix 16C) displayed 15 carbon signals assigned with the aid of DEPT-135 (300 MHz, $CDCl_3$) (Appendix 16D). One carbonyl carbon appeared at δ 161. 5 suggesting an ester carbonyl carbon. Two oxygenated sp^2 carbons were observed at δ 150.2 and 149.7 along with two more sp^2 quaternary carbons at δ 114.0 and 103.2. In addition, two aromatic methines were observed at δ 111.4 and 107.5 along with two olefinic methines at δ 143.3 and 113.3 of which the downfield chemical shift of the former suggest β-position to ester carbonyl carbon. Carbon signal at δ 56.4 was assigned to methoxy group. Two methylene groups, which are part of prenyl moiety appeared at δ 31.9 and 31.6 along with one methine at δ 31.6 and two methyl groups at δ 22.7 and 14.8. Thus, based on the above spectroscopic data and comparison with the data reported for suberosin (**253**) [201, 202], the structure of compound **252** was identified to be derivative of suberosin (**252**, Figure 32), which was previously reported from *Citrus grandis* by Wu (1988) [202], but reported herein for the first time from genus *Euphorbia*.

Table 15: ^{1}H NMR (300MHz) and ^{13}C NMR (75 MHz) chemical shifts (ppm) of compound (**252**) in $CDCl_3$.

Position	**252**		**[201]**	
	δ_H (in ppm), (*J* in Hz)	δ_C (in ppm)	δH (in ppm), (*J* in Hz)	δ_C (in ppm)
2	-	161.5		161.5
3	6.28 (*d*, *J* = 9.4)	113.3	6.20 (*d*, 9.4)	112.7
4	7.60 (*d*, *J* = 9.5)	143.3	7.59 (*d*, 9.5)	143.5
4a	-	114.1	-	127.7
5	6.91(*s*)	111.5	7.15 (s)	125.4
6	-	149.8	-	154.4
7	-	150.3	-	160.6
8	6.84 (*s*)	107.5	6.75 (*s*)	111.8
8a	-	103.2	-	98.8
$-OCH_3$	3.95 (*s*, 3H)	56.4	3.89 (*s*, 3H)	55.8
1’	2.32 (*t*, 7.9)	31.9	3.29 (*d*, 7.5)	133.6
2’	2.00 (*m*)	31.6	5.26 (*m*)	121.3
3’	2.00 (*m*)	23.4	-	27.2
4’	0.89 (*d*, *J*= 6.1)	22.7	1.76 (*s*)	25.7
5’	0.89 (*d*, *J*= 6.1)	14.1	1.68 (*s*)	17.5

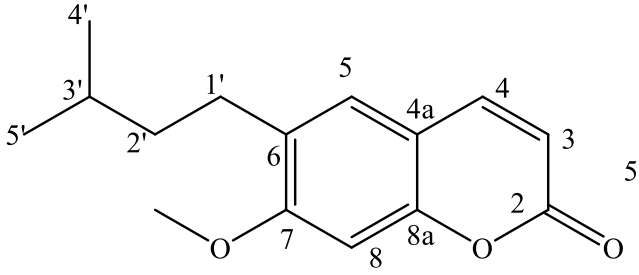

252

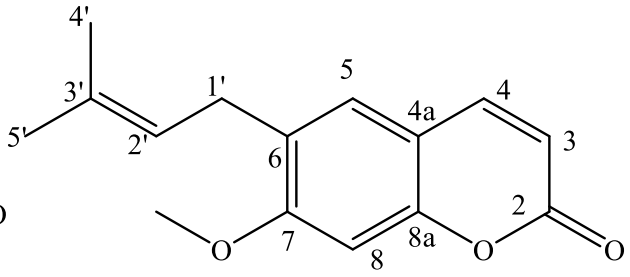

253

Figure 32: Compound (**252**) isolated from the roots extract of *E. shemepriana* and suberosin (**253**) [201]

4.1.5.2. Compound 254

Compound **254** was obtained as amorphous colorless. Its ^{1}H NMR (300 MHz, $CDCl_3$) (Table 16, Appendix 19A) showed a singlet peak at δ 5.75 for 4 protons belonged to two primary amine groups in the compound. The doublet peak at δ 5.18 (*d*, *J* = 3.7 Hz, 1H) assigned for a proton attached to anomeric carbon. The peaks at δ 3.78-3.12 (*m*, 11H) assigned for methine protons. In addition, peaks at 3.56 (*m*, 4 H) belonged to methylene protons.

The ^{13}C NMR (100 MHz, $CDCl_3$) supported by DEPT-135 spectra (Table 16, Appendix 19B-C) showed totally 13 carbon peaks. The anomeric carbon displayed at 104.5 (C-1'). Another methine carbons at δ 72.1 (C-2), 77.5 (C-3), 83.0 (C-4), 74.7 (C-5), 73.3 (C-2'), 73.2 (C-3'), 70.3 (C-4'), and 77.2 (C-5'), Two methylene carbons displayed at δ 62.6 (C-6) and 60.9 (C-6'). Furthermore, one methine linked with two amine groups were observed at δ 92.2 (C-1). Based on the spectroscopic data and literature of glycosylmethylamine [203], compound **254** was found to be glycosylmethylamine derivative (Figure 33, **254**) reported herein for the first time from plant source.

Table 16: ^{1}H NMR (300MHz) and ^{13}C NMR (75MHz) chemical shifts (ppm) of compound (**254**) in DMSO).

NO	**Compound (254)**		**[203]**
	δ_H (in ppm), (*J* in Hz)	δ_C (in ppm)	δ_C (in ppm)
-OH	5.75 (s, 4H)	-	-
1	3.84 (*dd*, *J*= 2.8, 3.4 Hz, 1H)	92.2	81.0
2	3.18-3.33 (*m*, 5H)	72.1	73.8
3		77.5	79.5
4		83.0	80.1
5		74.7	77.2
6	3.56 (*m*, 2H)	62.6	62.3
1'	5.18 (*d*, *J* = 3.7 Hz, 1H)	104.5	104.2
2'	3.18-3.33(*m*, 5H)	73.3	72.3

3’		73.2	72.3
4’		70.3	69.9
5’		77.2	76.7
6’	3.56 (*m*, 2H)	60.9	61.7
1” ($CH(NH_2)_2$	3.18-3.33(*m*, 1H	49.0	43.0($\underline{C}H_2NH_2$)

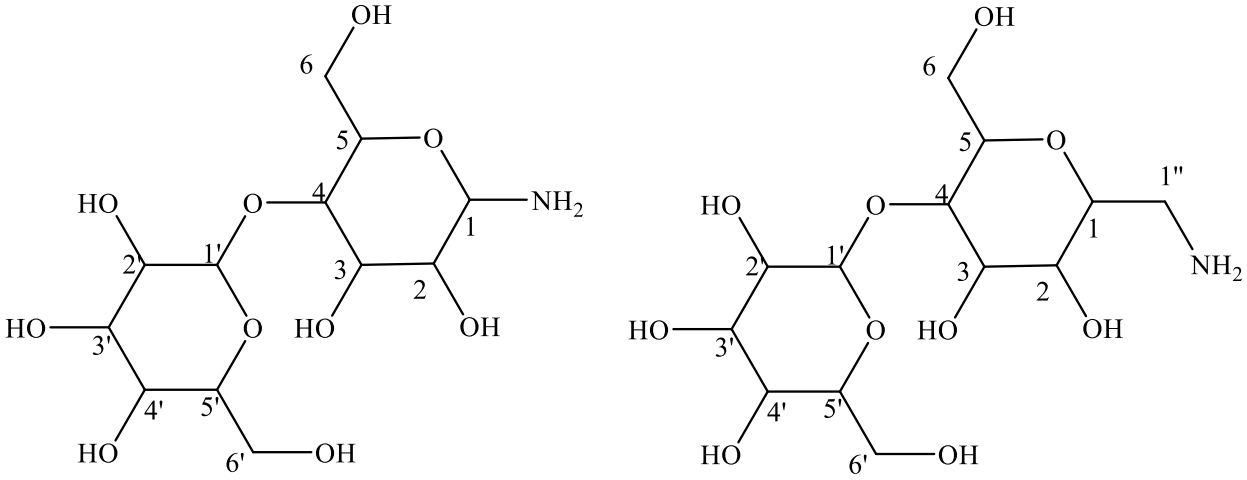

254 **255**

Figure 33: Compound **254** isolated from the roots extract of *E. schimeperiana* and glycosylmethylamine (**255**) [203]

4.1.5.3. GC/MS Analysis of fractions (12 -15)

Compound **155-160** were identified from fraction 12-15 (eluted with 30 and 35% Ethyl acetate fractions) as brownish amorphous. The GC (Figure 34) and GC/MS (Table 17, Appendix 20A-G) analysis of fraction 12-15 from roots of *E. schimperiana* revealed a total of six compounds (Figure 35, **155-160**), accounting 79.5 %. The structure of compounds were identified based on their mass spectra value comparing with the NIST library databases. The major constituents of which are lupane derivative (29.54%) (**258**), the oleane derivatives (14.19%) (**259**) and germanicol (12.23%) (**260**), the remaining compounds ranged from 4.75 to 8.15%.

Table 17: Chemical constituents fraction **12-15**.

No	**RT**	**Identified compounds**	**Molecular formula**	**Molecular weight**	**Compositions %**
255	33.11	13,27-Cycloursan-3-one-(13α)-	$C_{30}H_{48}O$	424.3	5.03
256	33.39	6a,14a-Methanopicene, perhydro-1,2,4a,6b,9,9,12aheptamethyl-10-hydroxy-	$C_{30}H_{50}O$	426.4	5.45
257	34.58	24-Methylenecycloartan-3-one	$C_{31}H_{50}O$	438.3	8.15
258	34.73	Lup-20(29)-en-3-ol, acetate, (3β)-	$C_{32}H_{52}O_2$	468.4	29.54
259	34.84	12-Oleanen-3-yl acetate, (3α)-	$C_{32}H_{52}O_2$	468.4	14.19
260	34.96	Germanicol	$C_{30}H_{50}O$	426.4	12.23
Total compositions					**79.50%**

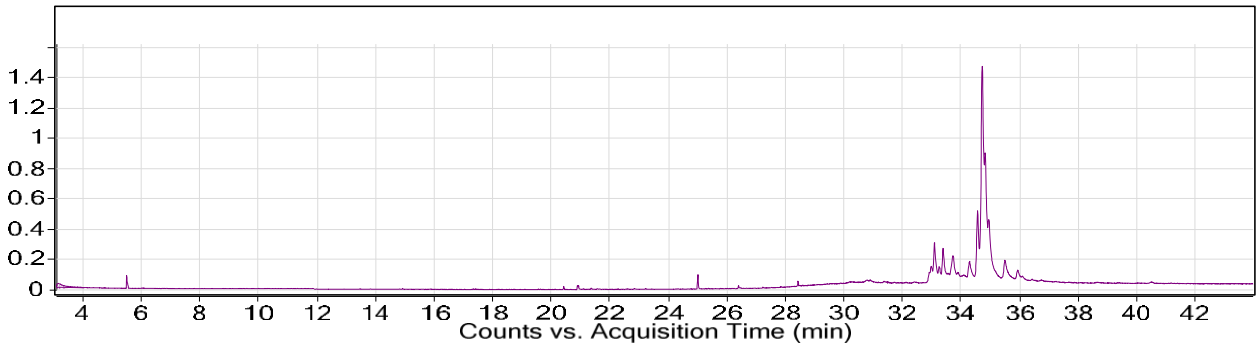

Figure 34: Chromatogram for compounds in the fraction **12-15.**

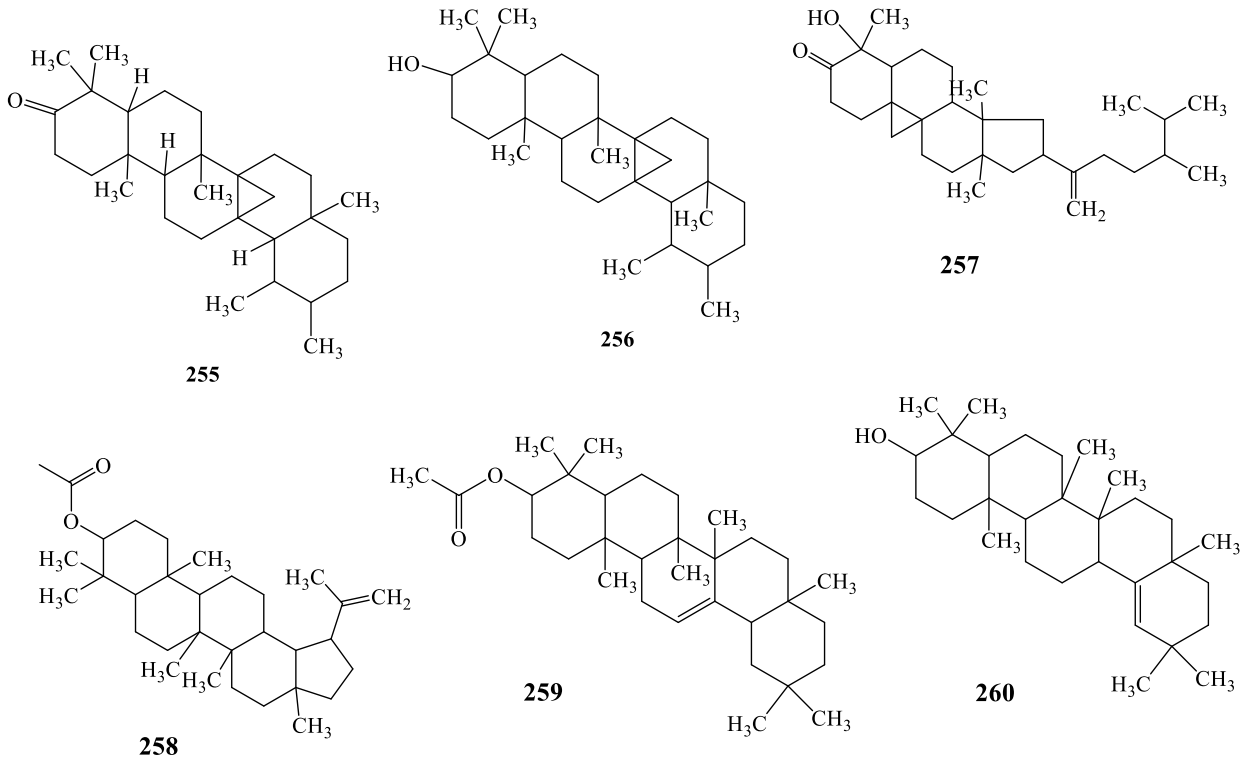

Figure 35: Compounds **255-260** identified from the roots extract of *E. schimperiana*.

4.1.6. Chemical Compositions of Essential Oils

The yield of essential oils obtained by hydrodistillation revealed 0.5, 2.7, 2.0 % (v/w) from the roots of *U. scheflerri*, fruits of Z. *chalybeum* and fruits of *V. dainelli*, respectively. The GC and GC-MS (Table 18, Appendix 21) analysis of essential oils from roots of *U. scheflerri* revealed a total of 58 chemical components, accounting 97.63 % of the total compositions, of which sesquiterpenes (51.8%), oxygenated sesquiterpenes (18.9%), oxygenated monoterpenes (17.2%), monoterpenes (6.9%) and benezenoid compounds (5.2%) are identified. The major constituents were alloaromadendrene (13.0%), camphene (10.0%), β-Maaliene (9.9%), (-)-borneol acetate (9.9%), and (-)-α-gurjunene (5.9%). The remaining compounds ranged from 0.10 to 5.1%. The results are comparable to a previous report [204], on the *Uvaria species*, which reported that thymoquinoldimethyl ether and benzyl benzoate as the major constituents. On the contrary to previous reports from *Uvaria* essential oils out of Ethiopian flora, our findings suggest that thymoquinoldimethyl ether is absent whereas benzyl benzoate was found as a minor constituent.

In the same way, GC and GC-MS (Table 19, Appendix 22) analysis of essential oil *of Z. chalybeum* revealed a total of 18 chemical components, accounting 99.5 % of the total compositions, of which the appreciable amounts were oxygenated monoterpenes (44.4%), followed by monoterpenes (33.3%), sesquiterpenes (16.7%), and oxygenated sesquiterpenes (5.6%). The principal constituents were tricycle [5.3.0.0(3, 9)] decane (82.8%), followed by 2-tridecanone (2.8%), decanal (2.6%), Phenol, 2, 2'-methylene bis [6-(1,1-dimethylethyl)-4-methyl- (2.40%) and limonene oxide trans-(2.2%). The remaining compounds ranged from 0.1 to 1.3%. The results are in consistent to previous studies [205, 206], in accordance with the classes of compounds reported from *Zanthoxylum* species. The recent study showed the major chemical constituents of leaves essential oils of this plant are β-phellanderene and β-myrcene [207]. However, the major constituent in the present study was tricyclo [5.3.0.0(3, 9)] decane (82.8%) suggesting that this compound reported herein for the first time in a fruit of *Zanthoxylum* species could be considered as marker constituent for Ethiopian species.

In a related study, GC and GC-MS (Table 20, Appendix 23) analysis of essential oils from fruits of *V. dainelli* revealed a total of 20 chemical compositions representing 98.8 % of the total oil contents. Meanwhile, the major compounds were sesquiterpenes (55.0%) of the total composition, followed by monoterpenes (25.0%), oxygenated sesquiterpenes (10.3%), and benezenoid compounds (5%). The most abundant chemical constituents were tricyclo [5.3.0.0(3, 9)] decane (69.8%), caryophyllene (5.8%), phenol, 2, 2'-methylenebis [6-(1, 1-dimethylethyl)-4-methyl-(4.8%), neoalloocimen (3.5%) and germacrene D (3.20%). Other chemical components were detected in the range of 0.19-2.99%. The previous studies regarding to essential oils composition of *Vepris* species suggest α-pinene (60.5%) [46] and terpinolene (49.7%) [208], as major constituents. On the contrary, the present study revealed that tricyclo [5.3.0.0(3, 9)] decane (69.9%) as major constituent and reported herein for the first time in a *Vepris* species suggesting this compound could be considered as marker for Ethiopian *Vepris* species.

Table 18: Chemical compositions of essential oils from roots of *U. shceffleri*.

No	**Chemical compositions**	**RT**	**Area (%)**
1.	α-Pinene	4.9748	0.406
2.	Camphene	5.4353	10.004
3.	D-Limonene	6.7197	0.435
4.	Eucalyptol	7.0544	0.244
5.	Bicyclo[2.2.1]heptane, 2-methoxy-1,7,7-trimethyl-	8.1991	0.300
6.	Neoalloocimene	8.5223	0.238
7.	(-)-trans-Myrtanyl acatate	9.303	0.139
8.	Camphene hydrate	9.7265	0.108
9.	endo-Borneol	10.2094	0.172
10.	Fenchyl acetate	10.2876	0.282
11.	2-Pentanone, 5-(2- methylenecyclohexyl)-, stereoisomer	10.5319	0.127
12.	Bicyclo[2.2.1]heptane-2-carboxylic acid, 3,3-dimethyl-, methyl ester	10.7743	0.432
13.	(-)-Borneol acetate	11.3448	9.901
14.	Isobornyl acetate	11.4167	0.486
15.	(+)-Cyclosativene	11.6735	1.581
16.	α-Copaene	11.7625	1.135
17.	Aromadendrene, dehydro-	11.8576	0.800
18.	(-)-α-Gurjunene	12.1795	5.933
19.	Isoledene	12.2867	0.416
20.	δ-Terpinene	12.4774	0.981
21.	α-Terpinyl propionate	12.5788	0.733
22.	11-Isopropylidenetricyclo [4.3.1.1(2,5)] undec-3-en-10-one	12.777	1.100
23.	γ-Amorphene	12.8705	0.253
24.	Rotundene	13.0146	1.922
25.	(+)-γ-Gurjunene	13.0986	0.128
26.	2,5-Dimethoxy-p-cymene	13.1438	0.387
27.	α-Gurjunene	13.1952	1.843

28.	α -Maaliene	13.2567	1.1539
29.	α.-Guaiene	13.4289	0.439
30.	- (+)-β-Selinene	13.5071	2.111
31.	Neoisolongifolene	13.5705	1.478
32.	1,5-Cadinadiene	13.6717	0.254
33.	(+)-δ-Cadinene	13.7702	2.592
34.	7-epi-α-Selinene	13.8639	0.232
35.	Guaia-9,11-diene	13.9008	0.336
36.	α-Cadinene	14.0144	0.164
37.	ButylatedHydroxytoluene	14.2254	0.073
38.	4-Isopropyl-1,6-dimethyl-1,2,3,4-tetrahydronaphthalene	14.3833	0.117
39.	δ-Guaiene	15.1142	0.1745
40.	(-)-Gleenol	15.2635	0.160
41.	Guaiol	15.5413	5.130
42.	Epicubenol	15.5887	0.567
43.	Naphthalene,1,2,3,4,4a,7-hexahydro-1,6-dimethyl-4-(1-methylethyl)-	15.7431	0.286
44.	Aromadendrene, dehydro-	15.8081	0.822
45.	1,1,7,7a-Tetramethyl-1a,2,6,7,7a,7b-hexahydro-1H-cyclopropa[a]naphthalene	15.8781	4.584
46.	β-Guaiene	15.9268	0.218
47.	β-Maaliene	16.0107	9.983
48.	Clovene	16.1513	0.213
49.	Isolongifolenone	16.2447	0.450
50.	Alloaromadendrene	16.3179	12.905
51.	Bulnesol	16.4006	2.269
52.	Neoisolongifolene, 8,9-dehydro-	16.5045	5.185
53.	Aristolediene	16.6404	0.445
54.	11,13-Dimethyl-12-tetradecen-1-ol acetate	16.9824	0.1238
55.	3-Azepan-1-yl-benzo[d]isothiazole 1,1-dioxide	17.6125	0.109

56.	Benzyl Benzoate	18.1853	4.101
57.	4-(p-Methoxyphenylazo)-m-phenylenediamine	21.2837	0.264
58.	Acetonitrile,2-(2-aminophenylamino)-	25.4219	0.203

Table 19: Chemical compositions of essential oils from fruits of *Z. chalybeum.*

No	**Chemical compositions**	**RT**	**Area (%)**
1.	Sabenene	5.936	1.13
2.	β-Thujene	6.109	0.50
3.	β-Myrcene	6.150	1.03
4.	Tricyclo[5.3.0.0(3,9)]decane	6.737	82.40
5.	β-Ocimene	7.123	0.60
6.	Octanal	7.253	0.83
7.	Linalool	8.818	0.25
8.	Limonene oxide, trans-	9.224	2.17
9.	Decanal	10.291	2.62
10.	(±)-Dihydrocarvone	10.810	0.19
11.	Cis-Carveol	10.983	0.23
12.	2-Undecanone	11.590	1.30
13.	β-copaene	12.637	0.47
14.	(-)-Isogermacrene D	12.866	0.11
15.	trans-2-Dodecen-1-ol	13.017	0.25
16.	Germacrene D	13.511	0.29
17.	2-Tridecanone	14.157	2.78
18.	Phenol, 2,2'-methylenebis[6-(1,1-dimethylethyl)-4-methyl-	17.433	2.40

Table 20: Chemical compositions of essential oils from fruits of *V. dainelli*.

No	**Chemical compositions**	**RT**	**Area (%)**
1.	D-Limonene	6.7272	0.97
2.	(+)-α-Pinene	6.8432	1.08
3.	Tricyclo[5.3.0.0(3,9)]decane	7.1348	69.86

4.	Neoalloocimene	8.5222	3.50
5.	Cosmene	8.8047	0.30
6.	δ-Elemene	11.2605	0.72
7.	β-Elemene	12.1817	0.90
8.	β-Copaene	12.4704	2.92
9.	Caryophyllene	12.6389	5.85
10.	ε-Muurolene	13.0417	0.85
11.	1,4,7,-Cycloundecatriene, 1,5,9,9-tetramethyl-, Z,Z,Z-	13.1359	0.44
12.	Germacrene D	13.511	3.21
13.	(Z)-γ-Bisabolene	13.5757	1.38
14.	β-Cubebene	13.6717	0.61
15.	δ-Cadinene	13.7711	0.39
16.	2-Tridecanone	14.1593	0.33
17.	Cadina-3,5-diene	15.2963	0.28
18.	τ-Cadinol	16.0085	0.19
19.	α-Cadinol	16.2897	0.24
20.	Phenol,2,2'-methylenebis[6-(1,1-dimethylethyl)-4-methyl-	17.4468	4.80

4.2. Biological Activity

4.2.1. Cytotoxicity and Cell Cycle Analysis

4.2.1.1. Cytotoxicity Analysis

The cytotoxicity assay of five alkaloids (**13, 17, 55, 67** and **245**) isolated from *V .dainelli* and *Z. chalybeum* were evaluated using the MTS assay against MDA-MB-231 and MCF-7 breast cancer cell lines. The results revealed that the alkaloids induced a significant reduction of cell growth of both breast cancer cell lines in a concentration-dependent manner. The IC_{50} values for tested alkaloids and positive control (doxorubicin) on MDA-MB-231 and MCF-7 cell lines are presented in Table 21. Among the studied alkaloids chelerythrine (**55)** isolated from the root extract of *Z. chalybeum* and evodiamine (**245)** from the fruit extract of *V. dainelii* showed the highest potency and selectivity against the aggressive and metastatic MDA-MB-231 cell line at low micromolar concentrations (IC_{50}= 1.73 ± 0.48 and 3.616±0.51 µM, respectively) with

respect to doxorubicin (0.23 µM). They are also effective against MCF-7 breast cancer cell lines while compared with standard doxorubicin. On other hand, dihydrochelyrithrine (**67**) displayed higher activity against MDA-MB-231 cell at lower concentration (IC_{50}= 24.14 ± 5.24 µM) compared to evoxanthine (**17**) and arbronine (**7**) (IC_{50}= 55.99 ± 12.17 and 69.30 ± 5.34 µM, respectively). In contrast, evoxanthine (**17**) exhibited higher cytotoxicity against MCF-7 cell line (IC_{50}= 17.44 ± 0.87 µM) compared with its lipophilic analogue arbronine (**13**) (IC_{50}= 40.63 ± 2.30 µM), as well as chelerythrine (**55)** and evodiamine (**245) (**IC_{50}= 22.47 ± 0.84 and 26.47 ± 5.95 µM, respectively). Dihydrochelerithrine (**67**) displayed weak activity against MCF-7 cell lines (IC_{50} = 109.11 ± 11.46 µM) compared with respect to standard doxorubicin (0.23 µM).

Table 21: Cytotoxicity activity against breast cancer cell lines.

Compounds	**MDA-MB-231**	**MCF7**
	IC_{50} (µM)	**IC_{50} (µM)**
17	55.99 ± 12.17	17.44 ± 0.87
13	69.30 ± 5.34	40.63 ± 2.30
245	1.73 ± 0.48	26.47 ± 5.95
55	3.616 ± 0.51	22.47 ± 0.84
67	24.14 ± 5.24	109.11 ± 11.46
Doxorubicin	0.23	9.6

Values of 50% inhibitory concentration (IC_{50}) are the average of three independent assays and expressed as mean ± standard error.

4.2.2. Cell cycle Analysis

In order to investigate the effect of studied five alkaloids (**13, 17, 55, 67** and **245**) on the cell cycle of MDA-MB-231 and MCF-7 cell lines the DNA levels was measured after treatment. The results showed that evodiamine (**245**) highly arrested the cells in the G2/M phase, especially in the case of MCF7 cell line where almost all the cells were arrested at this checkpoint, whereas studied acridones (**17** and **13**) showed slight influence on the cell cycle in both cell lines by arresting some cells in the G2/M phase, preventing cells with damaged DNA from entering mitosis (Figure 36). Chelerythrine (**55**) and dihydrochelerythrine (**67**) showed the influence on the cell cycle in MDA-MB-231 cell line by arresting some cells in the G_2/M phase, preventing

cells with damaged DNA from entering mitosis. However, these alkaloids did not show significant influence in MCF7 cells, which were mostly arrested in G_0/G_1 phase (Figure 37).

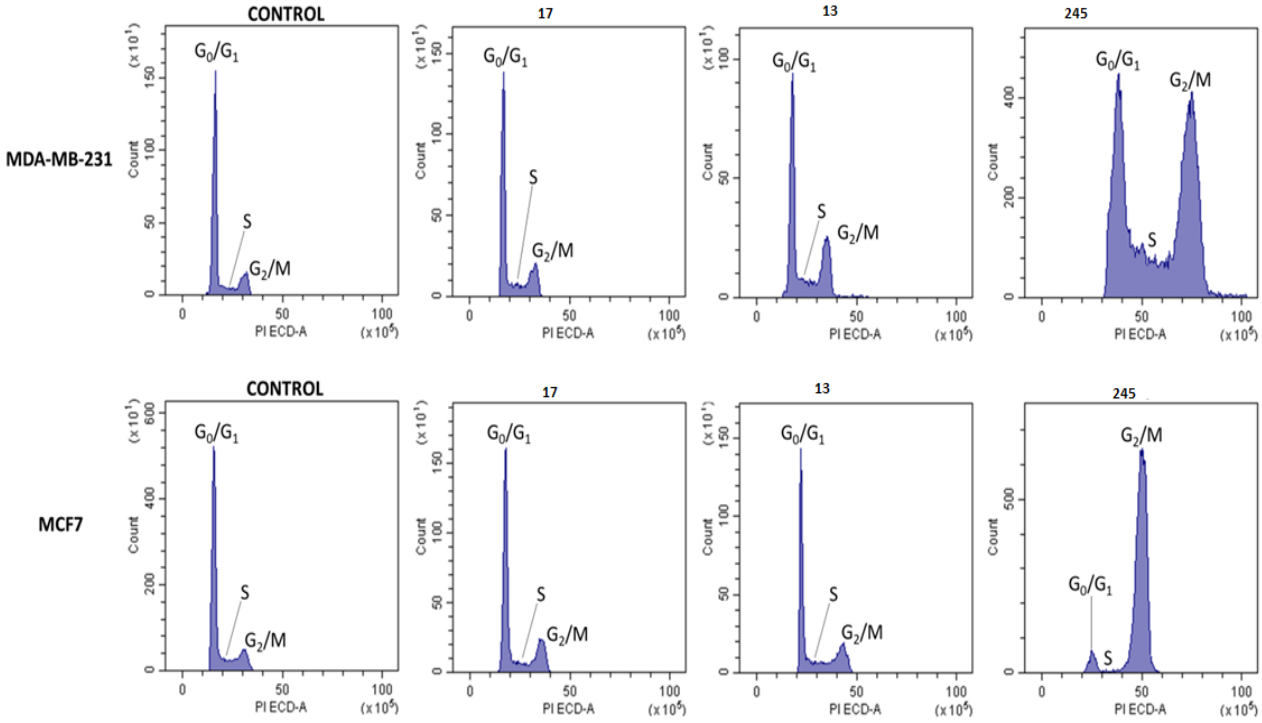

Figure 36: Cell cycle histograms obtained from the untreated cell lines (control) and after treatment of both cell lines with compounds at IC_{50} concentrations (**17**) (56 µM in MDA-MB.-231 and 17.4 µM in MCF7), (**13**) (69.3 µM in MDA-MB.-231 and 40.6 µM in MCF7) and (**245**) (1.7 µM in MDA-MB.-231 and 26.5 µM in MCF7).

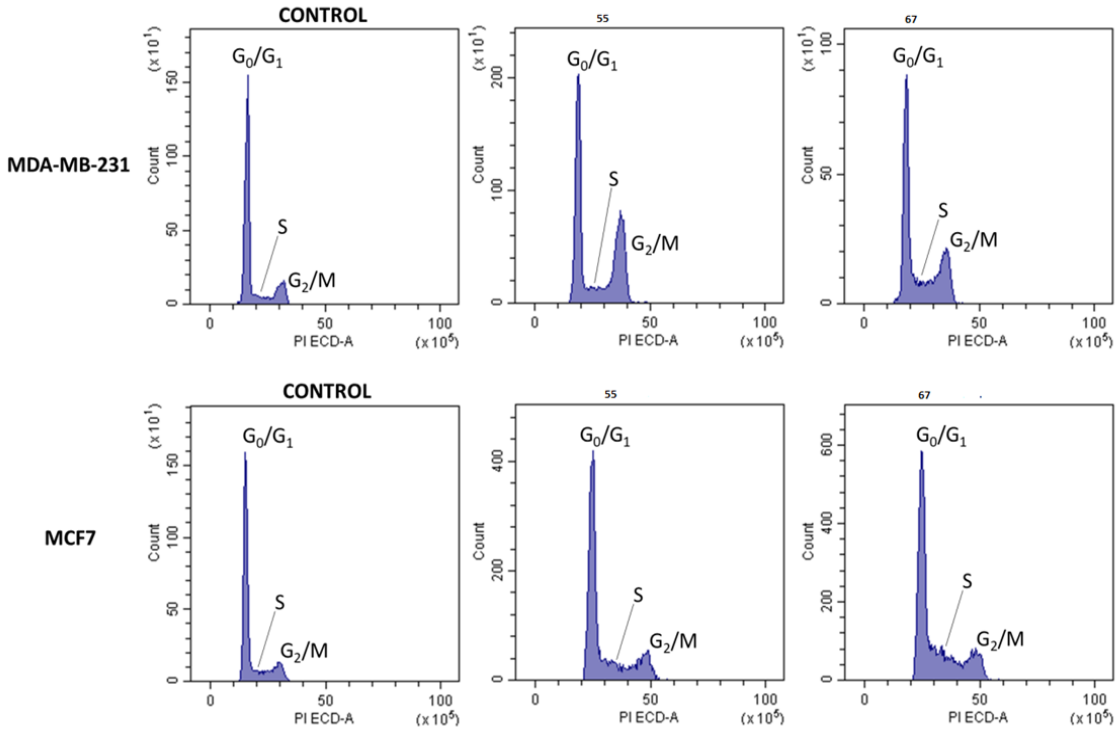

Figure 37: Cell cycle histograms obtained from the untreated cell lines (control) and after treatment of both cell lines with compounds (**55**) (3.6 µM in MDA-MB.-231 and 22.5 µM in MCF7) and (**67**) (24.1 µM in MDA-MB.-231 and 109.1 µM in MCF7).

4.2.3. Antimicrobial Analysis

The antimicrobial activity (Table 22) of root extract of *U. scheffleri* and isolated compounds (**13**, **17**, **55**, **67**, **98**, **245, 248**, **249,** and **252**) were tested *in vitro* against standard reference human pathogenic bacterial strains: gram positive (*S. aureus*) and gram negative (*E. coli*) as well as a fungal strain (*C. albicans*). The results showed chelerythrine (**55**), uvarindole-F (**248)**, and dichloromethane extract of *U. scheffleri* displayed potential antibacterial activity against *S. aureus* (MIC 12.5, 6.25, and 12.5 µg/mL) respectively, compared with gentamicin (5 µg/mL against *S. aureus*), and also compound (**55**) and compound (**248**) showed antifungal effect on *C. albicans* (50 and 12.5 µg/mL, respectively) compared with fluconazole (8 µg/mL against *C. albicans*). Evoxanthine (**13**), arbronine (**17**), evodiamine (**245**), isolated from *V. dainelli* dihydrochelerythrine (**67)** from *Z. chalybeum* and uvaindole-C derivative (**249**) isolated from *U. sheffleri* did not show any effect on both microorganisms. However, Lupeol (**98)** and suberosin derivative (**252)** isolated from *C. burgensis* and *E. schimperiana* respectively showed weak

antibacterial effect against both gram positive and gram negative bacterial strains, but were inactive to fungal stain. The results of benzophenathridine alkaloids (**55** and **67**) are in consistency with a previous reported study [209]. The antibacterial activity of dichloromethane extract of *U. sheffleri* showed higher activity than uvarindole–F (**248**) which was isolated from the same extract of *U. sheffleri* which might be accounted by synergic effects of compounds within the extract or minor constituents which were not isolated by our study might be responsible for the observed activity. Both extract and isolated compound (**248)** of root of *U. scheffleri*, **55** from *Z. chalybeum* were observed to be effective against gram positive bacterial strains only. The findings of this study support the traditional use of the root decoction of *U. scheffleri* and *Z. calybeum* for the treatment of infectious diseases caused by gram-positive bacteria strains such as pneumonia, asthma and sore throat [68, 79].

Table 22: Antimicrobial activity against selected microorganisms (MIC in µg/mL)

Compounds	***Staphylococcus aureus***	***Escherichia coli***	***Candida albicans***
13	NE	NE	NE
17	NE	NE	NE
245	NE	NE	NE
55	12.5 µg/mL	NE	50 µg/mL
67	NE	NE	> 400µg/mL
248	12.5 µg/mL	NE	6.25 µg/mL
249	NE	NE	NE
98	>100 µg/mL	>100 µg/mL	NE
252	>100 µg/mL	>100 µg/mL	NE
UE	6.25 µg/mL	NE	6.25 µg/mL
Gentamicin	5	5	ND
Fluconazole	ND	ND	8

UE, dichloromethane root extract of *U. scheffleri*, ND, not determined; NE. = no effect

4.2.4. *In vitro* Larvicidal Activity Essential Oils

The larvicidal activity of the essential oils were evaluated *in vitro* against *Anisakis* type I. The results revealed that *U. scheffleri* essential oils displayed potential larvicidal activity in marinade

solution against *Anisakis* type I at 0.1% concentration, the LT_{100} was 12 h., at 0.5 and 1% concentrations, was 7 h, whereas at high concentration 5%, was 5 h. The result showed the dose dependent activity of essential oils with respect to time. At low concentration the mobility of the larvae was decreased with respect to time, and died completely when the exposure time increased (Table 23, Figure 38).

In the same way, *Z. chalybeum* essential oils displayed potential larvicidal activity at the lowest concentrations, at 0.1% with 12 h, 0.5 and 1% with 7 h exposure time to achieve 100% mortality, whereas at 5% concentration LT_{100} was 3 h. The average motility rate revealed that the larvicidal activity is proportional to the concentration of the chemical constituents of the essential oil with respect to time (Table 23, Figure 38).

Accordingly, *V. dainelli* essential oils revealed significant larvicidal activity at 1 and 5%, with LT_{100} of 7 h and 5 h, respectively, and the larvicidal activity of LT_{100} observed at low concentrations of 0.1 and 0.5% was 24 and 12 h respectively. The larval movement was restricted as the concentration of essential oil increased. At the highest concentration of5%, the larvae started to die within 4h, and completely died in 5h; the potential larvicidal activity of *V. dainelli* essential oils revealed at high concentration with respect to time (Table 23, Figure 38).

The larvicidal capacity of the tested essential oils show the most effective essential oils at the lowest concentration of 0.1% are that of *U. scheflerri* and *Z. chalybeum*, but only after 12 h. Moreover, *Z. chalybeum* essential oil shows the most effective antiparasitic activity at the highest concentration tested of 5% after 3 h of marinating. The larvicidal activity of essential oils is related to the synergistic effects of the terpenes such as monoterpenes and sesquiterpenes identified in the essential oils, in agreement with previous reports [27, 171], and the high activity could be attributed to the damage caused to the cuticle and digestive apparatus of the parasite.

Furthermore, future studies should also include the mechanisms responsible for this larvicidal activity. The increase of worldwide prevalence of *anisakiasis* and the lack of effective pharmacological treatments as well as the effectiveness of tested essential oils against *Anisakis* larvae suggest that the essential oils could be applied in the sea food marinating processes to

prevent human anisakiasis. This initiative has interesting applications since marinated sea food products are always kept in oil after the marination process and the potential use of marinade solution enriched with essential oils of *U. scheflerri*, *Z. chalybeum*, and *V. dainelli* could represent, according to our results, an alternative method for the inactivation of Anisakidae larvae, but these results have to be supported by *in vivo* studies.

Table 23: LT100 (lethal time required to kill 100% of nematodes) and LT50 (lethal time required to kill 50% of nematodes) of *U. scheflerri*, *Z. chalybeum* and *V. dainelli* essential oils.

Essential oil	Concentrations	**LT_{50}**	**LT_{100}**
Uvaria scheflerri	5%	-	5
	1%	5	7
	0.5%	-	7
	0.1%	-	12
	0%	-	-
Zanthoxylum chalybeum	5%	-	3
	1%	5	7
	0.5%	5	7
	0.1%	5	12
	0%	-	-
Vepris dainelli	5%	-	5
	1%	-	7
	0.5%	-	12
	0.1%	-	24
	0%	-	-

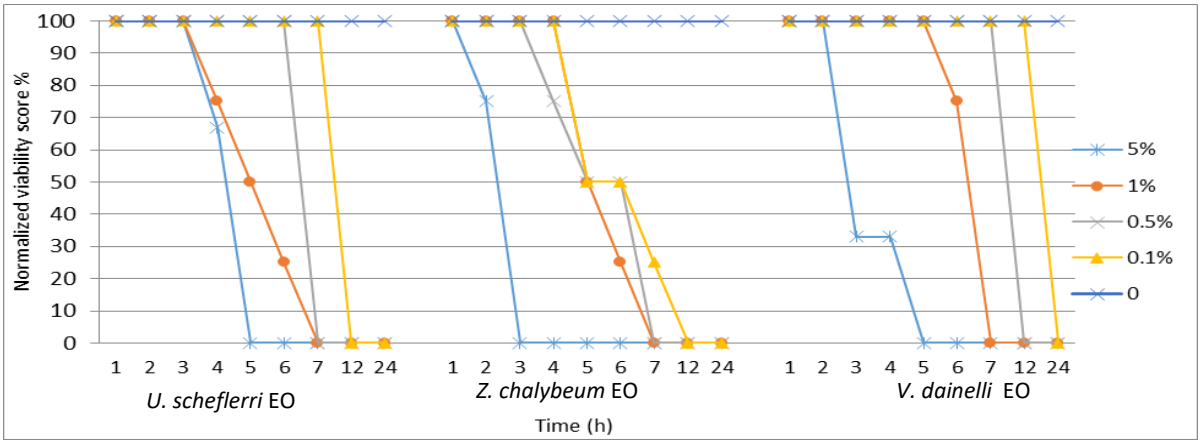

Figure 38: Viability score (%) of L3 larvae of Anisakis Type I in marinate solution with 0.1%, 0.5%, 1%, 5% of *U. scheflerri*, *Z. chalybeum* and *V. dainelli* essential oils (EOs) respectively. Control larvae remained alive along the experiment.

4.2.5. Cytotoxicity Analysis of Essential Oils

Results of cell viability assay on VERO cell line revealed the level of cytotoxicity increased with the increasing of concentrations or cytotoxic effects of each other in a concentration-dependent manner (Figure 39). According to Döll-Boscardin et al (2012) report, the cytotoxic level of essential oils with the IC_{50} values between 10–50 μg/mL represent a strong cytotoxic activity, between 50–100, 100-200, and 200-300 μg/mL indicate moderate, weak, and very weak cytotoxic properties, respectively. Furthermore, IC_{50} values higher than 300 μg/mL represent no cytotoxicity [210]. Considering this comparison, the essential oils of *U. sheffleri*, *Z. Chelybeum*, and *V. dainelli* demonstrated moderate cytotoxicty on VERO cell line, IC_{50} Values of 65.46 ± 0.48, 83.88 ± 2.30, and 96.82±5.95 µg/mL, respectively. This result indicated that, using the aforementioned EOs as a food preservative in marinating processes might be serve as anti Anisakiasis type I considering their weak cytotoxic effect at lower concentration which was possessed larvicidal properties.

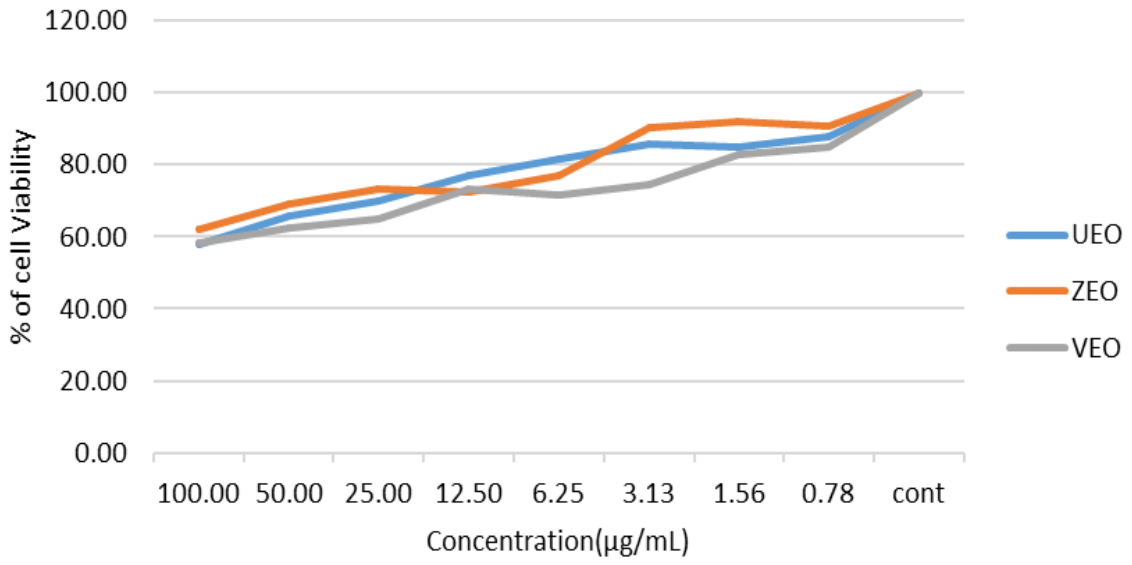

Figure 39: Effect of concentration on cytotoxicity of *U. scheflerri* (UEO), *Z. chalybeum* (ZEO) and *V. dainelli* (VEO) essential oils respectively against VERO cells after 24 h incubation by MTT assay.

4.3. Computational Study of Isolated Compounds

4.3.1. Molecular Docking Analysis of Isolated Compounds

Molecular docking is an important method for understanding the bioactivity mechanism of compounds by examining a ligand-protein interaction [211]. Thus, herein investigated the interactions of fourteen isolated compounds (**55**, **62, 247**, **67**, **248-250**, **98**, and **252**) with *E.coli* DNA gyrase B and (**244**, **17**, **13**, **245**, **9**, **55**, **62, 247**, **67**, **248-250**, **98**, and **252**) human DNA topoisomerase IIα, the target enzymes for antimicrobial and anticancer agents, respectively [212, 213].

4.3.1.1. Interactions of Isolated Compounds with Human DNA Topoisomerase IIα

The interactions of fourteen isolated compounds (**9**, **13**, **17**, **55**, **62**, **67, 98, 244**, **245**, **247-250** and **252**) with human DNA topoisomerase IIα, which enzyme is a target for many anticancer agents, revealed minimum binding energy ranging from -5.9 to -6.3 kcal/mol. The binding affinity, H-bond and residual interactions with human DNA topoisomerase II α were presented in Table 24 and Figure 40. Acridones (**13**, **17**, and **244**) and indolequinozoline alkaloid (**245**) isolated from *V. dainelli* showed better binding affinity (-5.9, -6.0, -6.0 and -6.3 kcal/mol), respectively. Among them

evodimine (**245**) displayed appreciable minimum binding energy (-6.3 kcal/mol) and DNA interactions profile with amino acid residues Asp-479, Ser-480, Glu-477, Ala-481, Arg-503, Gly-478, Gly-504 and nucleic acid residues DT-8, DT-9, DG-10, DG-12 and DG-13 compared to vosaroxin (-6.2 kcal/mol). Arborinine (**13**) and norevoxanthine (**244**) displayed moderate binding affinity but similar amino acid and DNA binding patterns within the binding pocket compared to vosaroxin. In the same study, benzophenanthridine alkaloids (**55**, **62**, **67** and **247**) isolated from the root extract of *Z. chalybeum* showed strong binding affinity ranged from -6.1 to -6.6 kcal/mol compared with standard vosaroxin (-6.2 kcal/mol). Chelerythrine (**55**) and dihydrochelerythrine (**67**) showed higher binding affinity (-6.4 and -6.3 kcal/mol), similar residual and DNA interaction profile with amino acid residues Asp-479, Ser-480, Glu-477, Ala-481, Arg-503, Gly-478, Gly-504 and nucleic acid residues DT-8, DT-9, DG-10, DG-12 and DG-13 compared to vosaroxin (- 6.2 kcal/mol). Furthermore, compounds **248** and **249** isolated from *U. shaffleri,* compounds **250** and **98** which were isolated from *C. bugenisis* and compound **252** isolated from *E. schimperiana* showed moderate binding affinity, -5.4 and -5.9 kcal/mol, similar residual Asp-479 and nucleic acid residues DC-8, DT-9 and DG-10, compared to vosaroxin (-6.2 kcal/mol). The docking study results- proved that compounds **13, 17, 55**, **67** and **247** could act as DNA topoisomerase IIα inhibitors. Topoisomerase IIα is an enzyme essential for DNA replication, chromosome condensation and chromosome segregation. Inhibitors of topoisomerase IIα are important drugs used in the therapy of many neoplasms including breast cancer, lung cancer, testicular cancer, lymphomas and sarcomas. Hence, our finding suggest that the aforementioned compounds could serve as potential anticancer agents.

Table 24: Molecular docking scores and residual amino acid interactions of isolated compounds against human DNA topoisomerase II α

Ligands	Affinity (kcal/mol)	H-bond	DNA	Residual interactions	
				Hydrophobic/Pi-Cation	Van dar Waals
244	-6.0	Ser-480	DC-8, DT-9, DG-10	Asp-497, Arg-503	Glu-477, Gly-478, Ala-481
17	– 5.9	--	DC-8, Dt-9	Arg-503, Asp-557	Asp-479, Glu-477, Gly-478, Gly-504
13	– 6.0	Asp-479, Ser-480	DC-8, DT-9, DG-10	Gly-477, Gly-478, Arg-503	Asp-557, Gly-504
245	– 6.3	Tyr-821	DT-8, DT-9, DG-10, DG-13	Asp-479. Arg-503, Gly-478	Gly-504
9	– 5.9	--	DT-8, DT-9, DG-13	Arg-503,	Asp-479, Glu-477, Ser-480, Gly-504, Ala-481, Asp-557
55	-6.4	Asp-479, Ser-480	DC-8, DT-9, DG-10, DG-13, DC-14	Arg-503	Glu-477, Gly-478, Gly-504
62	– 6.2	Asp-479	DT-9, DG-10, DG-12	Ser-480, Arg-503, Gly-478, Asp-557	Glu-477
247	– 6.1	Ser-480	DT-8, DT-9, DG-10, DA-13, DG-14	Asp-479, Arg-503, Glu-477, Thr-821, Asp-557	Gly-478
67	– 6.3	Asp-479	DC-8, DT-9, DG-10, DG-13, DC-14	Arg-503	Ser-480, Gly-478
248	-5.4	Ser-480,	DC-8, DT-9,	Tyr-821	Asp-479, Gly-

		Glu-477, Asp-577	DG-10		478, Ala-481, Gly-776
249	-5.6	Glu-477	DC-8, DT-9	Arg-503	Gly-478, Tyr-821, Asp-557
250	-5.3	Gln-778, Tyr-821	DG-7, DC-8, DT-9, DG-10	--	Asp-557, Glu-477, Asp-559, His-774
98	-5.5	--	DG-7, DC-8, DT-9, DG-10	His-775	Ala-779, Arg-503, Asp-479, Glu-477, Asp-561
252	-5.9	Ser-480, Asp-479	DC-8, DT-9, DG-10	Arg-503	Glu-477, Gly-478, Asp-557
Vosaroxin	– 6.2	Asp-479, Ser-480, Glu-477, Ala-481, Arg-503	DT-8, DT-9, DG-10, DA-12, DG-13	--	Gly-478, Gly-504

DA= Deoxyadenosine, DG= Deoxyguanosine, DT= Deoxythymidine, and DC = Deoxycytosine

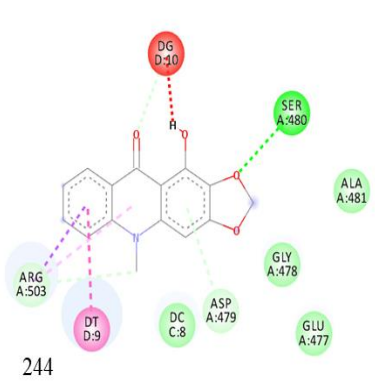

244

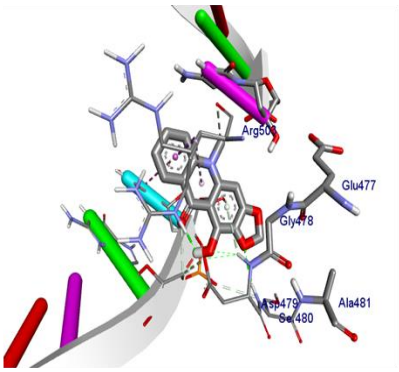

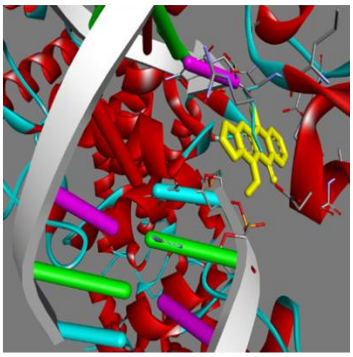

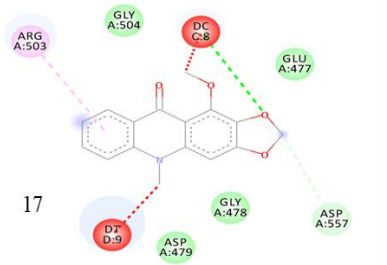
ARG A:503
GLY A:504
DC C:8
GLU A:477
GLY A:478
ASP A:557
DT D:9
ASP A:479

17

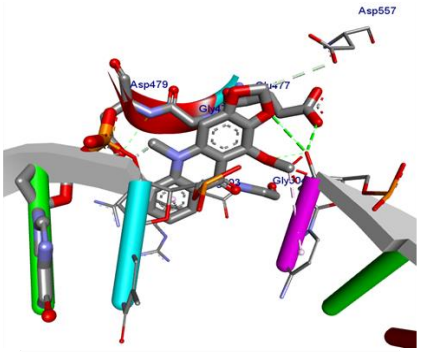
Asp557
Asp479
Gly504

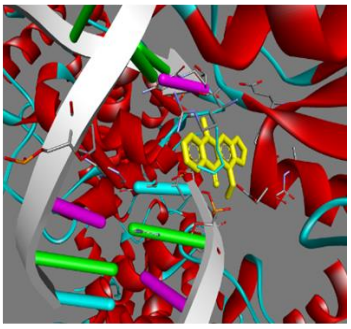

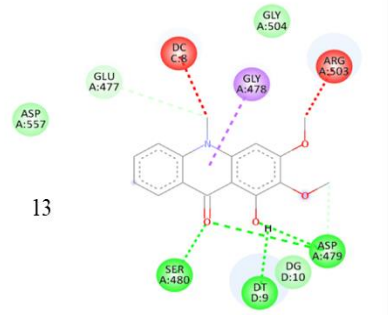
GLY A:504
DC C:8
GLU A:477
GLY A:478
ARG A:503
ASP A:557
ASP A:479
SER A:480
DG D:10
DT D:9

13

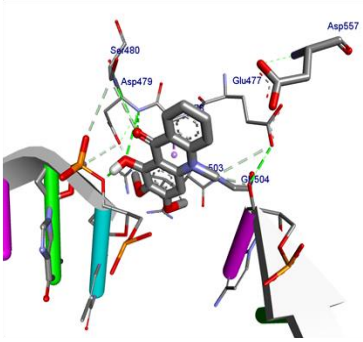
Asp557
Ser480
Asp479
Glu477
Gly504

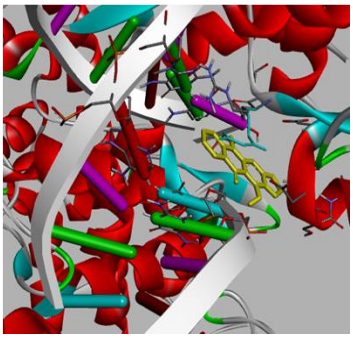

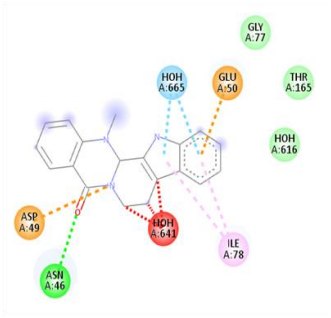
GLY A:77
HOH A:665
GLU A:50
THR A:165
HOH A:616
ASP A:49
HOH A:641
ILE A:78
ASN A:46

245

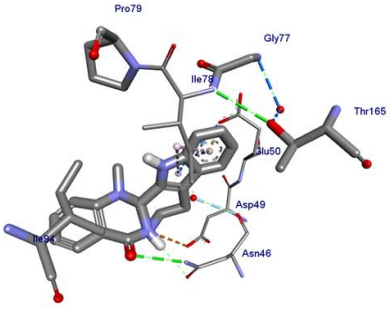
Pro79
Gly77
Ile79
Thr165
Glu50
Asp49
Asn46

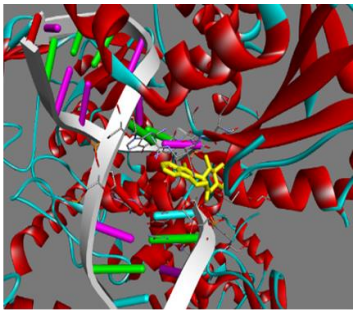

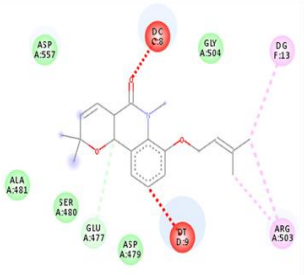
ASP A:557
DC C:8
GLY A:504
DG F:13
ALA A:481
SER A:480
GLU A:477
DT D:9
ASP A:479
ARG A:503

9

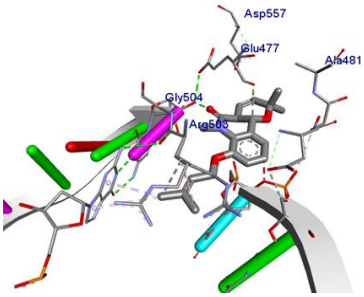
Asp557
Glu477
Ala481
Gly504
Arg508

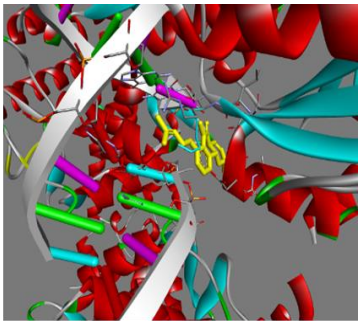

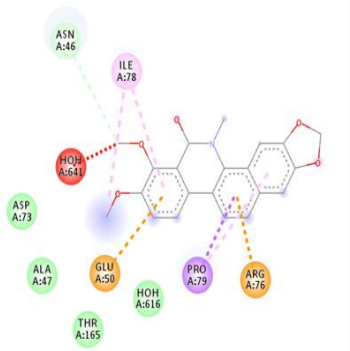
ASN A:46
ILE A:78
HOH A:641
ASP A:73
ALA A:47
GLU A:50
PRO A:79
ARG A:76
HOH A:616
THR A:165

55

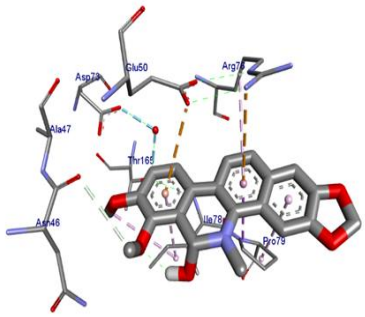
Asp73
Glu50
Arg76
Ala47
Thr165
Asn46
Ile78
Pro79

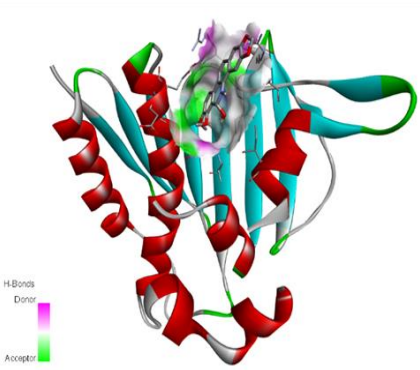
H-Bonds
Donor
Acceptor

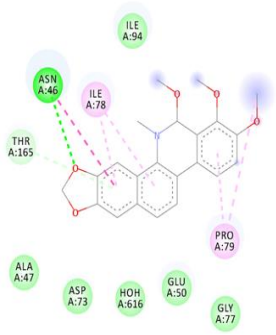
ILE A:94
ASN A:46
ILE A:78
THR A:165
PRO A:79
ALA A:47
ASP A:73
HOH A:616
GLU A:50
GLY A:77

62

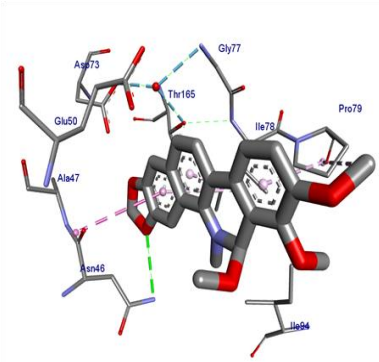
Asp73
Gly77
Thr165
Pro79
Glu50
Ile78
Ala47
Asn46
Ile94

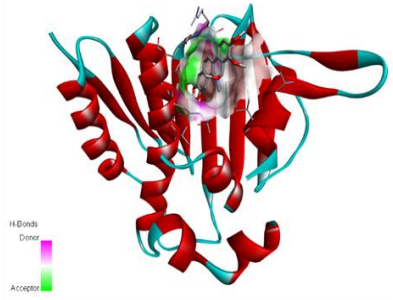
H-Bonds
Donor
Acceptor

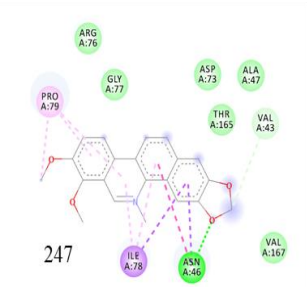
ARG A:76
GLY A:77
ASP A:73
ALA A:47
PRO A:79
THR A:165
VAL A:43
ILE A:78
ASN A:46
VAL A:167

247

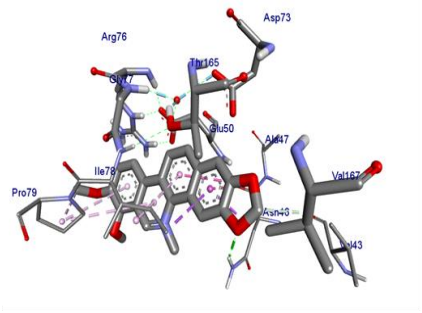
Asp73
Arg76
Thr165
Glu50
Ala47
Ile78
Pro79
Asn43
Val167

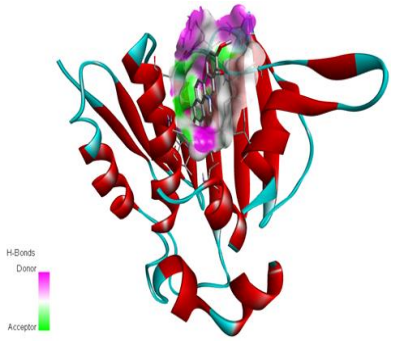
H-Bonds
Donor
Acceptor

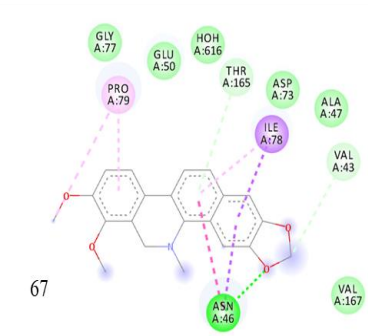
GLY A:77
GLU A:50
HOH A:616
THR A:165
PRO A:79
ASP A:73
ALA A:47
ILE A:78
VAL A:43
ASN A:46
VAL A:167

67

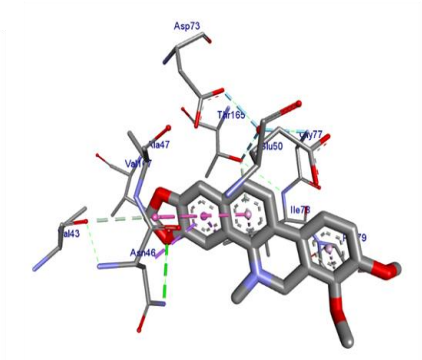
Asp73
Thr165
Ala47
Glu50
Gly77
Ile78
Asn46

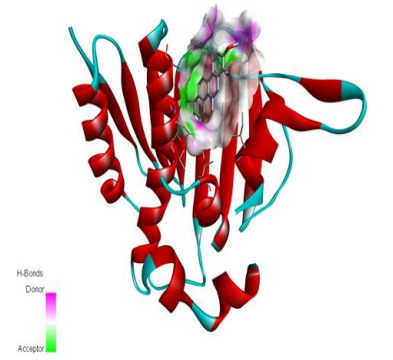
H-Bonds
Donor
Acceptor

248

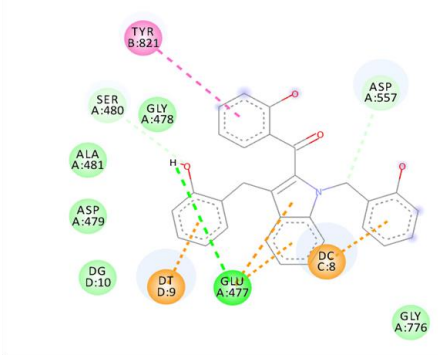
TYR B:821
SER A:480
GLY A:478
ASP A:557
ALA A:481
ASP A:479
DG D:10
DT D:9
GLU A:477
DC C:8
GLY A:776

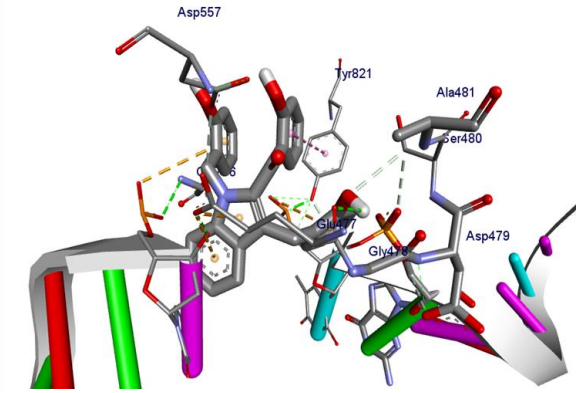
Asp557
Tyr821
Ala481
Ser480
Glu477
Gly478
Asp479

249

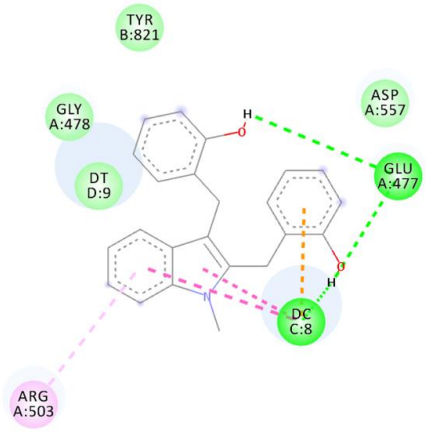
TYR B:821
GLY A:478
ASP A:557
DT D:9
GLU A:477
DC C:8
ARG A:503

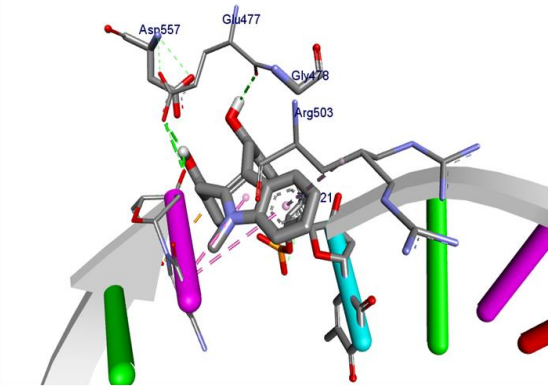
Asp557
Glu477
Gly478
Arg503

250

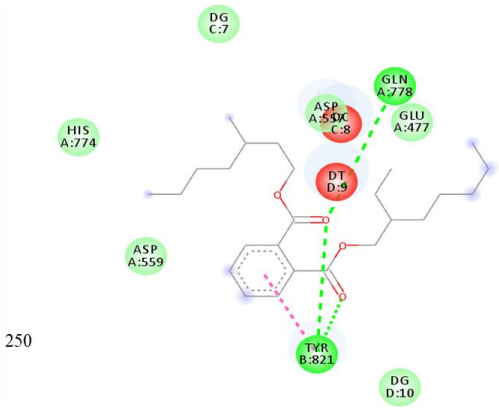
DG C:7
GLN A:778
ASP A:559
DC C:8
GLU A:477
HIS A:774
DT D:9
ASP A:559
TYR B:821
DG D:10

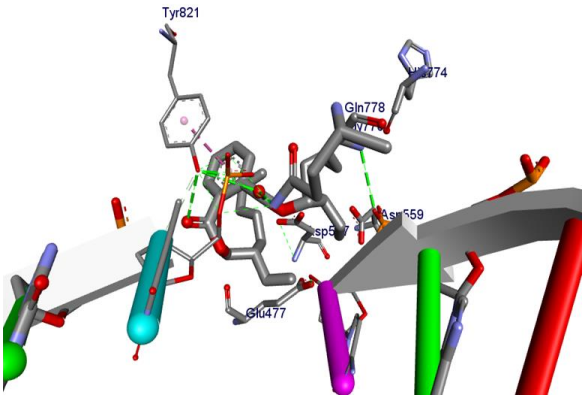
Tyr821
Gln778
Asn559
Glu477

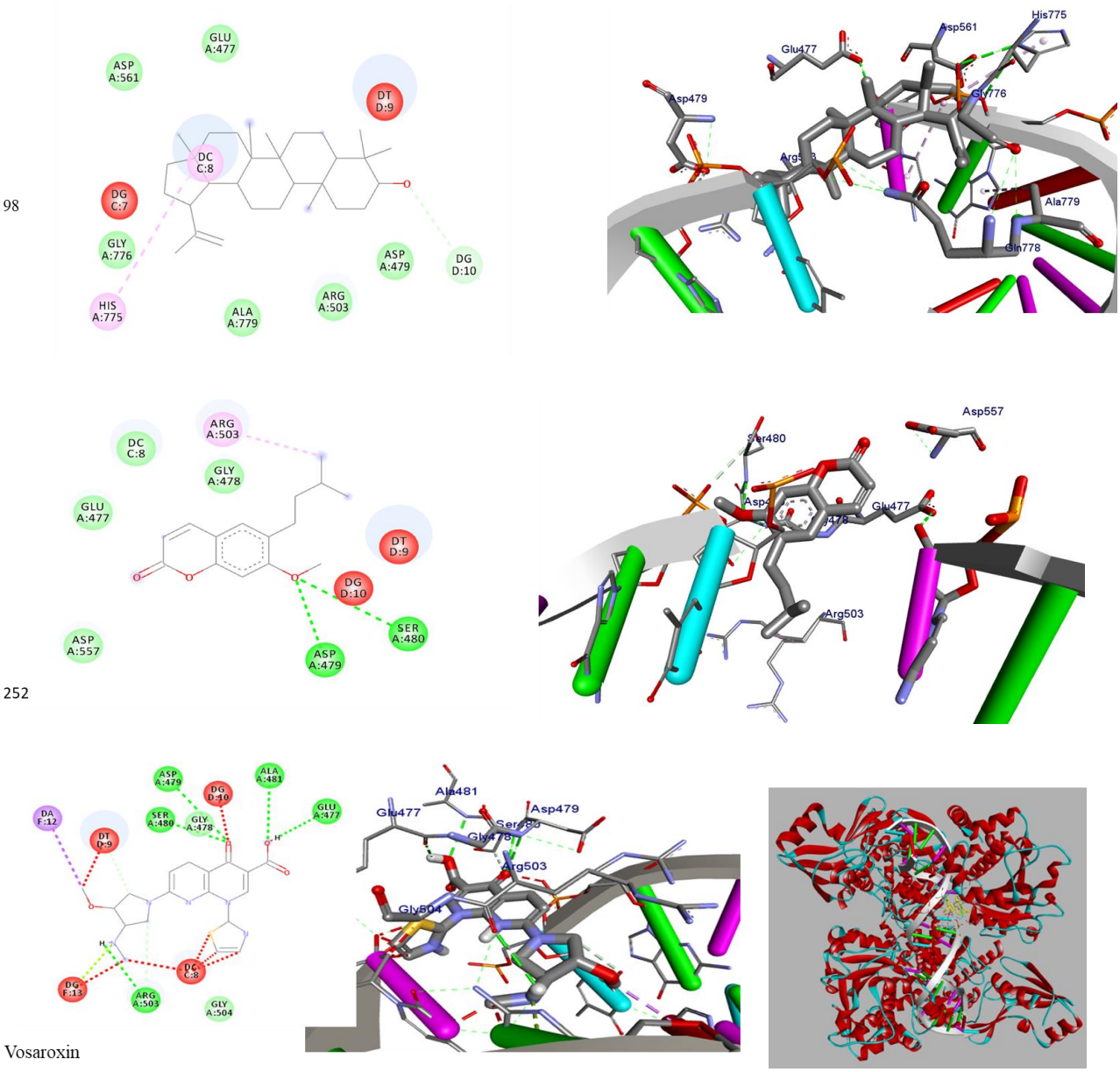

Figure 40: The 2D and 3D binding interactions of isolated compound **(9, 13, 17, 55, 62, 67, 98, 244, 245, 247-250 and 252)** and standard vosaroxin against human topoisomerase II α (PDB ID: 3QX3) respectively. Hydrogen bonds between compounds and amino acids are shown as green dash lines, hydrophobic interaction is shown as pink lines.

4.3.1.2. Interactions of isolated compounds with *E.coli* DNA gyrase B

Fourteen isolated compounds (**55**, **62**, **247**, **67**, **98**, **248-250**, **and 252**) were investigated herein for their interaction with *E.coli* DNA gyrase B, which enzyme is a potential target in study mode of

action to antibacterial agents [214]. The results obtained from the molecular docking demonstrated that all isolated compounds have showed binding affinity for target protein *E.coli* DNA gyrase B when compared with ciprofloxacin. The binding affinity, H-bond and residual interactions with *E.coli* DNA gyrase B are presented in Table 25 and Figure 41.

Benzophenanthridine alkaloids, the binding affinity ranging from -6.5 to -7.5 kcal/mol. Among them, compounds (**55**), (**247**), and (**67**) showed hydrogen bond interaction with active site amino acid residue Asn-46 at a distance of 1.5A^{o}. However, compound (**62)** does not form a hydrogen bond with any amino acid within the binding pocket. The hydrophobic interactions were observed for chelerythrine (**55**) with Ile-78, Pro-79, Val-43 amino acids, (**62**) with Arg-76, Asn-46, Glu-50, Ile-78, and Pro-79, (**247**) with Ile-78, Pro-79, and Thr-165, and (**67**) with Ile-78, Pro-79, Val-43, and Thr-165, suggesting the compounds may act as potential inhibitors of DNA gyrase B enzyme. In the same way compound (**248**-**250, 98,** and **252**), compound (**235**) which is isolated from *Uvaria schefflerri* have showed high minimum binding affinity (7.2 kcal/mol) to the docked protein. The rest other compounds (**249**, **250, 98** and **252**) were showed moderate binding affinity (-6.0 to -6.9 kcal/mol) with respect to standard ciprofloxacin (7.2 kcal/mol). Their hydrophobic interactions were indicated in Table 25.

From the docked ligands, chelerythrine (**55**) and dihydrochelerythrine (**67**), and Uvarindole-F (**248**) showed comparable binding affinity and amino acid interactions with the value ranged from 7.2-7.7 kcal/mol comparable to ciprofloxacin (-7.2 kcal/mol). The docking data supported by *in vitro* experimental study for Chelerythrine (**55**) and Uvaridole-F (**248**) showed a potential antibacterial effect against *S. aurues* suggesting that these compounds can be considered as lead drug candidates against human pathogenic microorganism.

Table 25: Molecular docking scores and residual amino acid interactions of isolated compounds against *E.coli* DNA gyrase B (PDB ID: 6F86).

Ligand	Affinity (kcal/mol)	H-bond	Residual interactions	
			Hydrophobic/Pi-Cation	Van der Waals
55	-7.4	Asn-46	Ile-78, Pro-79, Val-43	Asp-73, Ala-47, Arg-76, Gly-77, Thr-165, Val-167
62	–6.8	--	Arg-76, Asn-46, Glu-50, Ile-78, Pro-79	Asp-73, Ala-47, Thr-165
247	–6.5	Asn-46	Ile-78, Pro-79, Thr-165	Asp-73, Ala-47, Gly-77, Glu-50, Ile-94
67	–7.5	Asn-46	Ile-78, Pro-79, Val-43, Thr-165	Asp-73, Ala-47, Glu-50, Gly-77, Val-167
98	-6.6	Asn-46, Glu-50	Pro-79	Ala-47, Asp-49, Ile-78, Arg-76, Gly-77
248	-7.3	Asn-46	Ala-53, Glu-50, Ile-78, Ile-94	Asp-73, Gly-77, Val-120
249	-6.2	Arg-76, Glu-50	Ile-78, Pro-79, Ile-94	Asp-73, Asn-46, Gly-77
250	-6.0	Asn-46	Asp-49, Val-43, Val-71, Val-167, Ile-78, Ile-94	Asp-73, Thr-165, Glu-50, Gly-77, Pro-79
252	-6.9	Asp-73, Thr-165	Val-43, Ile-78, Ile-167	Glu-50, Gly-77, Val-71, Asn-46, Ala-47
Ciprofloxacin	**–7.2**	Asp-73, Arg-76, Thr-165	Asn-46, Ile-78, Glu-50, Gly-77	Ala-47, Pro-79

55

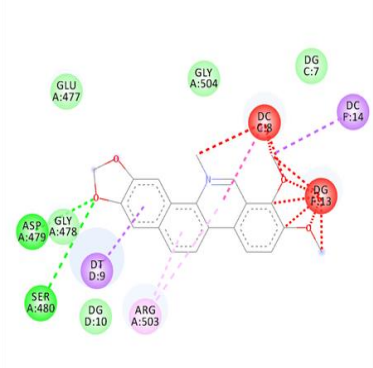
GLU A:477
GLY A:504
DG C:7
DC C:8
DC F:14
DG F:13
ASP A:479
GLY A:478
DT D:9
SER A:480
DG D:10
ARG A:503

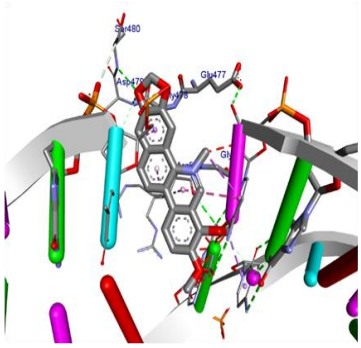
Ser480
Asp479
Glu477

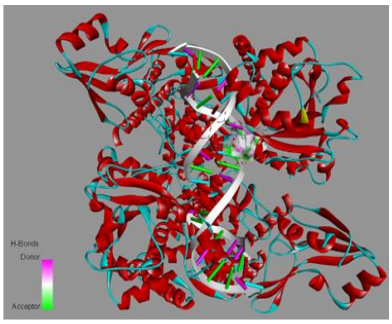
H-Bonds
Donor
Acceptor

62

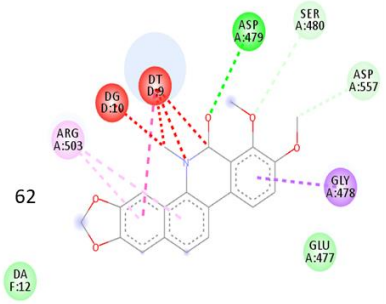
ASP A:479
SER A:480
DT D:9
DG D:10
ASP A:557
ARG A:503
GLY A:478
GLU A:477
DA F:12

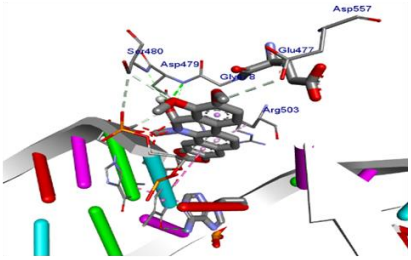
Asp557
Ser480
Asp479
Glu477
Arg503

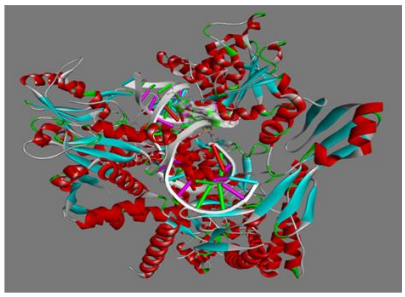

247

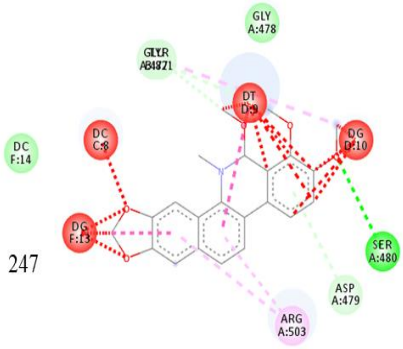
GLY A:478
DT D:9
DC C:8
DG D:10
DC F:14
DG F:13
SER A:480
ASP A:479
ARG A:503

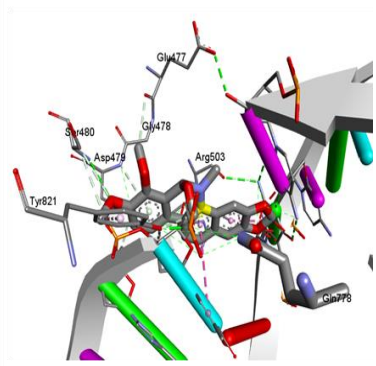
Glu477
Ser480
Gly478
Asp479
Arg503
Tyr821
Gln778

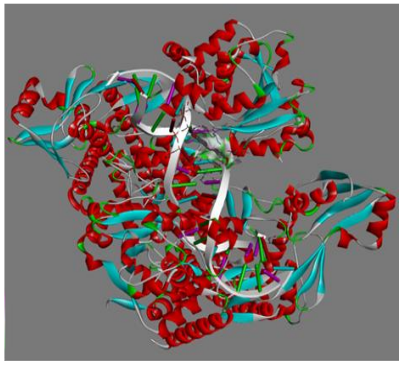

67

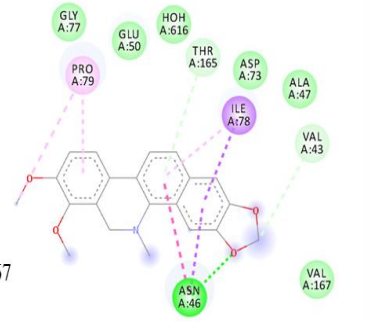
GLY A:77
GLU A:50
HOH A:616
PRO A:79
THR A:165
ASP A:73
ALA A:47
ILE A:78
VAL A:43
ASN A:46
VAL A:167

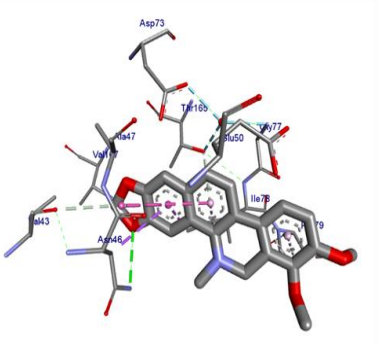
Asp73
Thr165
Ala47
Glu50
Ile78
Asn46

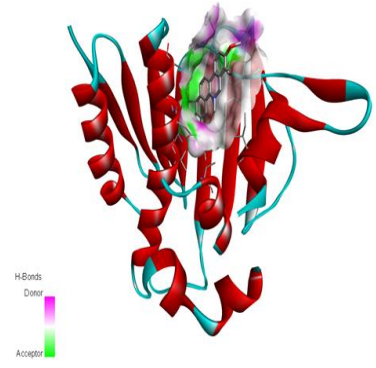
H-Bonds
Donor
Acceptor

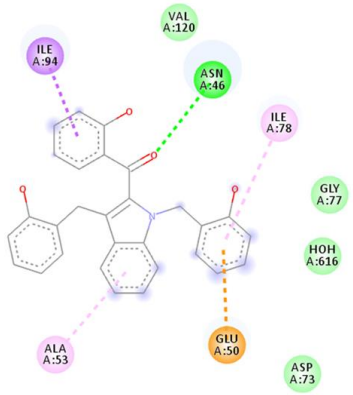
VAL A:120
ILE A:94
ASN A:46
ILE A:78
GLY A:77
HOH A:616
ALA A:53
GLU A:50
ASP A:73

248

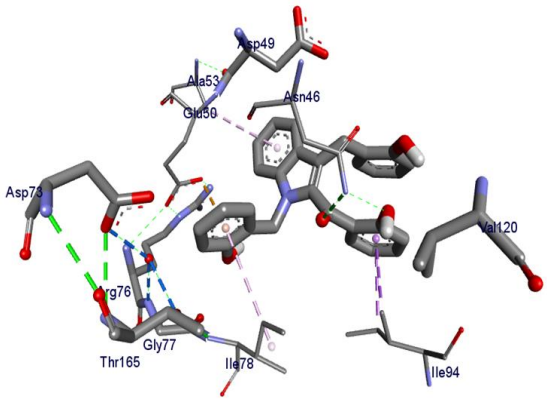
Asp49
Ala53
Asn46
Glu50
Asp73
Val120
Arg76
Gly77
Thr165
Ile78
Ile94

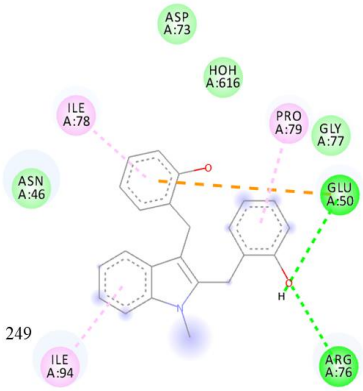
ASP A:73
HOH A:616
ILE A:78
PRO A:79
GLY A:77
ASN A:46
GLU A:50
ILE A:94
ARG A:76

249

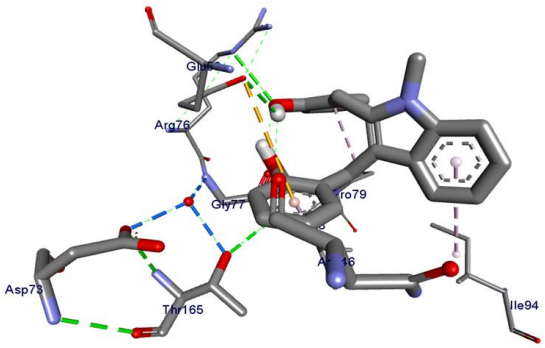
Arg76
Gly77
Asp73
Thr165
Ile94

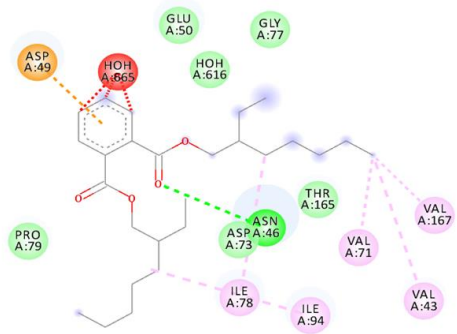
GLU A:50
GLY A:77
ASP A:49
HOH A:665
HOH A:616
THR A:165
VAL A:167
PRO A:79
ASN A:46
ASP A:73
VAL A:71
ILE A:78
ILE A:94
VAL A:43

250

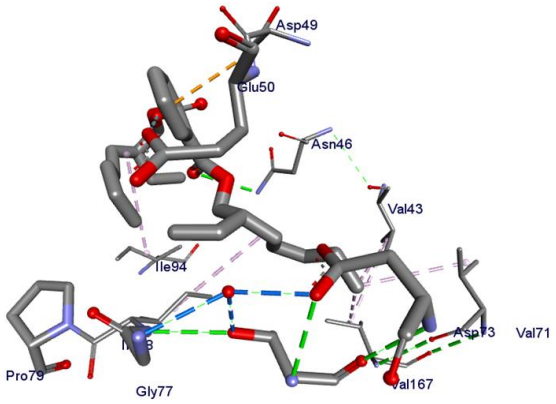
Asp49
Glu50
Asn46
Val43
Ile94
Asp73
Val71
Pro79
Gly77
Val167

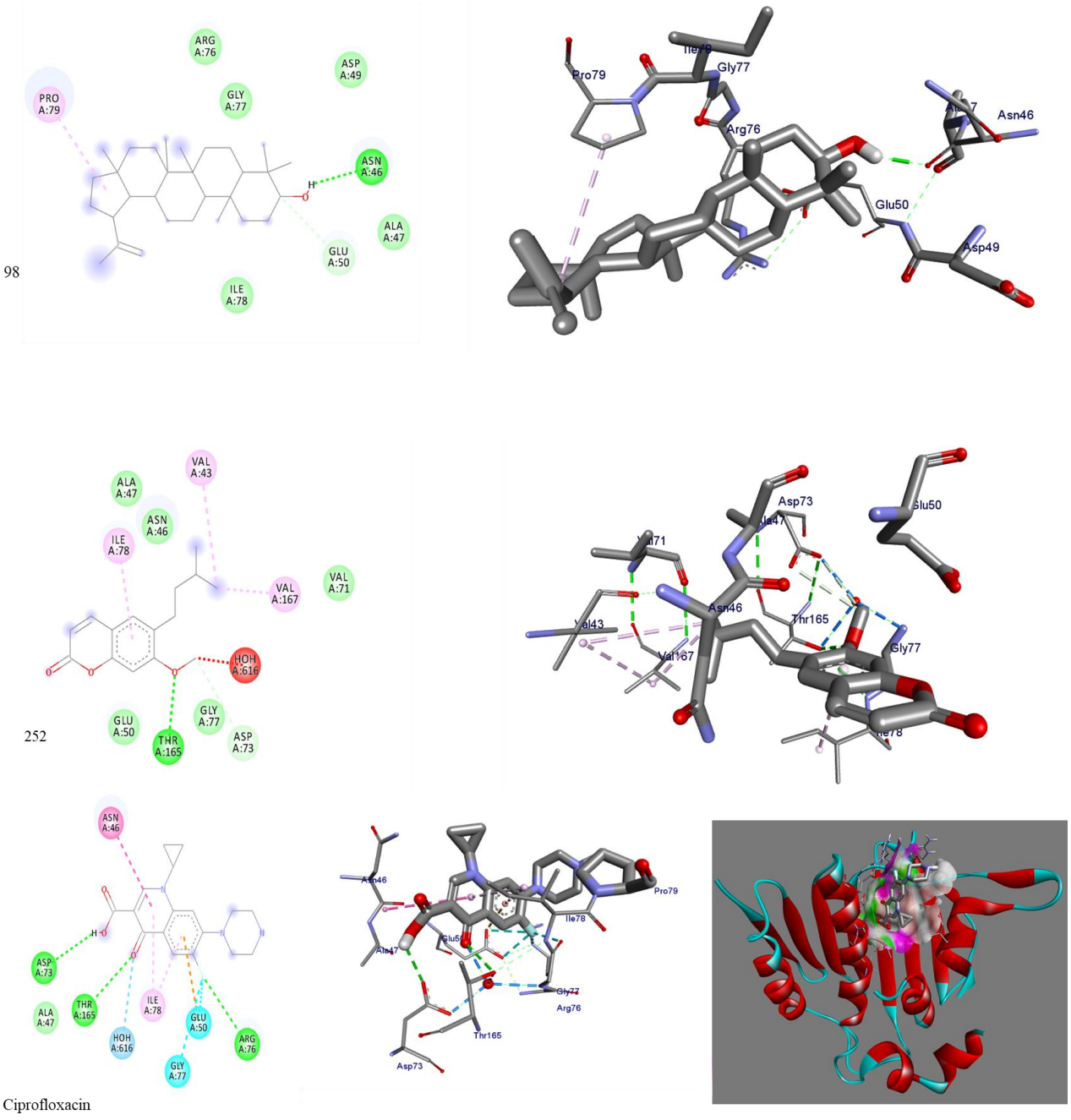

Figure 41: The 2D and 3D binding interactions compounds **(55, 62, 247, 67, 98, 248-250, and 252)** and standard ciprofloxacin against DNA gyrase B (PDB ID: 6F86) respectively. Hydrogen bonds between compounds and amino acids are shown as green dash lines, hydrophobic interaction are shown as pink line.

4.3.2. *In-Silico* Pharmacokinetics (Drug-likeness) and Toxicity analysis

The chemical structures of the isolated compounds (**9**, **13**, **17**, **55**, **62**, **67, 98, 244**, **245**, **247-250** and **252**) were converted to their canonical simplified molecular input line entry system (SMILE) and submitted to SwissADME tool to estimate *in-silico* pharmacokinetic parameters (drug likeness properties) according to 'Lipinski's rule of five'. It denotes that the drugs and/or candidates should obey rule of five parameters such as less than 5 hydrogen-bond donors (HBDs), less than 10 hydrogen-bond acceptors (HBAs), a molecular mass less than 500 Da, log P not greater than 5, and total polar surface area (TPSA) should not be > 140 Å [176] Drug-likeness is a prediction that screens whether a particular organic molecule has properties consistent with being an orally active drug Lipinski, et al., (1997)[176]. In the present studies the SwissADME prediction revealed, all the studied compounds did not violate any of the Lipinski's rule of five and are likely to be orally active (Table 26), except compound (**250**). The hydrogen bonding potential and bioavailability of molecules closely correlated to TPSA value. TPSA of the studied compounds was noticed in the range of 20.23 – 82.69 ˚A and is well below the limit of 160 ˚A. The number of rotatable bonds (NRB) measured the conformational stability of molecules [215]. All calculated values for the isolated compounds are less than 10, so these compounds are conformationally stable [211].

4.3.3. ADMET Properties

The ADMET of isolated compounds (**9**, **13**, **17**, **55**, **62**, **67, 98, 244**, **245**, **247-250** and **252**) were predicted using Swiss ADMET, which includes drug absorption, distribution, metabolism, excretion and toxicity. The skin permeability value (Kp) in cm/s denotes the skin absorption of molecules. The more positive the value of logKp the higher the skin absorption. The skin permeability, Kp, values of studied alkaloids ranged -1.90 to –6.97 cm/s indicating low skin permeability, are within the range of broad spectrum antibiotic ciprofloxin (-9.09 cm/s) and under the clinical trial anticancer agent vosoroxin (-9.43 cm/s). Additionally, gastrointestinal (GI) and blood brain barrier (BBB) permeation indicates the absorption and distribution of drug molecules [211, 217]. The *in-silico* predication results of absorption, distribution, metabolism, and excretion (ADME) of studied alkaloids are presented in Table 27. The Swiss ADME prediction parameters revealed all isolated compounds except (**250** and **98**) have high gastrointestinal (GI) absorption and blood brain barrier (BBB) permeation. As per previous

reports, a range of cytochromes (CYP's) regulates the drug metabolism, in which CYP1A2, CYP2C19, CYP2C9, CYP2D6 and CYP3A4 are vital for biotransformation of drug molecules [216]. In this regard, our findings revealed that acridone alkaloids (**244, 17 and 13**) inhibited all cytochromes except CYP2C19. Evodiamine (**245**) inhibited cytochromes except CYP2C9 and is substrate of permeability glycoprotein (P-gp). However, among studied quinolone alkaloids (**3**) inhibited only CYP2C19 and CYP2C9. In similar study, the SwissADME prediction of benzophenathrides (**55**, **62**, **67**, and **247**) showed that inhibited all cytochromes and substrate of permeability glycoprotein (P-gp). However, dihyrochelerythrine (**67**), do not inhibited CYP2D6. Regarding to compound (**98**, **248-250** and **252**), compound (**249**) inhibited all cytochromes except CYP2C9 and substrate of permeability glycoprotein (P-gp). Compound (**248**) inhibited cytochromes CYP2C19 and CYP2D6, (**250)** inhibited CYP2C9 and CYP3A4, whereas compound (**252**) inhibited CYP1A2, CYP2C19, CYP2C9, and CYP2D6 but both of them are not substrate of permeability glycoprotein (P-gp). However, compound (**98**) neither cytochromes inhibitor nor a substrate of permeability glycoprotein (P-gp). The toxicological prediction gives results of endpoints such as hepatotoxicity, carcinogenicity, mutagenicity, and cytotoxicity. Acute toxicity prediction results, such as toxicity class classification and LD_{50} values, predict that none of the isolated compounds has acute toxicity. The studied compounds were predicted to be non-carcinogenic and non-irritant. However, all compounds have shown hepatotoxicity and mutagenicity. Pre-ADMET and OSIRIS property explorer prediction analysis have shown in Table 28. Hence, based on ADMET prediction analysis, the isolated compounds (**9**, **13**, **17**, **55**, **62**, **67, 98, 244**, **245**, **247-250** and **252**) may be the good candidates in this investigation.

Table 26: Drug-likeness predictions of isolated compounds **(9, 13, 17, 55, 62, 67, 98, 244, 245, 247-250** and **252)**, computed by SwissADME.

Alkaloids	**Mol. Wt. (g/mol)**	**NHD**	**NHA**	**NRB**	**TPSA ($A^{\circ 2}$)**	**LogP (cLogP)**
244	269.25	1	4	0	60.69	2.5
13	283.28	0	4	1	49.69	2.61
17	287.31	1	4	2	59.00	2.35
245	303.36	1	1	0	39.34	2.25
9	325.40	0	3	3	40.46	3.86

55	365.38	1	5	2	60.39	3.35
62	379.41	0	5	3	49.39	3.76
247	349.38	0	4	2	40.16	3.59
67	348.37	0	4	2	40.8	0.22
248	449.5	6	4	3	82.69	3.29
249	343.42	4	2	2	45.39	2.79
250	418.61	18	4	0	52.6	5.23
98	426.72	1	1	1	20.23	4.89
252	246.3	4	3	0	39.44	3.12
Vosaroxin	401.45	2	9	5	136.13	0.963
All studied compounds obeyed Lipinski's rule of Five						

NHD = Number of Hydrogen donor, NHA = Number of Hydrogen acceptor, NRB = Number of rotatable bonds, and TPSA = total polar surface area

Table 27: ADME predictions of isolated compounds (**9**, **13**, **17**, **55**, **62**, **67, 98, 244**, **245**, **247-250** and **252**), computed by SwissADME and PreADMET.

Isolated compounds	**log Kp cm/s**	**GI Absorption**	**BBB Permeability**	**P-gp substrate**	**Inhibitor Interaction**				
					CYP1A2	**CYP2C19**	**CYP2C9**	**CYP2D6**	**CYP3A4**
244	-5.73	High	Yes	No	Yes	No	Yes	Yes	Yes
17	-5.97	High	Yes	No	Yes	No	Yes	Yes	Yes
13	-6.97	High	Yes	No	Yes	No	No	No	No
245	-5.95	High	Yes	Yes	Yes	Yes	No	Yes	Yes
9	-5.70	High	Yes	No	No	Yes	Yes	No	No
55	-5.9	High	Yes	Yes	Yes	Yes	Yes	Yes	Yes
62	-5.61	High	Yes	Yes	Yes	Yes	Yes	Yes	Yes
247	-5.41	High	Yes	Yes	Yes	Yes	Yes	Yes	Yes
67	-5.17	High	Yes	Yes	Yes	Yes	Yes	No	Yes
248	-4.3	High	No	No	No	Yes	No	Yes	No

249	-4.72	High	Yes	Yes	Yes	Yes	No	Yes	Yes
250	-2.8	Low	No	No	No	No	Yes	No	Yes
98	-1.9	Low	No	No	No	No	No	No	No
251	-4.96	High	Yes	No	Yes	Yes	Yes	Yes	No
Vosaroxin	-8.98	High	No	Yes	Yes	No	No	No	No

LogKp = Skin permeation value, GI = Gastro-Intestinal, BBB = Blood Brain Barrier, P-gp = P glycoprotein, CYP = Cytochrome-P

Table 28: Predication of Toxicity of isolated compounds (**244**, **17**, **13**, **245**, **9**, **55**, **62**, **247**, **67**, **248-250**, **98**, and **252)** computed by Pre-ADMET and OSIRIS Property Explorer.

Isolated compounds	**LD $_{50}$ (mol/kg)**	**Toxicity Class**	**Organ Toxicity**				
			Hepatotoxicity	**Carcinogenicity**	**Cytotoxicity**	**Mutagenicity**	**Irritant**
244	2.618	3	Yes	No	No	Yes	No
17	2.507	3	Yes	No	No	Yes	No
13	2.653	3	Yes	No	No	Yes	No
245	2.697	2	Yes	No	No	Yes	No
9	3.083	3	Yes	No	Yes	Yes	No
55	2.557	3	Yes	No	Yes	Yes	No
62	2.502	3	Yes	No	Yes	Yes	No
247	2.678	3	Yes	No	No	Yes	No
67	2.678	3	Yes	No	No	Yes	No
248	2.000	4	Inactive	Inactive	Inactive	Inactive	Inactive
249	1.600	4	Inactive	Inactive	Inactive	Inactive	Inactive
250	1.340	4	Inactive	Active	Inactive	Inactive	Inactive
98	2.000	4	Inactive	Inactive	Active	Inactive	Inactive
251	3.200	4	Inactive	Inactive	Active	Inactive	Inactive
Vosaroxin	2.188	4	Yes	No	No	Yes	No

4.3.4. DFT analysis

DFT (density functional theory) study is an important approach to explore the relationship between geometry and electronic properties of chemical compounds [215]. Therefore**,** we report herein DFT calculation with the basis sets B3LYP/6-31 G (d,p) involving optimized geometries (Figure 42), molecular electrostatic potential (MEP), Mullikan's atomic charges, highest occupied molecular orbital (HOMO), lowest unoccupied molecular orbital (LUMO) and energy gap for fourteen isolated compounds from selected Ethiopian medicinal plants (**244, 17, 13, 245, 9, 55, 62, 247, 67, 248-250, 98** and **252**). The determination of the MEP region is the best fit for identifying sites for intra- and inter-molecular interactions (Figure 43). Red/Yellow regions indicate negative electrostatic potentials and the blue region shows positive, and green color designates neutral potential region. The Mullikan's atomic charges (Figure 44) of DFT calculation revealed a charge distribution in individual atoms, the charges on carbon atoms were exhibited either positive or negative value. All hydrogen atoms were displayed a net positive charge and act as acceptor atoms. In addition, all oxygen atoms of the optimized compound were shown to have negative charge, which act as donor atoms. The HOMO, LUMO and energy gap (ΔE) of isolated compounds are presented in table 29. The results revealed that all studied compounds showed the least energy gap (ΔE) suggesting that high chemical reactivity and considerable intramolecular charge transfer from electron donor (HOMO) to electron acceptor (LUMO) groups. Additionally, all studied compounds have large electronegativity (χeV), global softness (σ eV^{-1}), and global electrophilicity (ωeV) (Table 29). Based on the results isolated compounds have better bioactivity.

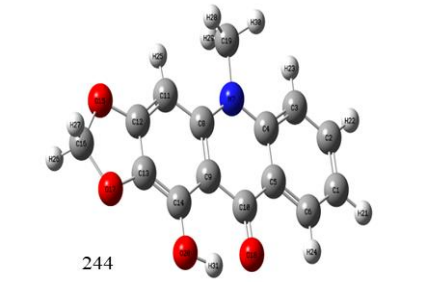

244

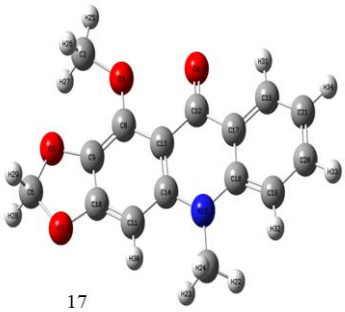

17

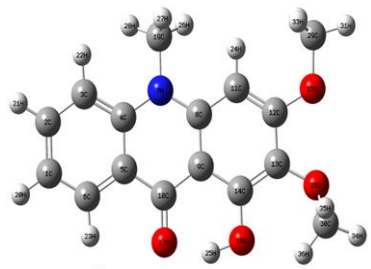

13

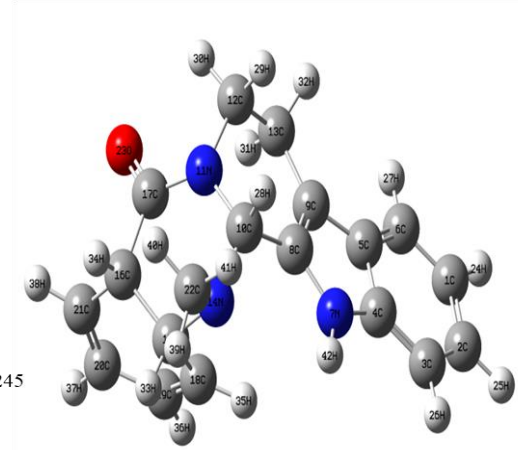

245

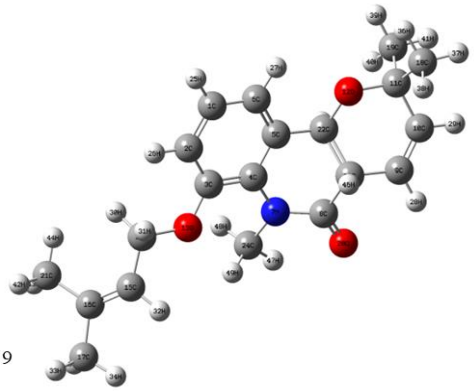

9

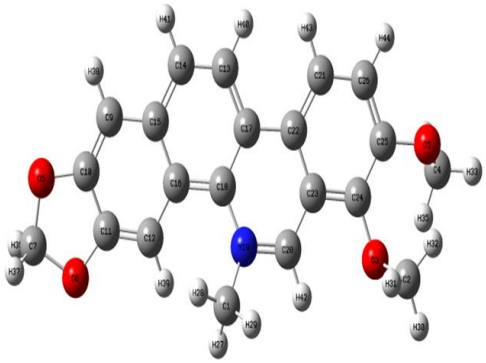

55

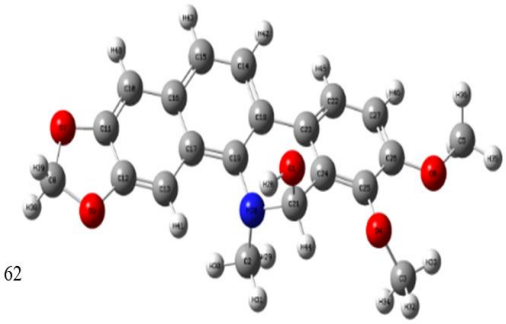

62

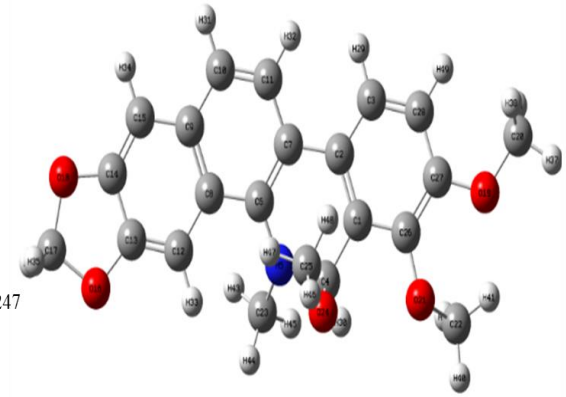

247

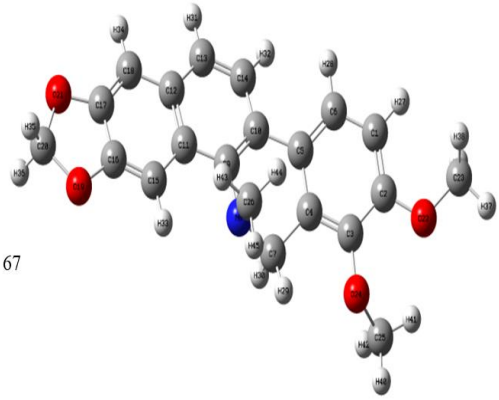

67

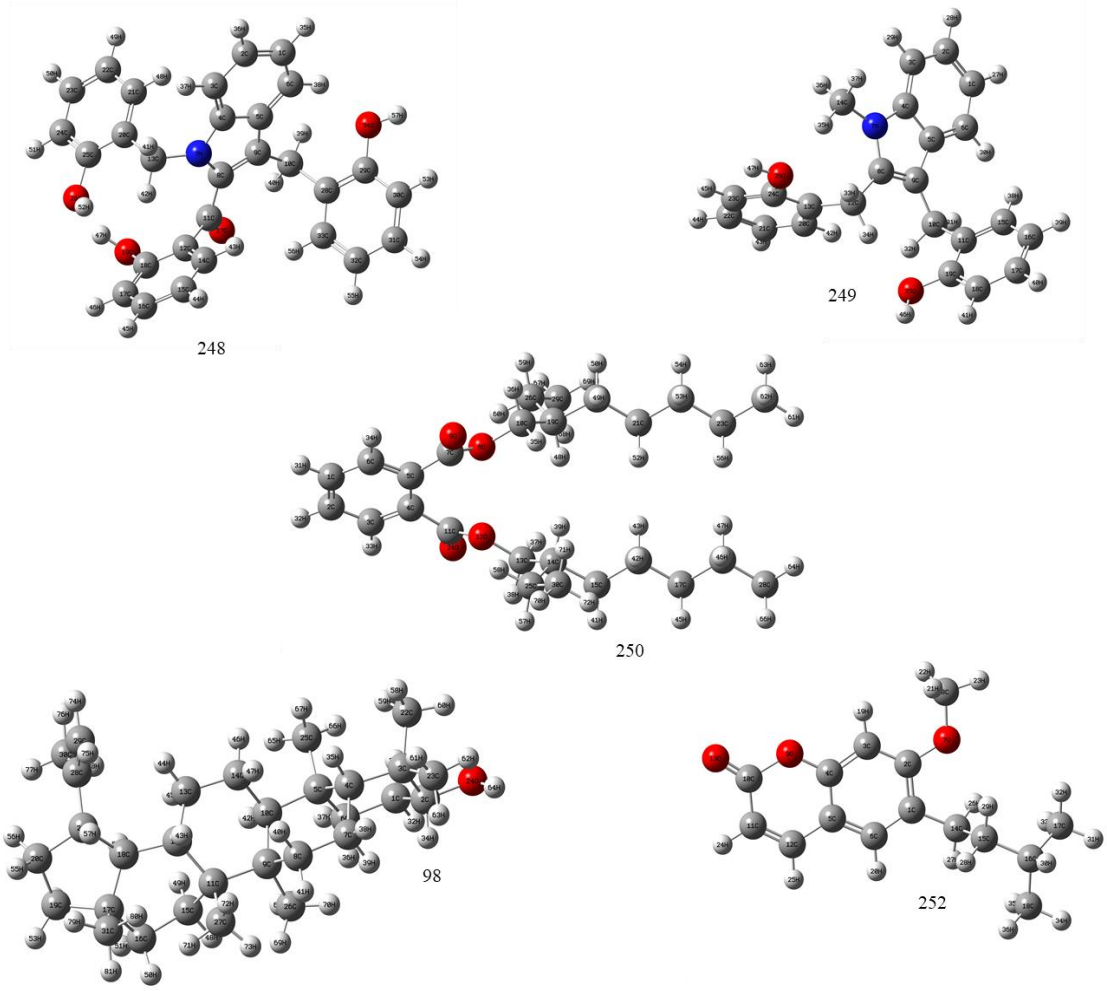

Figure 42: The optimized structures of isolated compounds

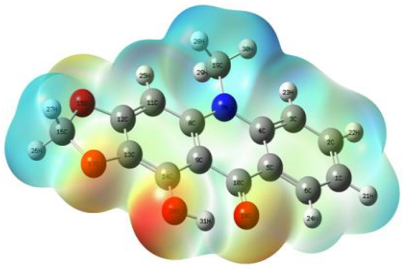

244

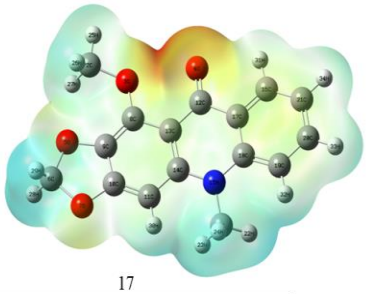

17

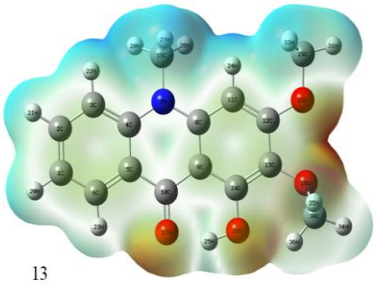

13

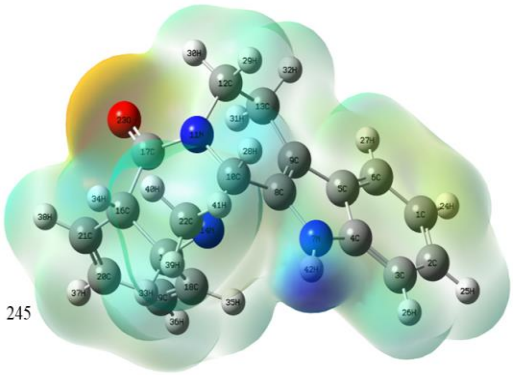

245

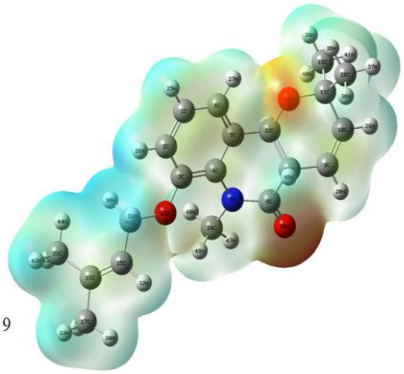

9

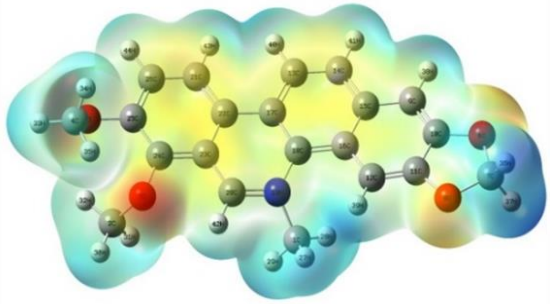

55

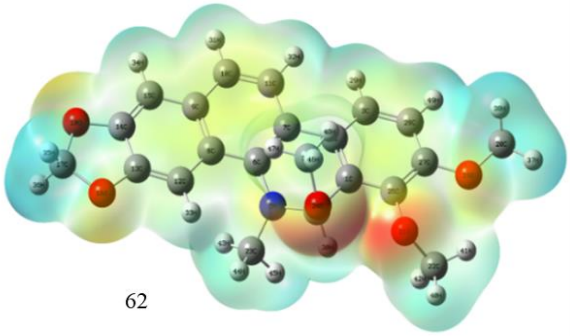

62

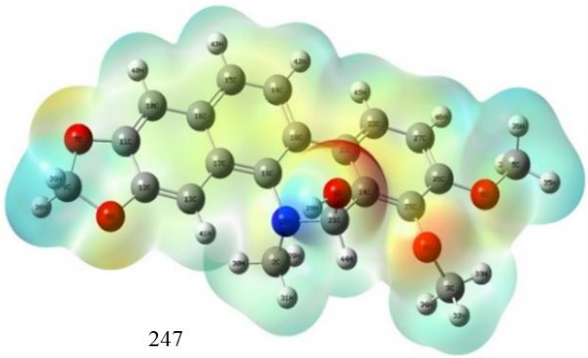

247

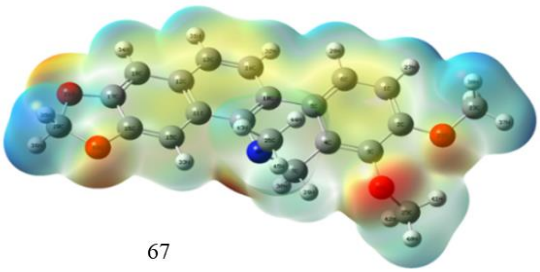

67

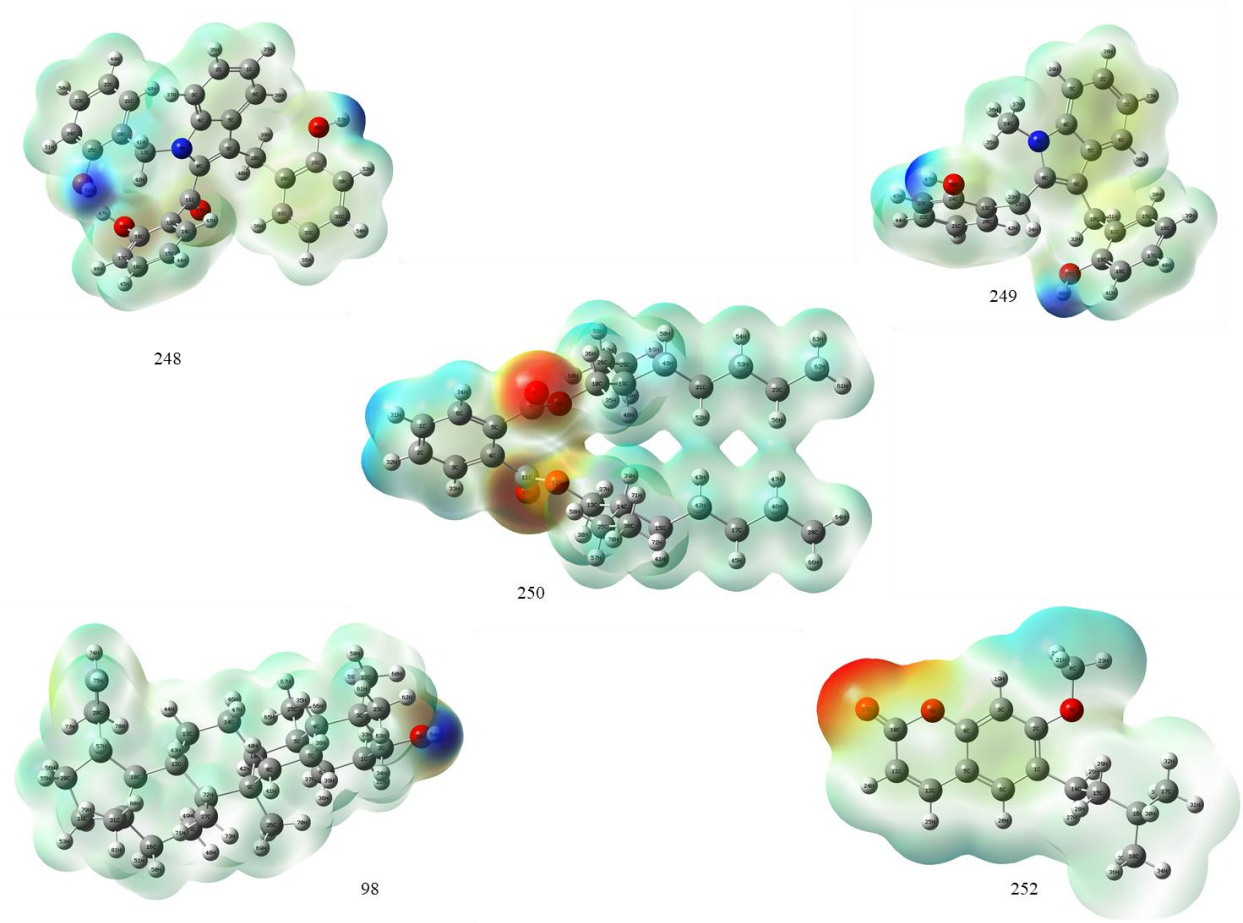

Figure 43: Molecular electrostatic potential surface of isolated compounds

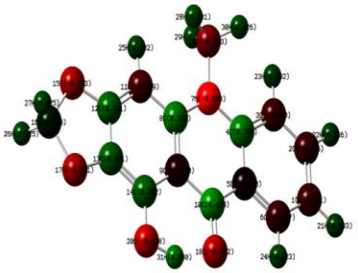

244

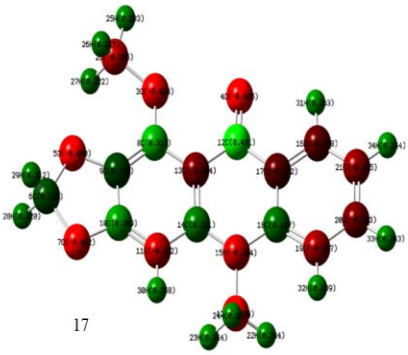

17

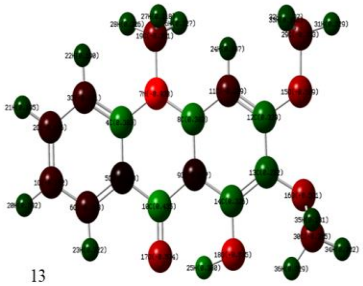

13

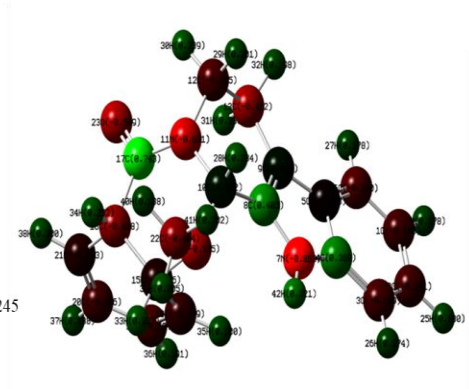

245

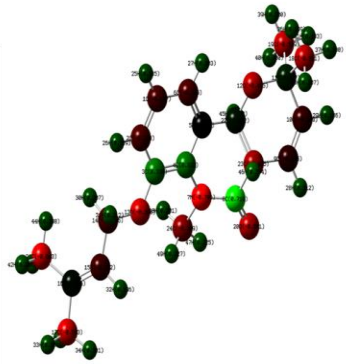

9

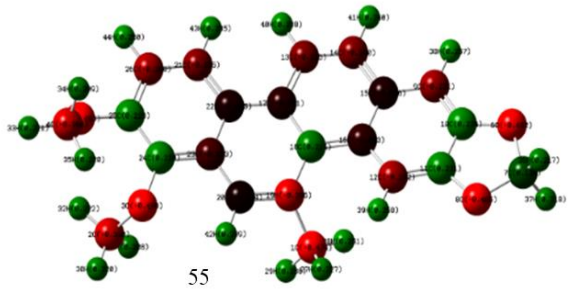

55

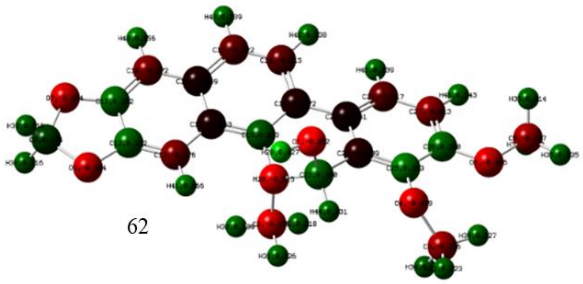

62

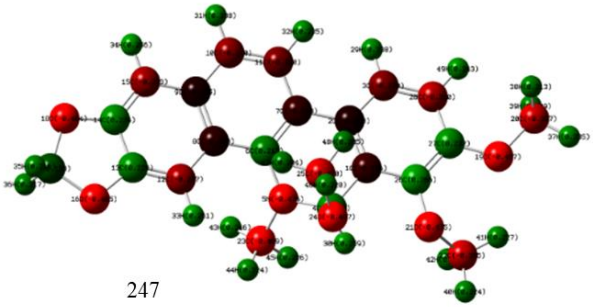

247

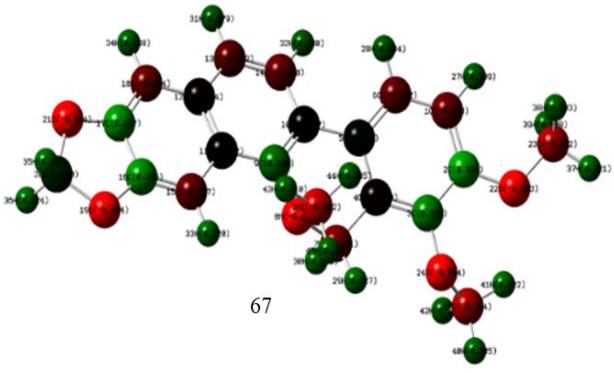

67

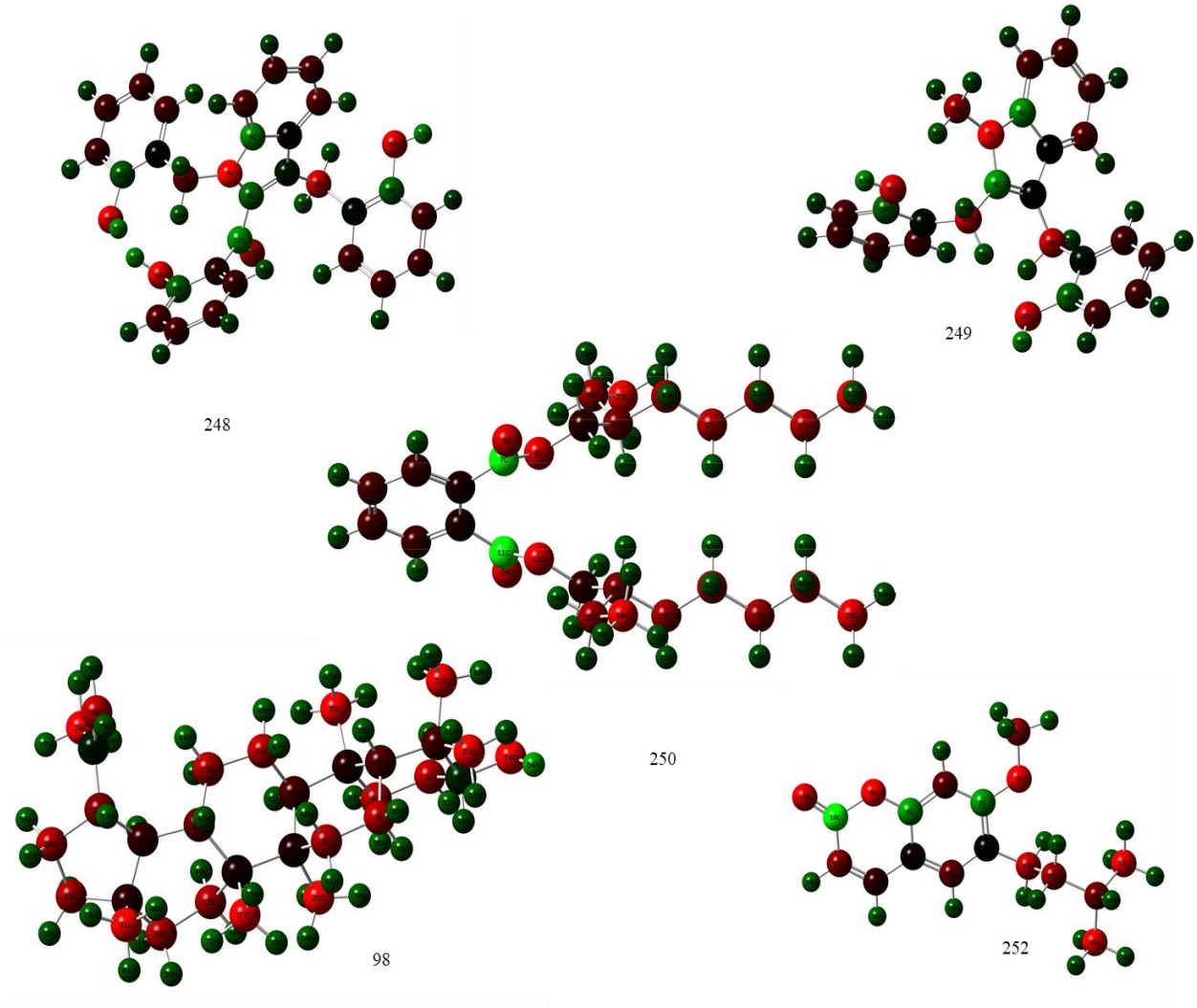

Figure 44: The DFT calculated Mulliken's atomic charges of isolated compounds.

Table 29: The various quantum chemical parameters of isolated compounds.

NO	E_{HUMO} (eV)	E_{LUMO} (eV)	Energy Gap ΔE (eV)	Electron egativity χ (eV)	Global Hardness η (eV)	Global Softness σ (eV^{-1})	Global Electrophilicity ω (eV)
244	-0.1913	-0.0591	0.1322	0.1252	0.0661	15.1274	0.1186
13	-0.1895	-0.0397	0.1498	0.1146	0.0749	13.3475	0.0876
17	-0.1882	-0.0562	0.1320	0.1222	0.0660	15.1469	0.1132
245	-0.1960	-0.0266	0.1693	0.1113	0.0846	11.8070	0.0731
9	-0.1987	-0.0071	0.1916	0.1029	0.0558	10.4384	0.0553
55	-0.1880	-0.0326	0.1554	0.1103	0.0777	12.8667	0.0783
62	-0.1751	-0.0287	0.1464	0.1019	0.0732	13.6602	0.0710
247	-0.1851	-0.0309	0.1542	0.1080	0.0771	12.9676	0.0756
67	-0.1196	-0.0359	0.0837	0.0778	0.0418	23.8891	0.0723
248	-0.2037	-0.0544	0.1493	0.1290	0.0746	13.3931	0.1115
249	-0.1788	-0.0009	0.1778	0.0899	0.0889	11.2441	0.0454
250	-0.2565	-0.0560	0.2005	0.1563	0.1002	9.9740	0.1218
98	-0.2336	0.0313	0.2649	0.1011	0.1325	7.5474	0.0385
252	-0.2171	-0.0582	0.1588	0.1377	0.0794	12.5881	0.1193

CHAPTER FIVE

5. CONCLUSIONS AND RECOMMENDATIONS

5.1. Conclusions

- From the roots and fruits extract of *V. dainelli* eight compounds such as N-methyl-8-(3",3"-dimethylallyloxy)-findersine (**9**), arborinine (**13**), evoxanthine (**17**), kokusaginine (**51**)**,** skimmianine (**25**), Norevoxanthine (**244**) evodiamine **(245**) and tetrahydropyranyl Octadeca-9, 12-dienoate (**246**) were reported herein for the first time of which evoxanthine (**17**), arborinine (**13**) and evodiamine **(245**) exhibited a cytotoxic effect against the estrogen-responsive MCF-7 and the estrogen-unresponsive MDA-MB-231 human breast cancer cell lines by MTS assay, also supported by computational analysis against human topoisomerase IIα, indicating that these compounds could be a drug candidate for the treatment of human breast cancer.

- The root extract of *Z. chalybeum* afforded four benzophenanthridine alkaloids such as chelerythrine (**55)**, 6-hyroxydihydrochelerythrine (**62**), dihyrochelerythrine (**67**), and 6-methoxydihyrochelerythrine (**247**) of which 6-hyroxydihydrochelerythrine (**62**) and 6-methoxydihyrochelerythrine (**247**) are isolated herein for the first time from this plant. Chelerythrine (**55**) and dihydrochelerythrine (**67**) induced a significant reduction of cell growth of MDA-MB-231 and MCF-7 breast cancer cell lines in a dose-dependent manner. Chelerythrine (**55**) showed the highest potency and selectivity against the aggressive and metastatic MDA-MB-231 cell line at low micromolar concentrations compared to dihydrochelerythrine (**67**) which displayed selectivity at higher concentration. Antimicrobial effects of chelerythrine (**55**) showed promising result against *S. aureus* and *C. albinais* at lower concentration. Therefore, chelerythrine (**55**), suggesting a potential lead compound against infectious diseases and human breast cancer cells.
- The root extract of *U. scheffleri* afforded two new uvrindole-F and G (**248** and **249**), along with known dihydrochalcone uvaretin (**112**). Dichloromethane extract and uvrindole-F (**248**) showed potential antibacterial activity against *S. aureus* (IC_{50} = 6.125 and 12.5 µg/mL) compared with Gentamicin (5 µg/mL against *S. aureus*) whereas uvrindole-F (**248**) also

showed antifungal activity against *C. albicans* (IC_{50} = 12.25 µg/mL) compared with fluconazole (2.5 µg/mL against *C. albicans*), therefore, uvrindole-F (**248**) suggesting a lead compound against infectious diseases caused by microorganisms.

- Silica gel column separation of root of *C. burgensis* afforded three compounds such as lupeol (**98**), bis(2-ethylheptyl) phthalate (**250**) and stearic acid (**251**) for the first time from the species. Lupeol (**98**) was evaluated for antimicrobial activity against *S. aureus* and *E. coli* and *C. albicans*, showed weak antimicrobial activity.
- Phytochemical analysis on the roots of *E. schimperiana* afforded eight compounds such as pernylated coumarin (**252)**, compounds **(254-260)**) for the first time from the species. Perynlated coumarin **252** displayed weak antimicrobial activity against *S. aureus* and *E. coli*.
- Hydrodistillation of roots of *U. scheffleri* and fruit of *V. dainelli* and *Z. chalybum* provided 58 (97.63%), 20 (98.8%) and 18 (99.5%) chemical constituents. Essential oils showed moderate toxicity and potential larvicidal activity against anisakis L_3. Thus results obtained suggest that the studied essential oils could serve as larvicidal agents in treating human anisakidosis. The observed weak cytotoxicity at low concentrations points out the possibility of developing effective and safe botanical larvicides.
- The results obtained from molecular docking, drug-likeness properties, ADMET analysis and the DFT calculation are in a good agreement with those obtained from experimental studies of *Vepris dainelli*, *Zanthoxylum chalybeum* and *Uvaria scheffleri* compounds suggesting the potential use of the isolated compounds as medicine which corroborate with the claimed traditional uses of these plants.

5.2. Recommendations

- *In vivo* studies against animal models for those active compounds arborinine (**13**), evoxanthine (**17**), chelerithrine (**55**), evodiamine (**245**) and uvarindole -F (**248**) should be carried out to determine their bioactivity.
- The alkaloids (**13, 17, 55, 67** and **245**) should evaluate for their toxicity with normal cell line in different concentration to determine their toxicity level.

- Cytotoxicity of alkaloids (**13, 17, 55, 67** and **245**) of the genus *Vepris and Zanthoxylum* and their structure-activity relationship should further studied for providing potential lead drugs with low cytoxicity against human breast cancer.
- *Uvaria scheffleri* crude extracts are more active than the pure compounds (**248** and **249**) against *S. aureus*. It is therefore interesting to find out if there is synergy between the isolated compounds or other more active compounds which should be isolated and identified.
- Future studies need to be done on a combination of the compounds isolated from these plants with standard first line drugs *in vitro* and *in vivo*. Likewise, in vivo cytotoxicity study of combination *Vepris* and *Zanthoxylum* should be done along with existing first line drugs.
- Synthetic derivatives of alkaloids (**13, 17, 55, 67 and 245**) of the *Vepris* and *Zanthoxylum* should be synthesized and conduct structure-activity relationship in search for lead drugs with low cytoxicity against human breast cancer.

REFERENCES

[1]. WHO (2013), *Traditional Medicine Trade*, 134, p. 1–4.

[2]. Balandrin, M. F. Kinghorn, A. D. and Farnsworth, N. R. (1993). P*lant-Derived Natural Products in Drug Discovery and Development*, ACS Symposium Series, American Chemical Society: Washington, DC, p. 2–12.

[3]. Payyappallimana, U. (2010). Role of traditional medicine in primary health care: An overview of perspectives and challenges, *Yokohama J. Soc. Sci*, 14(6): p. 7–77.

[4]. David J. Phillipson (2001). Phytochemistry and medicinal plants, *Phytochemistry*, 56(3): p. 237–243.

[5]. Kong, J.M., Ngoh-Khang, G., Lian-Sai, C., and Tet-Fatt, C. (2003). Recent advances in traditional plant drugs and orchids, *Acta Pharmacol. Sin*, 24(1): p. 7–21.

[6]. Rashid, M. A. (2013). Recent trends in natural product research and Bangladesh perspective, *Biochem Pharmacol*, 2(5): p. 179.

[7]. Cragg G. M. and Newman, D. J. (2013). Natural products: A continuing source of novel drug leads, *Biochim. Biophys. Acta - Gen. Subj*, 1830 (60): p. 3670–3695.

[8]. Dias, D. A. Urban, S., and Roessner, U. (2012). A Historical overview of natural products in drug discovery, *Metabolites*, 2(2): p. 303–336.

[9]. Ramawat, K.G. (2009). *Herbal Drugs: Ethnomedicine to Modern Medicine*, Springer-Verlag: Berlin, Heidelberg, Germany, 22, p. 32.

[10]. Rahman, A. H. M. M. (2018). A Review on Medicinal Plants with Anticancer Activity Available In Bangladesh, *Mod Appl Pharm Pharmacol*,1(4): p. 1–6,.

[11]. Siegel, R. L., Miller, K. D., and Jamal, A. (2020). Colorectal cancer statistics, *CA: A Cancer Journal for Clinicians*, 70 (3): p.145-164.

[12]. Tao, Z. Q., Shi, A., Lu, C., Song, T., Zhang, Z., and Zhao, J. (2015). Breast Cancer: Epidemiology and Etiology, *Cell Biochem. Biophys.*, 72(2): p. 333–338.

[13]. Dumitrescu, R. G. and Cotarla, I. (2005). Understanding breast cancer risk - Where do we stand in 2005?, *J. Cell. Mol. Me*, 9, no. 1, pp. 208–221, 2005.

[14]. Foroodi, F., Duivenvoorden, W. C., Singh, G. (2009). Interactions of doxycycline with

chemotherapeutic agents in human breast adenocarcinoma MDA-MB-231 cells, *Anticancer. Drugs*, 20(2): p. 115–122.

[15]. Razak, N. A., Abu, N., Ho, W. Y., Zamberi, N. R., Tan, S. W., Alitheen, N. B., Long , K. and Yeap, S. K (2019). Cytotoxicity of eupatorin in MCF-7 and MDA-MB-231 human breast cancer cells via cell cycle arrest, anti-angiogenesis and induction of apoptosis, *Sci. Rep*, 9(1): p. 1–12.

[16]. Greenwell, M. and Rahman, P. K. S. M.(2015). Medicinal Plants: Their Use in Anticancer Treatment., *Int. J. Pharm. Sci. Res*, 6(10): p. 4103–4112.

[17]. Gajdács, M. Urbán, E,. Stájer, A., and Baráth, Z. (2021). Antimicrobial resistance in the context of the sustainable development goals: A brief review, *Eur. J. Investig. Heal. Psychol. Educ*, 11(1). 71–82.

[18]. Jones, K. E., Patel, N. G., Levy, M. A., Storeygard, A., Balk, D., Gittleman, J. L., and Daszak, P. (2008). Global trends in emerging infectious diseases, *Nature*, 451(7181): p. 990–993.

[19]. Cassell, G. H. and Mekalanos, J. (2001). Development of antimicrobial agents in the era of new and reemerging infectious diseases and increasing antibiotic resistance, *JAMA*, 285(5): p. 601–605.

[20]. Blaser, M. J. (2006). Who are we? Indigenous microbes and the ecology of human diseases, *EMBO Rep*, 7(10): p. 956–960.

[21]. Chai, J., Murrell, D. K., and Lymbery, A. J. (2005). Fish-borne parasitic zoonoses : Status and issues, 35(0020): p. 1233–1254.

[22]. Lymbery, A. C. F (2007). *Anisakid Nematodes and Anisakiasis. In: Murrell K.D., Fried B. (eds) Food-Borne Parasitic Zoonoses. World Class Parasites, 11, Springer, Boston, MA*.

[23]. Aibinu, I. E. Smooker , P. M., and Lopata, A. L. (2019). Anisakis Nematodes in Fish and Shellfish- from infection to allergies, *IJP Parasites Wildl*, 9: p. 384–39.

[24]. Mattiucci, S., Cipriani, P., Paoletti, M., Levsen, A., and Nascetti, G. (2017). Reviewing biodiversity and epidemiological aspects of anisakid nematodes from the North-east Atlantic Ocean, *J. Helminthol, 91(4): p.* 422-439.

[25]. Giarratana, F. P. A. (2012). *Study of the Resistance Variability of Anisakis Larvae to Some*

Technological Stressors. In: Pugliese A., Gaiti A., Boiti C. (eds) Veterinary Science. Springer, Berlin, Heidelberg, 13, pp. 155–159.

[26]. Hierro, I., Valero, A., and Navarro, M. C. (2006). In vivo larvicidal activity of monoterpenic derivatives from aromatic plants against L 3 larvae of Anisakis simplex s . l . 13: p. 527–531,

[27]. Giarratana, F., Muscolino, D., Beninati, C., Giuffrida, A. and Panebianco, A. (2014). Activity of *Thymus vulgaris* essential oil against Anisakis larvae, *Exp. Parasitol*, 429(1): p. 7–10.

[28]. Hierro, I., Valero, A., Pérez, P., González, P., Cabo, M. M., Montilla, M. P. and Navarro, M. C. (2004). Action of different monoterpenic compounds against Anisakis simplex s . l . L_3 larvae, *Phytomedicine* 11: 77–82.

[29]. Kassa, D. and Abebe, A. (2008). Species composition, abundance, distribution and habitat association of rodents of wondo genet, ethiopia, *Ethiop. J. Sci*, 31(2): p. 141–146.

[30]. Abebe, W. (2016). An Overview of Ethiopian Traditional Medicinal Plants Used for Cancer Treatment, *European J Med Plants*, 14(4): p. 1–16.

[31]. Santiago, P. R., Blanco, A., Morales, F., Marcelain, K., Harismendy, O., Herrera, M.S., Armisén, R. (2021). Immune-related IncRNA LINC00944 responds to variations in ADAR1 levels and it is associated with breast cancer prognosis, *Life Sci*, 268: p. 118956.

[32]. Tesfaw, A., Alebachew, W., and Tiruneh, M. et al (2020). Why women with breast cancer presented late to health care facility in North-west Ethiopia? A qualitative study, *PLoS One*, 15(12), p.1-15.

[33]. Enioutina, E.Y. Teng, L. Fateeva, T. V. Brown, J.C.S. Job, K.M. Bortnikova, V. V. Krepkova, L. V. Gubarev, M.I. Sherwin, C.M.T. (2017). Phytotherapy as an alternative to conventional antimicrobials: combating microbial resistance, Expert Rev. Clin. Pharmacol. 10 (11): p 1203–1214.

[34]. Penchovsky, R. and Traykovska, M. (2015). Designing drugs that overcome antibacterial resistance: Where do we stand and what should we do?, Expert Opin. Drug Discov. 10 (6): P, 631–650.

[35]. Dallavalle, S., Dobričić, V., Lazzarato, L.; Gazzano, E., Machuqueiro, M., Pajeva, I.,

Tsakovska, I., Zidar, N., Fruttero, R. (2020). Improvement of conventional anti-cancer drugs as new tools against multidrug resistant tumors, *Drug Resist. Updat*, 50(1):. p. 100682.

[36]. Tan, J., Tay, J., Hedrick, J., Yang, Y.Y. (2020). Synthetic macromolecules as therapeutics that overcome resistance in cancer and microbial infection, *Biomaterials*, 252(1): p. 120078.

[37]. Sofowora, A., Ogunbodede, E., and Onayade, A. (2013). The role and place of medicinal plants in the strategies for disease prevention, *Afr. J. Tradit. Complement. Altern. Med*, 10(5): p. 210–229.

[38]. Kebebew, M, R. and Mohammed, E. E. (2013). Distribution, Abundance and Population Status of Four Indigenous Threatened Tree Species in the Arba Minch, 2(1): p. 1–8.

[39]. Engeu, O. P., Ralph, T., Moses, A., Gerosome, M., Kyeyune, G. N., Badru, G., and Paul, W. (2008). Repeat-dose effects of *Zanthoxylum chalybeum* root bark extract: A traditional medicinal plant used for various diseases in Uganda, *African J. Pharm. Pharmacol*, 2(6): p. 101–105.

[40]. Regassa, R. (2013). Assessment of indigenous knowledge of medicinal plant practice and mode of service delivery in Hawassa city , southern Ethiopia, 7(9): p. 517–535.

[41]. Macabeo, A. P. G., Rubio, P. Y. M., Higuchi, T., Umezawa, N., Faderl, C., Budde, S., Bangcaya, P.S., & Jonathan D, G. A. (2014). Tetrahydroxanthene-1,3(2 H)-dione derivatives from *Uvaria valderramensis*, *J. Nat. Prod.*, 77(12): p. 2711–2715.

[42]. Scott, K. D., McIntyre, C. L., and Playford, J. (2000). Molecular analyses suggest a need for a significant rearrangement of Rutaceae subfamilies and a minor reassessment of species relationships within Flindersia, *Plant Syst. Evol*, 223,(1–2): p. 15–27.

[43]. Sivoko, I. P., Kibagendi, O. E., Said, N. A., Japheth O. O., Kiplagat P. C. (2014). A review on chemistry of some species of genus *Vepris* (Rutaceae family), 3(3): p. 357–362.

[44]. Dagne, E., Yenesew, A., Waterman, P. G., & Gray, A. I. (1988). The Chemical Systematics of the Rutaceae , Subfamily Toddalioideae , in Africa, 16(2): p. 179–188.

[45]. Denu D.and Desissa, D. (2013). Abundance and use of *Vepris dainellii* (Pichi-Serm .) Kokwaro , an Ethiopian endemic plant , in Melokoza woreda ," *Ethiop. J. Educ. Sc.*, 8(2):

p. 1–10.

[46]. Patiño, L. O. J., Prieto, R. J. A., and Cuca, S. L. E. (2008). *Zanthoxylum Genus as Potential Source of Bioactive Compounds*, Prof. Iraj Rasooli (Ed.), InTech. *Bioact. Compd. Phytomedicine*, pp. 185–218.

[47]. Orwa, C., Mutua, A., Kindt, R., Jamnadas, R. and Anthony, S. (2009). Persea americana Miller Lauraceae *Persea americana* Miller, *Agroforestry Database 4.0*, p. 1–5.

[48]. Egydio, A. P. M. and Yara, A. C. S (2015). *Chapter 9 - Nutritional Value of the Pulp of Different Sugar Apple Cultivars (Annona squamosa L.),* In: Monique S.J. Simmonds, Victor R. Preedy (Eds), Nutritional Composition of Fruit Cultivars, Academic Press, USA, P. 195-214.

[49]. Chen,Y. and Yu, D. Q. (1996). Tonkinecin, a novel bioactive annonaceous acetogenin from *Uvaria tonkinesis*, *J. Nat. Prod.*, 59(5): p. 507–509.

[50]. https://www.worldwidefruits.com/genus-uvaria.html. [Online]. Available: Google Search. [Accessed: 13-Sep-2018].

[51]. Zhou, L., Su, Y. C. F., and Saunders, R. M. K. (2009). Molecular phylogenetic support for a broader delimitation of *Uvaria* (Annonaceae), inclusive of *Anomianthus*, *Cyathostemma*, *Ellipeia*, *Ellipeiopsis* and *Rauwenhoffia*, *Syst. Biodivers*, 7(3): p. 249–258.

[52]. Moshi, M., Joseph, C., Innocent, E., & Nkunya, M. (2004). *In Vitro* Antibacterial and Antifungal Activities of Extracts and Compounds from *Uvaria scheffleri*, *Pharm. Biol*, 42(4–5): p. 269–273.

[53]. Kuma, M. and Shibru, S. (2015). Floristic Composition , Vegetation Structure and Regeneration Status of Kimphe Lafa Natural Forest, *J. Bot.*, 5(1) p. 19–32.

[54]. https://en.wikipedia.org/wiki/Ranunculaceae "Ranunculaceae.[online], accessed 2021."

[55]. Jin, F. (2012). The Pharmaceutical Potential of Compounds from Tasmanian Clematis species, Thesis, P. 330.

[56]. Rahman, A. H. M. M., & Akter, M. (2013). Taxonomy and Medicinal Uses of Euphorbiaceae (Spurge) Family of Rajshahi , Bangladesh, *Int. Res. J. Plant Sci*, 1(3): p. 74–80.

[57]. Jassbi, A. R. (2006) Chemistry and biological activity of secondary metabolites in

Euphorbia from Iran ,Phytochemistry, 67 (1): p. 1977–1984.

[58]. Hedberg, I., Hedberg, O., Madat, P. J., Mshigeni, K. E., Mshiu, E. N., and Samuelsson, G. (1983). Inventory of plants used in traditional medicine in Tanzania. II. Plants of the families dilleniaceae-Opiliaceae, *J. Ethnopharmacol*, 9(1): p. 105–127.

[59]. Gurib-Fakim, A., Sewraj, M., Gueho, J., and Dulloo, E. (1993). Medicalethnobotany of some weeds of Mauritius and Rodrigues, *J. Ethnopharmacol*, 39(3): p. 175–185.

[60]. Chhabra, S. C., Mahunnahb, R. L. A., & Mshiub, E. N. (1991). Plants used in traditional medicine in Eastern Tanzania. V. Angiosperms (Passifloraceae to Sapindaceae) S.C, *J. Ethnopharmacol*, 33: p. 143–157.

[61]. Innocent, E., Moshi, M. J., Masimba, P. J., Mbwambo, Z. H., Kapingu, M. C., and Kamuhabwa, A. (2009). Screening of traditionally used plants for *in vivo* antimalarial activity in mice, *African J. Tradit. Complement. Altern. Med.*, 6(2): p. 163–167.

[62]. Moshi, M. J., Mbwambo, Z. H., Nondo, R. S. O., Masimba, P. J., Kamuhabwa, A., Kapingu, M. C., Thomas, P., and Richard, M (2006). Evaluation of ethnomedical claims and brine shrimp toxicity of some plants used in Tanzania as traditional medicines, *African J. Tradit. Complement. Altern. Med.*, 3(3): p. 48–58.

[63]. Arnold H. J. and Gulumian M. (1984). Pharmacopoeia of traditional medicine in Venda," *J. Ethnopharmacol.*, 12(1): p. 35–74.

[64]. Poitou, F., Masotti, V., Viano, J., Gaydou, E. M., Andriamahavo, N. R., Mamitiana, A., and Andriantsiferana, M. (1995). Chemical Compositon of *Vepris elliotii* Essential Oil, *J. Essent. Oil Res*, 7(4): p. 447–449.

[65]. Hamzah, A. S., Lajis, N. H., and Sargent, M. V. (1994). Kaempferitrin from the leaves of *Hedyotis verticillata* and its biological activity, *Planta Med*, 60(4): pp. 388–389.

[66]. Rasoanaivo, P., Federici, E., Palazzino, G., and Galeffi, C. (1999). Acridones of *Vepris sclerophylla*: their ^{13}C-NMR data, *Fitoterapia*, 70, (6): p. 625–627.

[67]. Emmanuel, T., Djibo, D., Jean-noël, N., Laurent, S., Luce, V. E., Bernard, D., & Joseph, M. (2015). Research Article Two new compounds from stem barks of *Vepris heterophylla* (Engl .) R . Let . (Rutaceae), 7(7): p. 553–557.

[68]. Nordeng, H., Al-Zayadi, W., Diallo, D., Ballo, N., and Paulsen, B. S. (2013). Traditional

medicine practitioners knowledge and views on treatment of pregnant women in three regions of Mali, *J. Ethnobiol. Ethnomed*, 9(1): p. 1-9.

[69]. Tesfaye, A., and Sebsebe, D. (2009). Ethnobotanical study of medicinal plants in Kafficho people, southwestern Ethiopia," *16th Int. Conf. Ethiop. Stud.*, p. 711–726.

[70]. Patiño, L. O. J., Prieto, R. J. A., and Cuca, S. L. E. (2008). *Zanthoxylum Genus as Potential Source of Bioactive Compounds*, Prof. Iraj Rasooli (Ed.), InTech. *Bioact. Compd. Phytomedicine*, p. 185–218

[71]. Adesina, S. K. (2005). The Nigerian Zanthoxylum; Chemical and Biological Values Abstract, *Afr. J. Trad. CAM*, 2(3): p. 282–301.

[72]. Ross, S. A., Sultana, G. N. N., Burandt, C. L., ElSohly, M. A., Marais, J. P. J., and Ferreira, D. (2004). A new Antiplasmodial (+)-Norepinephrine Derivative from *Zanthoxylum syncarpum*, *J. Nat. Prod.*, 67(1): p. 88–90.

[73]. Munda, S. and Bhusan, B. K (2017). Pharmacological evaluation of methanolic extract of *zanthoxylum oxyphyllum* edgw. With special reference to anti-inflammatory and analgesic activity Sunita, *Int. J. Appl. Biol. Pharm. Technol*, 8(4) p. 5–10.

[74]. Agwaya, M. S., California, P. V., and Masawi , A. N. (2016). Hypoglycemic Activity of Aqueous Root Bark Extract *Zanthoxylum chalybeum* in Alloxan-Induced Diabetic Rats, *J. Diabetes Res*, p. 1-5.

[75]. Parmar, V. S., Malhotra, A., Singh, S. K., Bisht, K. S., and Jain, R. (1993). Novel Constituents of *Uvaria* Species, *Nat. Prod. Rep*, 11, 219-224.

[76]. Moriyasu, M., Takeuchi, S., Ichimaru, M., Nakatani, N., Nishiyama, Y., Kato, A., and ChaloMutiso, P. B. (2012). Pyrenes and pyrendiones from *Uvaria lucida*, *J. Nat. Med*, 66(3): p. 453–458.

[77]. Ichimaru, M., Nakatani, N., Takahashi, T., Nishiyama, Y., Moriyasu, M., Kato, A., Mathenge, S. G., Juma, F. D., and Nganga, J. N. (2004). Cytotoxic C-benzylated dihydrochalcones from *Uvaria acuminata*, *Chem. Pharm. Bull (Tokyo)*, 52(1): p. 138–141.

[78]. Okpekon, T. A., Dade, J. M. E., Say , M. V., Yapo, D. K., Champy, P., Séon-Ménie, B., Yolou, S. F., and Bories , C. (2015). Bingervone, an antiprotozoal β-triketone derivative from the roots of *Uvaria afzelii* (annonaceae), *Int. J. Pharm. Sci. Res*,.6(10) p. 4210–4215.

[79]. Wanzala, W., Syombua, M., Joseck Olukusi, J. A. (2016). A survey of the applications and use of ethnomedicinal plants and plant products for healthcare from the Ukambani region in Eastern Kenya, *Indian J. Ethnophyopharmaceuticals*, 2 (2): p. 6–58.

[80]. Chawla, R., Kumar, S., & Sharma, A. (2012). The genus *Clematis* (Ranunculaceae): Chemical and pharmacological perspectives, *J. Ethnopharmacol*, 143(1): p. 116–150.

[81]. Won, C., Mi, S., Zhao, R., Lee, C., Chun, W., Son, Y., Hun, S.K., Yun, J. J., Hwan, J.K., Je , I.C., Kwang, S.K., Woo,Y. K., Ju , S. A., Chan , S.K., and An, W. G. (2015). Hederagenin , a major component of *Clematis mandshurica* Ruprecht root , attenuates inflammatory responses in RAW 264 . 7 cells and in mice, *Int. Immunopharmacol*, 29(2): p. 528–537.

[82]. Fu, Q., Chen, J., Yuan, H., Ma, Y., Yu, T., and Zou, L. (2016). Alkaloids and phenolic glycosides from *Clematis mandshurica* and their inhibitory effects against no production in LPS-induced RAW 246 . 7 macrophages, *Phytochem. Lett*., 17(1): p. 238–241.

[83]. Ding, Q., Yang, L., Yang, H., Jiang, C., Wang, Y., and Wang, S. (2009). Cytotoxic and antibacterial triterpenoids derivatives from *Clematis ganpiniana*, *J. Ethnopharmacol*, 126(1): p. 382–385.

[84]. Zhao, M., Da-wa, Z., Guo, D., Fang, D., Chen, X., Xu, H., Gu Y., Xia, B., Chen L., Ding, L. and Zhou, Y. (2016). Cytotoxic triterpenoid saponins from *Clematis tangutica*, *Phytochemistry*, 130(1): 228–237.

[85]. Hawaze, S., Deti, H., and Suleman, S. (2012). I*n vitro* antimicrobial activity and phytochemical screening of *clematis* species indigenous to Ethiopia, *Indian J. Pharm. Sci*, 74(1): p. 29.

[86]. Huang, C., Luo , S., Li, Y., Li, C., Hua, J., Shu-Xi Jing, Y., Wang, Y., Yang, M., and Li, S. (2014). Antifeedant and Antiviral Diterpenoids from the Fresh Roots of *Euphorbia jolkini*, *Nat. Prod. Bioprospect, 4:91–100*.

[87]. Yang, M. C. Y. (2013). New jatropholane-type diterpenes from J*atropha curcas* cv, Multiflorum CY Yang, Nat. Prod. Bioprospect, 3: p. 99–102.

[88]. Ma, Y., Yuan, X. T. W., Ding, X., and Hao, Y. D. X. (2018). Abietane Diterpernoids from the Roots of *Euphorbia ebracteolata, Nat. Products Bioprospect.*, 8(2): p. 131–135.

[89]. Wang, A., Gao, X., Huo, X., Huang, S., Feng, L., Sun, C., Zhang, B., Ma, X., Jia, J., and Wang, C. (2017). Antioxidant acetophenone glycosides from the roots of *Euphorbia ebracteolata* Hayata, *Nat. Prod. Res.*, 6419: p. 1–6.

[90]. Hu, R., Gao, J., Rozimamat, R., and Rozimamat, H. A. (2018). Jatrophane diterpenoids from Euphorbia sororia as potent modulators against P-glycoprotein-based multidrug resistance, *Eur. J. Med. Chem*, 146, p. 157–170.

[91]. Rozimamat, R., Hu, R., and Akber, H. (2018). New isopimarane diterpenes and nortriterpene with cytotoxic activity from *Ephorbia alatavica* Boiss," *Fitoterapia*, 127: p. 328–333.

[92]. Jian, B. Zhang, H., and Liu, J. (2018). Structural Diversity and Biological Activities of Diterpenoids Derived from *Euphorbia*, *Molecules*, 23,(935); p. 1–12.

[93]. Benabdelaziz, I., Gómez-Ruizb, S., Benkhaleda, M., Carralerob, S., Schenkerc, P., Salmc, A., Gertschc, J., Haba, H. (2018). New cycloartane-type ester triterpenes from E*uphorbia pterococca* and biological evaluation, *Fitoterapia*, 127: p. 271–278.

[94]. https://www.prota4u.org/database, 1843. [Online]. Available: https://www.prota4u.org/database/protav8.asp?g=pe&p=Euphorbia+schimperiana+Scheele. [Accessed: 12-Nov-2021].

[95]. Fouda, A. A., Aristide, F. A. T., Langat, M. K., Ngeufa, E. H., Leonard, L. M. M., Mulholland, A. D., François, A.K.W., Sewald, N., and Duplex, J.W. (2017). Acridone alkaloids from *Vepris verdoorniana* (Excell & Mendonça) Mziray (Rutaceae), *Phytochem. Lett*, 19: p. 191–195

[96]. Brader, G., Bacher, M. Grege, H., and Hofer, O. (1996). pyranoquinolones and acridones from *Vepris bilocularis Phytochemistry*. 42(3): p. 881-884.

[97]. Kiplimo, J. J., Islam,S. M., and Koorbanally, N. A. (2012). Ring A- seco limonoids and flavonoids from the Kenyan *Vepris uguenensis* Engl . and their antioxidant activity, *Phytochemistry*, 83: p. 136–143.

[98]. Kiplimo J. J. and Koorbanally N. A. (2012) Antibacterial activity of an epoxidised prenylated cinnamaldehdye derivative from *Vepris glomerata*, *Phytochem. Lett.*, 5(3): p. 438–442.

[99]. Kiplimo, J. J., Islam,S. M., and Koorbanally, N. A. (2011). A Novel Flavonoid and Furoquinoline Alkaloids from *Vepris glomerata* and their Antioxidant Activity, *Nat Prod Commun*, 6 (12): 1847 - 18502.

[100]. Chaturvedula, V. S. P., Schilling, J. K., Miller, J. S., Andriantsiferana, R., Rasamison, V. E., and Kingston, D. G. I. (2004) New cytotoxic terpenoids from the wood of *Vepris punctata* from the madagascar rainforest, *J. Nat. Prod,* 67(5): p 895–898.

[101]. Krane, B. D. Moses 0. Fagbule, M. S. (1984).The Benzophenanthridine alkaloids, *J. Nat. Prod*, 47(1), p. 1–43.

[102]. Wang, C., You, C., Yang, K., Guo, S., Geng, Z., Fan, L., Du, S., Deng, Z.& Wang, Y. (2015). Antifeedant activities of methanol extracts of four Zanthoxylum species and benzophenanthridines from stem bark of *Zanthoxylum schinifolium* against Tribolium castaneum, *Ind. Crops Prod.*,. 74: p. 407–411.

[103]. Chen, I. S., Wu, S. J., Tsai, I. L., Wu, T. S., Pezzuto, J. M., Lu, M. C., & Teng, C. M. (1994). Chemical and bioactive constituents from *Zanthoxylum simulans, J. Nat. Prod.*, 57(9): p. 1206–1211.

[104]. Kerubo, O. L., Martin, M. G., Korira,E., Omoled, R., Seob, E., Yenesewa, A., Heydenreichc, M., Jacob Ogweno, M. J., and Efferth, T. (2019). Cytotoxicity of fagaramide derivative and canthin-6-one from *Zanthoxylum* (Rutaceae) species against multidrug resistant leukemia cells Leonidah. Nat. Prod. Res. P 1-8.

[105]. Patiño Ladino, O. J., & Cuca Suárez, L. E. (2010). Isoquinoline alkaloids of *Zanthoxylum quinduense* (Rutaceae)," *Biochem. Syst. Ecol*, 38(4): p. 853–856.

[106]. Patiño O. J. and Cuca, L. E. (2011). Monophyllidin, a new alkaloid L-proline derivative from *Zanthoxylum monophyllum*, *Phytochem. Lett*, 4(1): p. 22–25.

[107]. Emerson F. Q., Anne-Emmanuelle H., Fatima C., Daphnevan D., Drissa D. K. H. (2006). New and Bioactive Aromatic Compounds from *Zanthoxylum zanthoxyloides*, *Planta Med*, 72(8): 746-750.

[108]. Mukhlesur, R. M., Islam, M. A., Khondkar, P., and Gray, A. I. (2005). Alkaloids and lignans from *Zanthoxylum budrunga* (Rutaceae), *Biochem. Syst. Ecol,* 33(1): p. 91–96.

[109]. Chen, I., Tsai, I., Teng, C., Chen, J., Chang, Y., Ko, F., Lu, M.C., and Pezzuto, J. M.

(1997). Pyranoquinoline alkaloids from *Zanthoxylum simulans*, *Phytochemistry*, 46(3): p. 525 529.

[110]. Liu, S., Tsai, I., and Ishikawa, T. (2000). Bishordeninyl Terpene Alkaloids from *Zanthoxylum integrifoliolum*, *J Chin. Chem. Soc*, 47(3): pp. 571–574.

[111]. Sheen W. and Teng, C. (1996). Indolopyridoquinazoline Alkaloids with Antiplatelet Aggregation Activity from *Zanthoxylum integrifoliolum, Planta Med.* 62(2):175-176.

[112]. Diehl, E. E., Poser, G. L. Von, and Henriques, H. T. (2000). Constituents of *Zanthoxylum rugosum*, *Biochem. Syst. Ecol*, 28: p. 275–277.

[113]. Ferreira, M. E., Arias, A. R. De, Ortiz, S. T. De, Inchausti, A., & Nakayama, H. (2002). Leishmanicidal activity of two canthin-6-one alkaloids, two major constituents of *Zanthoxylum chiloperone* var . angustifolium, *J Ethnopharmacol*, 80(2-3): p. 7–10.

[114]. Ju, Y., Still, C. C., Sacalis, J. N., Li, J., & Ho, C.-T. (2001). Cytotoxic coumarins and lignans from extracts of the Northern prickly ash (Zanthoxylum americanum). Phytotherapy Research, 15(5), 441–443.

[115]. Young, S. J., Huong, D. H. L., Bae, K., Lee, M. K., and Kim, Y., (2002). Monoamine oxidase inhibitory coumarin from *Zanthoxylum schinifolium, Planta Med*, 68(1): p. 84–85.

[116]. Li, W., Sun, Y. N., Yan, X. T., Yang, S. Y., Kim, E., Kang, H. K., and Kang, H. K. (2000) Coumarins and Lignans from *Zanthoxylum schinifolium* and Their Anticancer Activities, *J. Agric. Food Chem*, 61(45): p 10730–10740.

[117]. Saqib, Q. N. Hui, Y.-H., Anderson, J. E., and McLaughlin, J. L. (1990). Bioactive furanocoumarins from the berries of *Zanthoxylum americanum*, *Phyther. Res*, 4(6): p. 216–219.

[118]. Chen, I. S., Chen, T., Chang, Y., Teng, C., and Lin, W. (1999). Chemical constituents and biological activities of the fruit of *Zanthoxylum integrifoliolum*, *J. Nat. Prod*, 62(6):p. 833–837.

[119]. Omosa, L. K., Mbogo, G. M., Korir, E., Omole, R., Seo, E.-J., Yenesew, A., and Efferth, T. (2019). Cytotoxicity of fagaramide derivative and canthin-6-one from *Zanthoxylum* (Rutaceae) species against multidrug resistant leukemia cells. *Nat.Prod. Res*, 35 (4): p.1–8.

[120]. Anza, M., Haile, E., Tadesse, S., Fikre Mammo,F., and Endale, M.. (2015). A coniferyl

alcohol derivative from the roots of *Zanthoxylum chalybeum*, 2(12): p. 970–974.

[121]. Chagonda, L., Mazuru Gundidza, M., Wijesuria A. M. S. and Mavi, S. (1994). Composition of the leaf oil of *Zanthoxylum chalybeum* Thunb, *J. Essent. Oil Res.*, 6(6): p. 561–563.

[122]. Salae, A. W., Chairerk, O., Sukkoet, P., Chairat, T., Prawat, U., Tuntiwachwuttikul, P., Chalermglin, P., and Ruchirawat, S. (2017). Antiplasmodial dimeric chalcone derivatives from the roots of *Uvaria siamensis*, *Phytochemistry*, 135(1): p. 135–143.

[123]. Weenen, H., Nkunya, M. H. H., Mgani, Q. A., Posthumus, M. A., Waibel, R., and Achenbach, H. (1991). Tanzanene, a Spiro Benzopyranyl Sesquiterpene from *Uvaria tanzaniae* Verdc. *J. Org. Chem*, 56, (20): p. 5865–5867.

[124]. Weenen, H., Nkunya, M. H. H., El-Fadl, A. A., Harkema, S., and Zwanenburg, B. (1990). Lucidene, a Bis(benzopyranyl) Sesquiterpene from *Uvaria lucida* ssp. lucida, *J. Org. Chem*, 55 (17): p. 5107–5109.

[125]. Muhammad I. and Waterman, P. G. (1988). Chemistry of the annonaceae, part XXVI. The uvarisesquiterpenes, a novel type of benzylated sesquiterpene from uvaria angolensis, *J. Nat. Prod.*, 51 (4): p. 719–724.

[126]. Lasswell W. L. and Hufford, C. D. (1977). Cytotoxic C-Benzylated Flavonoids from *Uvaria chamae, J. Org. Chem*, 42(8):p. 1295–1302.

[127]. Fall, D., Duval, R. A., Gleye, C., Laurens, A., & Hocquemiller, R. (2004). Chamuvarinin, an acetogenin bearing a tetrahydropyran ring from the roots of *Uvaria chamae*, *J. Nat. Prod*, 67(6): p. 1041–1043.

[128]. Ankisetty, S., ElSohly, H. N., Li, X. C., Khan, S. I., Tekwani, B. L., Smillie, T., & Walker, L. (2006). Aromatic constituents of *Uvaria grandiflora*, *J. Nat. Prod*, 69, (4): p. 692–694.

[129]. Akendengue, B., Roblot, F., Loiseau, P. M., Bories, C., Ngou-Milama, E., Laurens, A., & Hocquemiller, R. (2002). Klaivanolide, an antiprotozoal lactone from *Uvaria klaineana*, *Phytochemistry*, 59(8): p. 885–888.

[130]. Seangphakdee, P., Pompimon, W., Meepowpan, P., & Panthong, A. (2013). Anti-inflammatory and anticancer activities of (−)-zeylenol from stems of *Uvaria grandiflora*,

39: p. 610–614.

[131]. Waterman, P. G., and Mohammad I. (1984). Chemistry of the Annonaceae. Structures of Uvarindoles A-D, Four New Benzylated lndole Alkaloids from Uvaria angolensis, *j. Chem. Soc., chem. Commun*, 1984: p. 1280–1281.

[132]. Muhammad I. and Waterman, P. G. (1985). Chemistry of the annonaceae, part 18.1benzylated indoles and dihydrochalcones in uvaria angolensis from tanzania, *J. Nat. Prod.*, vol. 48(4): p. 571–580.

[133]. Macabeo, A. P. G., Rubio, P. Y. M., Higuchi, T., Umezawa, N., Faderl, C., Budde, S., Bangcaya, P.S., & Jonathan D, G. A. (2017*).* Polyoxygenated seco-cyclohexenes and other constituents from *Uvaria valderramensis*, *Biochem. Syst. Ecol*, 71: p. 200–204.

[134]. Lekphrom, R., Kanokmedhakul, K., Schevenels, F., & Kanokmedhakul, S. (2018) Antimalarial polyoxygenated cyclohexene derivatives from the roots of Uvaria cherrevensis, *Fitoterapia*, 127(2): p. 420–424.

[135]. Macabeo, A. P. G., Letada, A. G., Budde, S., Faderl, C., Dahse, H. M., Franzblau, S. G., Jonathan D. G. A., Pierens G. K., & Garson, M. J. (2017). Antitubercular and Cytotoxic Chlorinated seco-Cyclohexenes from *Uvaria alba*. *Journal of Natural Products*, *80*(12), 3319–3323.

[136]. Ichimaru, M., Nakatani, N., Moriyasu, M., Nishiyama, Y., Kato, A., Mathenge, S. G. & Chalo Mutiso, P. B. (2010). Hydroxyespintanol and scheffleri chalcone: Two new compounds from *Uvaria scheffleri*, *J. Nat. Med*, 64,(1): p. 75–79.

[137]. Lin Yuan, Wenzhong Huang, Y. M. and Z. Du. (2012). Two new phenolic constituents from Clematis connata, *Afr. **J**. Pharm. Pharmacol*, 6(14): p. 1050–1055.

[138]. Zhang, L. J., Huang, H. T., Huang, S. Y., Lin, Z. H., Shen, C. C., Tsai, W. J., and Kuo, Y. H. (2015). Antioxidant and Anti-Inflammatory Phenolic Glycosides from *Clematis tashiroi*, *J. Nat. Prod*, 78(7): p. 1586–1592.

[139]. Liu, L. F., Ma, X. L., Wang, Y. X., Li, F. W., Li, Y. M., Wan, Z. Q., and Tang, Q. L. (2009). Triterpenoid saponins from the roots of *clematis chinensis* osbeck," *J. Asian Nat. Prod. Res*, 11(5): p. 389–396.

[140]. Fu, Q., Qiu, L., Yuan, H., Du, Y., Cheng, X., and Tang, T. (2017) Triterpenoid saponins

from *Clematis chinensis* and their inhibitory activities on NO production, *Phytochem. Lett*, 21(1): 206–210.

[141]. Mimaki, Y., Yokosuka, A., Hamanaka, M., Sakuma, C., and Yamori, T. (2004).Triterpene Saponins from the Roots of *Clematis chinensis*, *J. Nat. Prod*. 67, p. 1511-1516.

[142]. Cheng, L., Shi, L., Wu, J., Zhou, X., Li, X., Sun, X., Zhu., L., Xia, T., and Ding, Q. (2018). A hederagenin saponin isolated from *Clematis ganpiniana* induces apoptosis in breast cancer cells via the mitochondrial pathway, *Oncol. Lett.*, 15(2): p. 1737-1743.

[143]. Sun, F., He, Q., Gen, P., and Yu, Y. (2007). A new triterpenoid saponin from *Clematis ganpiniana*, *Chin. Chem. Lett*,18(9): p. 1078–1080.

[144]. Chen, J. H., Du, Z. Z., Shen, Y. M., and Yang, Y. P. (2009). Aporphine alkaloids from *Clematis parviloba* and their antifungal activity, *Arch. Pharm. Res*, 32(1): p. 3–5.

[145]. Shi, S., Tu, P., Dong, C., and Jiang, D. (2006). Alkaloids from Clematis manshurica Rupr, *J. Asian Nat. Prod. Res.*, 8(1–2): p. 73–78.

[146]. Li, W., Yang, B., Zhu, W., Gong, M., Xu, X., Lu, X., Sun, L., Tian, J., and Zhang, L. (2013). A new indole alkaloidal glucoside from the aerial parts of *Clematis terniflora*,, *Nat. Prod. Res*, 27(24): p. 37–41.

[147]. Shi, Q., Su, X., and Kiyota, H. (2008). Chemical and Pharmacological Research of the Plants in Genus *Euphorbia*, *Chem. Rev.*108(10): p. 4295–4327.

[148]. Dong, M., Chen, X., Chen, C., & Li, R. (2018). Terpenes from *Euphorbia antiquorum* and Their in Vitro Anti-HIV Activity, *Chem. Biodivers*, 15 (5): p. 1–7.

[149]. Mai, Z., Ni, G., Liu, Y., Li, L., Li, J., & Yu, D. (2018). Heliojatrones A and B, Two Jatrophane-Derived Diterpenoids with a 5/10 Fused-Ring Skeleton from *Euphorbia helioscopia* : Structural Elucidation and Biomimetic Conversion,. *Org. Lett*, 20(10): p. 3124–3127.

[150]. Kim, Y., Ahn, J., Chae, H., Hee, Y., Kim, J., & Chin, Y. (2018). Two new lathyrane-type diterpenoid glycosides with IL-6 production inhibitory activity from the roots of *Euphorbia kansui*, *Bioorg. Med. Chem. Lett*, 28(7): p. 1207–1210.

[151]. Sook, Y., Takeda, Y., Fukaya, H., Fuchino, H., Kawahara, N., Takahashi, S., Takahashi,

Y., and Inoue, H. (2018). A new ent-norabietant diterpenoid from roots of *Euphorbia lathyris* L .," *Tetrahedron Lett*, 59(29): p. 2813–2815.

[152]. Shaker, K. H.(2015). Antioxidant Compounds from *Euphorbia schimperiana* scheele in Aseer Region, Saudi Arabia Kamel, *J. Pharm. Sci. Rev. Res,* 32(21): p. 117–122.

[153]. Wansi, J.D., Mesaik, M.A., Chiozem, D.D., Devkota, K.P., Gaboriaud-Kolar, N., Lallemand, M.-C. (2008). Oxidative burst inhibitory and cytotoxic indoloquinazoline and furoquinoline alkaloids from *Oricia suaveolens*, *J. Nat. Prod*, 71(11): p. 1942–1945.

[154]. Lacroix, D., Prado, S., Kamoga, D., Kasenene, J., and Bodo, B. (2012). Absolute configuration of 2′(R)-acetylmontrifoline and 2′(R)-montrifoline, furoquinolines from the fruits of *Teclea nobilis*, *Phytochem. Lett*, 5(1): p. 22–25.

[155]. Wansi, J., Happi, E., Bavoua, J., Devkota, K., and Sewald, N. (2011). Bioactive β -indoloquinazoline Alkaloids from *Oricia renieri*, *Planta Med*, 78(1): 71-75.

[156]. Nouga, A. B., Ndom, J. C., Mpondo, E. M., Nyobe, J. C. N., Njoya, A., Meva'a, L. M., and Wansi, J. D. (2016). New furoquinoline alkaloid and flavanone glycoside derivatives from the leaves of *Oricia suaveolens* and *Oricia renieri* (Rutaceae), *Nat. Prod. Res*, 30 (3): p. 305–310.

[157]. Tillequin, F. (2007). Rutaceous alkaloids as models for the design of novel antitumor drugs, *Phytochem. Rev*, 6(1): p. 65–79.

[158]. Cordero, C. P., Gómez-González, S., León-Acosta, C. J., Morantes-Medina, S. J., and Aristizabal, F. A. (2004). S. Gómez-González, C. J. León-Acosta, S. J. Morantes-Medina, and F. A. Aristizabal, Cytotoxic activity of five compounds isolated from Colombian plants, *Fitoterapia*, 75(2): p. 225–227.

[159]. Manikandarajan, P.A., Sathish, M., Suresh, R., and Suresh, A.J (2018). Isolation, characterization, docking and anti-cancer activity of quercetin from leaves of *Euphorbia heterophylla* linn, *Int. J. Pharm. Sci. Res.*, 9(1): p. 197–202.

[160]. Diéguez-Hurtado, R., Garrido-Garrido, G., Prieto-González, S., Iznaga, Y., González, L., Molina-Torres, J., Curini , M., Epifano, F., and Marcotullio, M. C (2003). Antifungal activity of some Cuban *Zanthoxylum* species, *Fitoterapia*, 74(3): p. 384–386.

[161]. Tatsadjieu, L. N., Essia Ngang, J. J., Ngassoum, M. B., and Etoa, F. X. (2003).

Antibacterial and antifungal activity of Xylopia aethiopica, Monodora myristica, *Zanthoxylum xanthoxyloïdes* and *Zanthoxylum leprieurii* from Cameroon, *Fitoterapia*, 74(5): p. 469–472.

[162]. Hufford, C. D. and Oguntimein, B. O. (1987). Angoluvarin, an Antimicrobial Dihydrochalcone from *Uvaria angolensis*, 52(23): p. 5286–5288.

[163]. Padmaja, V., Thankamany, V., and Hisham, A. (1993). Antibacterial, antifungal and anthelmintic activities of root barks of *Uvaria hookeri* and *Uvaria narum*, *J. Ethnopharmacol*, 40(3): p. 181–186.

[164]. Bhatt, H. (2016). Preliminary phytochemical , physicochemical , antioxidant and antimicrobial studies of *Clematis montana* leaves, *Int J Curr Pharm Res*, 8,(4): p. 33-36.

[165]. Giridhar, A., Chawla, A., Jain, S., Jain, N., and Giridhar, S. (2010). Acridone alkaloids – a brief review. Int.J. Pharma. Res. Develop, 1(1): p 010

[166]. Dewick, P.M. (2009) Medicinal Natural Products: A Biosynthetic Approach. 3rd Edition, John Wiley & Sons, New York.

[167]. Sarker, S.D., Nahar, L., and Gray, A.I., (2006). Natural Products Isolation. Second Edition, edited by Satyajit D. Sarker, Zahid Latif, and Alexander I. Gray, Human press, Totowa New Jersey.p.529.

[168]. Palomino-Schätzlein, M., Montaño, M., Escrig, P., Boira, H., Corma, A., Pineda-Lucena, A., Primo, J., and Cabedo, N. (2017). Identification of Bioactive Compounds in Polar and Nonpolar Extracts of *Araujia sericifera*, *Planta Medica Int. Open*, 4(3): p. 93–103,.

[169]. Valgas, C. Machado, S. S., Smânia, E. F. A., and Smânia, A. J. (2007). Screening methods to determine antibacterial activity of natural products, *Brazilian J. Microbiol*, 38(2): p. 369–380.

[170]. Madrid, E., Galan-Puchades, T., and Marius V. F. (2012). Risk analysis of human anisakidosis through the consumption of the blue whiting, micromesistius poutassou, sold at Spanish supermarkets, *Foodborne Pathog. Dis*, 9(10): p. 934–938.

[171]. Giarratana, F., Muscolino, D., Ziino, G., Giuffrida, A., Marotta, S. M., Presti, V. L., Chiofalo, V. and Panebianco, A. (2017). Activity of Catmint (*Nepeta cataria*) essential oil against Anisakis larvae, *Trop. Biomed*, 34(1): 22–31.

[172]. Kavitha, N., Chen, Y., Kanwar, J. R. and Sasidharan, S. (2017). In situ morphological assessment of apoptosis induced by Phaleria macrocarpa (Boerl.) fruit ethyl acetate fraction (PMEAF) in MDA-MB-231 cells by microscopy observation, *Biomed. Pharmacother*, 87(1): p. 609–620.

[173]. Narramore, S., Stevenson, C. E. M., Maxwell, A., Lawson, D. M., and Fishwick, C. W. G. (2019). New insights into the binding mode of pyridine-3-carboxamide inhibitors of E . coli DNA gyrase, *Bioorg. Med. Chem.*, 27(16): p. 3546–3550.

[174]. Trott O. and Olson, A. J. (2009). Software News and Update AutoDock Vina : Improving the Speed and Accuracy of Docking with a New Scoring Function , Efficient Optimization , and Multithreading, *J. Comput.Chem*, 31(2): p. 455-461.

[175]. Seeliger D.and De Groot, B. L. (2010). Ligand docking and binding site analysis with PyMOL and Autodock / Vina, *J Comput Aided Mol Des*, 24(5): p. 417–422, 2010.

[176]. Lipinski, C. A., Franco; L., Dominy, B. W., and Feeney, P. J. (1997). Experimental and computational approaches to estimate solubility and permeability in drug discovery and development settings, *Adv.Drug.Deliv. Rev*. 23 (1-3):p. 3-25.

[177]. Oduselu, G. O., Ajani, O. O., Ajamma, Y. U.; Brors, B., and Adebiyi, E. (2019) Homology Modelling and Molecular Docking Studies of Selected Substituted Benzo[d]imidazol-1-yl)methyl)benzimidamide Scaffolds on Plasmodium falciparum Adenylosuccinate Lyase Receptor, *Bioinform. Biol. Insights*, 13(2): p 1-10.

[178]. Behrouz, S., Navid, M., Rad, S., Taghavi, B., Mohammad, S., Behrouz, M., and Mirkhani, H. (2018). Design , synthesis , and in silico studies of novel eugenyloxy propanol azole derivatives having potent antinociceptive activity and evaluation of their β - adrenoceptor blocking property, *Mol. Divers, 23(1): 147–164*.

[179]. Abu-melha, S. (2018). Design, Synthesis and DFT/DNP Modeling Study of New 2-Amino-5-arylazothiazole Derivatives as Potential Antibacterial Agents, *molecules*, *23*(2): 434.

[180]. Pegei, K. H. (1969). South African Plant Extractives. Part II. Alkaloids of Alkaloids of *Teclea natalensis*, J. Chem. SOC.1969(3): p. 2327–2329.

[181]. Bowie, J. H. et al (1967). The Mass Spectra of Acridone, *Aust. J. Chem*, 20(2): p.1179-

1193

[182]. Kenmogne Kouam, A. D., Kenmogne, S. B., Songue Lobe, J., Ngeufa Happi, E., Stammler, H.-G., Kamdem Waffo, A. F., Sewald, N., and Wansi, J. D. (2019). A rotameric tryptamide alkaloid from the roots of *Vepris lecomteana* (Pierre) Cheek & T. Heller (Rutaceae), *Fitoterapia*, 135(1): p. 9–14.

[183]. Shoji, N. Umeya, A., Takemo, T., Kajiwa, A., and Ohizumi, Y. (1986). Isolation of Evodiamine, a Powerful Cardiotonic Principle, from *Evodia rufaecarpa* Bentham (Rutaceae), *J. Pharm. Sci*, 75(6): p. 612-613.

[184]. Joshi, B. S., Moore, K. M., and Pelletier, S.W. (1991). Alkaloids of *Zanthoxylum budrunga* Wall. : NMR Assignments of Dihydrochelerythrine , Evodiamine and Zanthobungeanine, *Phytochem Anal*, 2(1): p. 20–25.

[185]. Khaljd, S. A and Waterman, P. G (1982). Furoquinoline and pyrano-2-quinolone alkaloids, *J. Nat. Prod*, 45(3): p. 343–346.

[186]. Paulini, H., Waibel, R., and Schimmer, O. (1989) Mutagenicity and structure-mutagenicity relationships of furoquinolines, naturally occurring alkaloids of the Rutaceae, Mutat. Res. Lett., 227(3): p. 179–186.

[187]. Wu, T.-S., Shi, L.-S., Wang, J.-J., Iou, S.-C., Chang, H.-C., Chen, Y.-P., Kuo, Y.-H., Chang, Y.-L. and Tenge, C.-M. (2003). Cytotoxic and Antiplatelet Aggregation Principles of Ruta graveolens, 50 (1): p. 171–178.

[188]. Cisneros, J. A., Vandevoorde, S., Ortega-Gutie´rrez, S., Paris, C., Fowler, C. J., and Lo´pez-Rodrı´guez, M. L. (2007). Structure-activity relationship of a series of inhibitors of monoacylglycerol hydrolysis - Comparison with effects upon fatty acid amide hydrolase," *J. Med. Chem*, 50(20): p. 5012–5023.

[189]. Sai, C., Wang, J., Li, B., Ding, L., Wang, H., Wang, Q., Hua, H., Zhang, F., and Ren, Q. (2020). Isolation and identification of alkaloids from M*macleaya microcarpa* by UHPLC–Q-TOF-MS and their cytotoxic activity in vitro, antiangiogenic activity in vivo, *BMC Chem*, 14(1): p. 1–11.

[190]. Kato, A., Moriyasu, M., Ichimaru, M., Nishiyama, Y., Juma, F.D., Nganga, J.N., Mathenge, S.G., Ogeto, J.O. (1996). Isolation of alkaloidal constituents of *Zanthoxylum*

usambarense and *Zanthoxylum chalybeum* using ion-pair HPLC, *J. Nat. Prod,* 59(3): pp. 316–318.

[191]. Sandjo, L. P., Kuete, V., Tchangna, R. S., Efferth, T., and Ngadjui, B. T. (2014). Cytotoxic Benzophenanthridine and Furoquinoline Alkaloids from *Zanthoxylum buesgenii* (Rutaceae), *Cardiovasc. Interv. Ther*, 8(1): p. 1–5.

[192]. Bodede, O. (2016). Phytochemical Analysis with Antioxidant and Cytotoxicity Studies of the Bioactive Principles from *Zanthoxylum capense* (Small Knobwood), 17(1). 627–634.

[193]. Wang, C., Fan, L., Tian, M., and Du, S. (2015). Cytotoxicity of benzophenanthridine alkaloids from the roots of *Zanthoxylum nitidum* (Roxb .) DC . var . fastuosum How ex Huang, Nat. Prod. Res, 29(14): p. 1380–1383.

[194]. Miao, F., Yang, X., Zhou, L., Hu, H., and Zheng, F. (2011). Structural modification of sanguinarine and chelerythrine and their antibacterial activity, *Nat. prod. res*, 25(9): p. 863–875.

[195]. Muhammad, I and Waterman, P. G. (1985). Chemistry of the annonaceae, part 18.1 benzylated indoles and dihydrochalcones in *Uvaria angolensis* from tanzania, *J. Nat. Prod,* 48(4): p. 571–580.

[196]. Allahresani, A., Ghorbanian, F., Nasseri, M. A., and Kazemnejadi, M. (2020). Isolation and characterization of bis(2-ethylheptyl) phthalate from *Cynodon dactylon* (L.) and studies on the catalytic activity of its Cu(II) complex in the green preparation of 1,8-dioxo-octahydroxanthenes, *Q. J. Iran. Chem. Commun*, 8(3): p. 212–227.

[197]. Li, Y., Qian, Z., and Kim, S.(2008). Cathepsin B inhibitory activities of three new phthalate derivatives isolated from seahorse , Hippocampus Kuda Bleeler, *Bioorg. Med. Chem. Lett.*, 18(23): p. 6130–6134.

[198]. Laghari, A. H., Memon , S., Nelofar, A., and Khan, K. M. (2011). Alhagi maurorum: A convenient source of lupeol, *Ind. Crops Prod.*, 34(1): p. 1141–1145.

[199]. Jain P. S. and Bari, S. B. (2010). Isolation of lupeol, stigmasterol and campesterol from petroleum ether extract of woody stem of Wrightia tinctoria, *Asian J. Plant Sci*, 9(3): p. 163–167.

[200]. Di Pietro, M. E., Mannu, A., and Mele, A. (2020). NMR determination of free fatty acids

in vegetable oils, *Processes*, 8(4): p. 1-15.

[201]. El-Shafae A. M. and Ibrahim, M. A (2003). Bioactive kaurane diterpenes and coumarins from *Fortunella margarita*, *Pharmazie*, 58(2): p. 143–147.

[202]. Wu, T. S. (1988). Alkaloids and coumarins of *Citrus grandis*, *Phytochemistry*, 27(11): p. 3717–3718.

[203]. Petrus, L., Alföldi, J., Matulová, M., and Bílik, V. (1984). Preparation and 13C NMR spectra of some disaccharide glycosylmethylamines. Chem. Papers 39 (3): p 401-406.

[204]. Oguntimein, B., Ekundayo, O., Laakso, I., and Hiltunen, R. (1989). Volatile Constituents of Uvaria chamae Leaves and Root Bark, *Planta Medica*, 55(1): p. 312–313.

[205]. Phuyal, N., Jha, P. K., Raturi, P. P., Gurung, S.and Rajbhandary, S. (2019). Essential oil composition of *Zanthoxylum armatum* leaves as a function of growing conditions, *Int. J. Food Prop*, 22(1): p. 1873–1885.

[206]. Theeramunkong, S. and Utsintong, M. (2018). Comparison between Volatile Oil from Fresh and Dried Fruits of *Zanthoxylum rhetsa* (Roxb .) DC . and Cytotoxicity Activity Evaluation, 10(5): p. 827–832.

[207]. Molla, T. Babu, G. N. (2020). Variation in Chemical Composition and Antimicrobial Activities of Essential oil of Leaves of Knob Wood, *Zanthoxylum chalybeum* Collected from Three Different Places of Eastern Ethiopia, *Orient. J. Chem.*, 36(3): p. 513–523.

[208]. Garcia, G., Charmillon, J. M., Roux, E., Sutour, S., Rakotozafy, J. B., Désiré, O., Paoli, M., Tomi, F., and Rabehaja, D. J. R. (2017). Chemical composition of leaf and bark essential oils of *Vepris unifoliolata* from Madagascar, *J. Essent. Oil Res*, 29(3): p. 214–220.

[209]. Kosina, P., Gregorova, J., Gruz, J., Vacek, J., Kolar, M., Vogel, M., Werner, R., Kathrin, N., Vilim, S., and Ulrichova, J. (2010). Phytochemical and antimicrobial characterization of *Macleaya cordata* herb, *Fitoterapia*, 81(80): p. 1006–1012.

[210]. Döll-Boscardin, P. M., Sartoratto, A., Sales Maia, B. H. L. de N., Padilha de Paula, J., Nakashima, T., Farago, P. V., & Kanunfre, C. C (2012). In vitro cytotoxic potential of essential oils of *Eucalyptus benthamii* and its related terpenes on tumor cell lines, *Evidence-based Complement. Altern. Med.*, 2012,(1): p.1-8.

[211]. Abdelrheem, D. A., Rahman, A. A., Elsayed, K. N. M., Abd El-Mageed, H. R., Mohamed, H. S., and Ahmed, S. A. (2021). Isolation, characterization, in vitro anticancer activity, dft calculations, molecular docking, bioactivity score, drug-likeness and admet studies of eight phytoconstituents from brown alga sargassum platycarpum, *J. Mol. Struct*,. 1225(1): p. 129245.

[212]. Pan, X., Hartley, J.M., Hartley, J.A., White, K.N., Wang, Z., and Bligh, S.W.A. (2012). Evodiamine, a dual catalytic inhibitor of type i and II topoisomerases, exhibits enhanced inhibition against camptothecin resistant cells, *Phytomedicine*, 19(7): p. 618–624

[213]. Wang, J. C. (2002). Cellular roles of DNA topoisomerases: A molecular perspective, *Nat. Rev. Mol. Cell Biol*, 3(6): p. 430–440

[214]. D'Atanasio, N., Capezzone de Joannon, A., Di Sante, L., Mangano, G., Ombrato, R., Vitiello, M., Bartella, C., Magarò, G., Prati, F., Milanese, C., Vignaroli, C., Paolo Di Giorgio, F., and Tongiani, S. (2020). Antibacterial activity of novel dual bacterial DNA type II topoisomerase inhibitors, *PLoS One*, 15(2): p. 1–21.

[215]. Mumit, M.A., Pal, T.K., Alam, M.A., Islam, M.A.A.A.A., Paul, S., Sheikh, M.C. (2020). DFT studies on vibrational and electronic spectra, HOMO–LUMO, MEP, HOMA, NBO and molecular docking analysis of benzyl-3-N-(2,4,5-trimethoxyphenylmethylene)hydrazinecarbodithioate, *J. Mol. Struct*, 1220(1): p. 128715.

[216]. Rodriguez-Antona, C., and Ingelman-Sundberg, M .(2006). Cytochrome P450 pharmacogenetics and cancer, *Oncogene*, 25, (11): p. 1679–1691.

[217]. Eswaramoorthy, R., Hailekiros, H., Kedir, F., Endale, M. (2021). In silico Molecular Docking, DFT Analysis and ADMET Studies of Carbazole Alkaloid and Coumarins from Roots of *Clausena anisata*: A Potent Inhibitor for Quorum Sensing. *Adv. Appl. Bioinform. Chem, 14*(7): p 13-24.

APPENDIXES

Appendix 1A: ^{1}H NMR spectrum of norevoxanthine (**244**), $CDC1_3$, 500 MHz

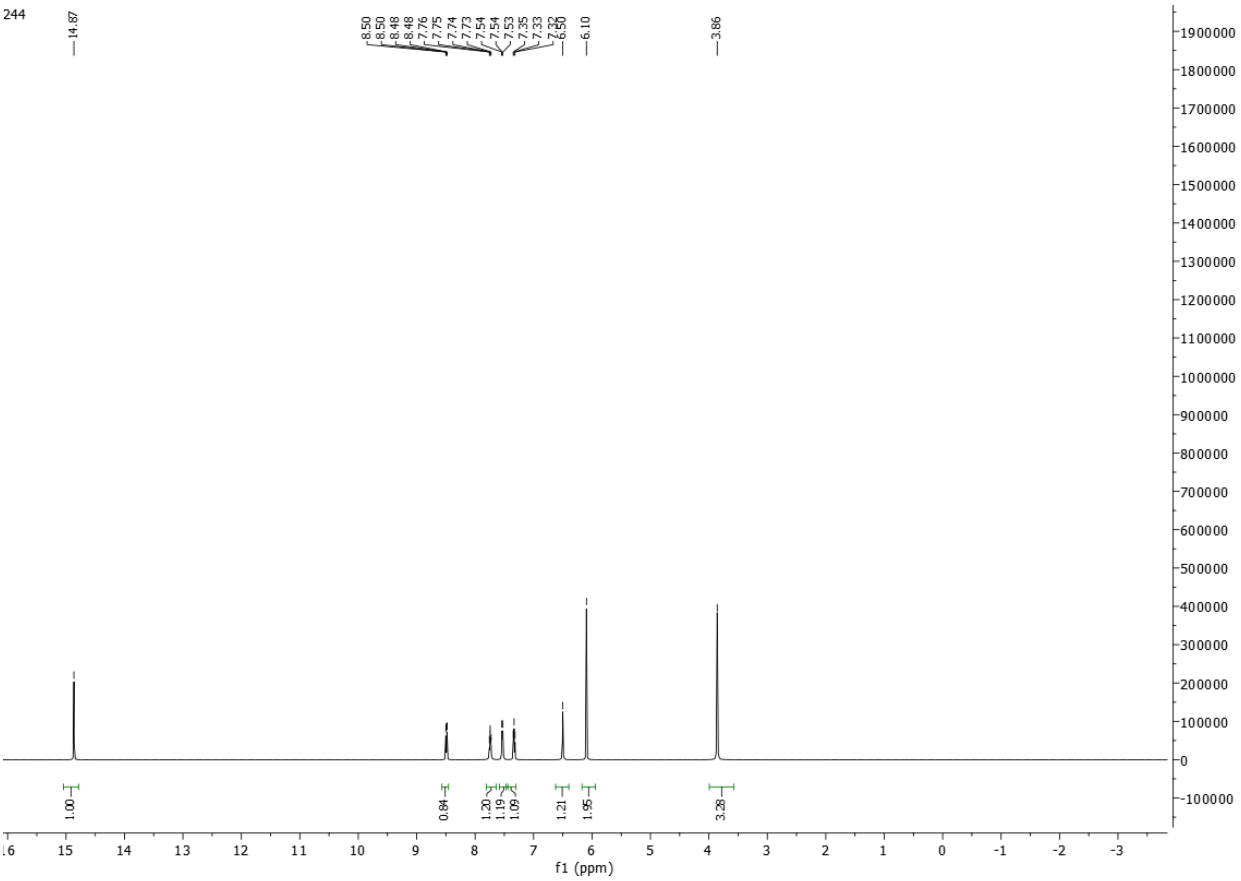

Appendix 1B: ^{13}C NMR spectrum of norevoxanthine (**244**), $CDC1_3$, 125 MHz

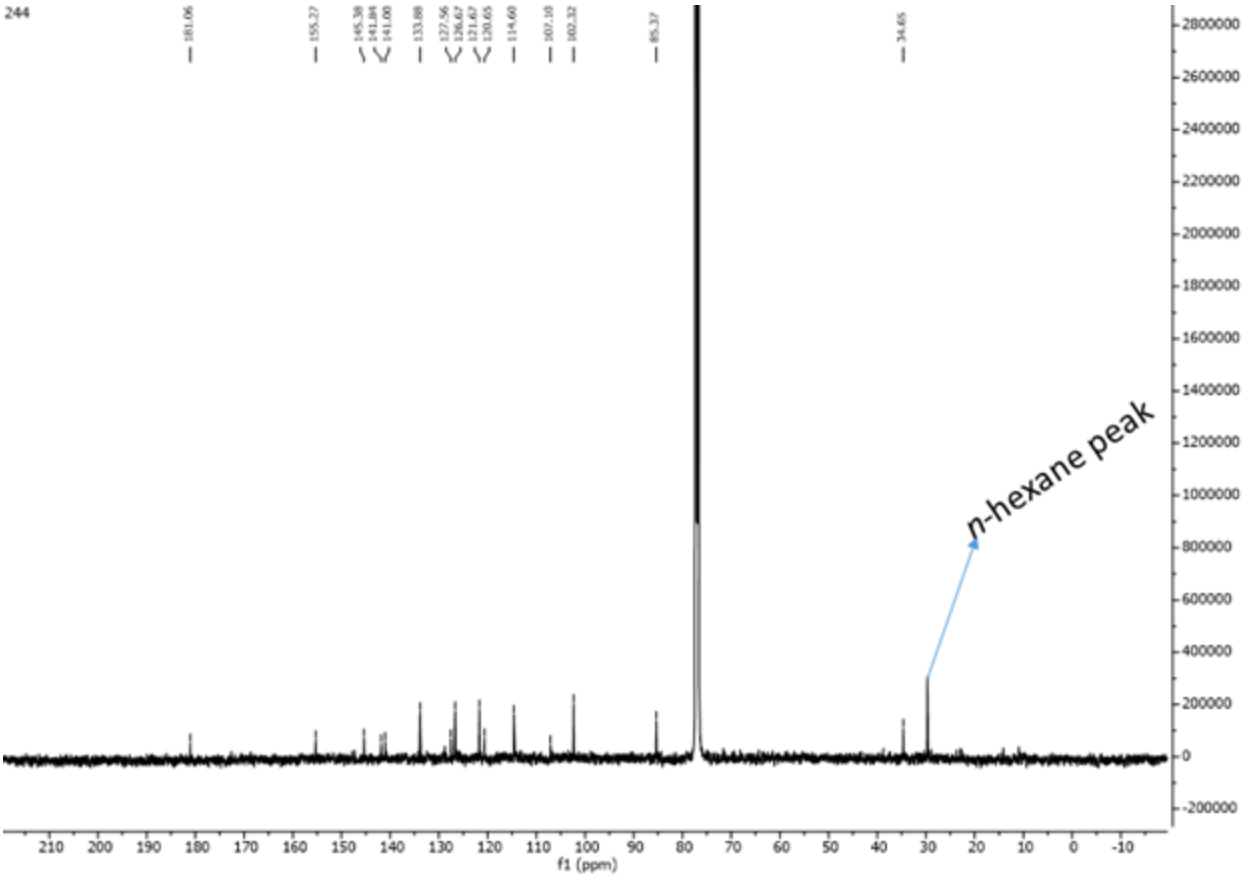

Appendix 1C: DPT-135 spectrum of norevoxanthine (**244**), $CDC1_3$, 125 MHz

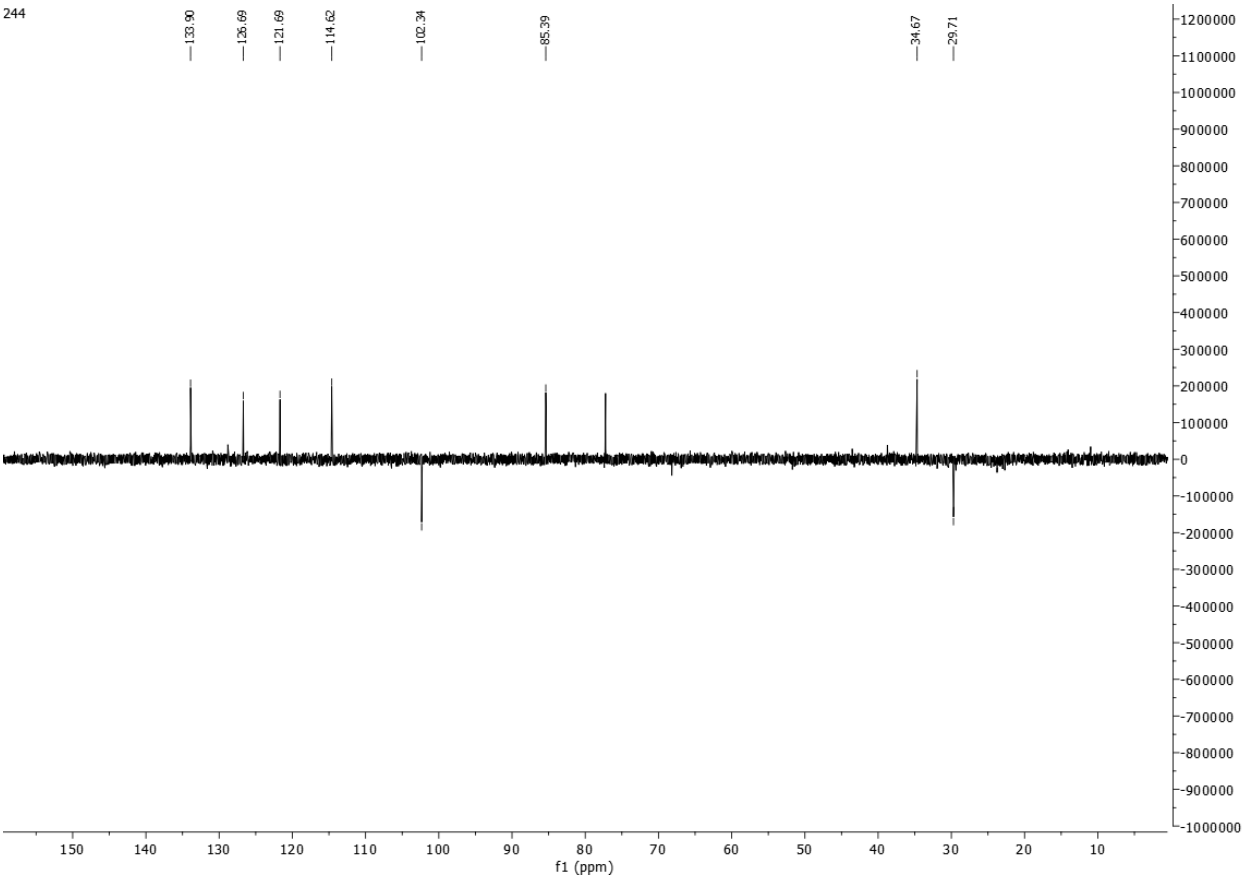

Appendix D: HSQC spectrum of Norevoxanthine (**244**), $CDC1_3$, 125 MHz

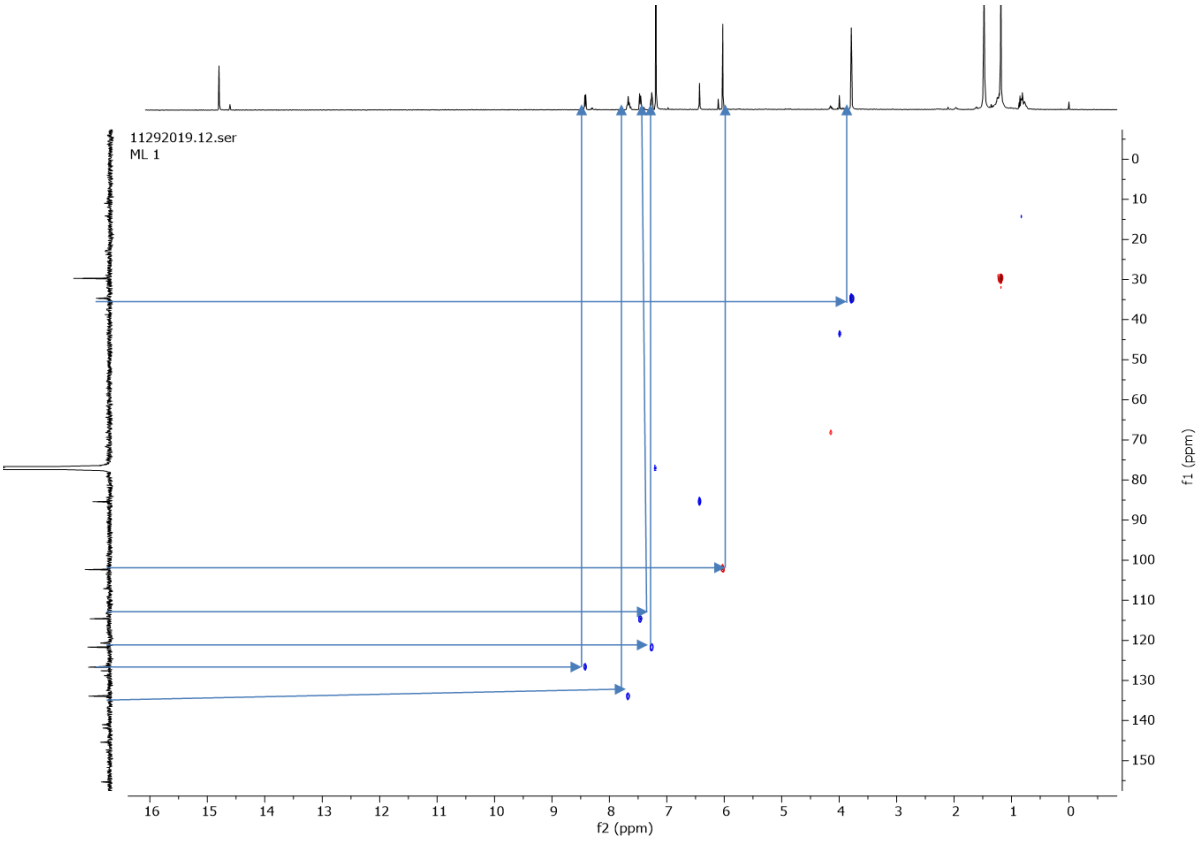

67

Appendix 2A: ^{1}H NMR spectrum of evoxanthine (**17**), $CDC1_3$/MeOD, 300 MHz

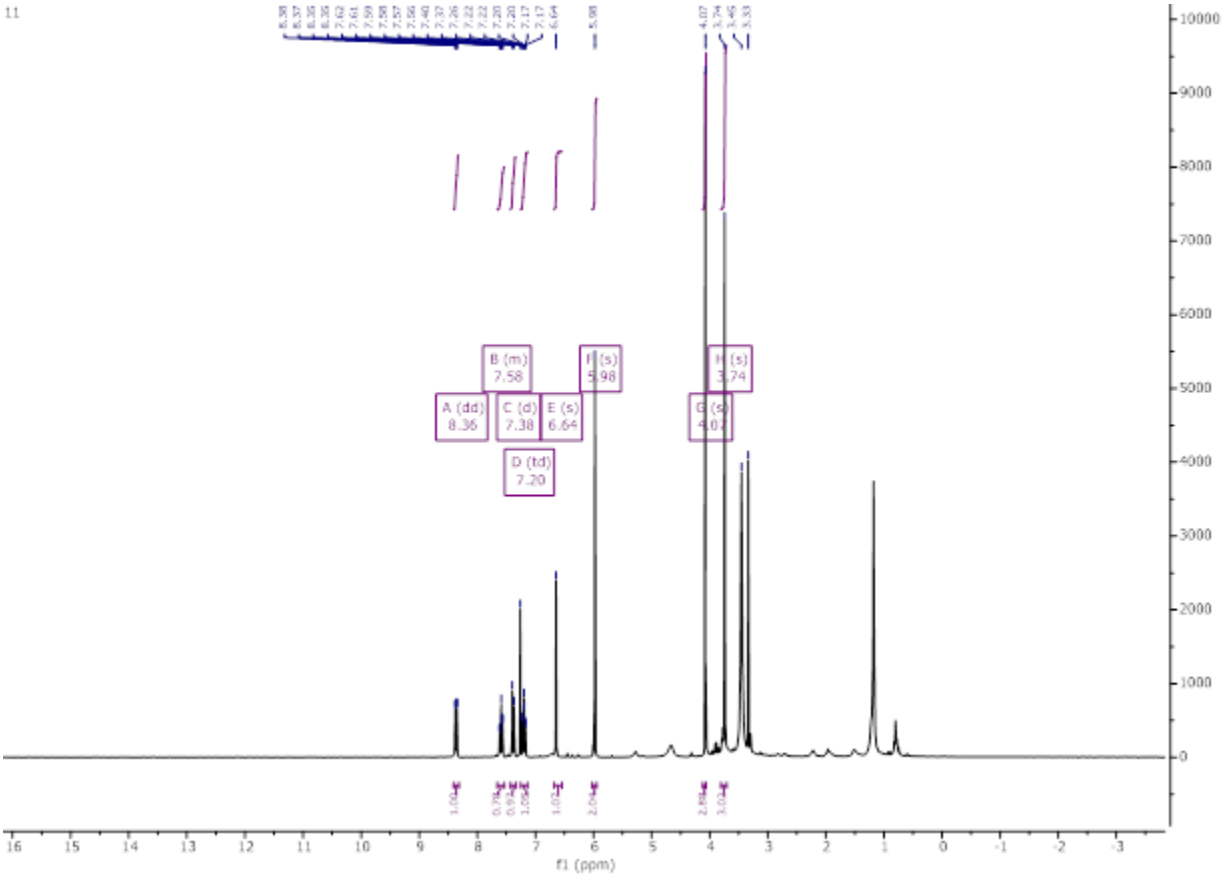

Appendix 2B: ^{13}C NMR spectrum of evoxanthine (**17**), 75 MHz in $CDC1_3$/MeOD, 300 MHz

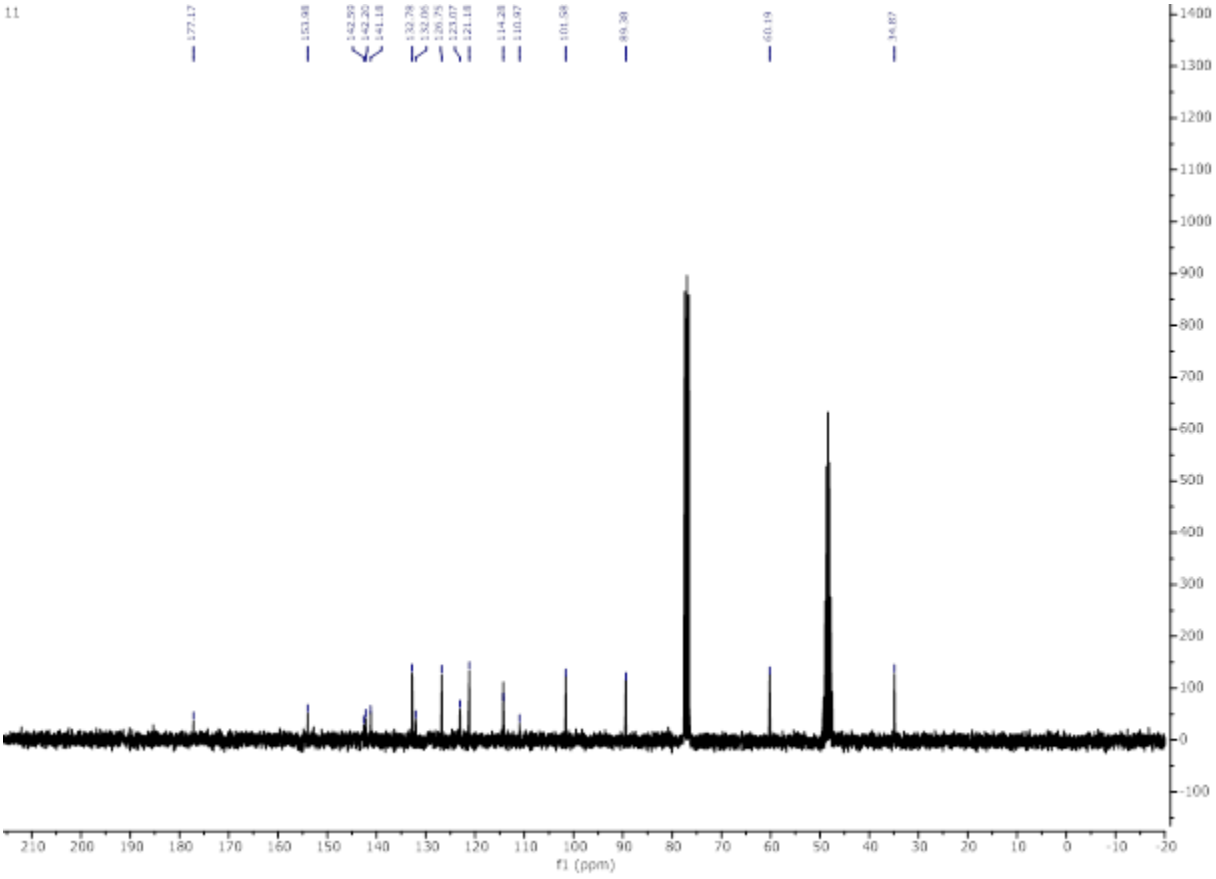

Appendix 3A: ^{1}H NMR spectrum of arborinin (**13**), $CDC1_3$, 300 MHz

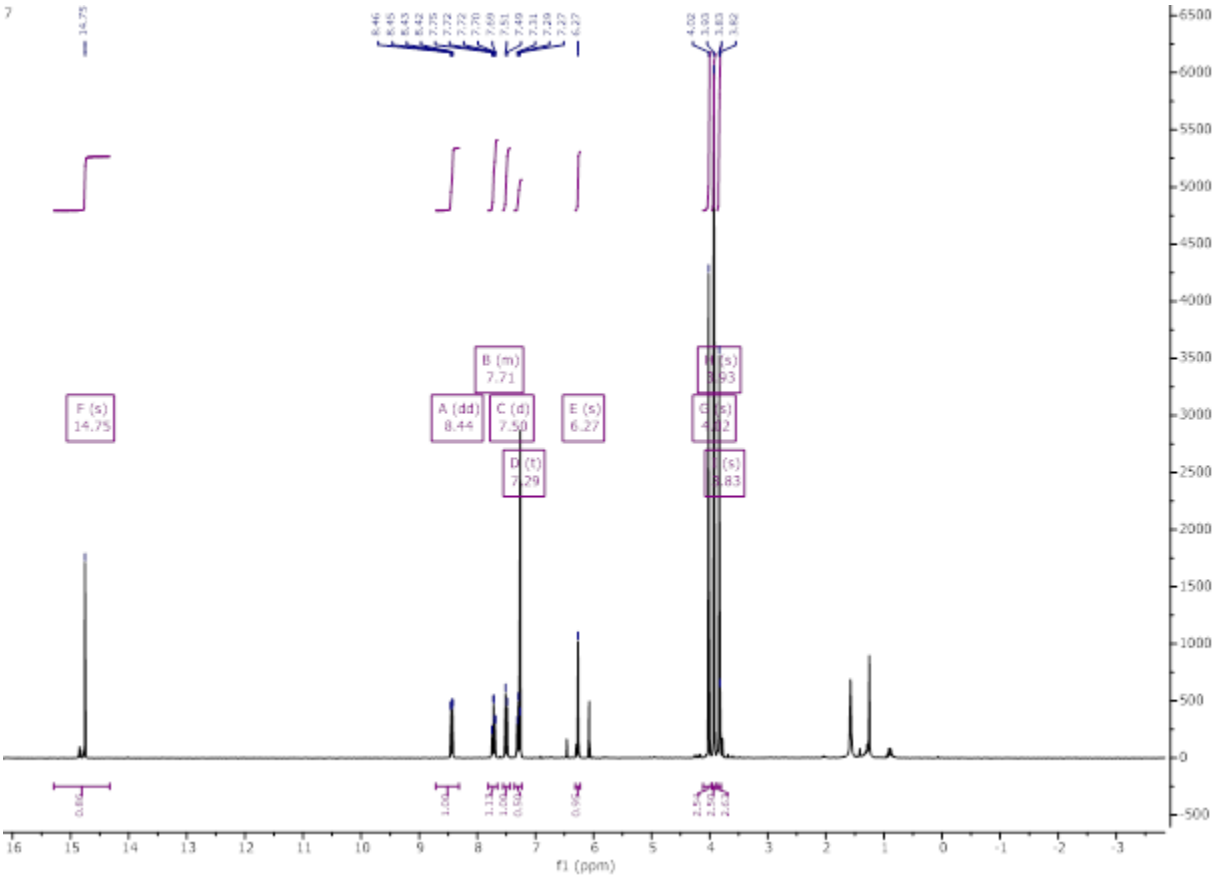

Appendix 3B:^{13}C NMR spectrum of arborinin (**13**), $CDC1_3$, 75 MHz

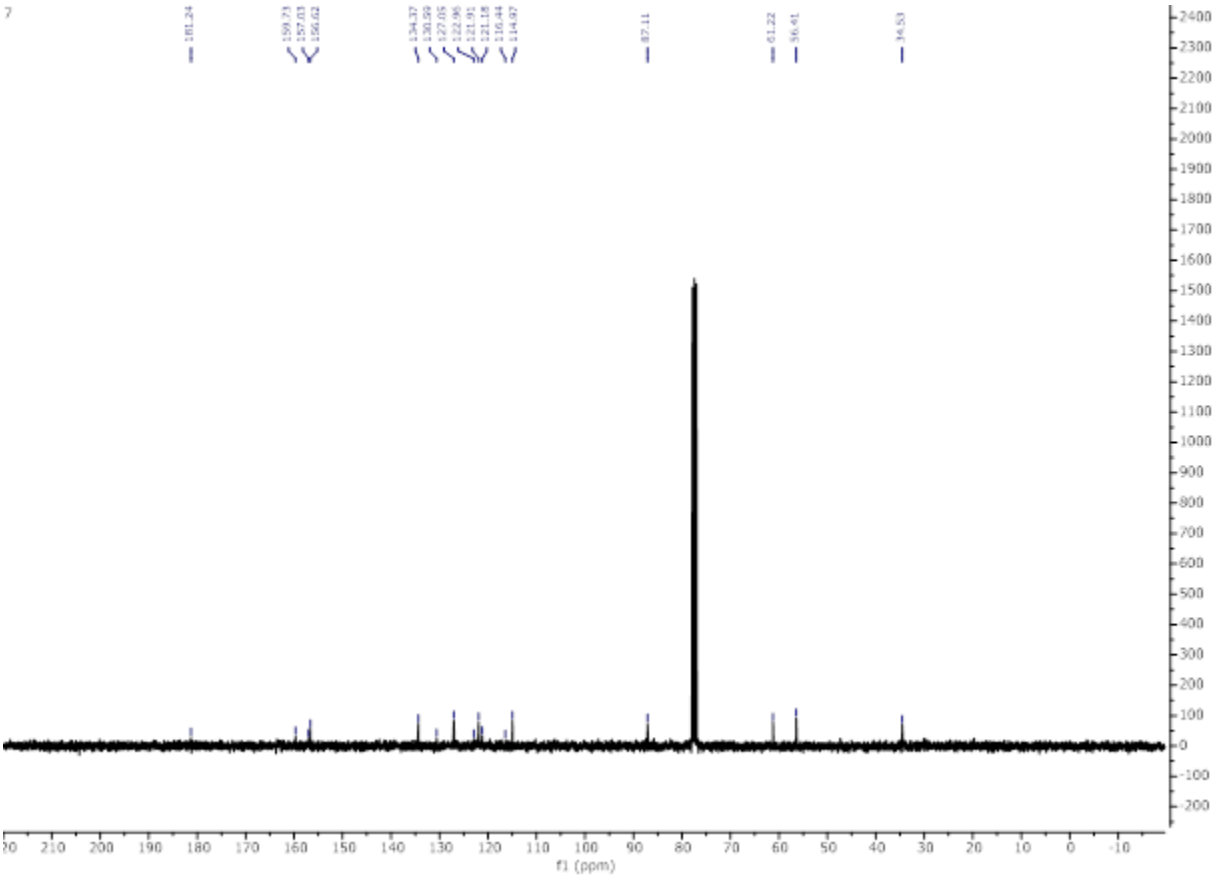

Appendix 4A:1H NMR spectrum of evodiamine (**245**), 300 MHz, DMSO-d_6

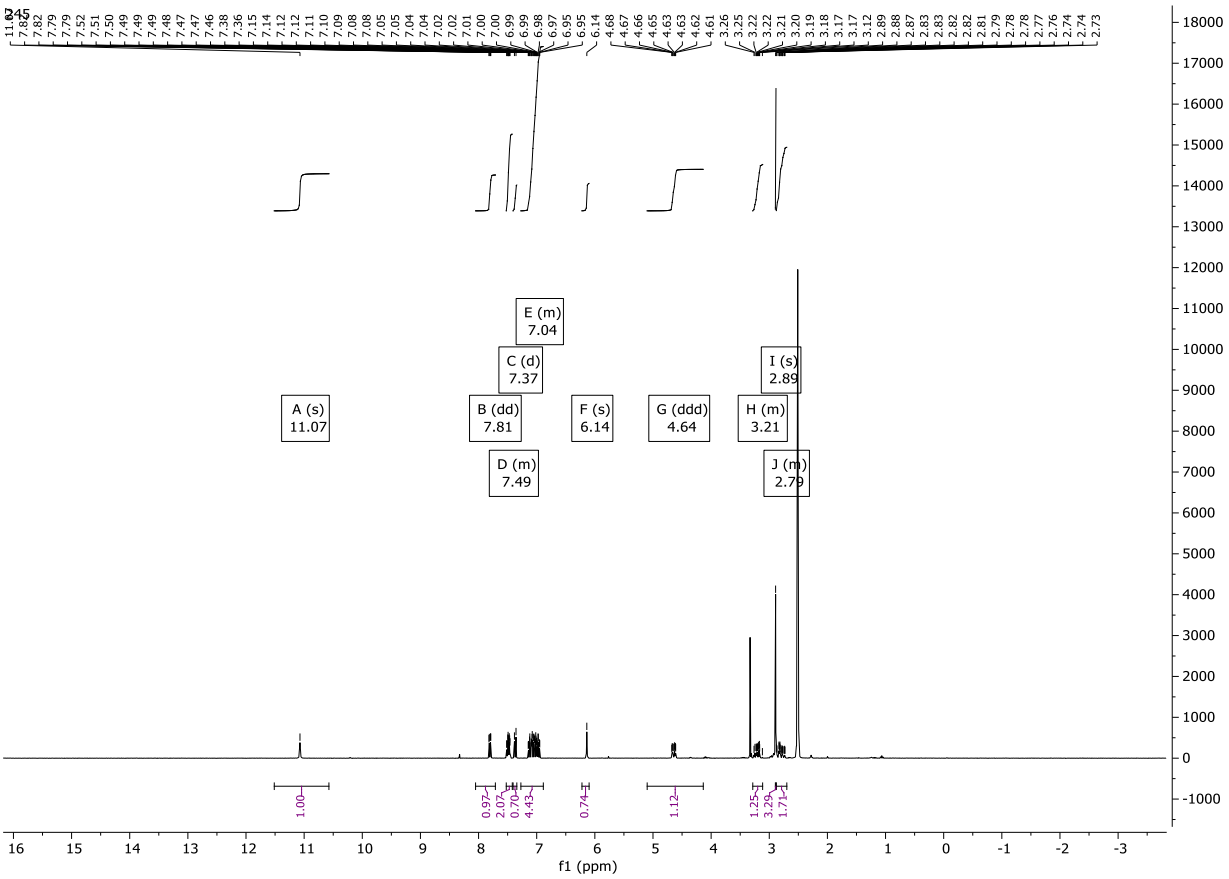

Appendix 4B: 13C NMR spectrum of evodiamine (**245**), 75 MHz, in $CDC1_3$/MeOD

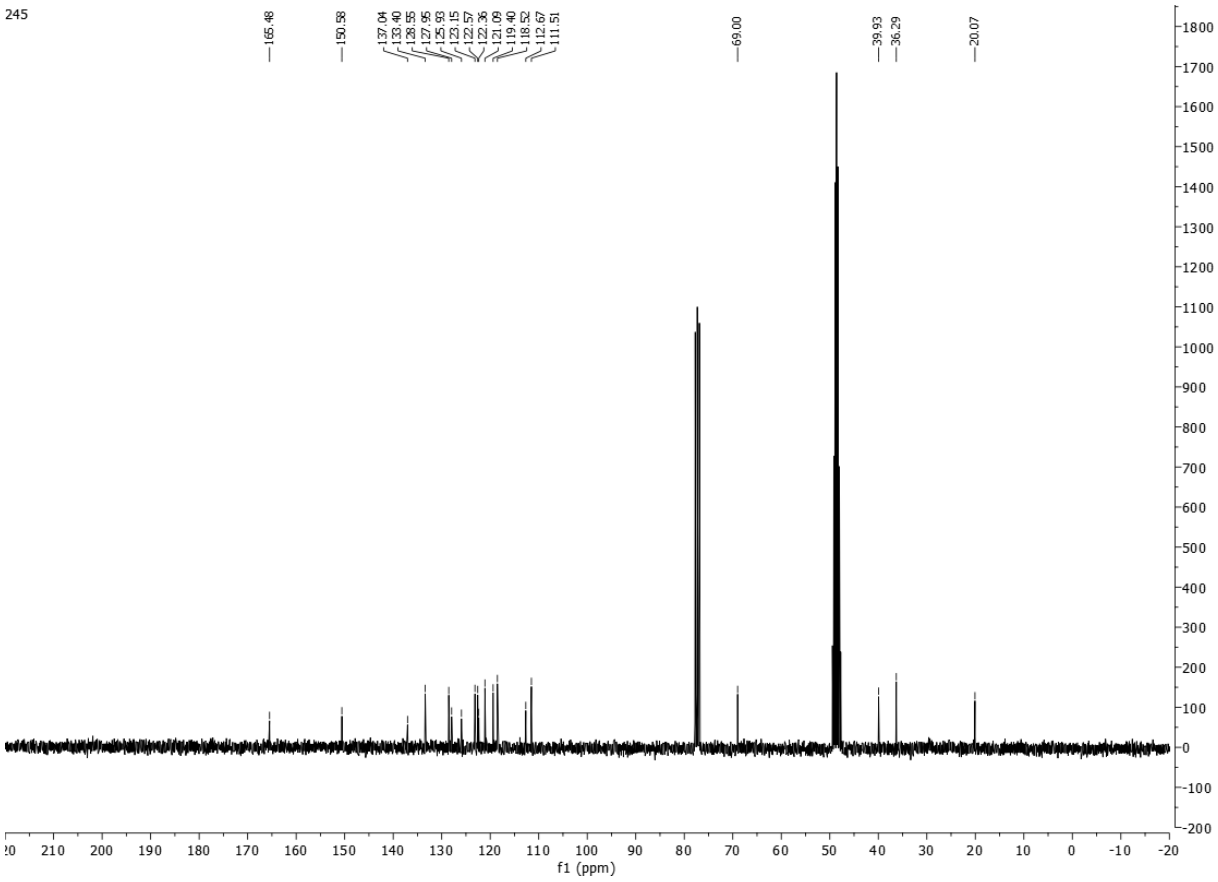

Appendix 4C: DPT-135 spectrum of evodiamine (**245**), 75 MHz, in $CDC1_3$/MeOD

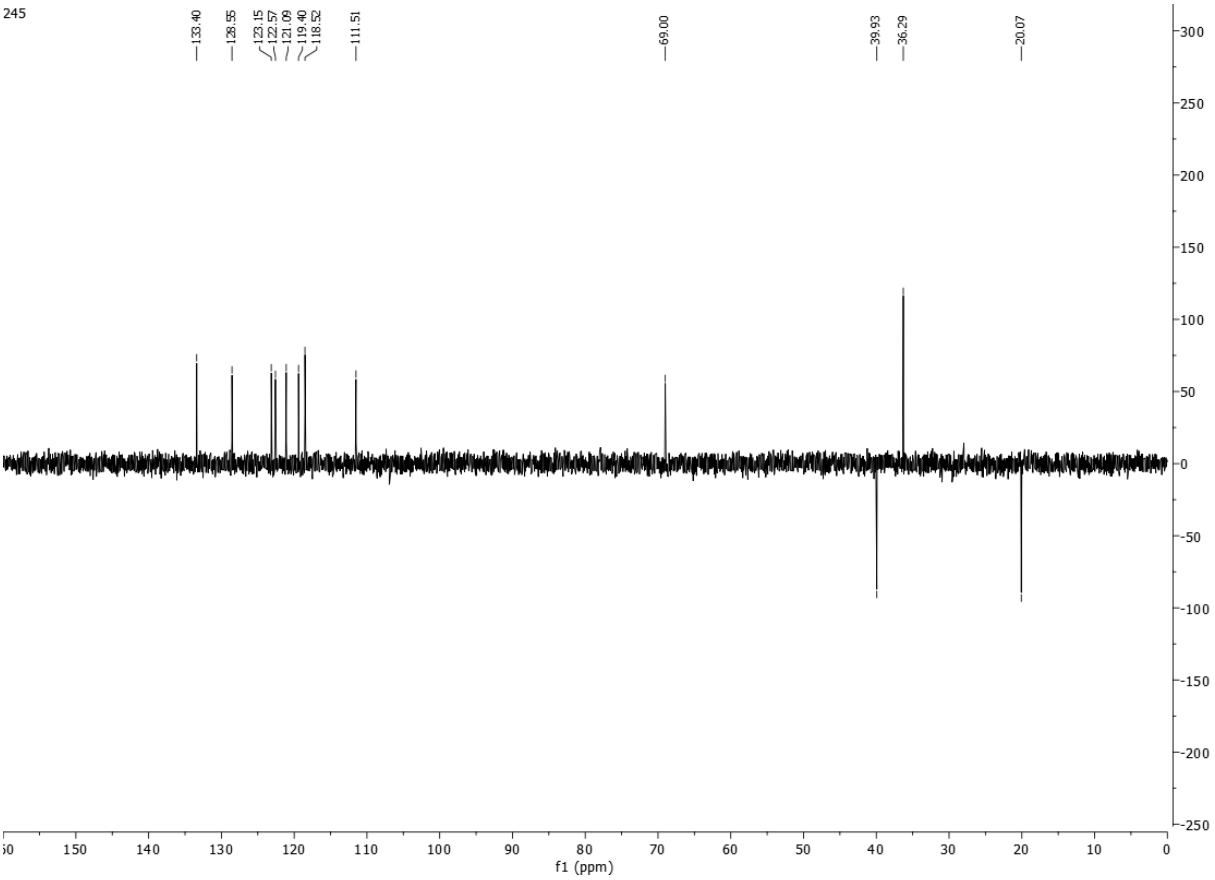

Appendix 4D: COSY spectrum of evodiamine (**245**), 300 MHz, DMSO-d_6

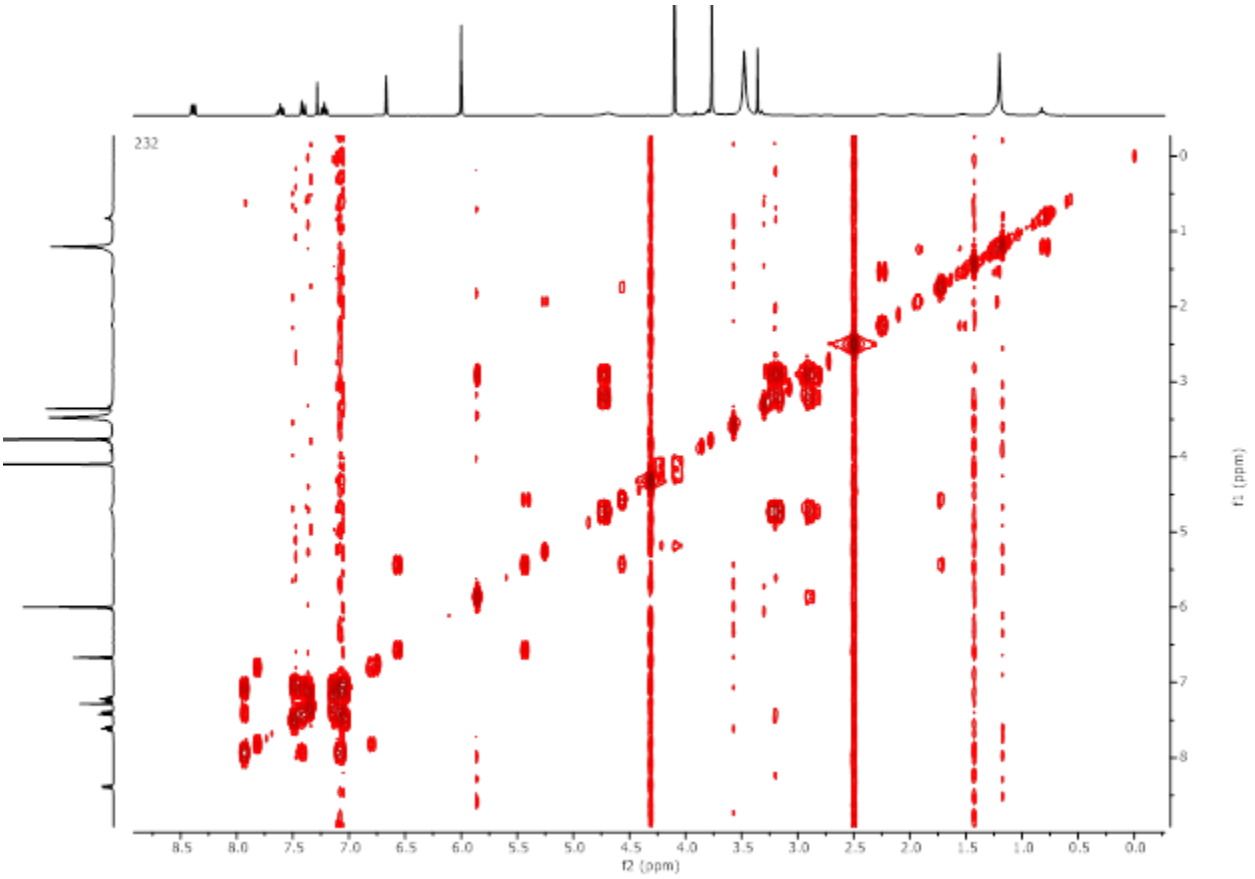

Appendix 4E: HSQC spectrum of evodiamine (**245**)

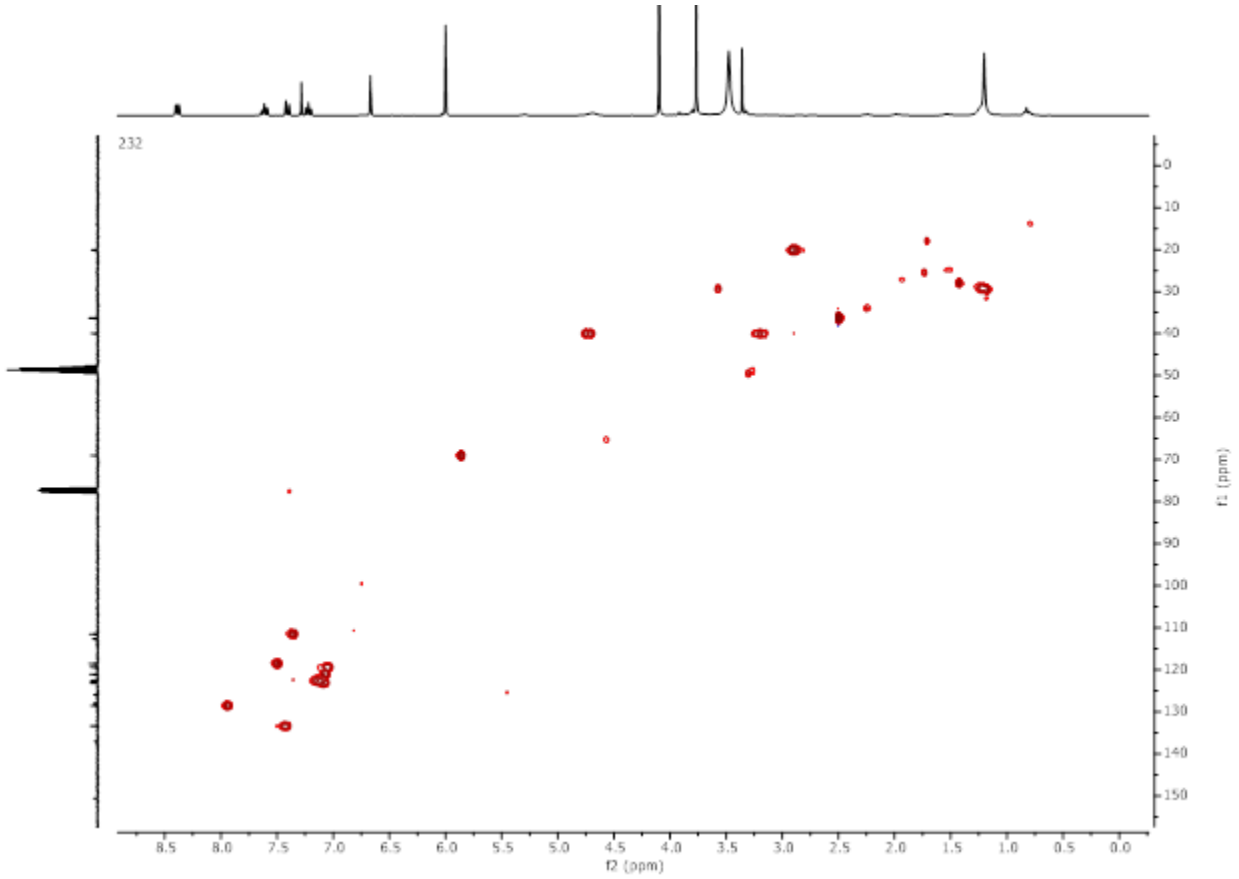

Appendix 4F: HMBC spectrum of evodiamine (**245**)

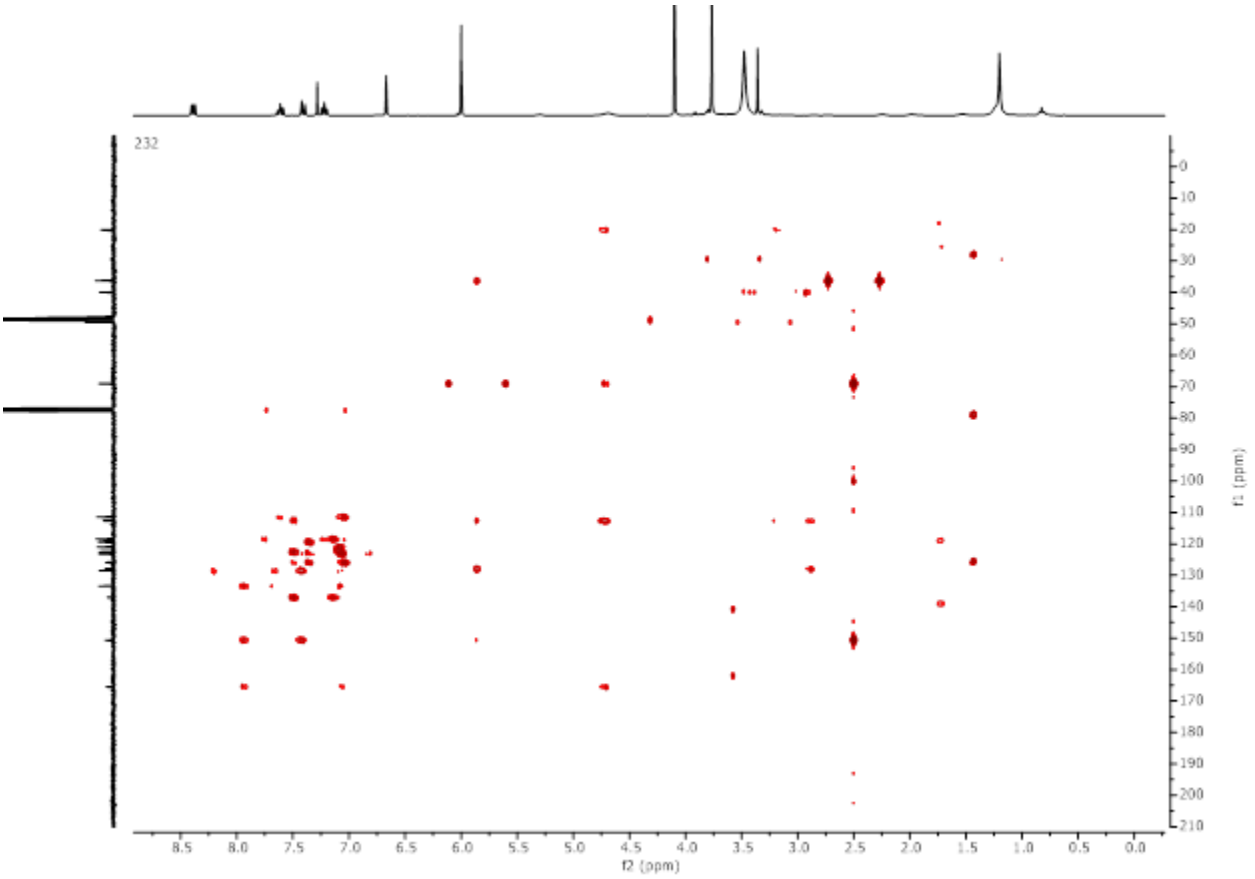

Appendix 5A: 1H NMR spectrum of N-methyl-8-(3", 3"-dimethylallyloxy)-findersine (**9**), $CDC1_3$, 300 MHz

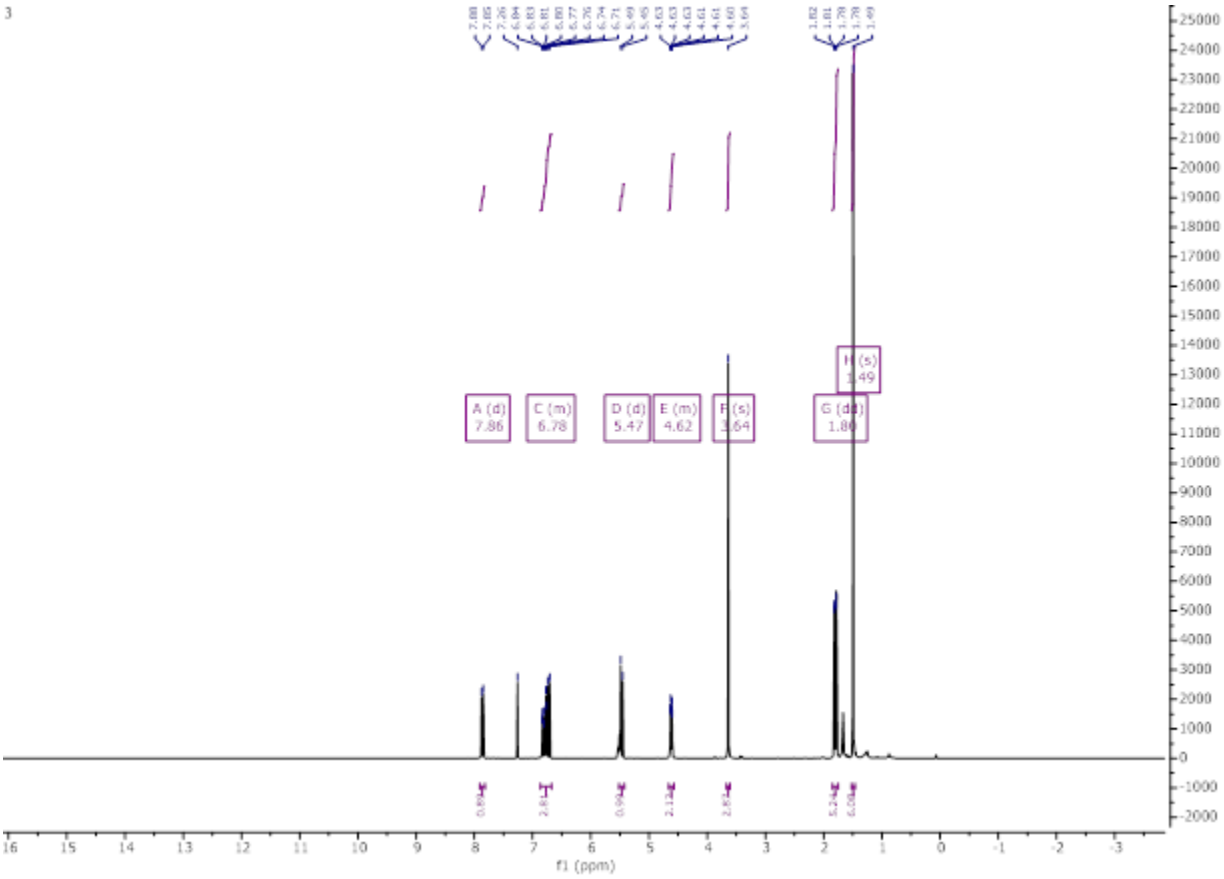

Appendix 5B: 13C NMR spectrum of N-methyl-8-(3", 3"-dimethylallyloxy)-findersine (**9**), CDC13, 75 MHz

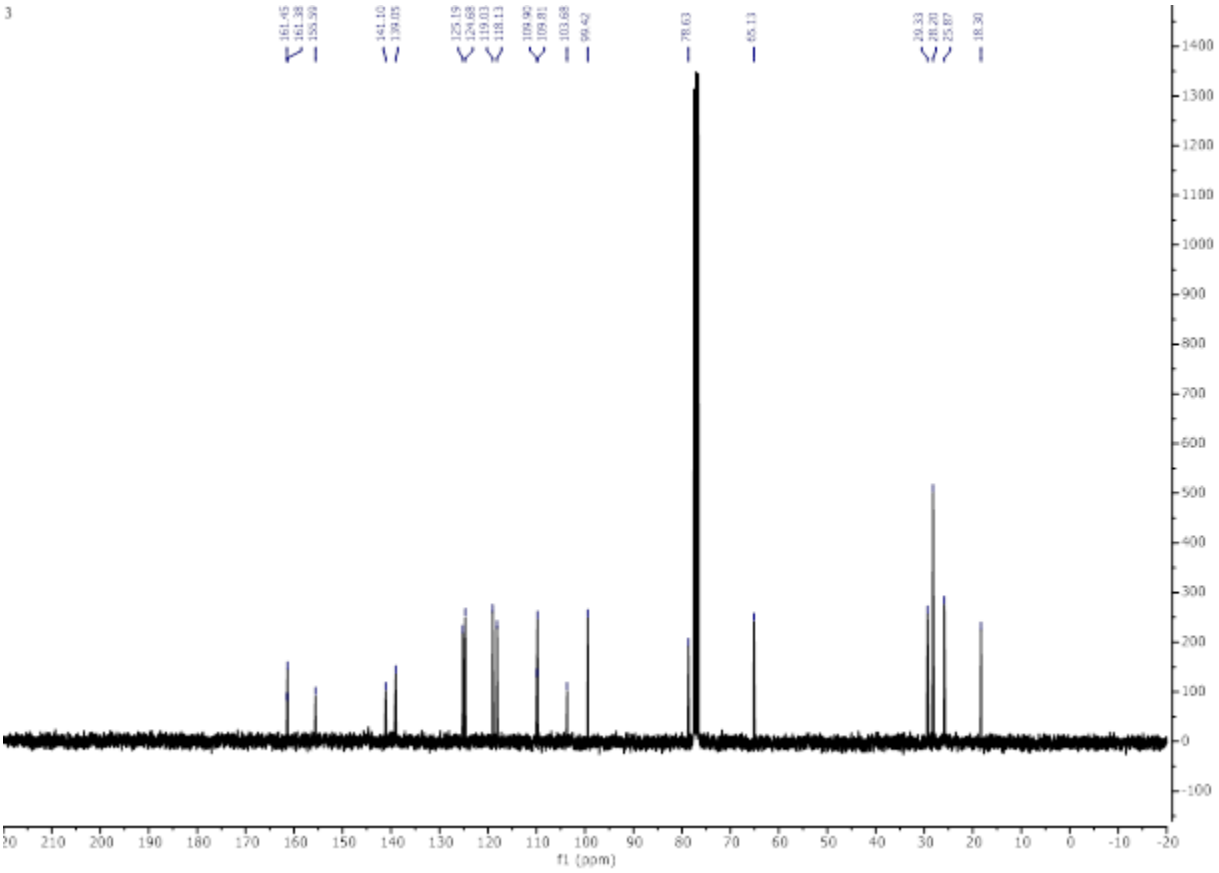

Appendix 5C: DPT-135 spectrum of N-methyl-8-(3", 3"-dimethylallyloxy)-findersine (**9**), CDC13, 300 MHz

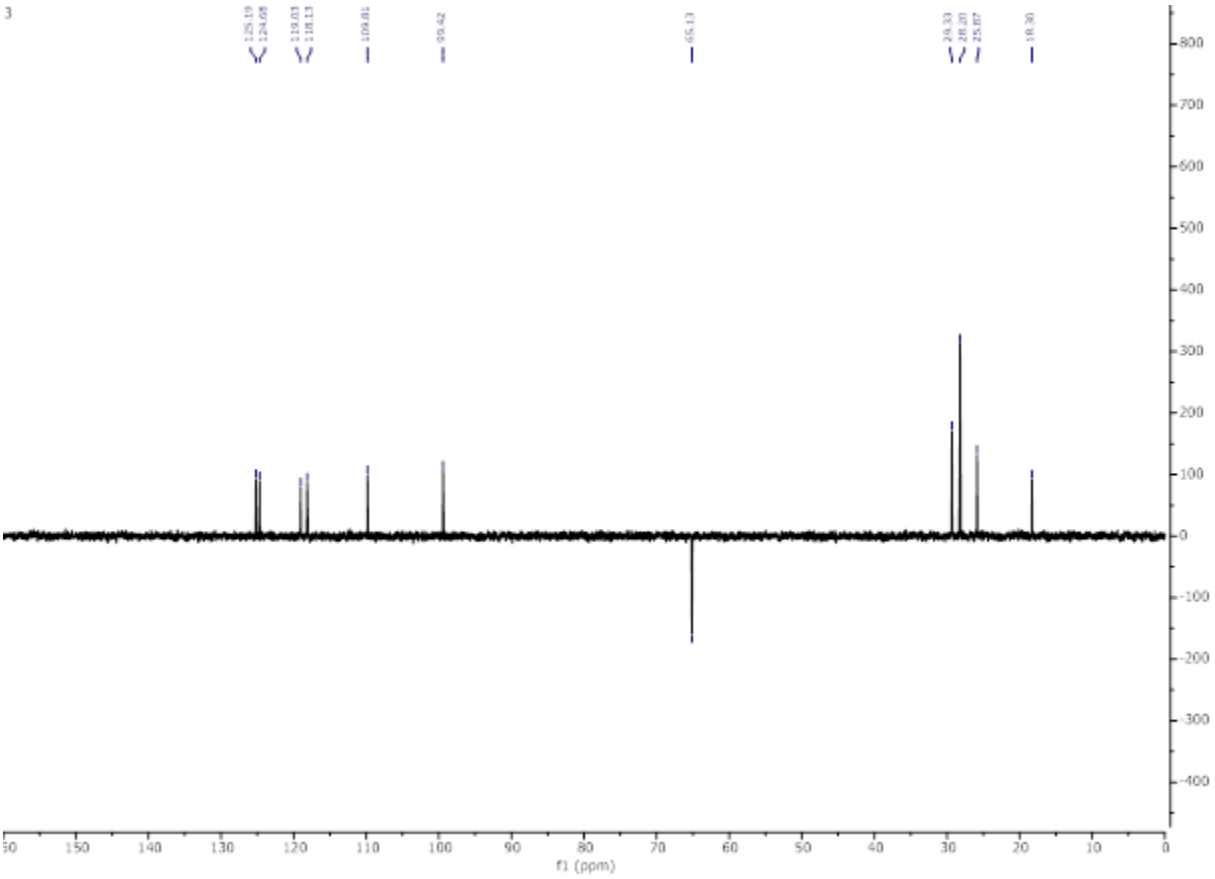

Appendix 5D: COSY spectrum of N-methyl-8-(3", 3"-dimethylallyloxy)-findersine (**9**), CDC13, 300 MHz

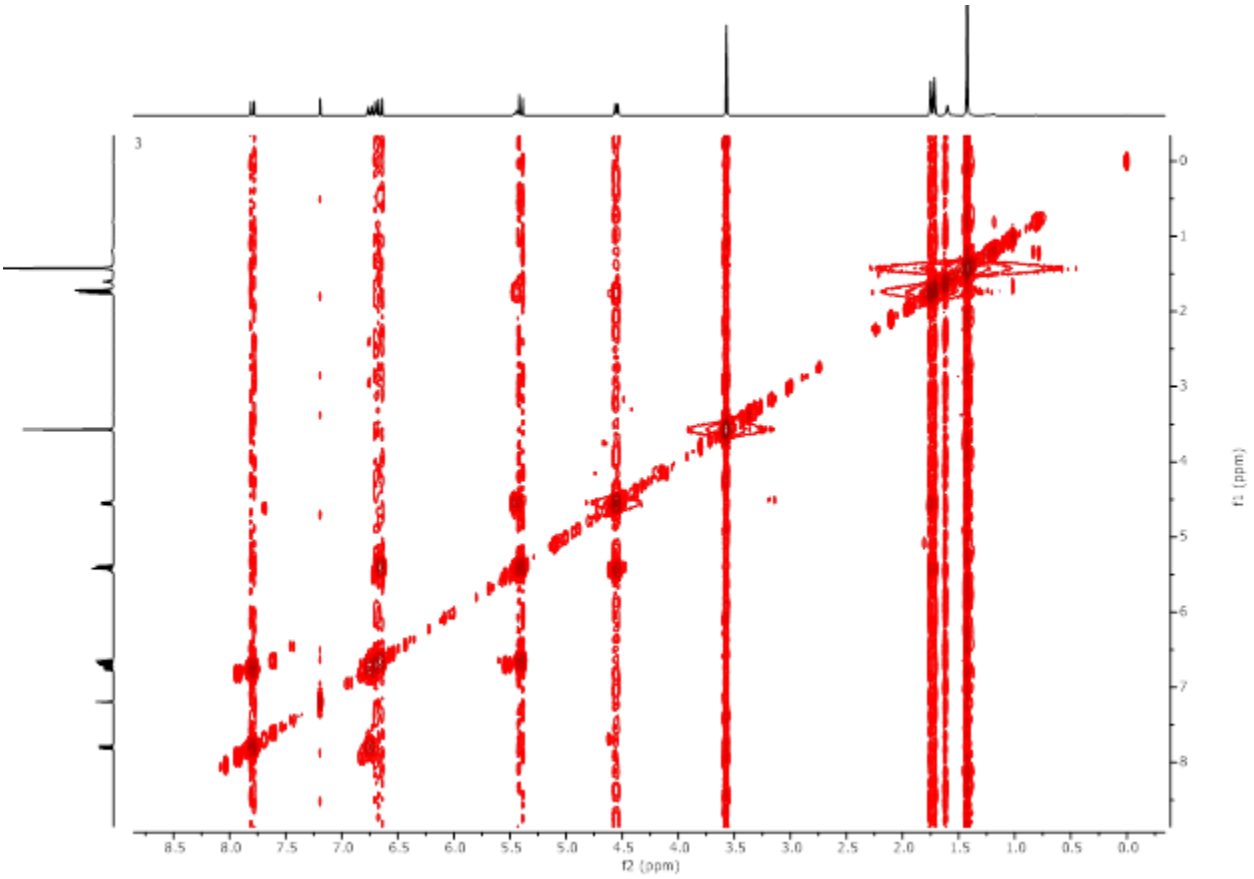

Appendix 5E: HSQC spectrum of N-methyl-8-(3", 3"-dimethylallyloxy)-findersine (**9**), $CDC1_3$, 300MHz

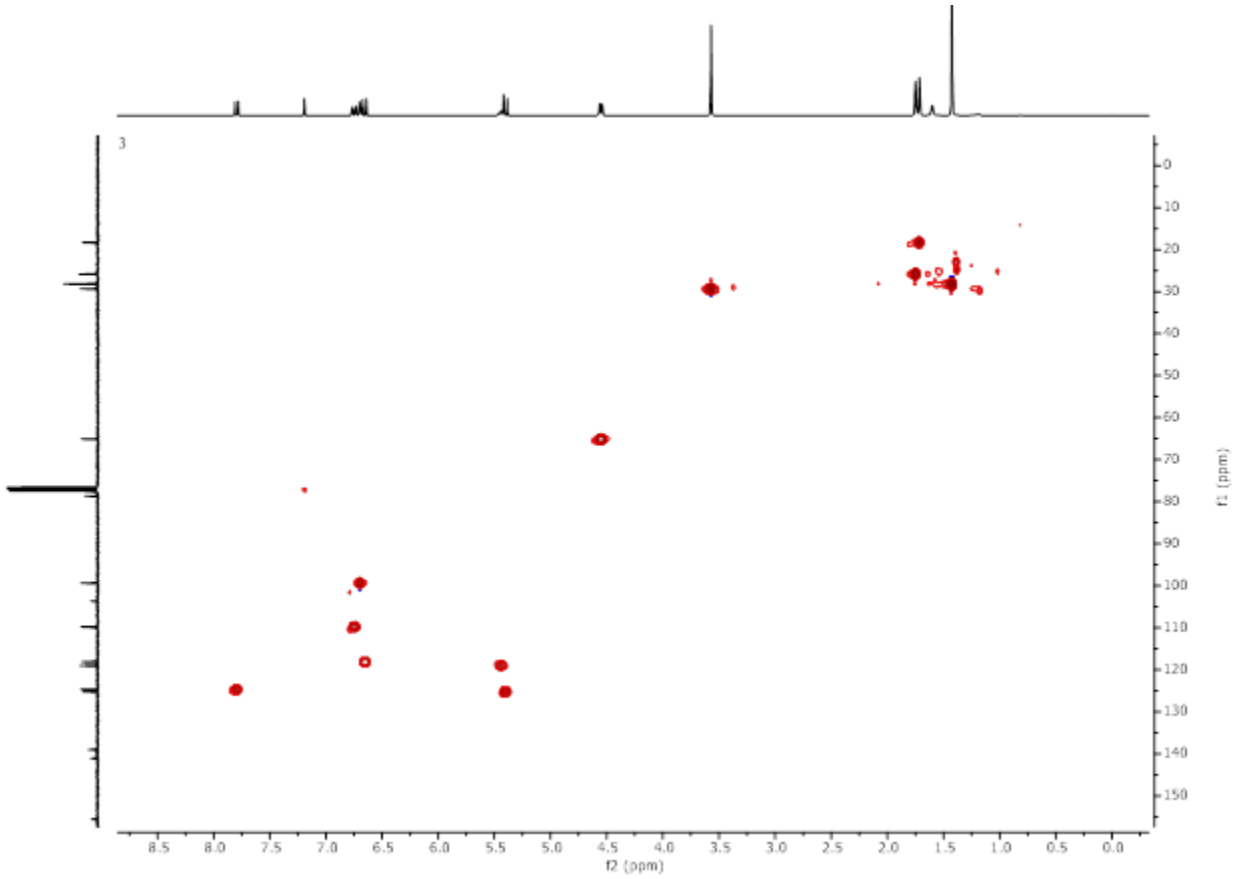

Appendix 5F: HMBC spectrum of N-methyl-8-(3", 3"-dimethylallyloxy)-findersine (**9**)

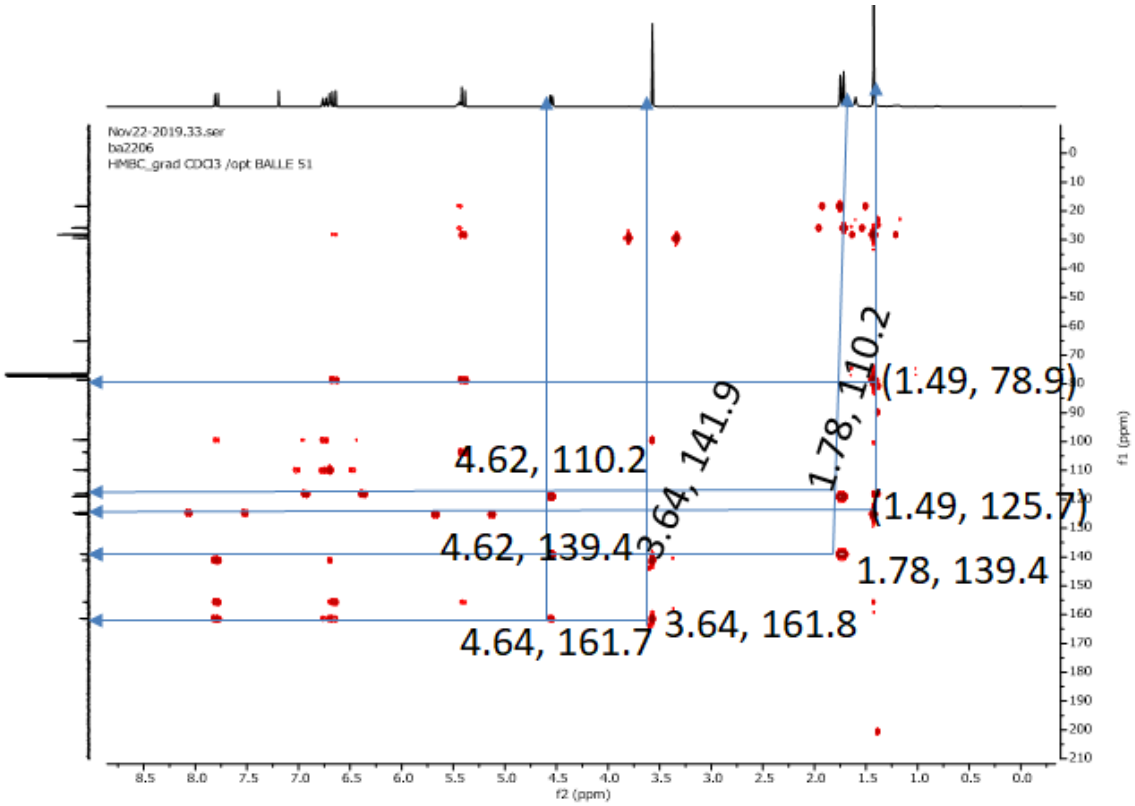

56

Appendix 6A: ^{1}HNMR Kokusaginine (**51**) and skimmianine (**25**), $CDC1_3$, 300 MHz

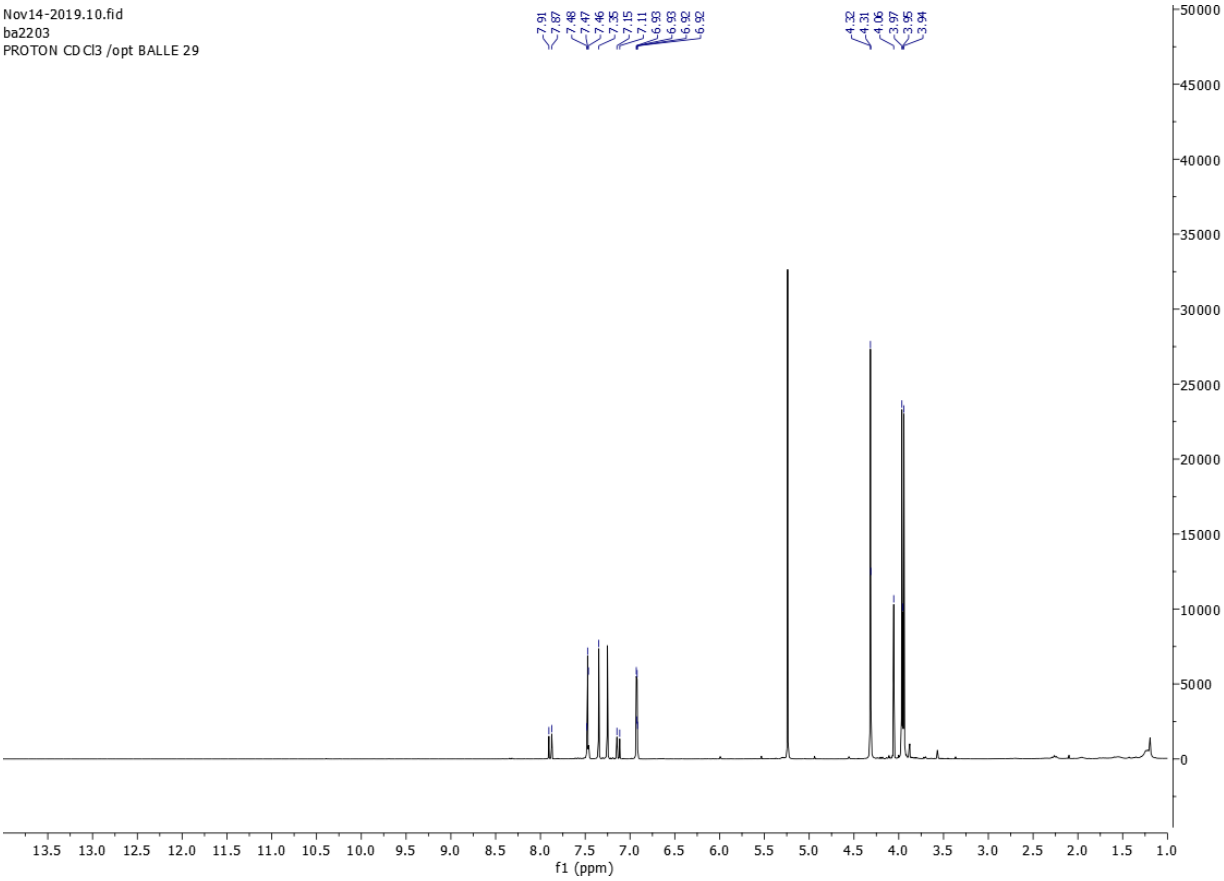

Appendix 6B: ^{13}CNMR Kokusaginine (**51**) and skimmianine (**25**), $CDC1_3$, 300 MHz.

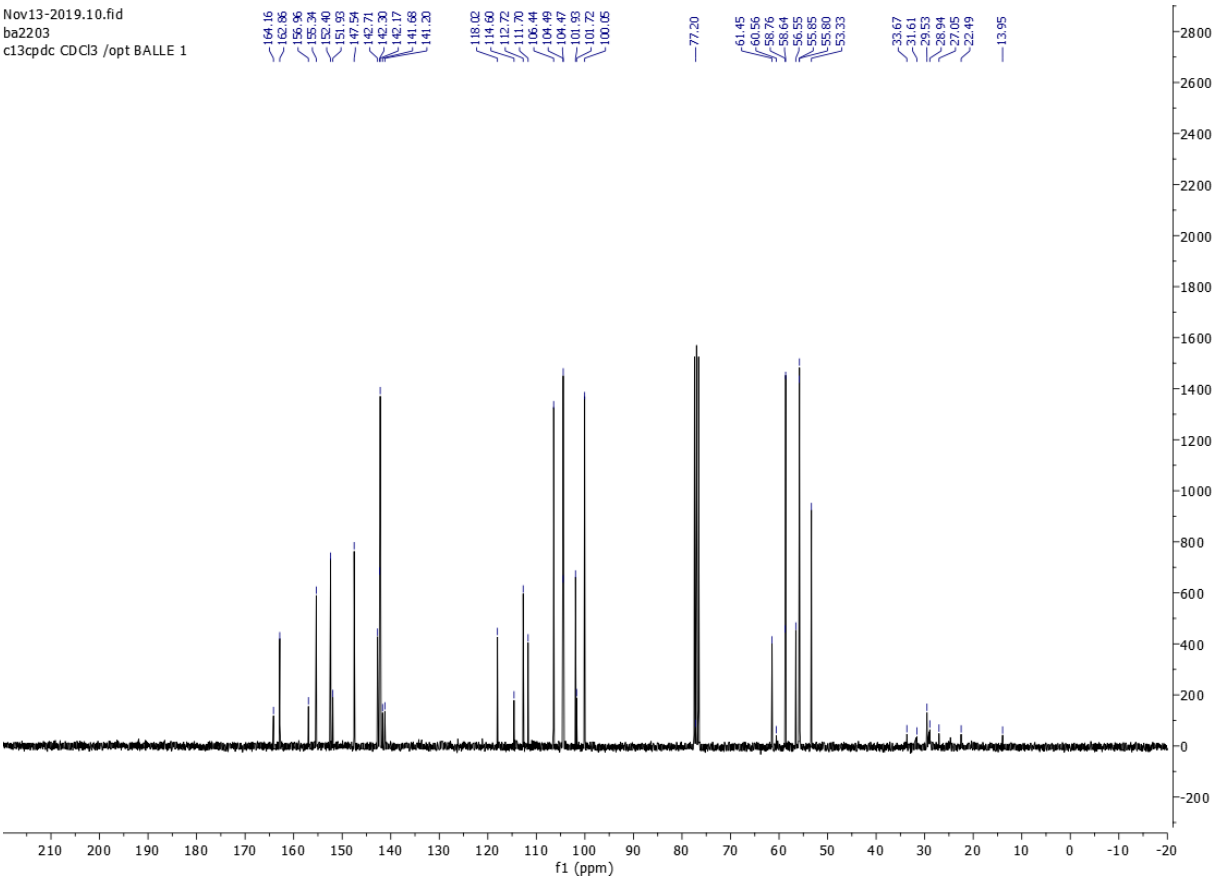

Appendix 6C: Dept-135 spectra of Kokusaginine (**51**) and skimmianine (**25**), CDC13, 300 MHz.

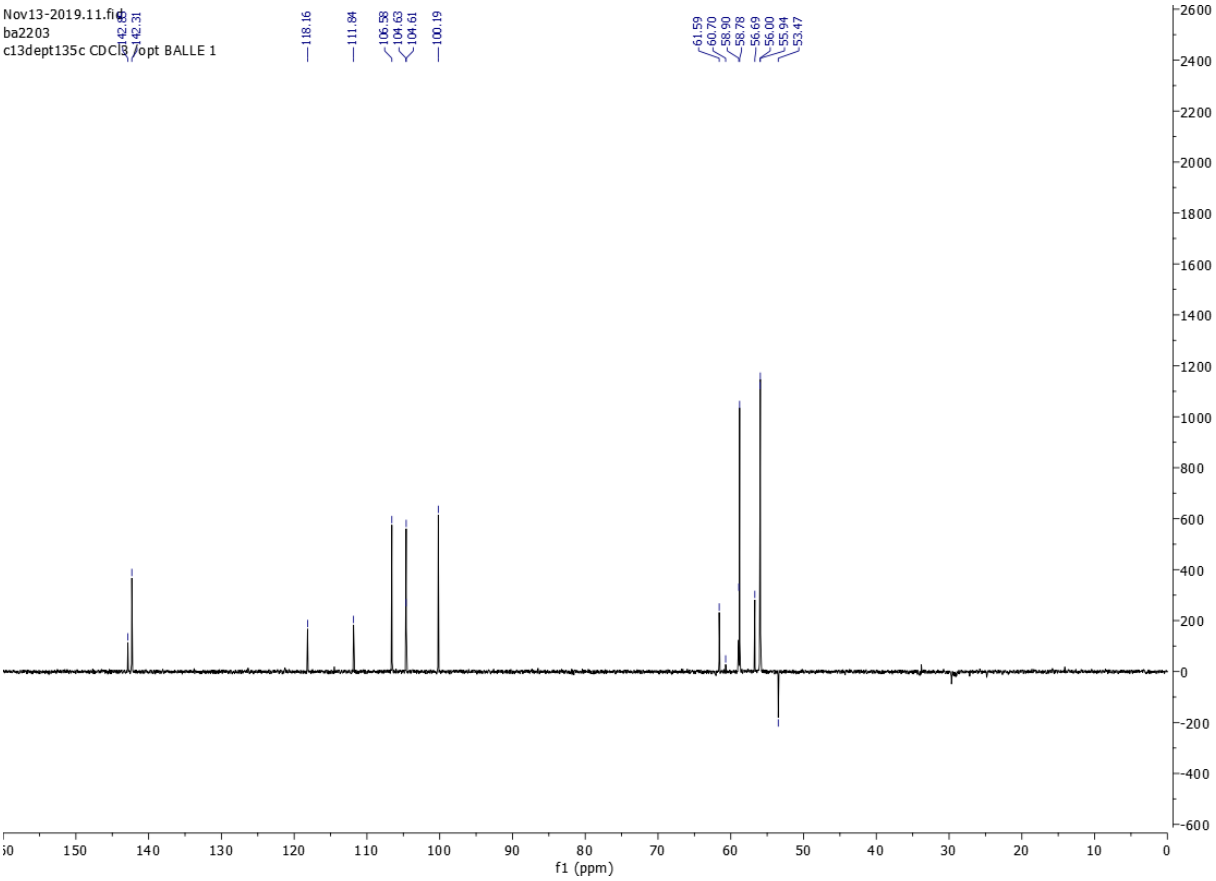

Appendix 6D: Cosy Spectra of Kokusaginine (**51**) and skimmianine (**25**)

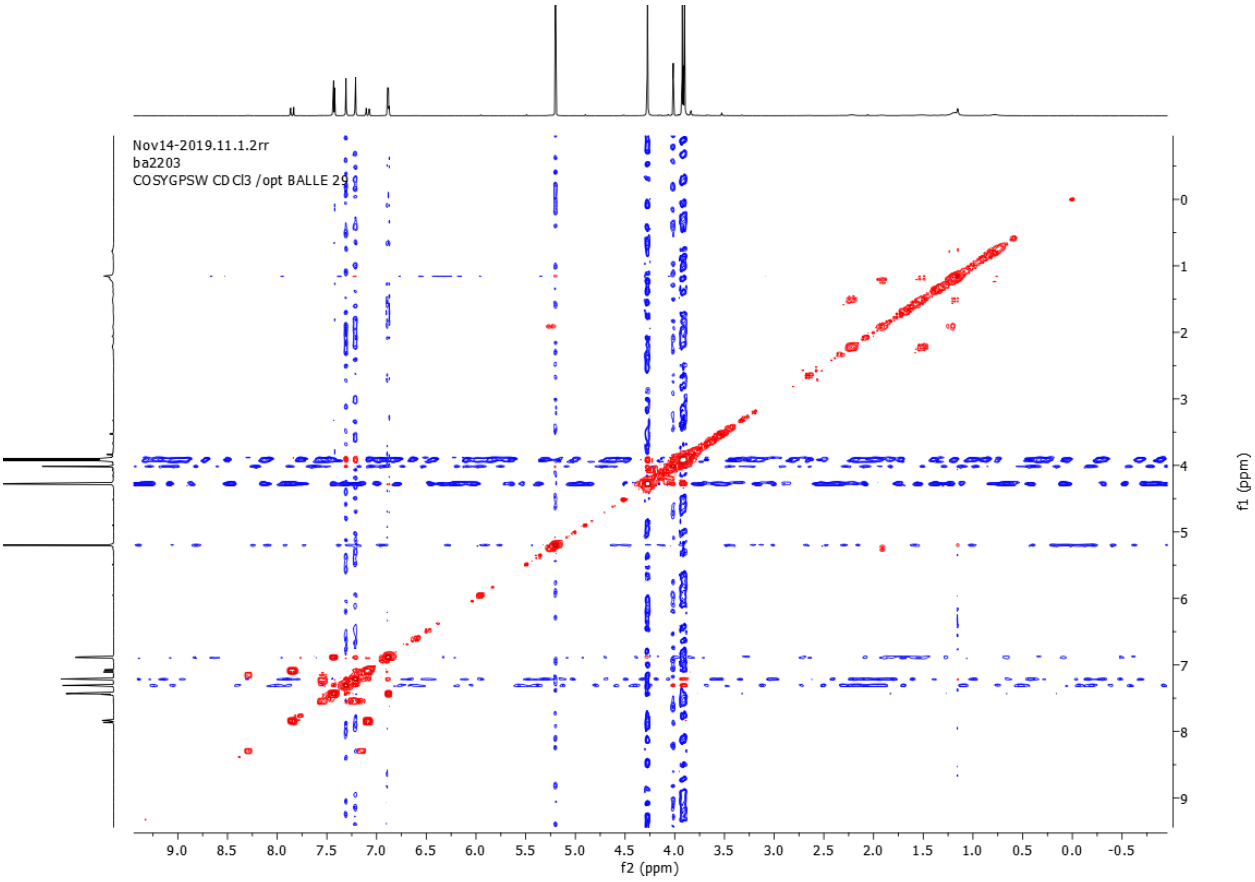

Appendix 6E: HSQC spectra of Kokusaginine (**51**) and skimmianine (**25**).

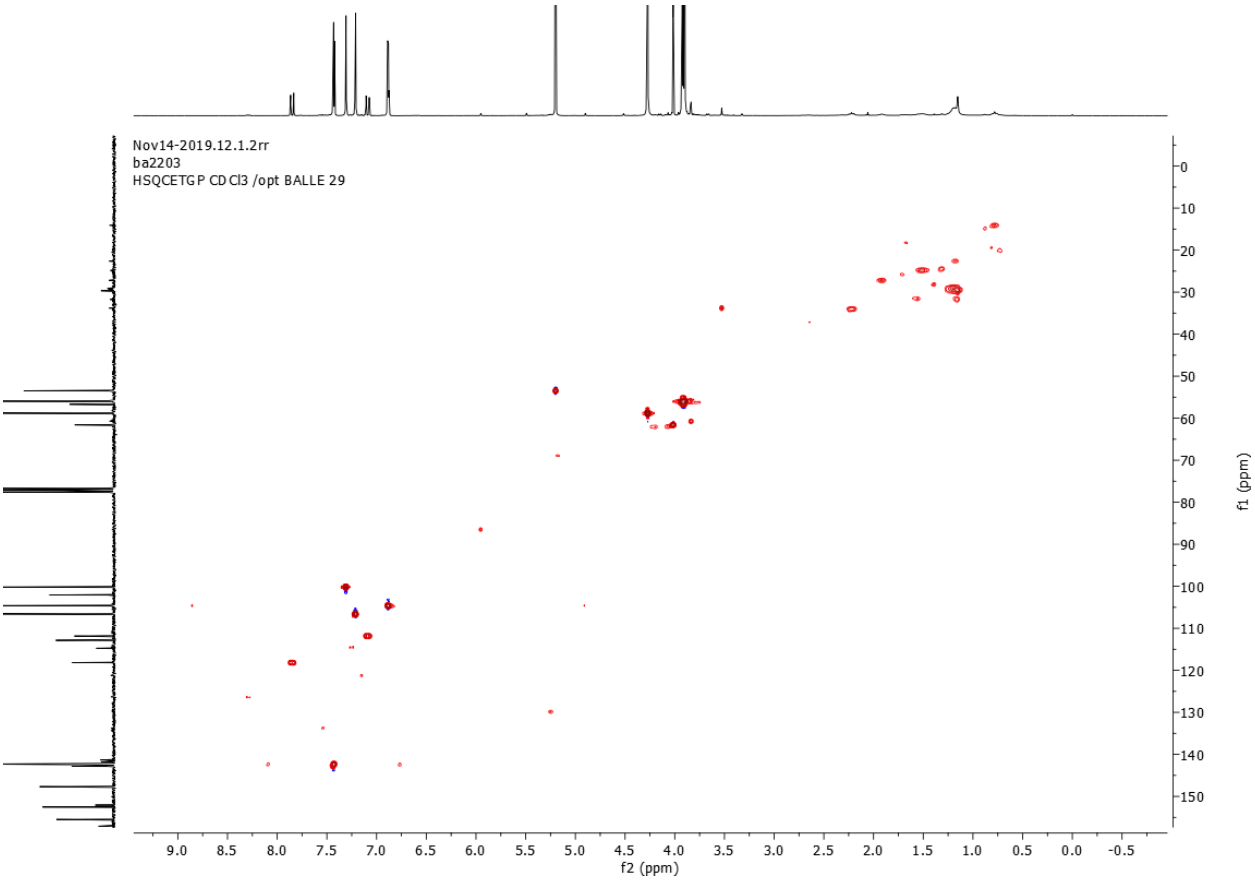

Appendix 6F: ^{1}HMBC spectra of Kokusaginine (**51**) and skimmianine (**25**)

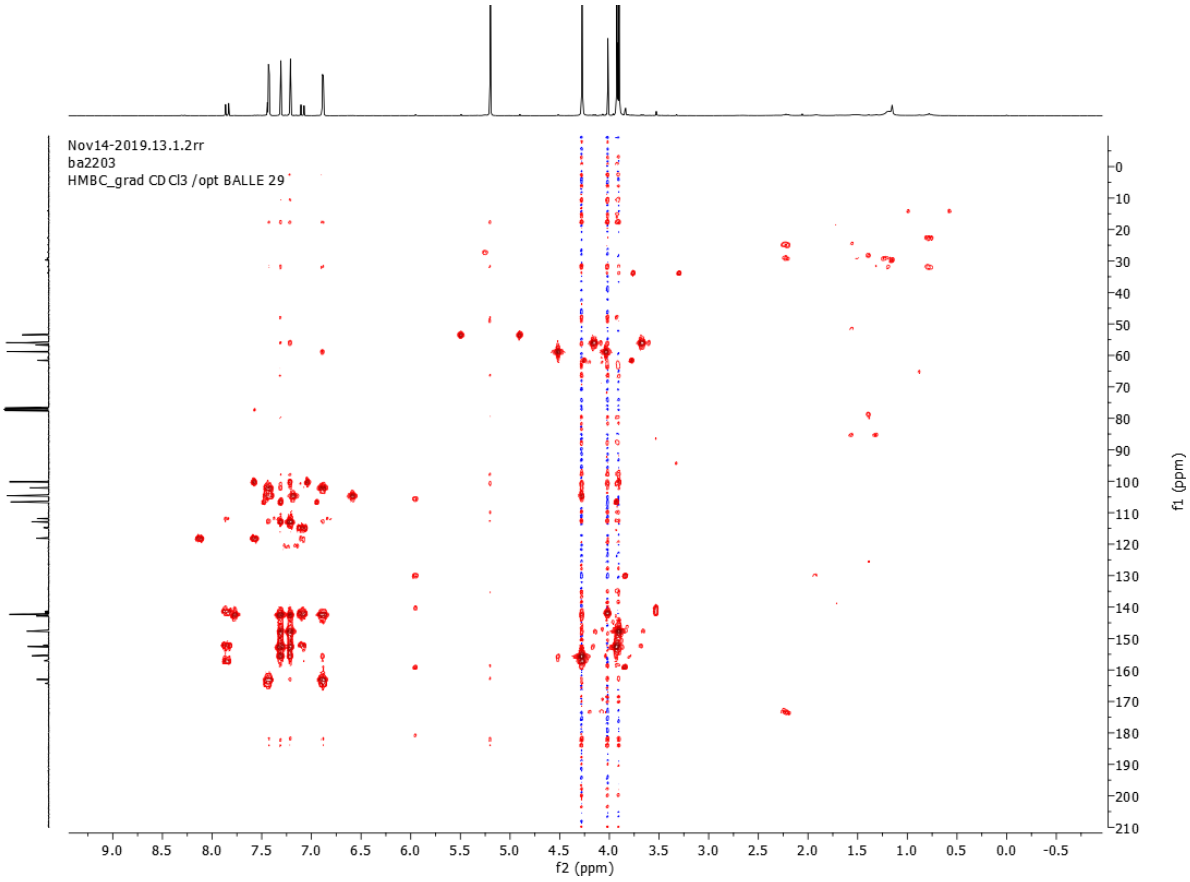

Appendix 7A: HRMS of tetrahydropyranyl Octadeca-9,12-dienoate (**246**)

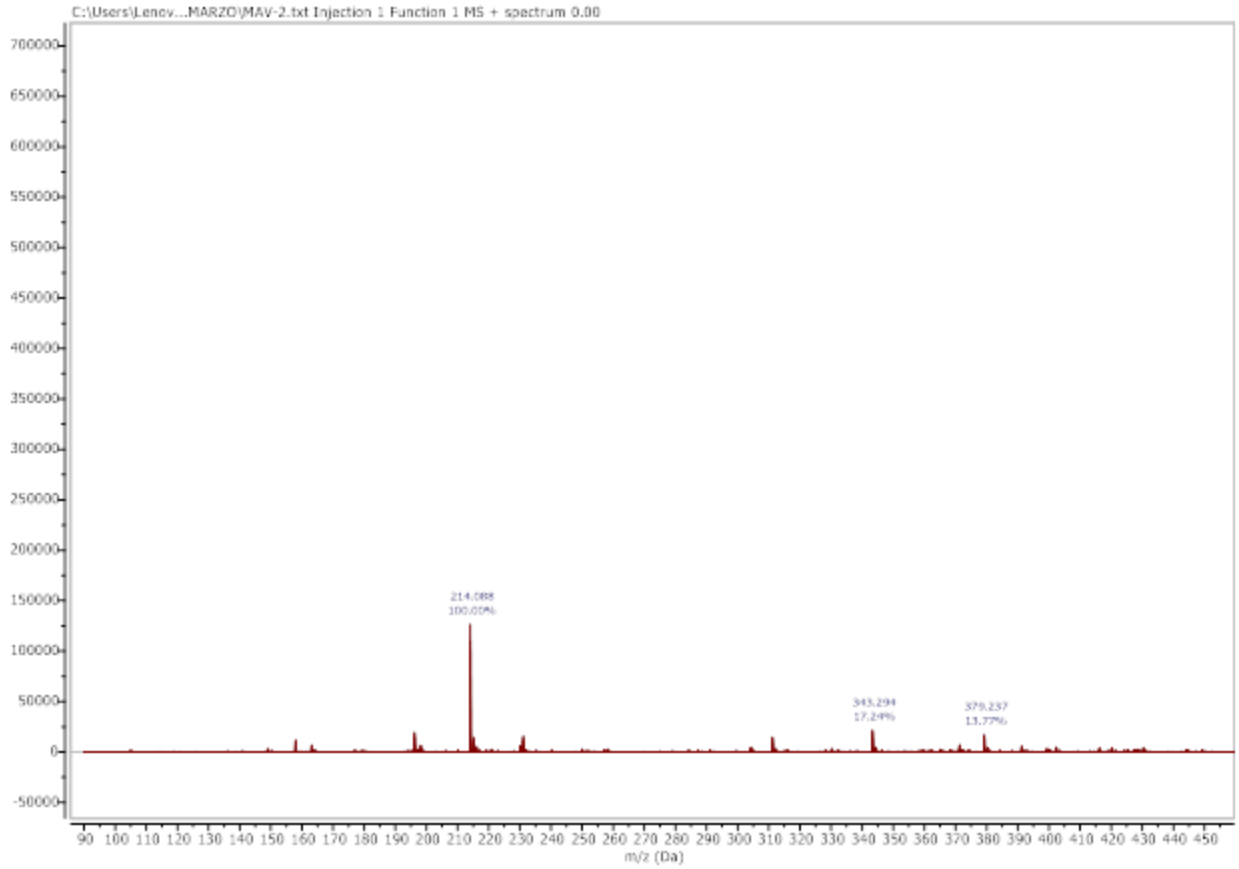

Appendix 7B: 1HNMR spectrum of tetrahydropyranyl octadeca-9,12-dienoate (**246**), $CDC1_3$, 300 MHz

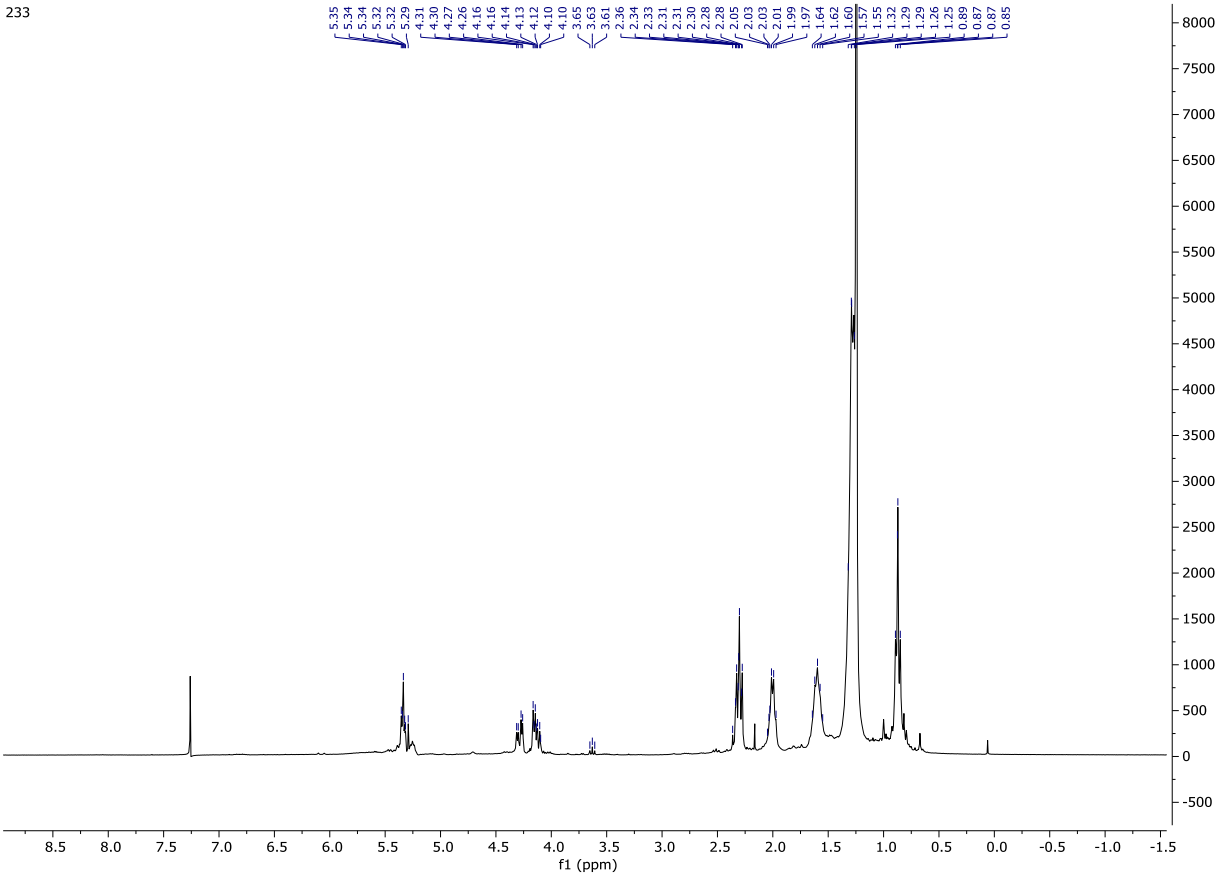

Appendix 7C: 13C NMR spectrum of tetrahydropyranyl octadeca-9,12-dienoate (**246**), $CDC1_3$, 75 MHz

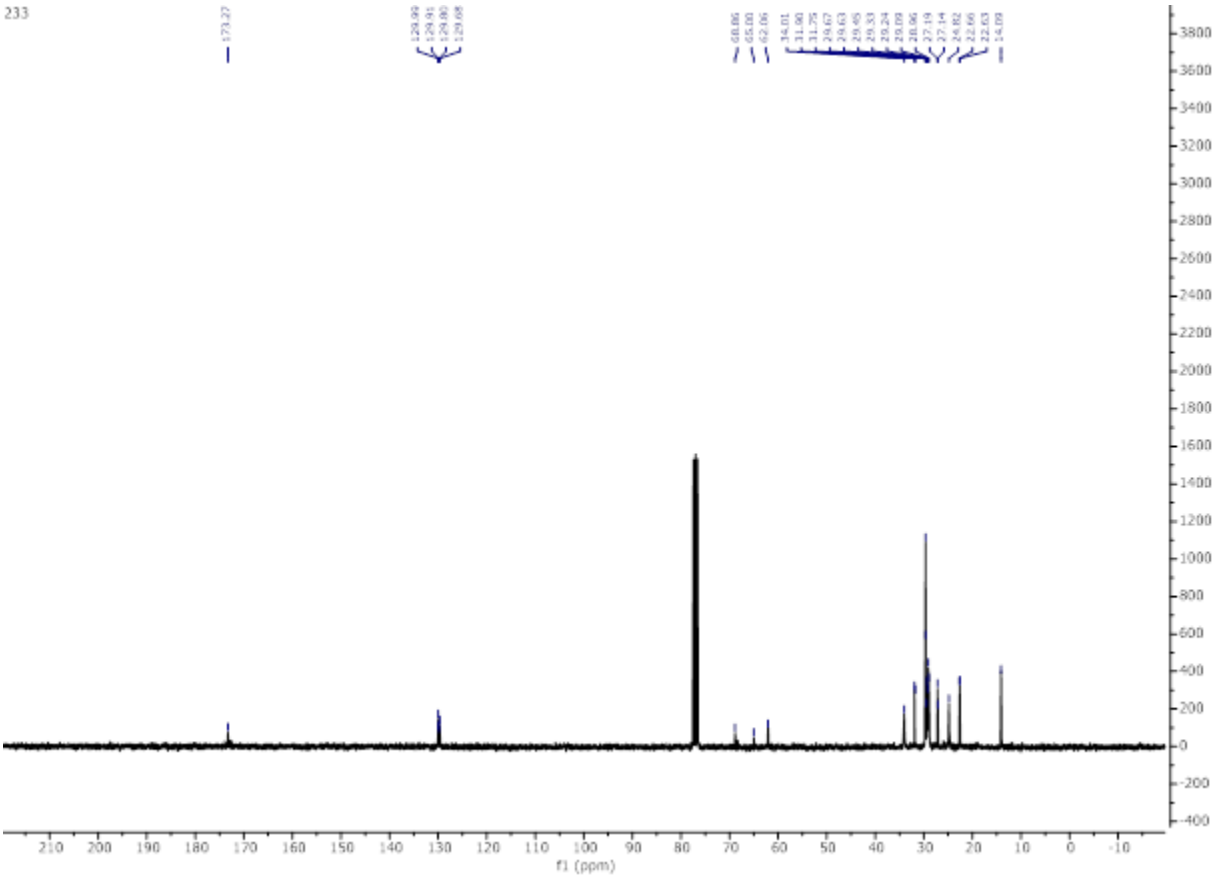

Appendix 7D: DEPT-135 spectrum of tetrahydropyranyl Octadeca-9,12-dienoate (**246**), $CDC1_3$, 300 MHz

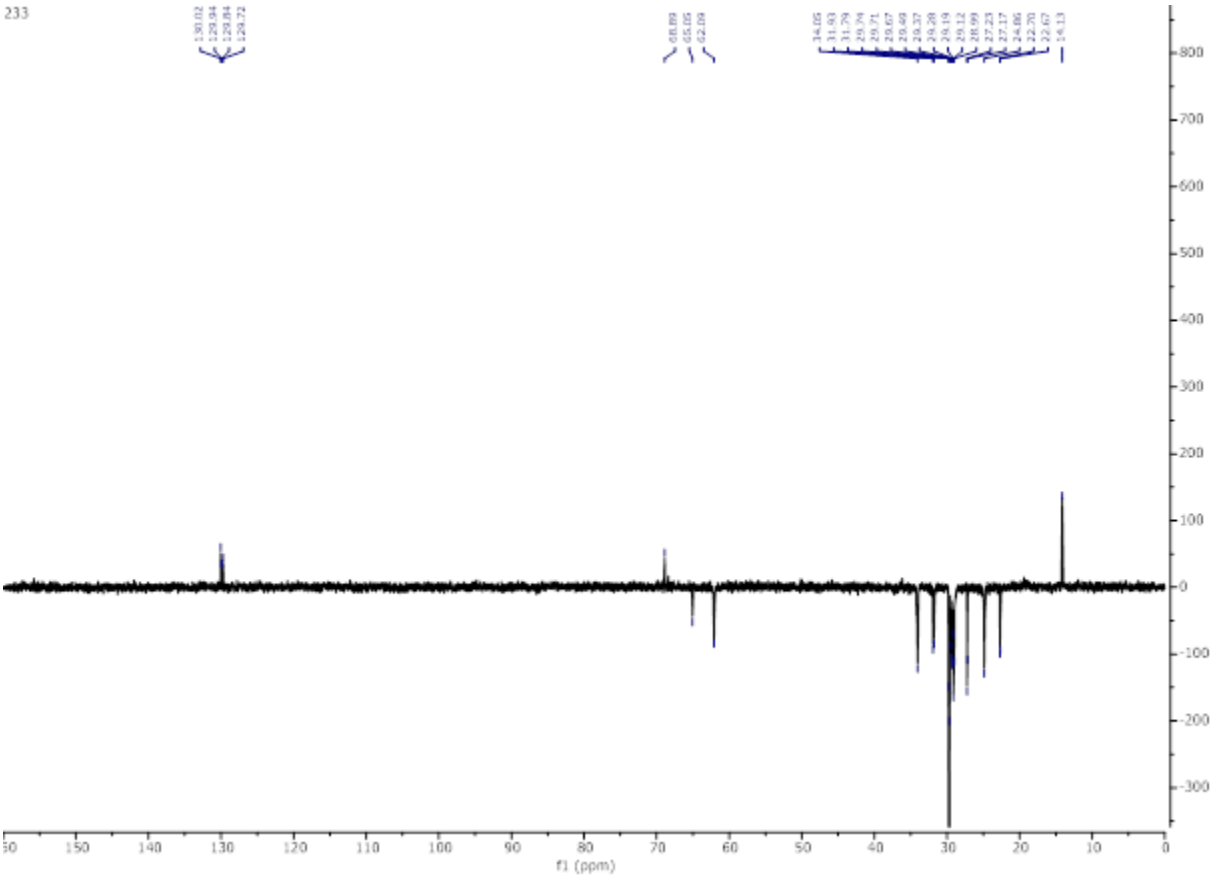

Appendix 8A: 1H NMR spectrum of chelerythrine (**55**), DMSO, 300 MHz

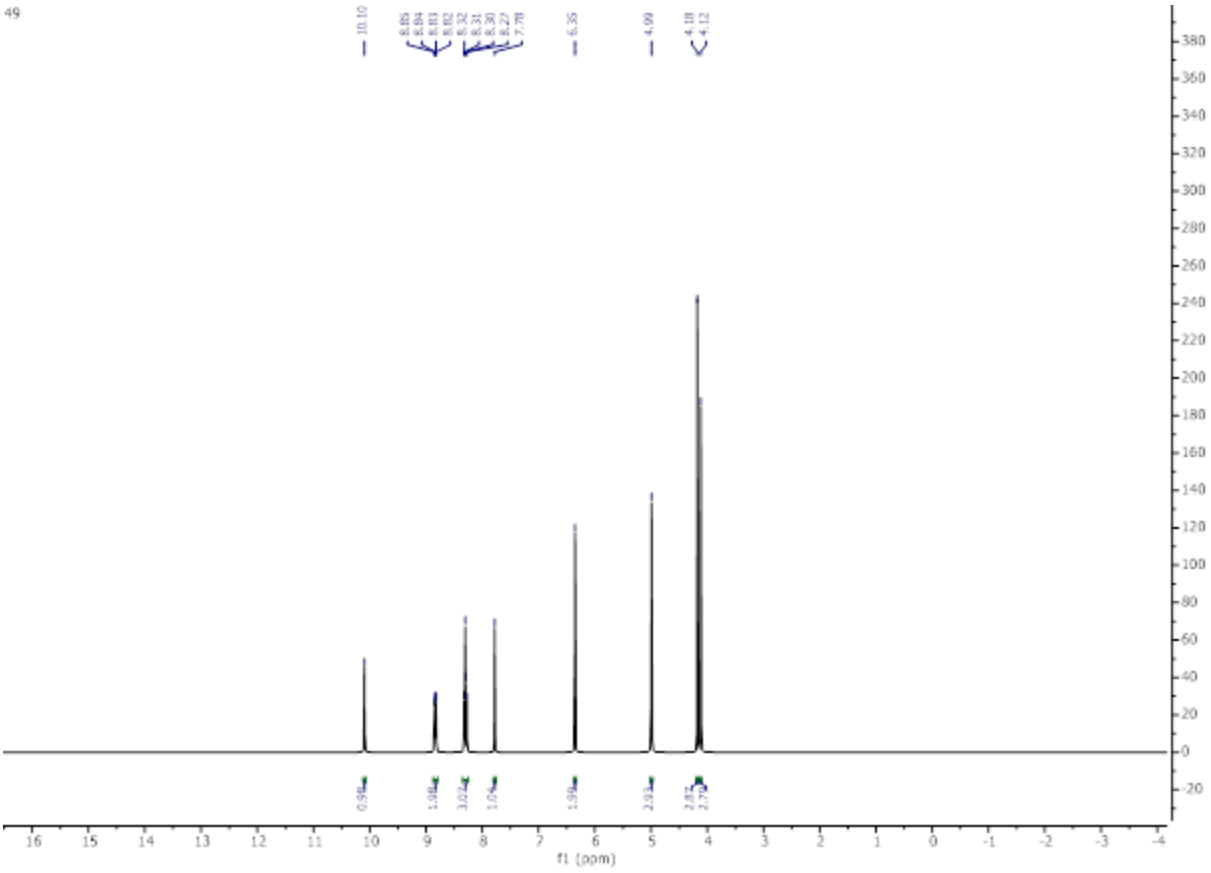

Appendix 8B: 13C NMR spectrum of chelerythrine (**55**), DMSO, 75 MHz

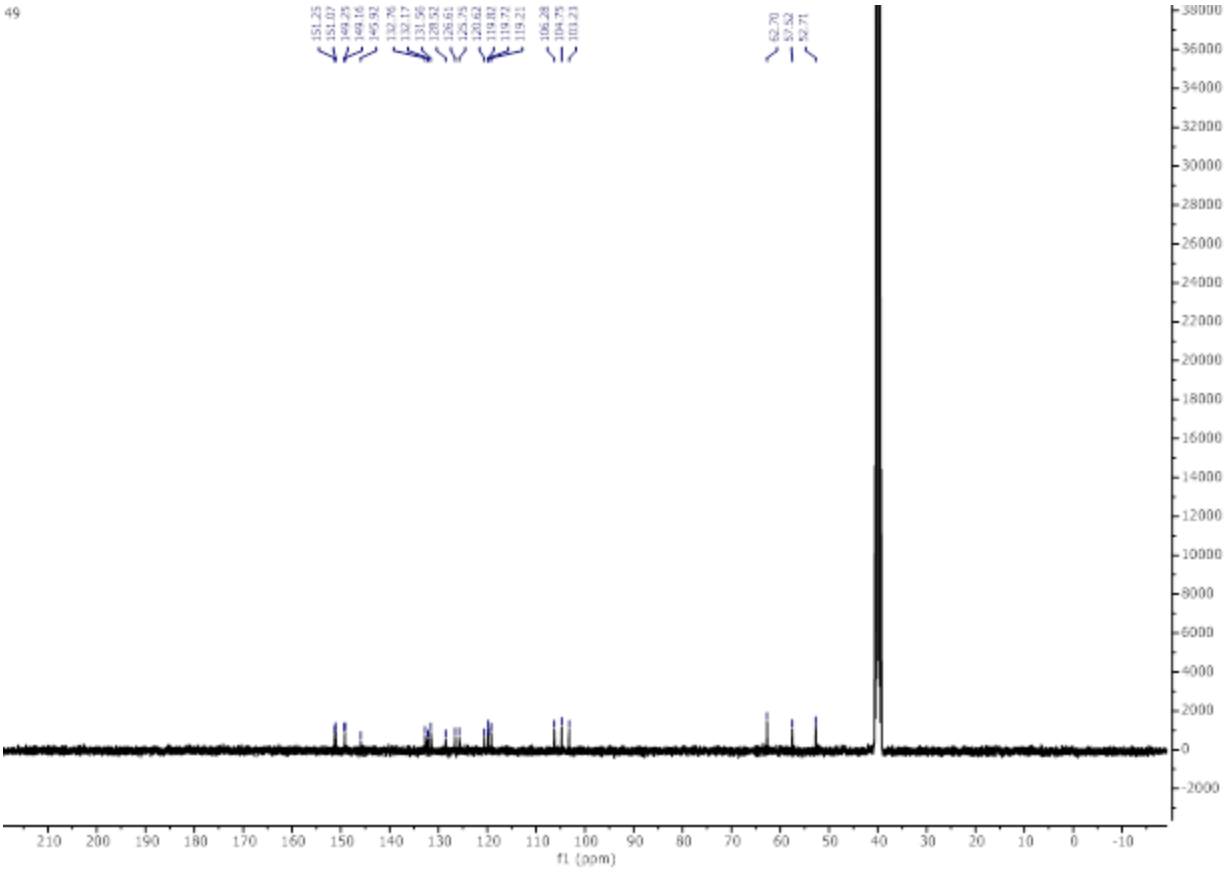

Appendix 8C: DEPT-135 spectrum of chelerythrine (**55**), DMSO 75 MHz

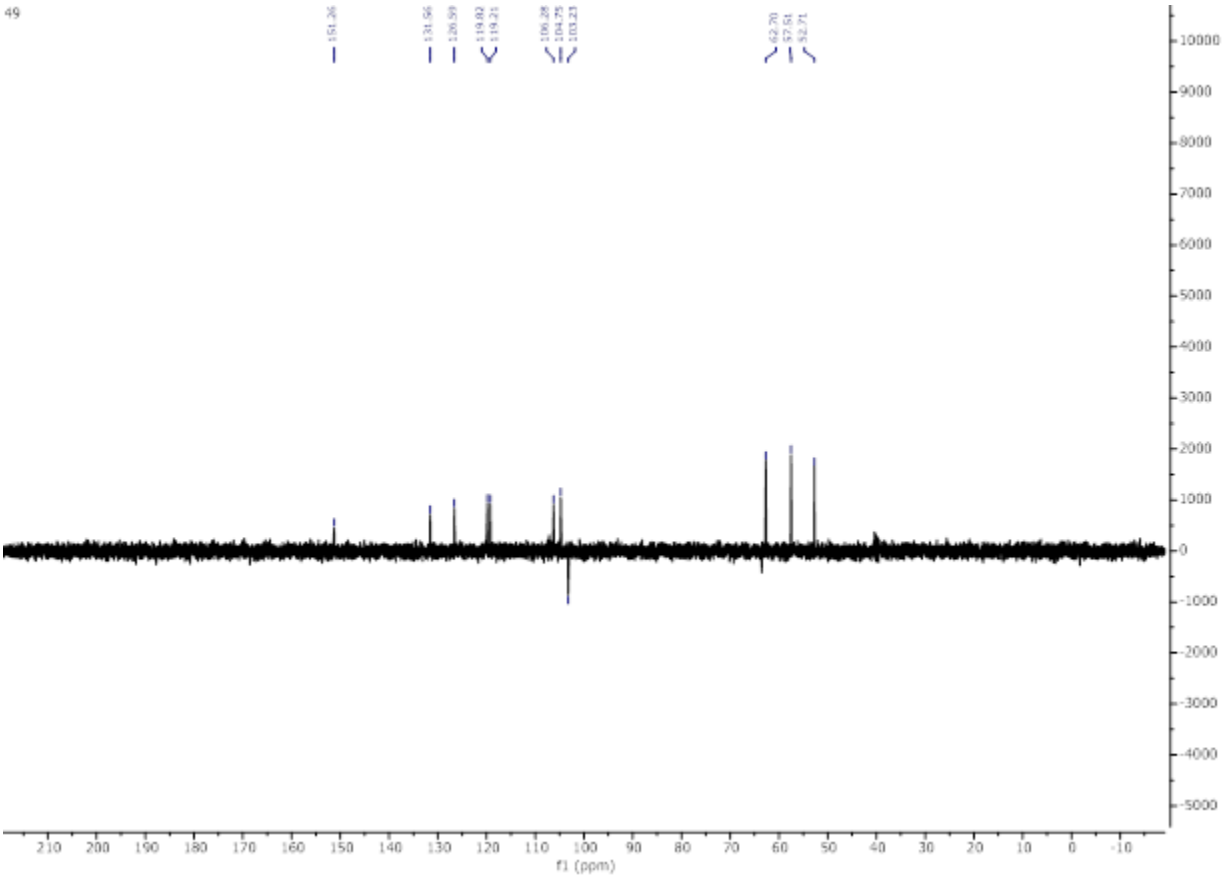

Appendix 8D: HSQC spectrum of chelerythrine **(55)**

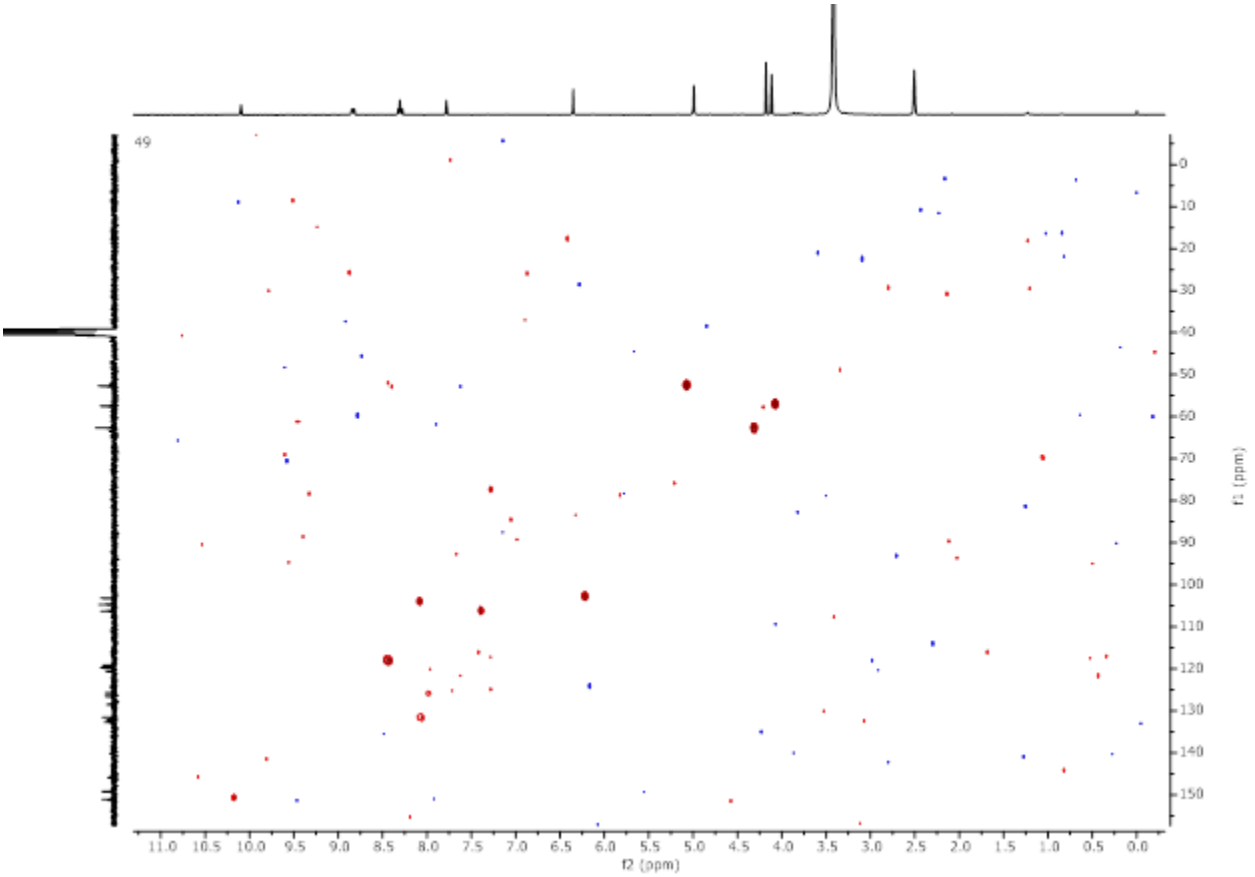

Appendix 9A: 1H NMR spectrum of 6-hydroxydihydrochelerythrine (**62**), $CDC1_3$, 300 MHz

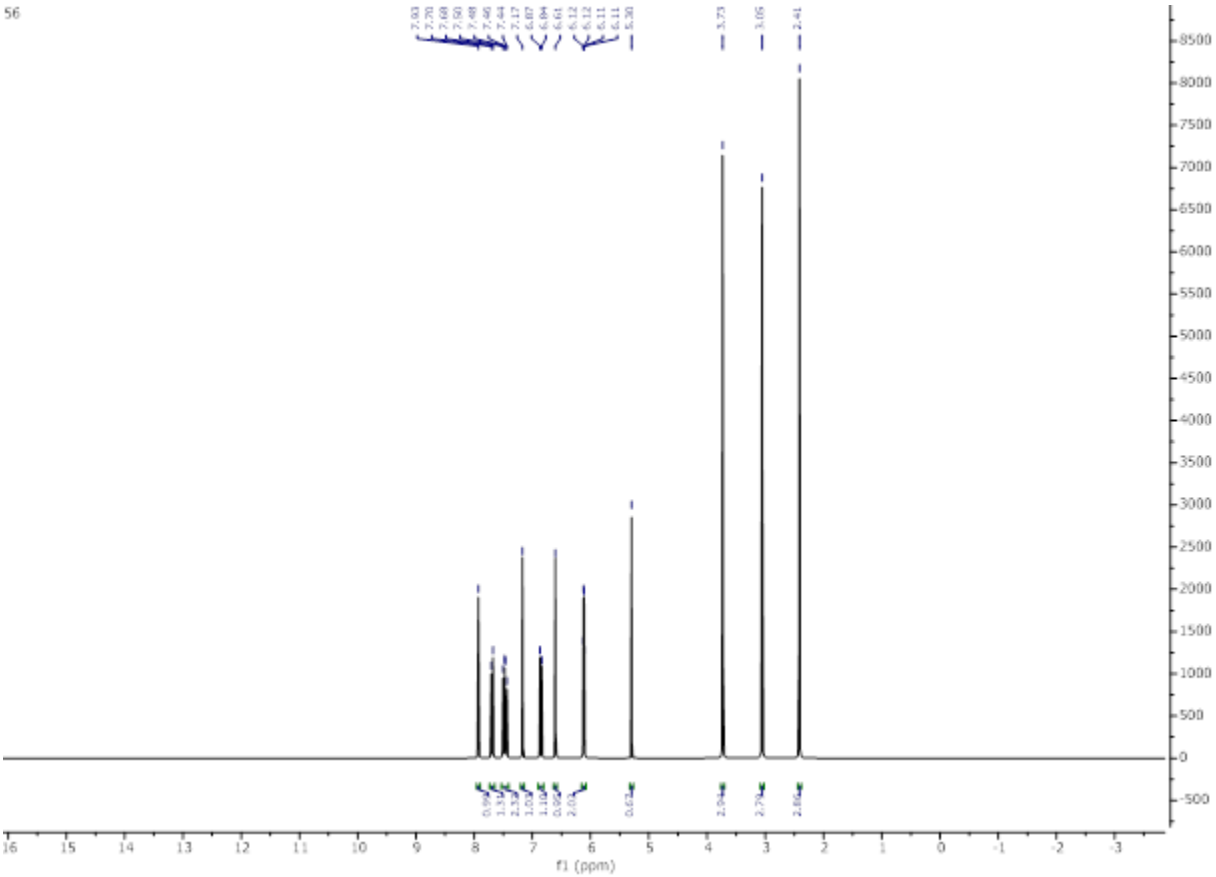

Appendix 9B: 13C NMR spectrum of 6-hydroxydihydrochelerythrine (**62**), $CDC1_3$, 75 MHz

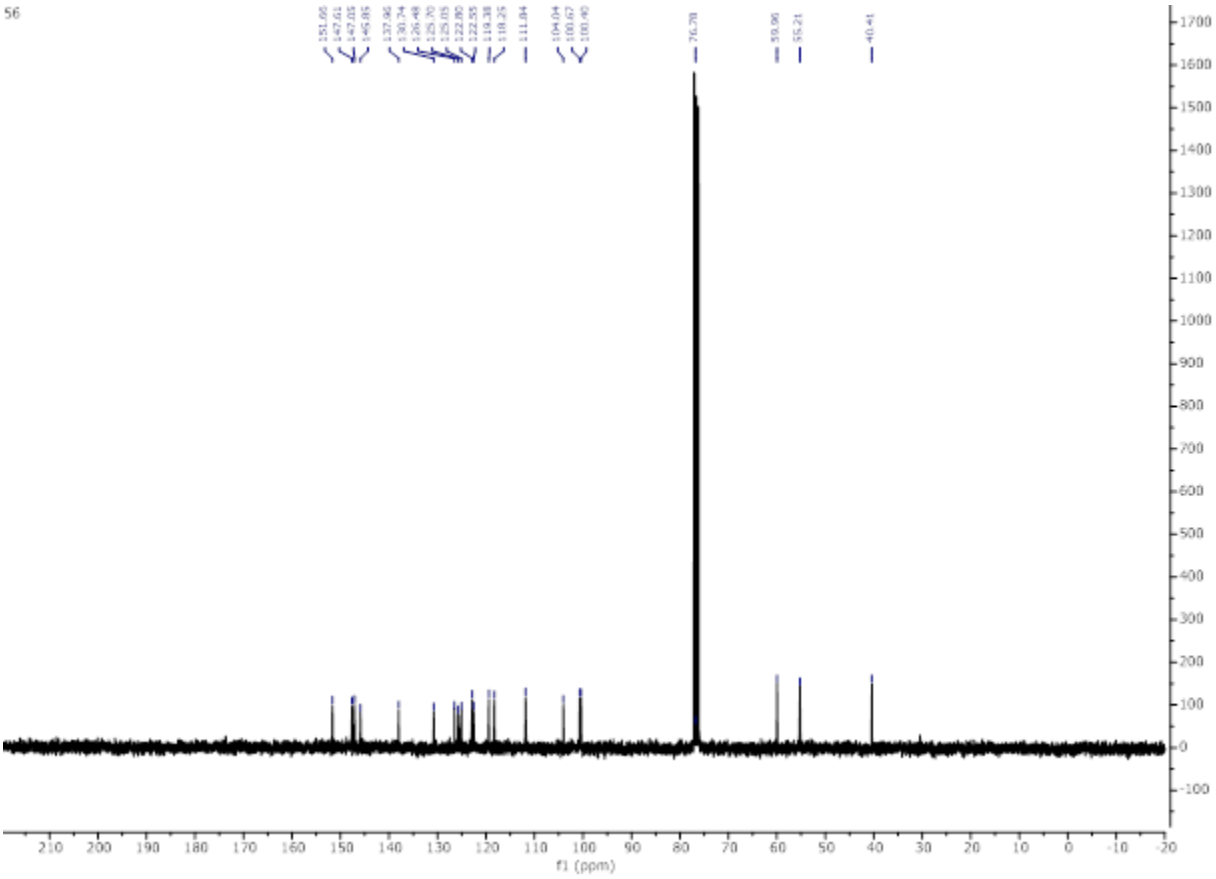

Appendix 9C: DEPT-135 spectrum of 6-hydroxydihydrochelerythrine (**62**), $CDC1_3$, 75 MHz

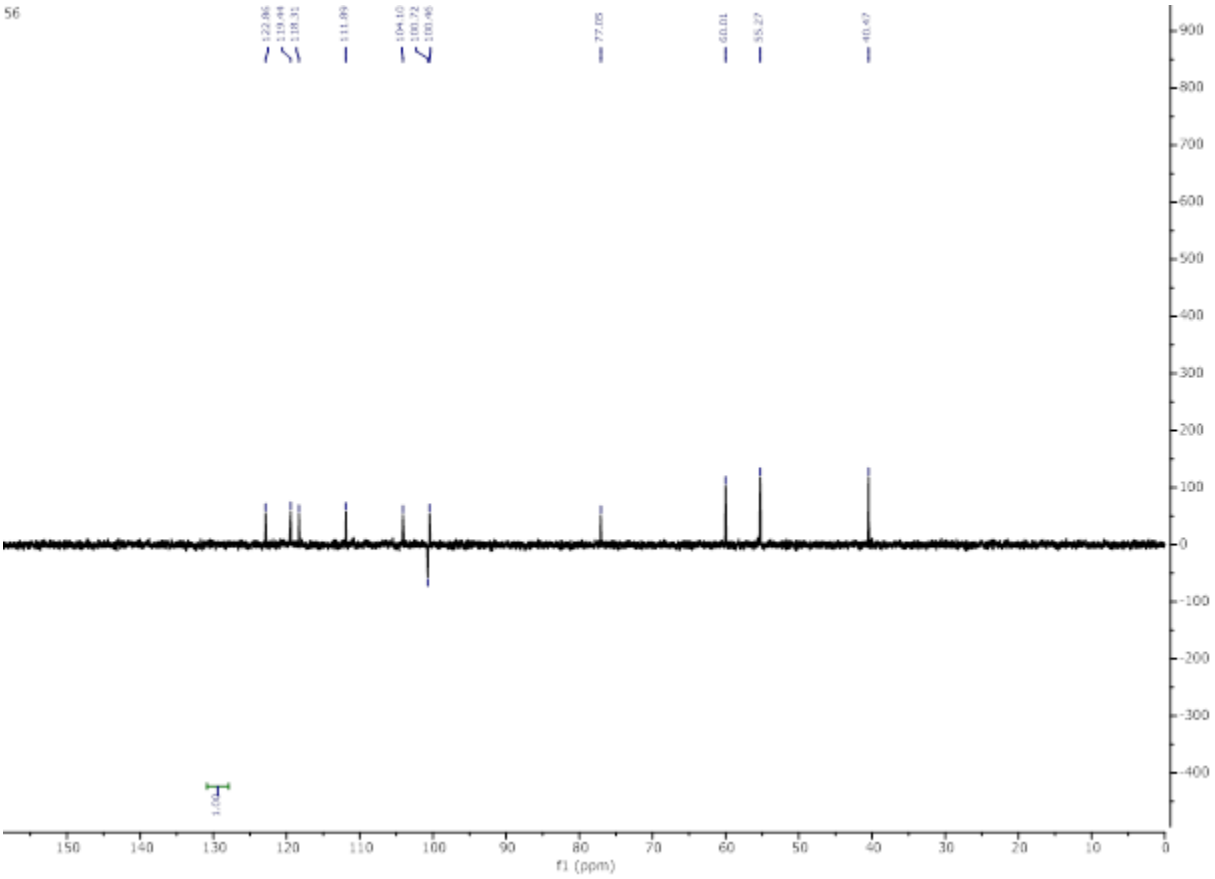

Appendix 10A: 1H NMR spectrum of 6-methoxydihydrochelerythrine (**247**), $CDC1_3$, 300 MHz

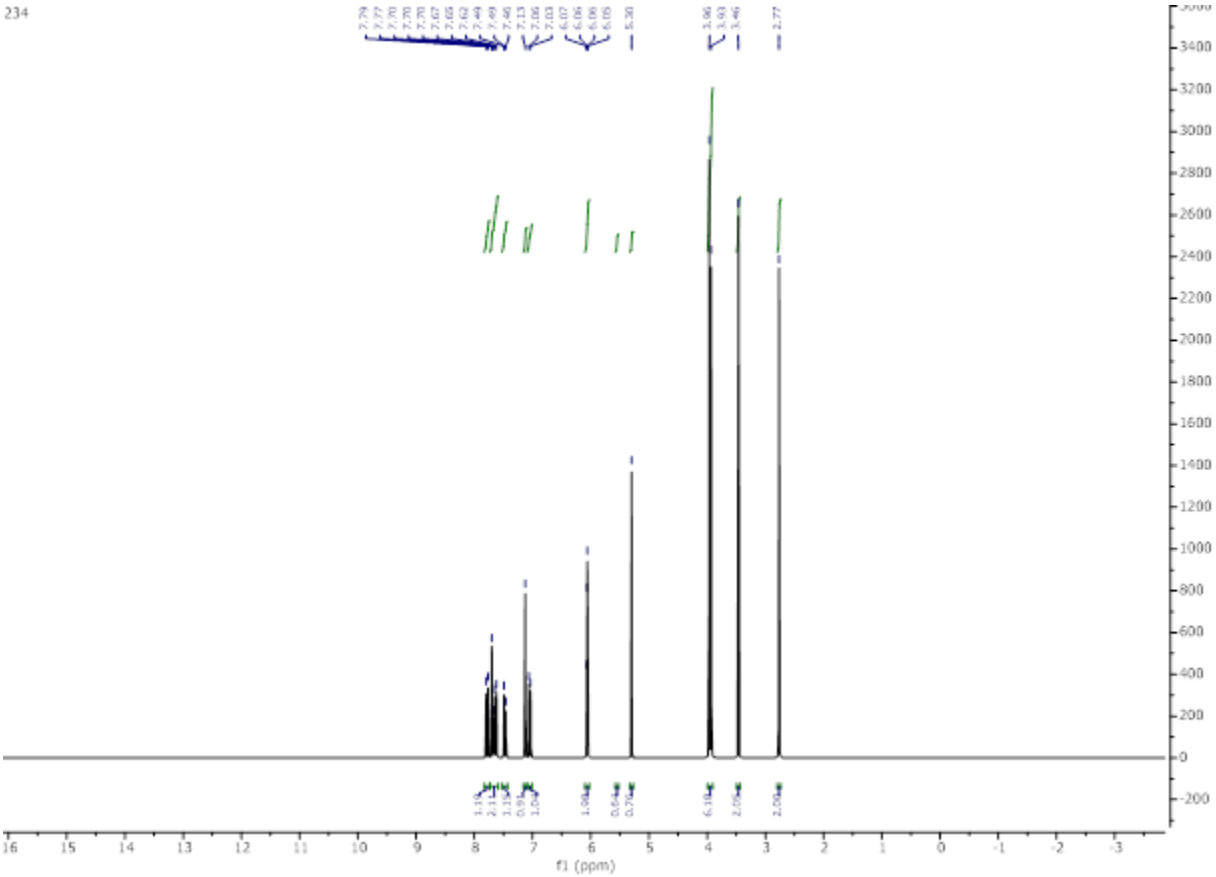

Appendix 10B: 13C NMR spectrum of 6-methoxydihydrochelerythrine (**247**), $CDC1_3$, 75 MHz

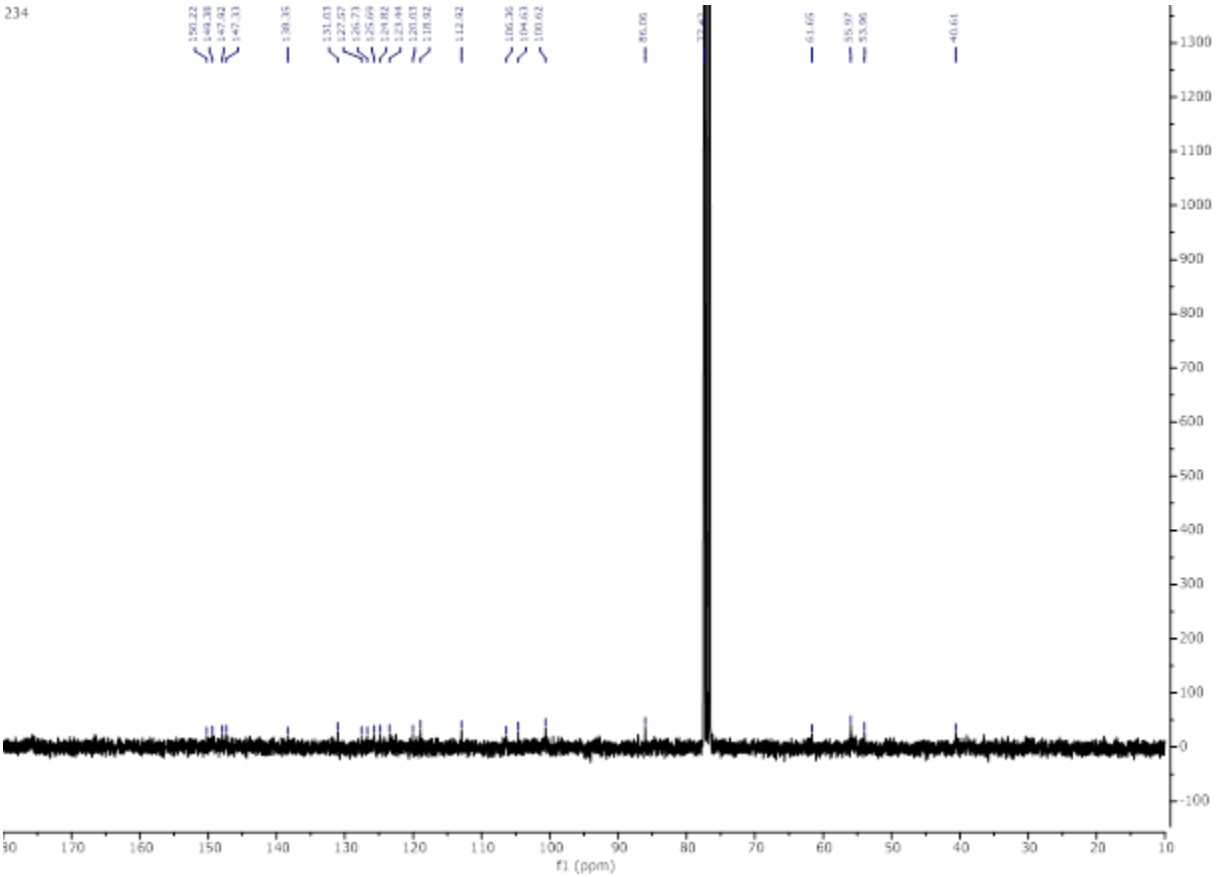

Appendix 10C: DEPT-135 spectrum of 6-methoxydihydrochelerythrine (**247**), $CDC1_3$, 75 MHz

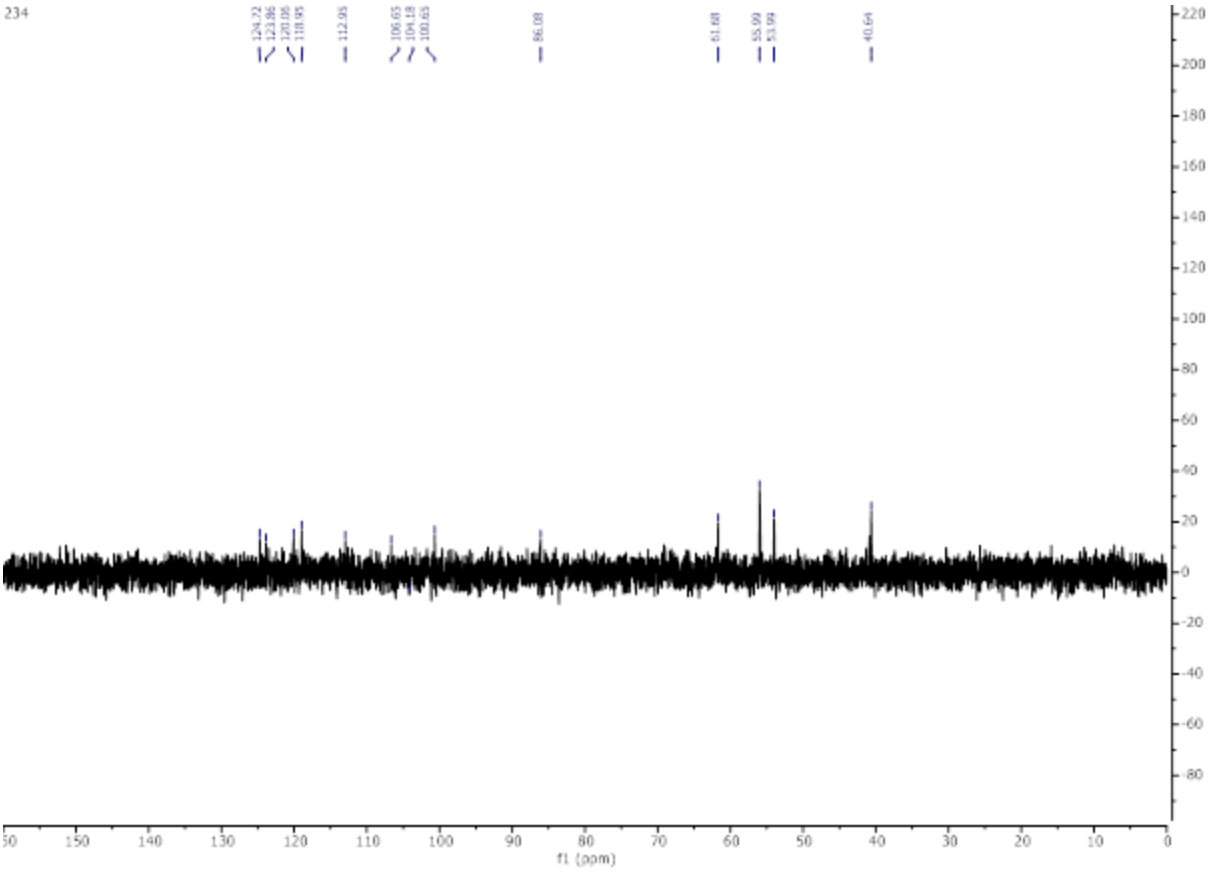

Appendix 10D: HSQC spectrum of 6-methoxydihydrochelerythrine (**247**)

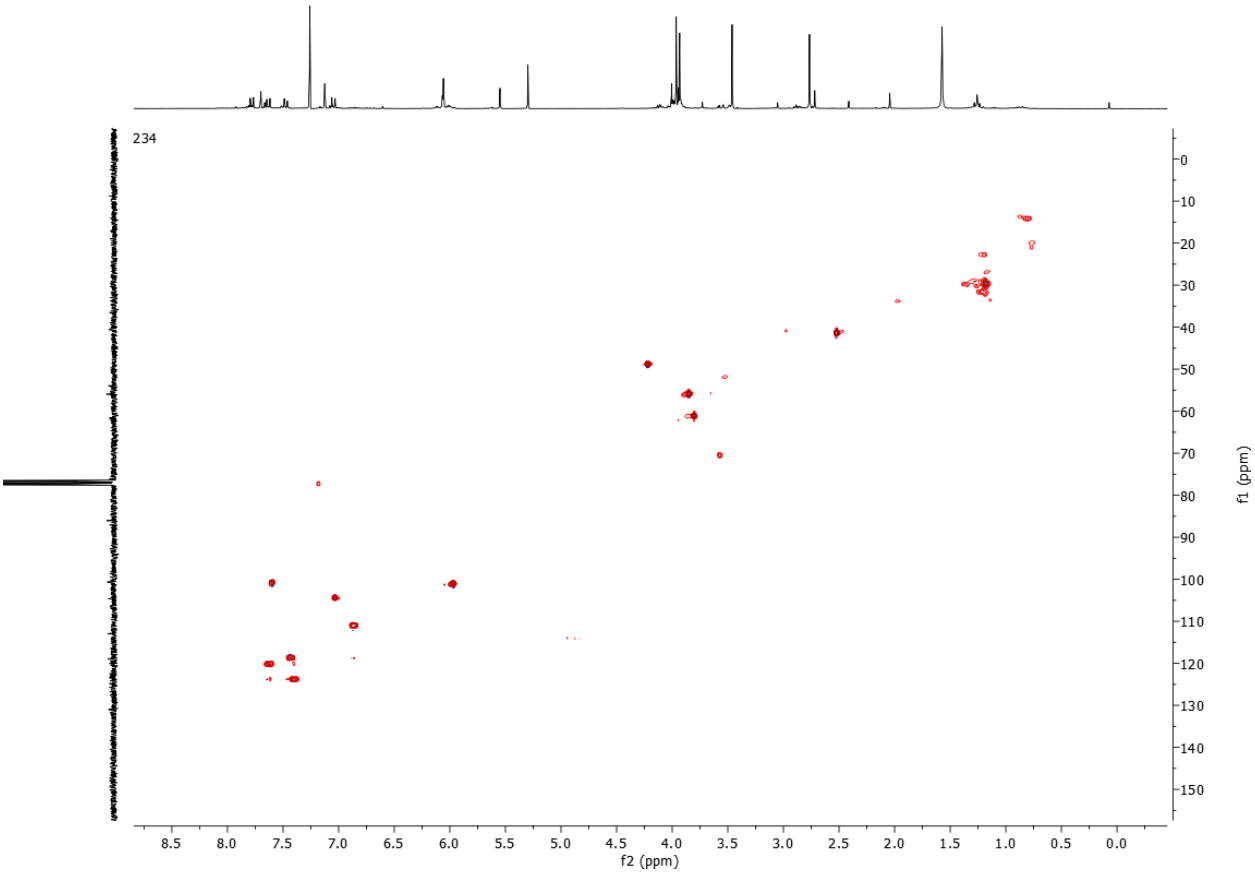

Appendix 11A: 1H NMR spectrum of dihydrochelerythrine (**67**), $CDC1_3$, 300 MHz

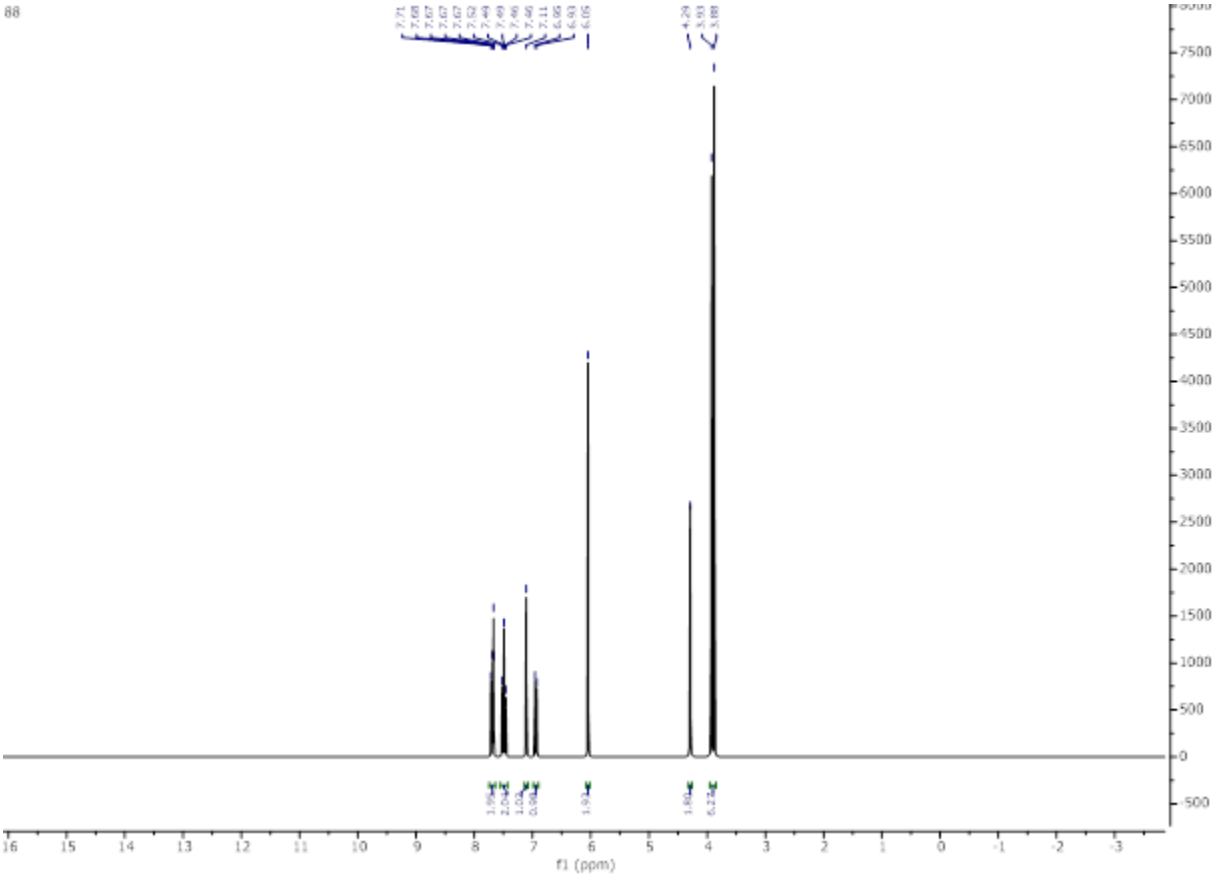

Appendix 11B : 13C NMR spectrum of dihydrochelerythrine (**67**), $CDC1_3$, 75 MHz

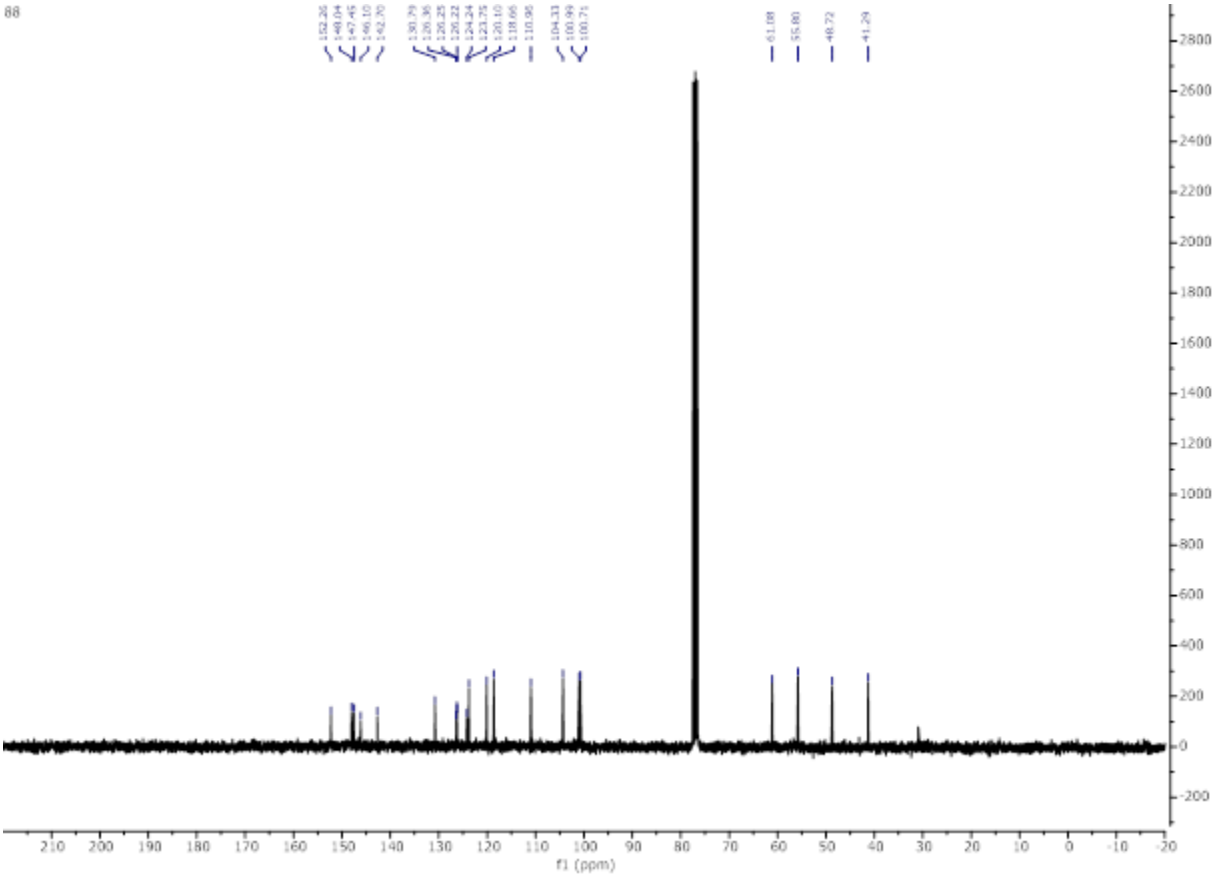

Appendix 11C: DEPT-135 spectrum of dihydrochelerythrine (**67**), $CDC1_3$, 75MHz

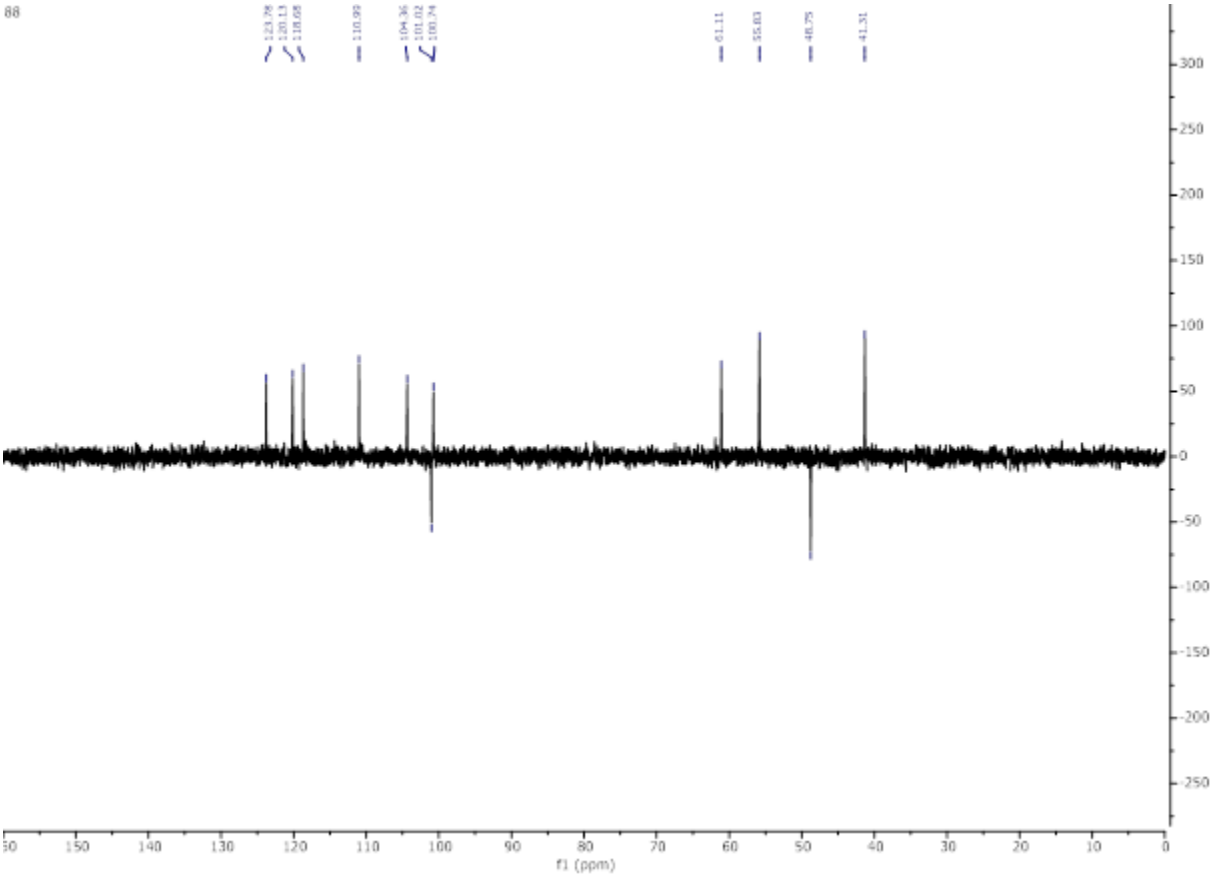

Appendix 12A: HRMS spectrum of u uvarindole-F (**248**)

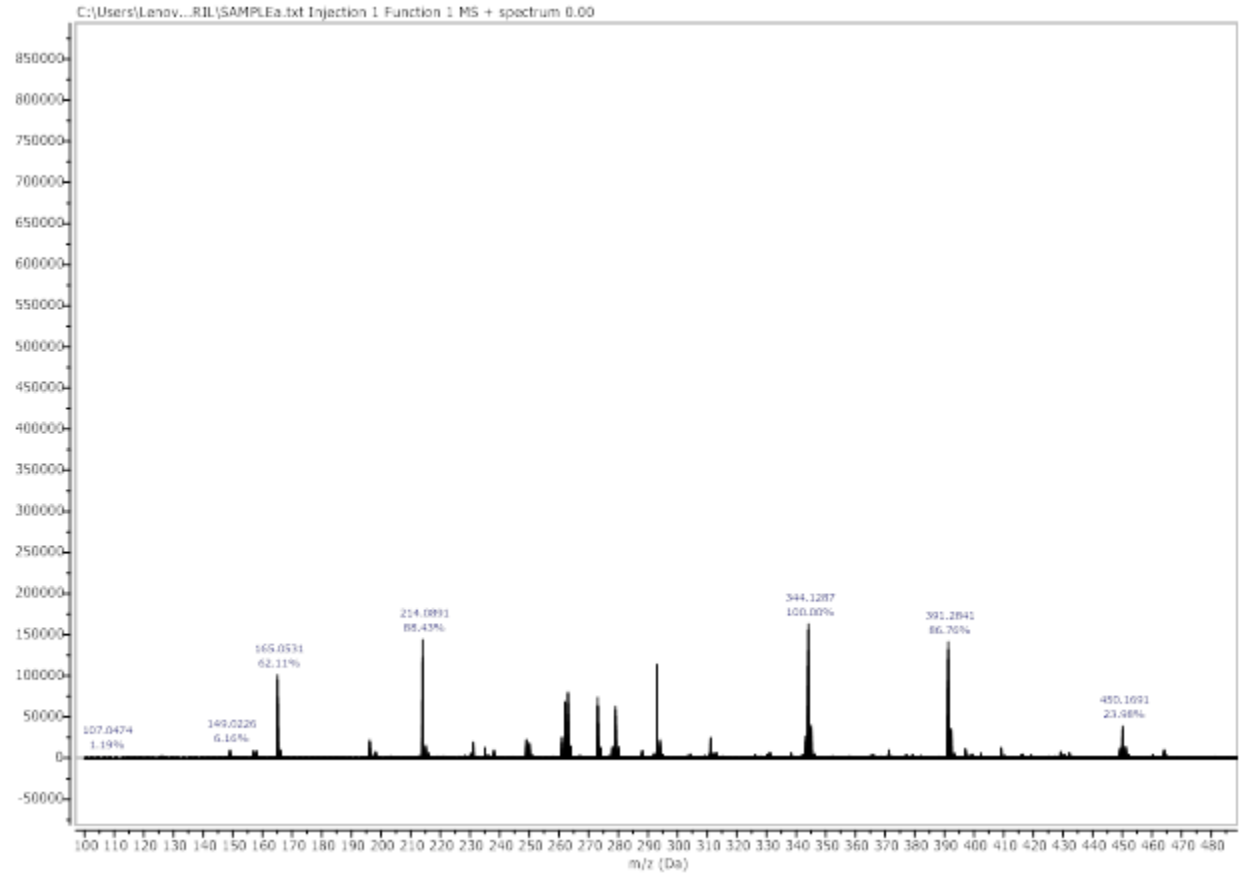

Appendix 12B: 1H NMR spectrum of uvarindole-F (**248**), $CDC1_3$, 500 MHz

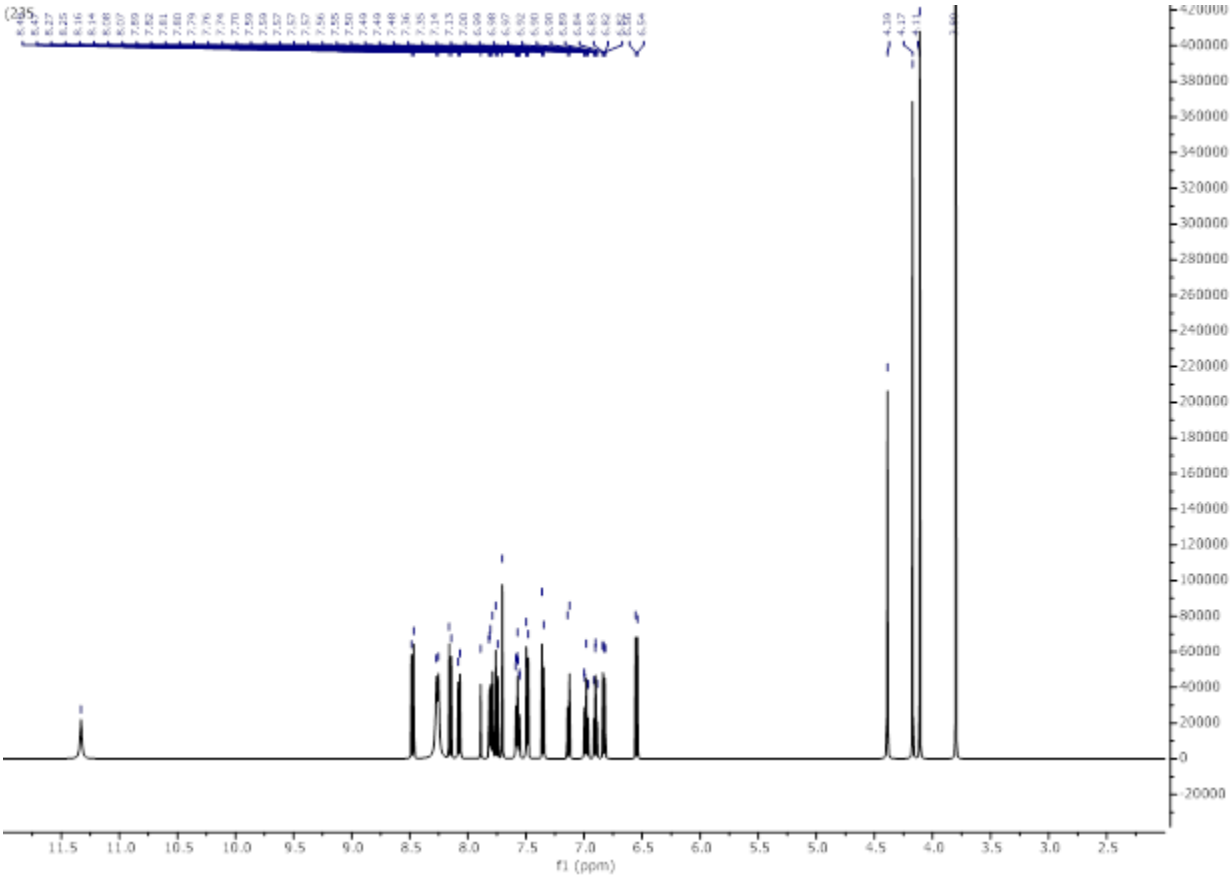

Appendix 12C: 13C NMR spectrum of uvarindole-F (**248**), $CDC1_3$, 125MHz

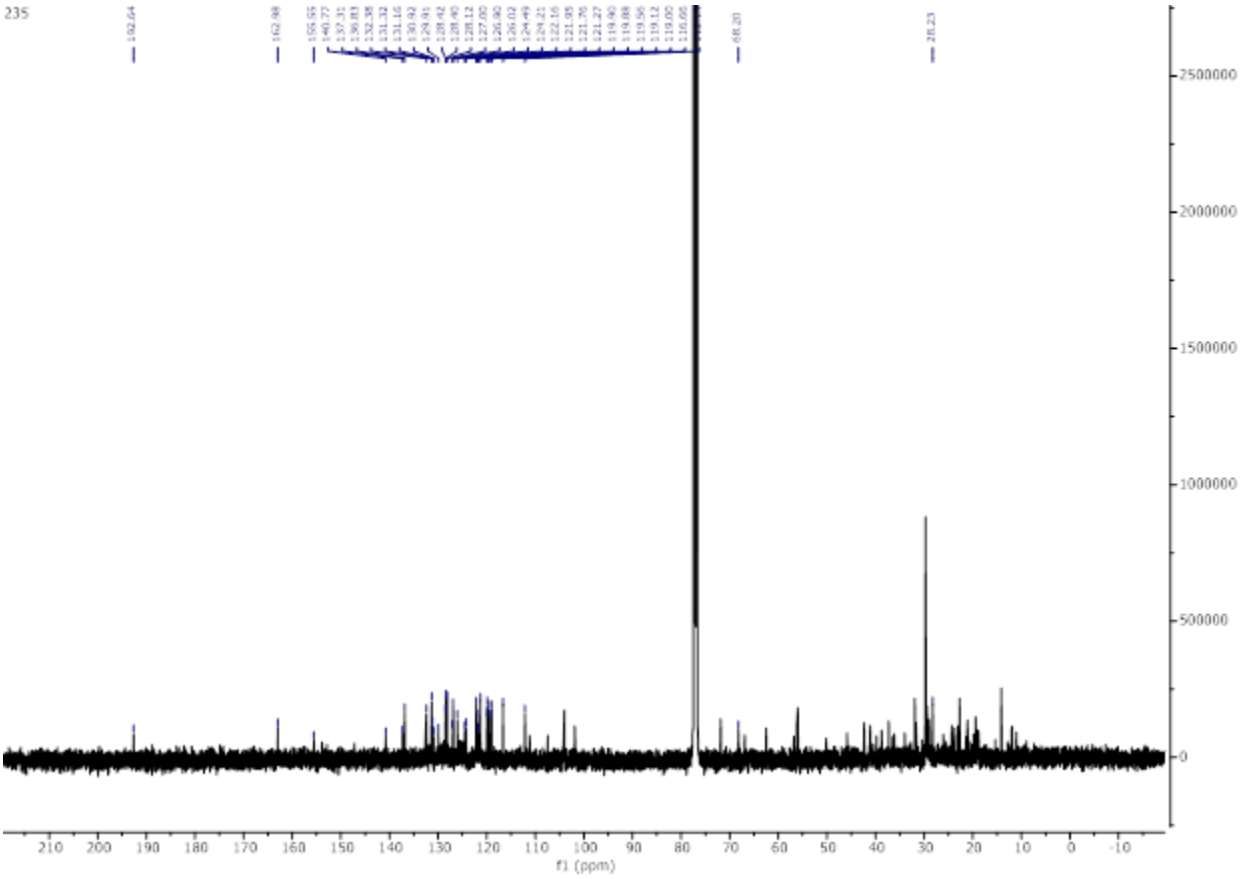

Appendix 12D: DEPT-135 spectrum of uvarindole-F (**248**), $CDC1_3$, 125 MHz

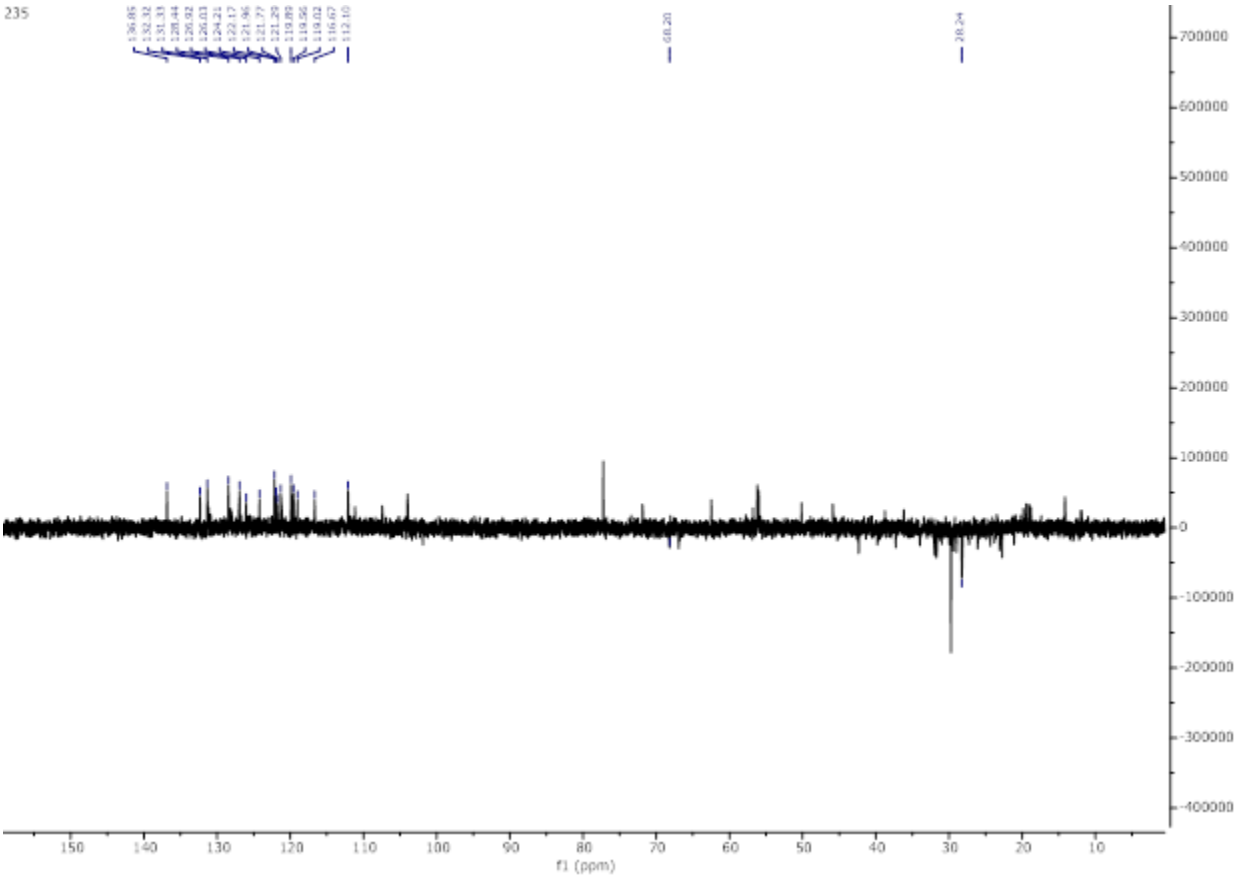

Appendix 12E: COSY spectrum of uvarindole-F **(248)**

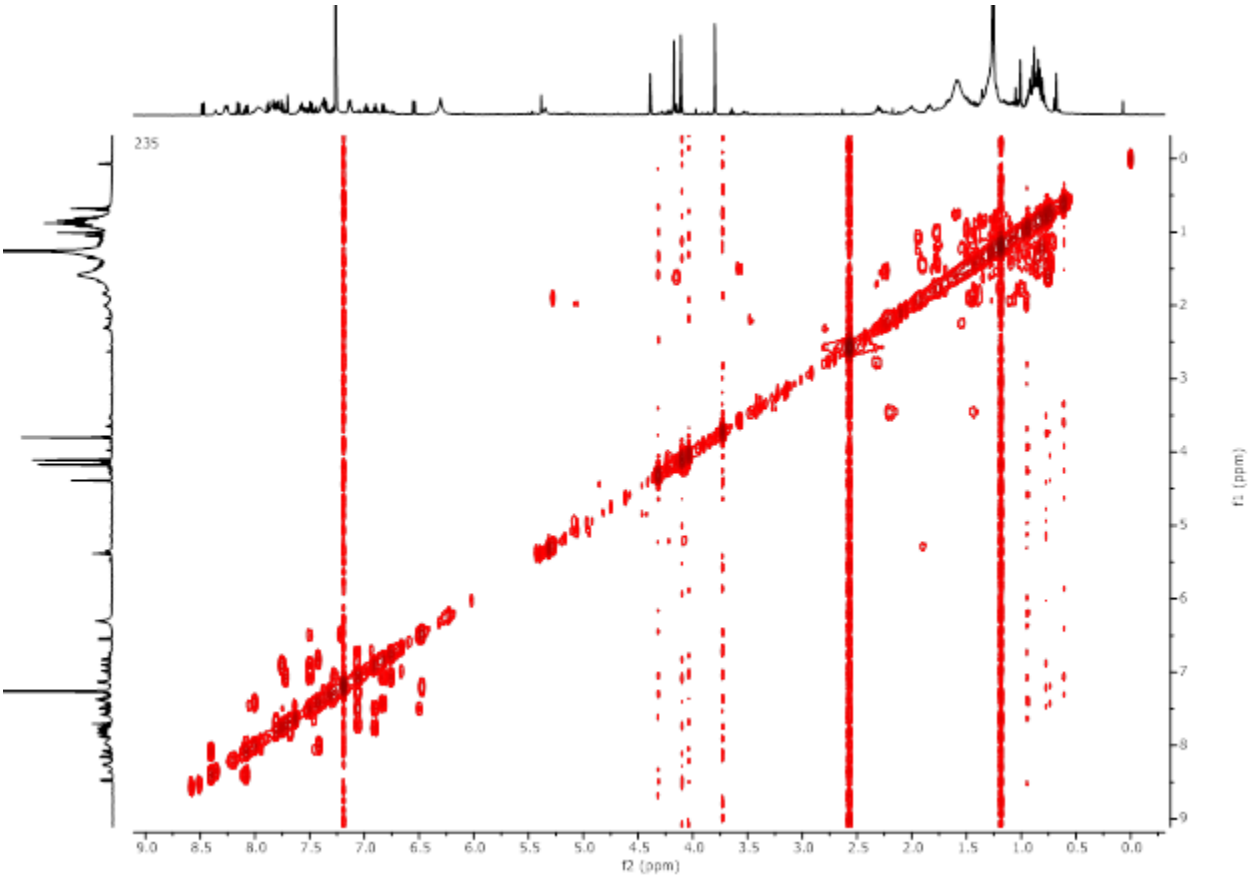

Appendix 12F: HSQC spectrum of uvarindole-F (**248**)

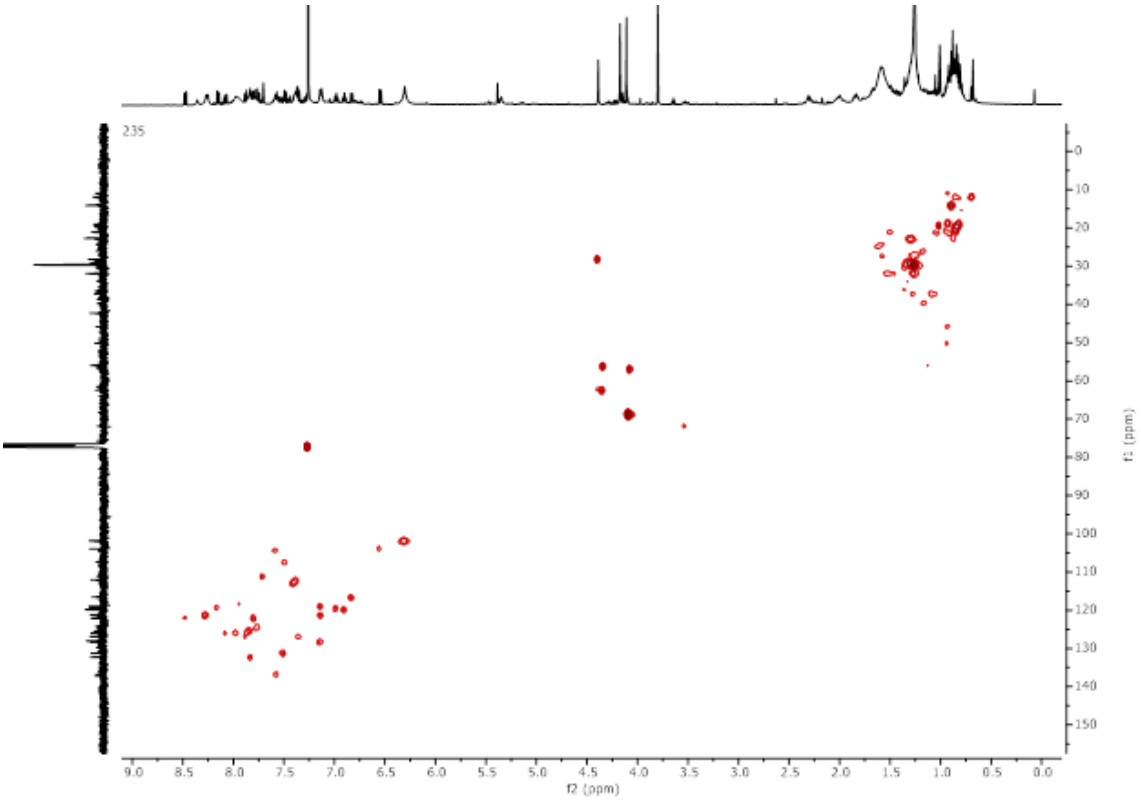

Appendix 12G: HMBC spectrum of uvarindole-F (**248**)

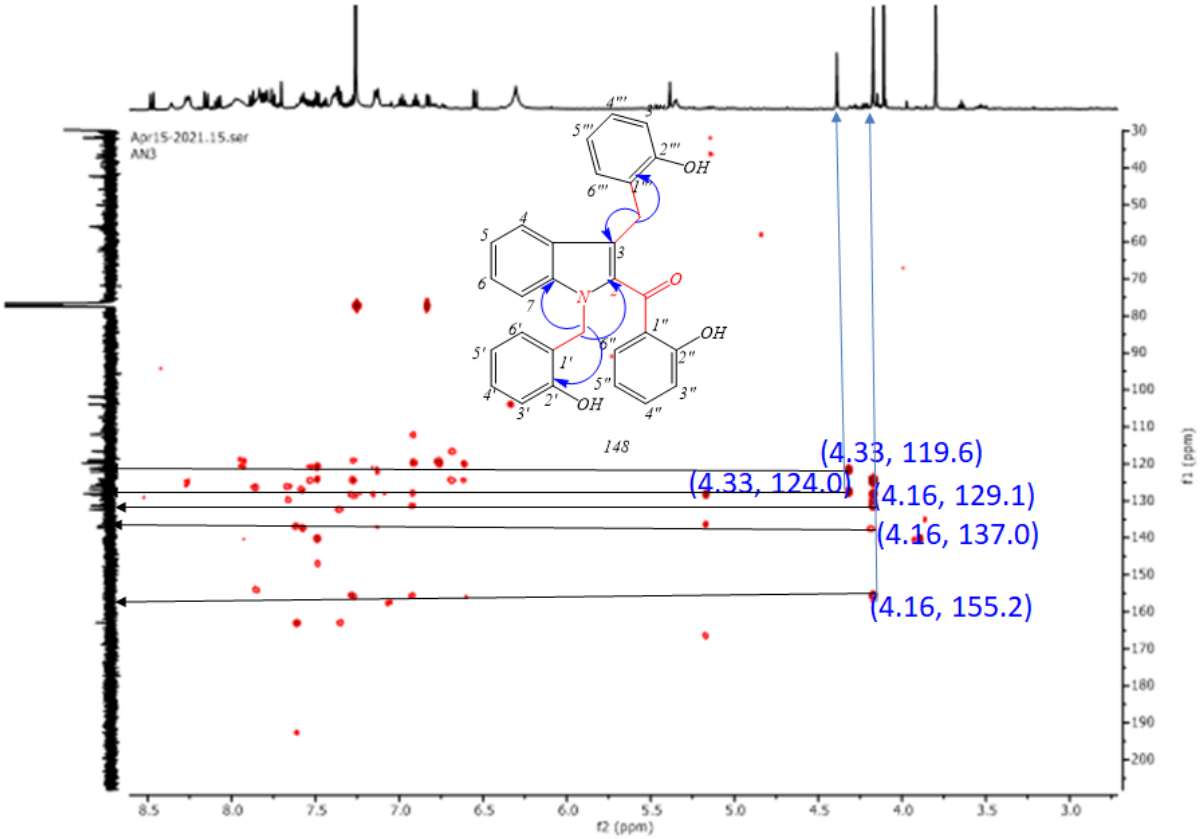

84

Appendix 13A: HRMS spectrum of uvarindole-G (**249**)

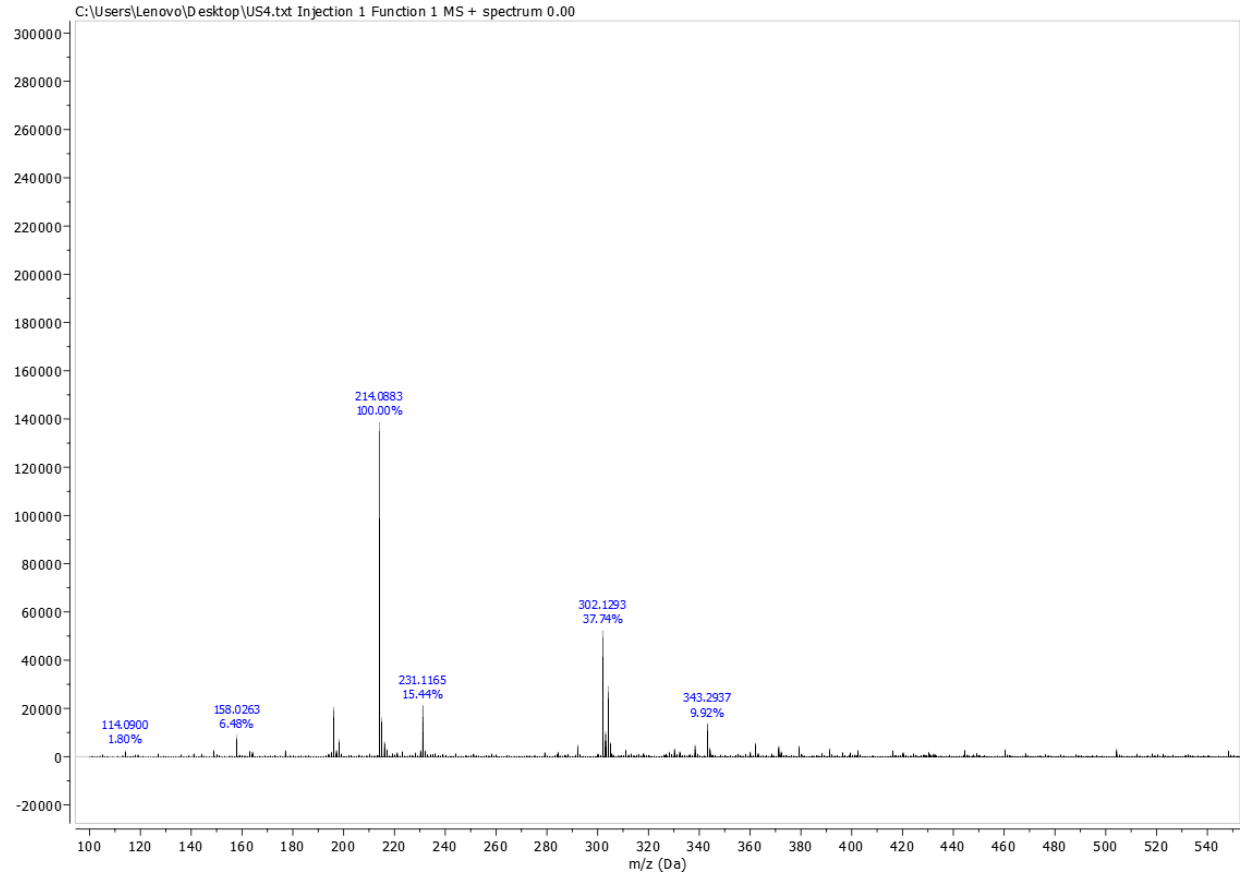

Appendix 13B: ^{1}H NMR spectrum of uvarindole-G (**249**), $CDC1_3$, 500 MHz

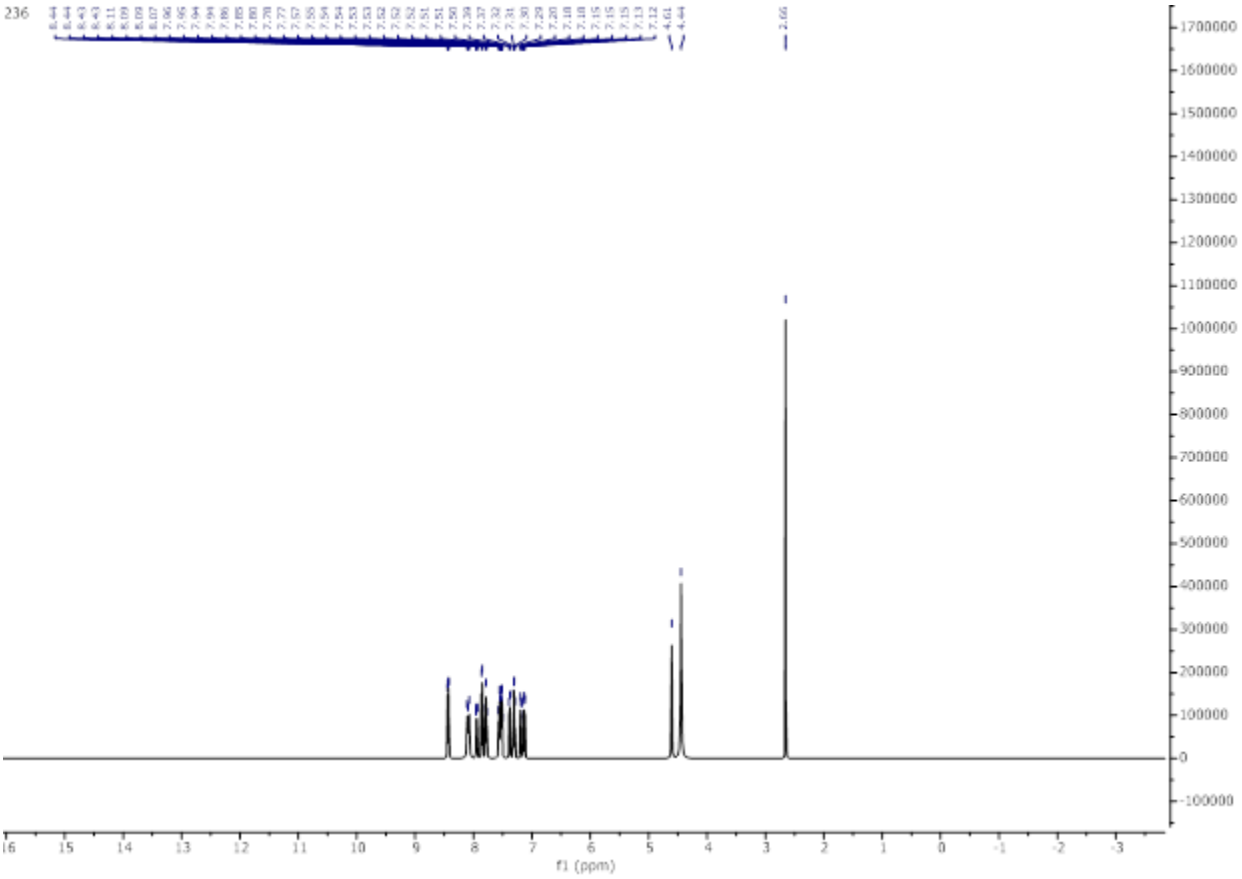

Appendix 13C: ^{13}CNMR spectrum of uvarindole-G (**249**), $CDC1_3$, 125 MHz

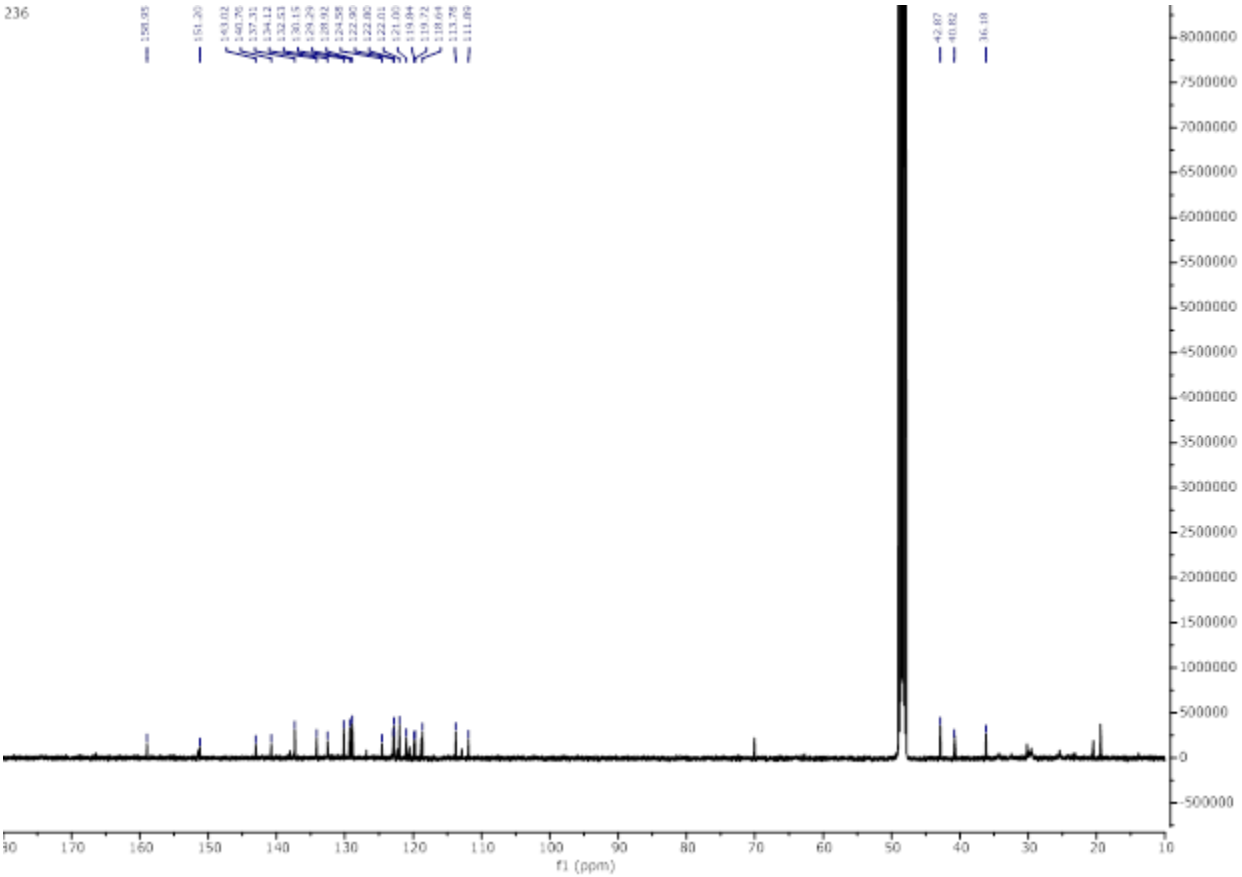

Appendix 13D: DEPT-135 spectrum of uvarindole-G (**249**), $CDC1_3$, 125 MHz

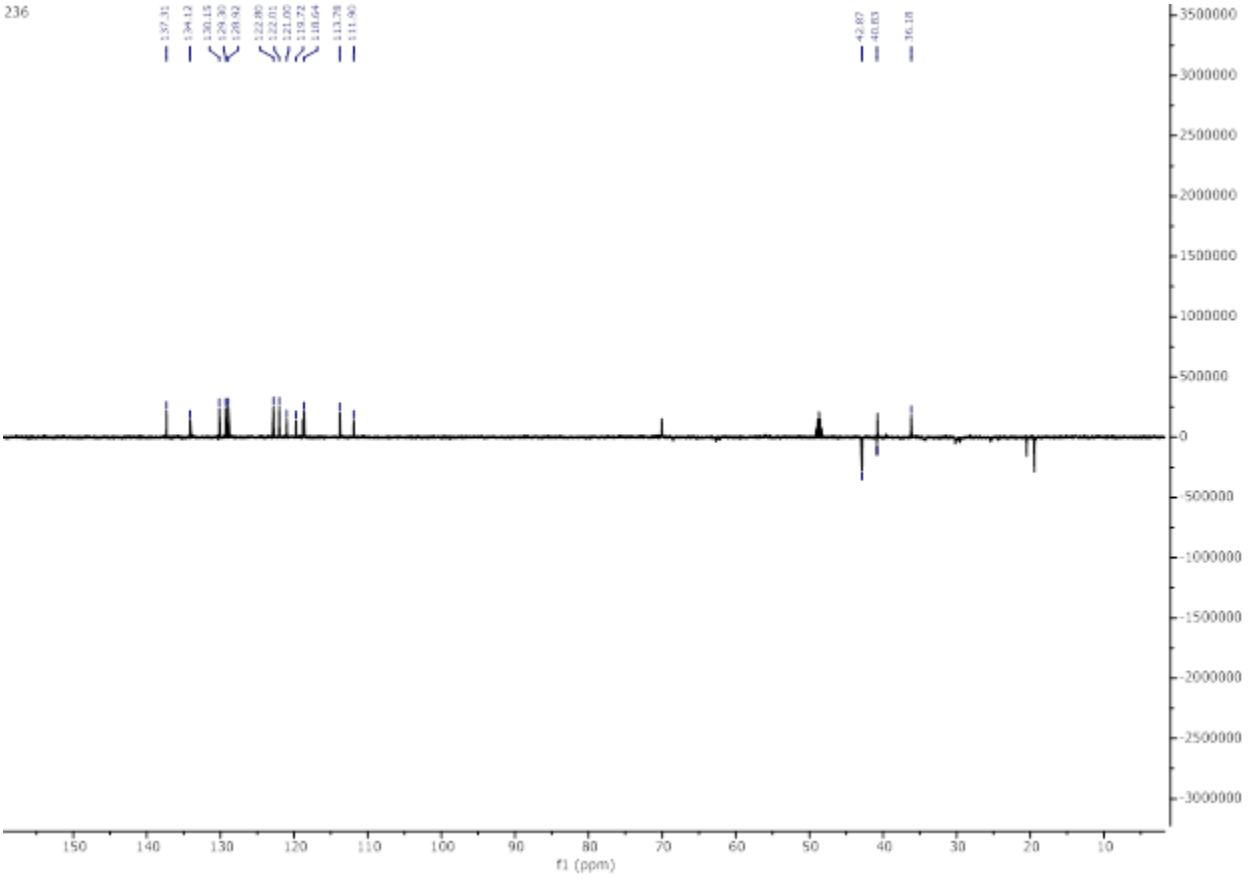

Appendix 13E: DEPT-135 spectrum of uvarindole-G (**249**), $CDC1_3$, 300 MHz

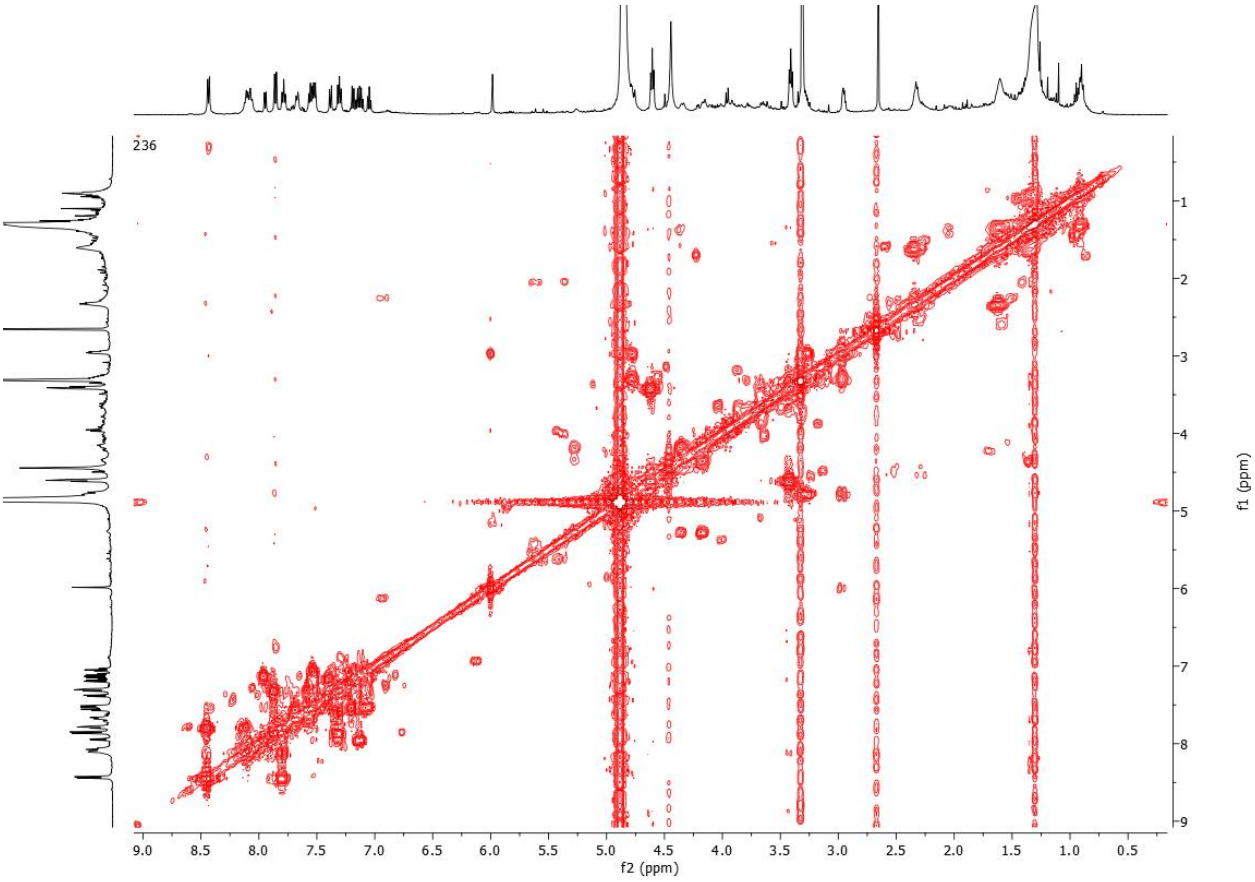

Appendix 13F: HSQC spectrum of uvarindole-G (**249**)

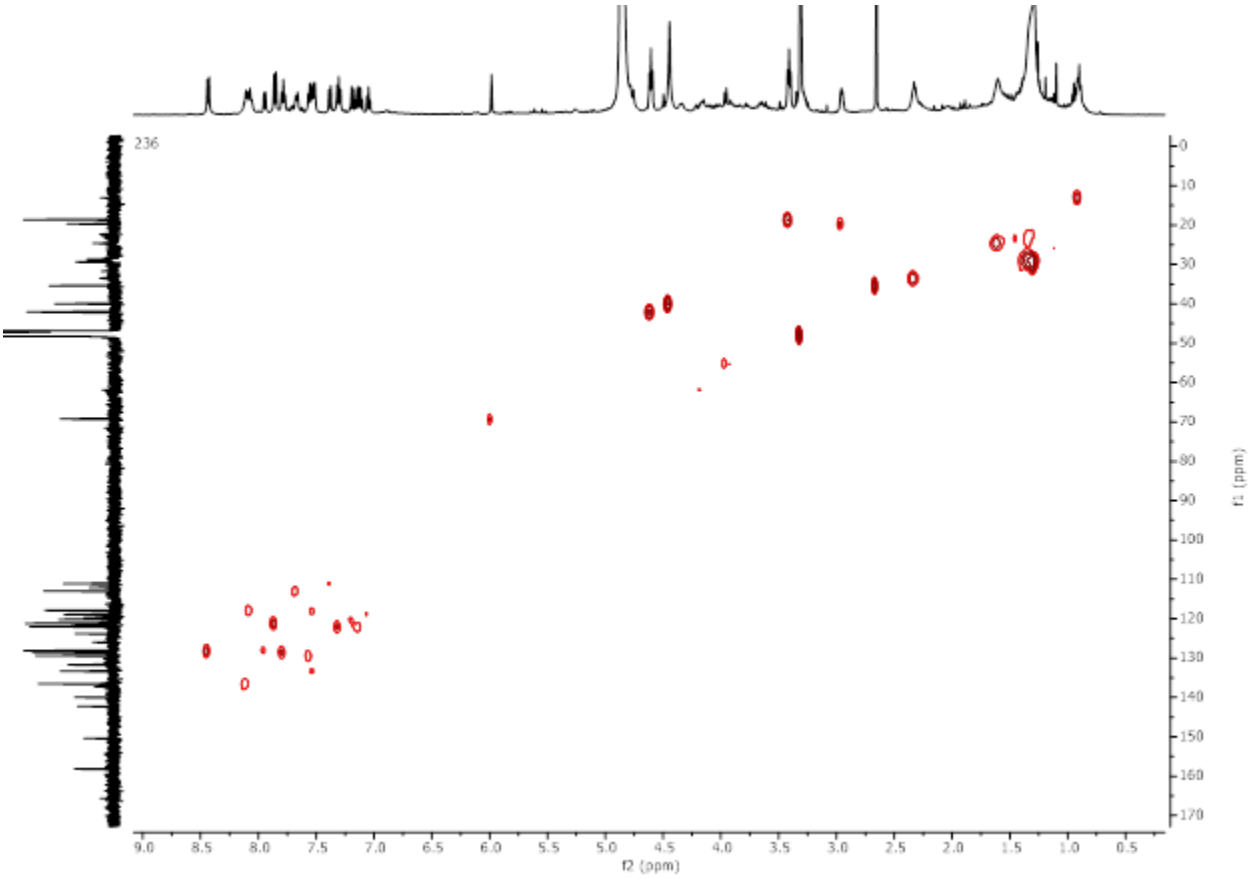

Appendix 13G: HMBC spectrum of uvarindole-G (**249**)

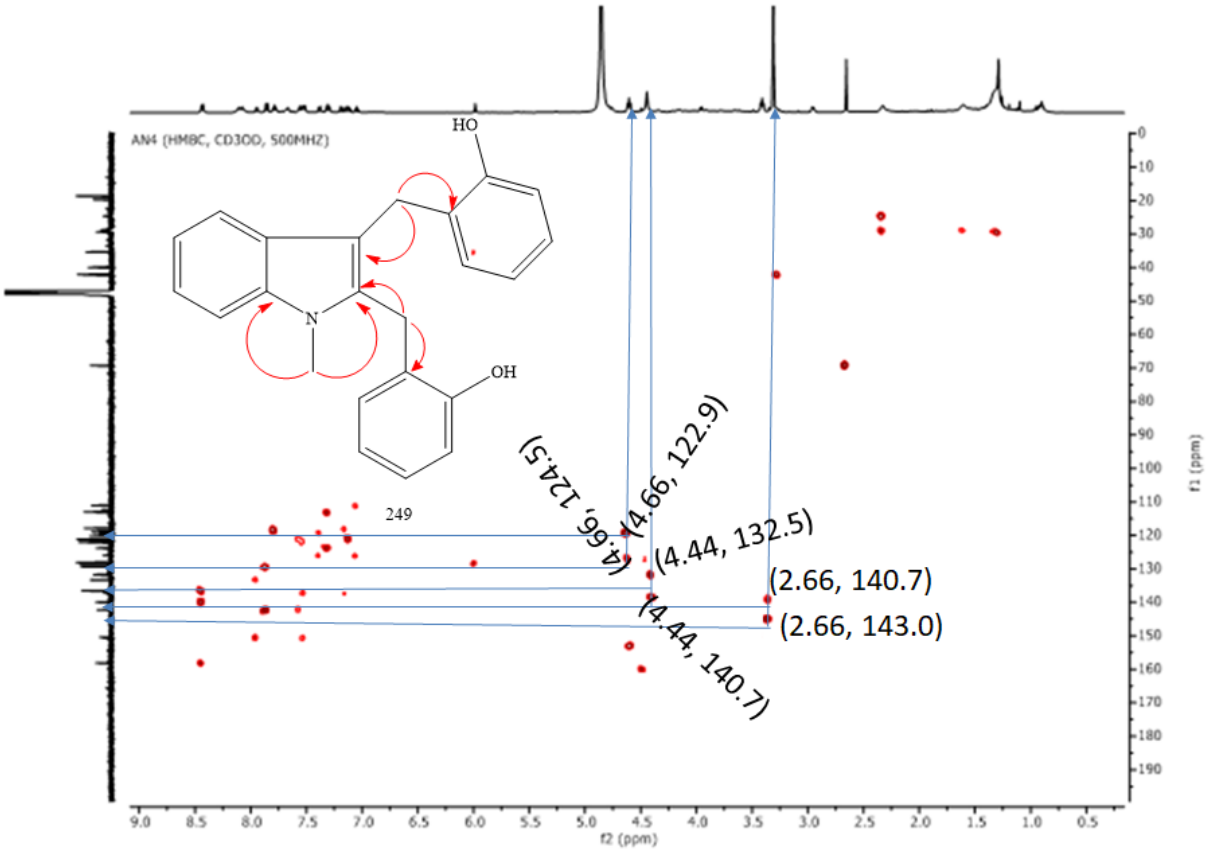

93

Appendix 14A: ^{1}H NMR spectrum of Uvaretin (**112**), $CDC1_3$, 300 MHz

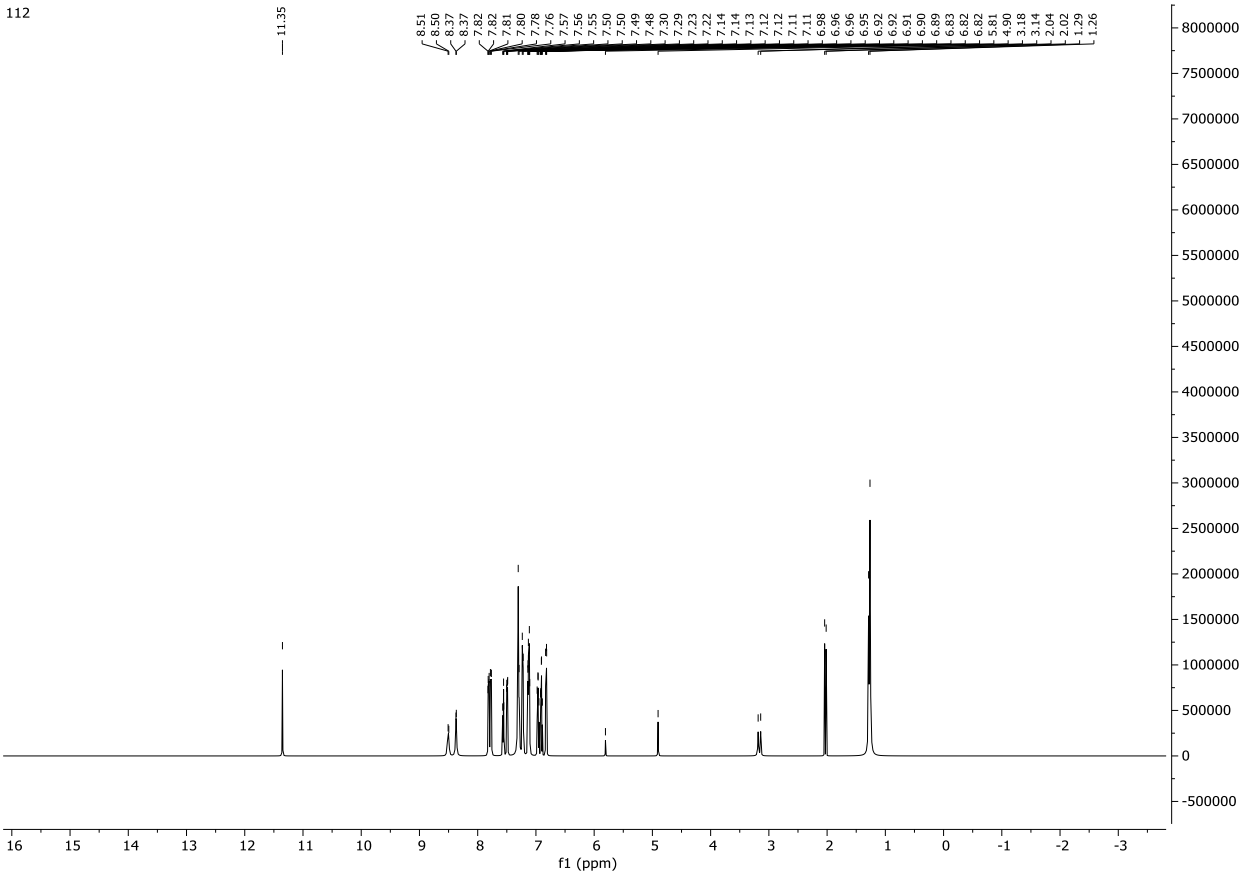

Appendix 14B: ^{13}CH NMR spectrum of Uvaretin (**112**), $CDC1_3$, 75 MHz

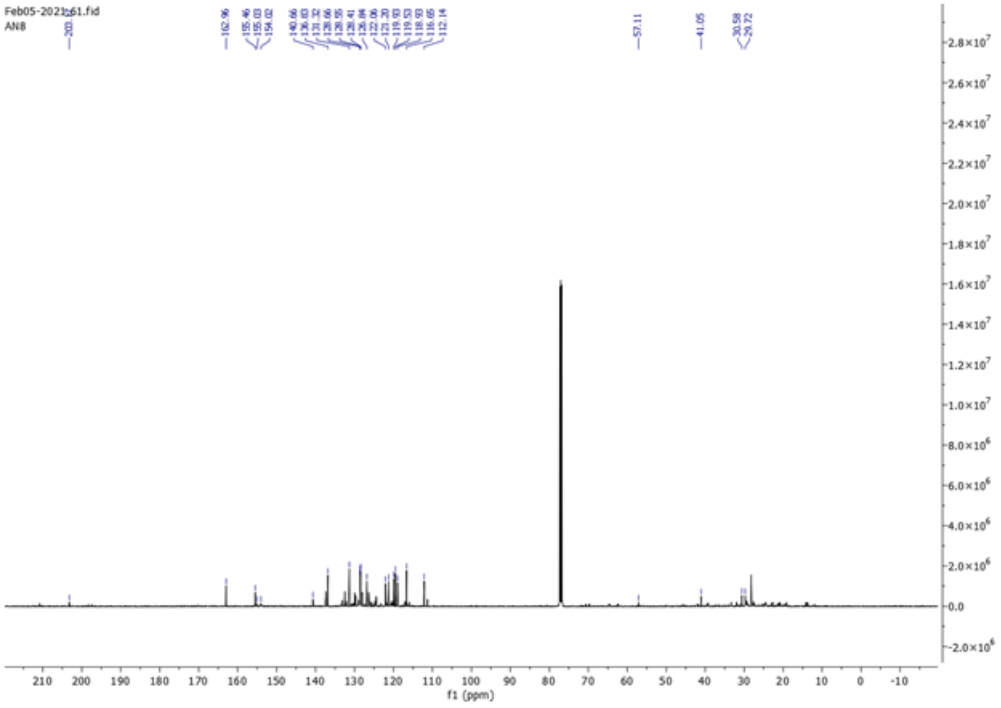

Appendix 14C: Dept-135 NMR spectrum of Uvaretin (**112**), $CDC1_3$.

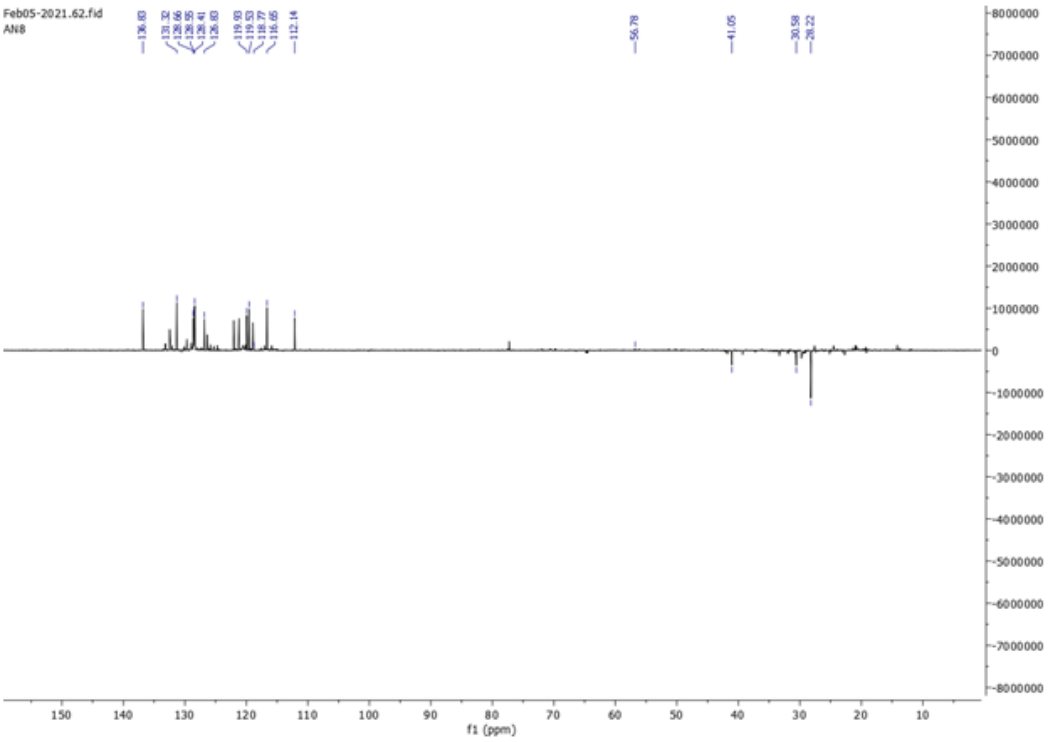

Appendix 15A:HRMS spectrum of bis(2-ethylheptyl) phthalate (**250**)

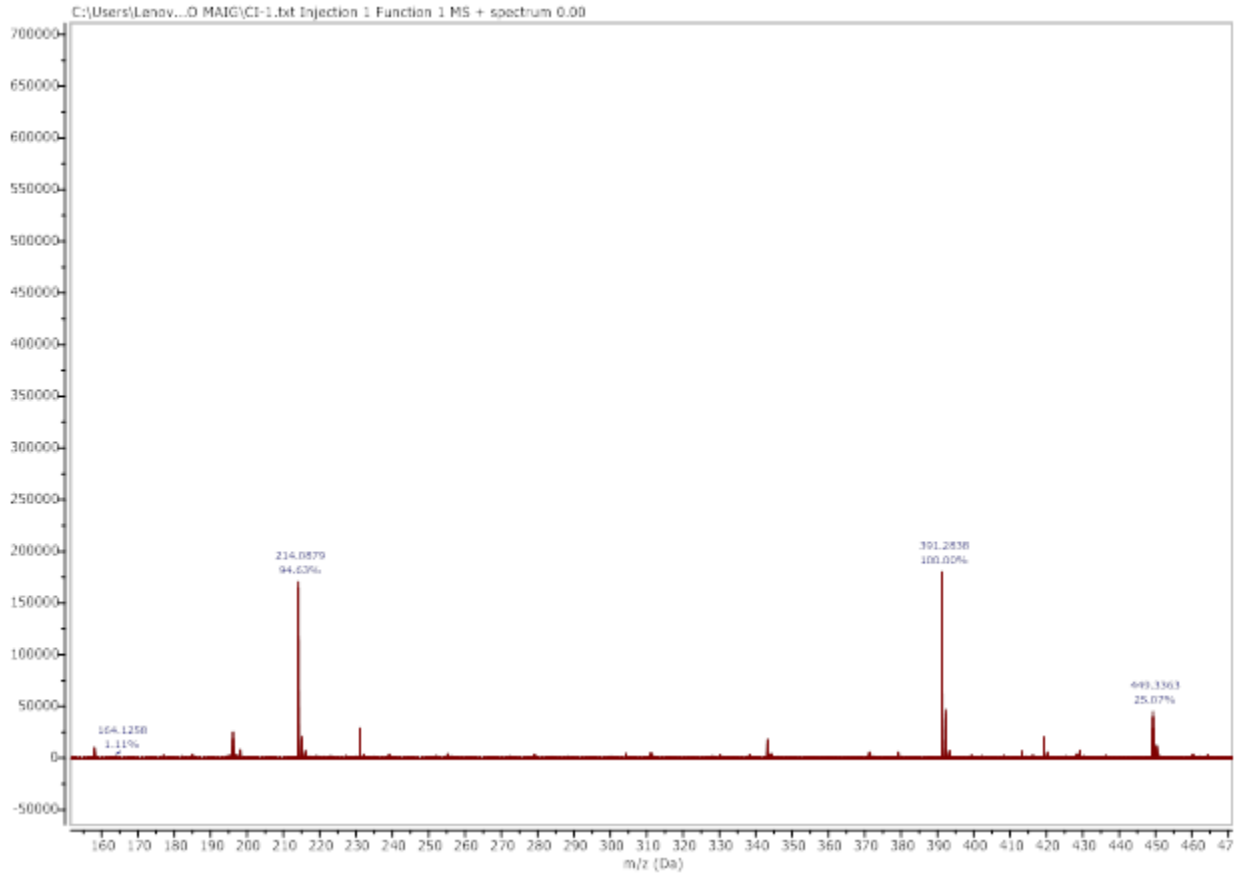

Appendix 15B: ^{1}H NMR spectrum of bis(2-ethylheptyl) phthalate (**250**), $CDC1_3$, 300 MHz

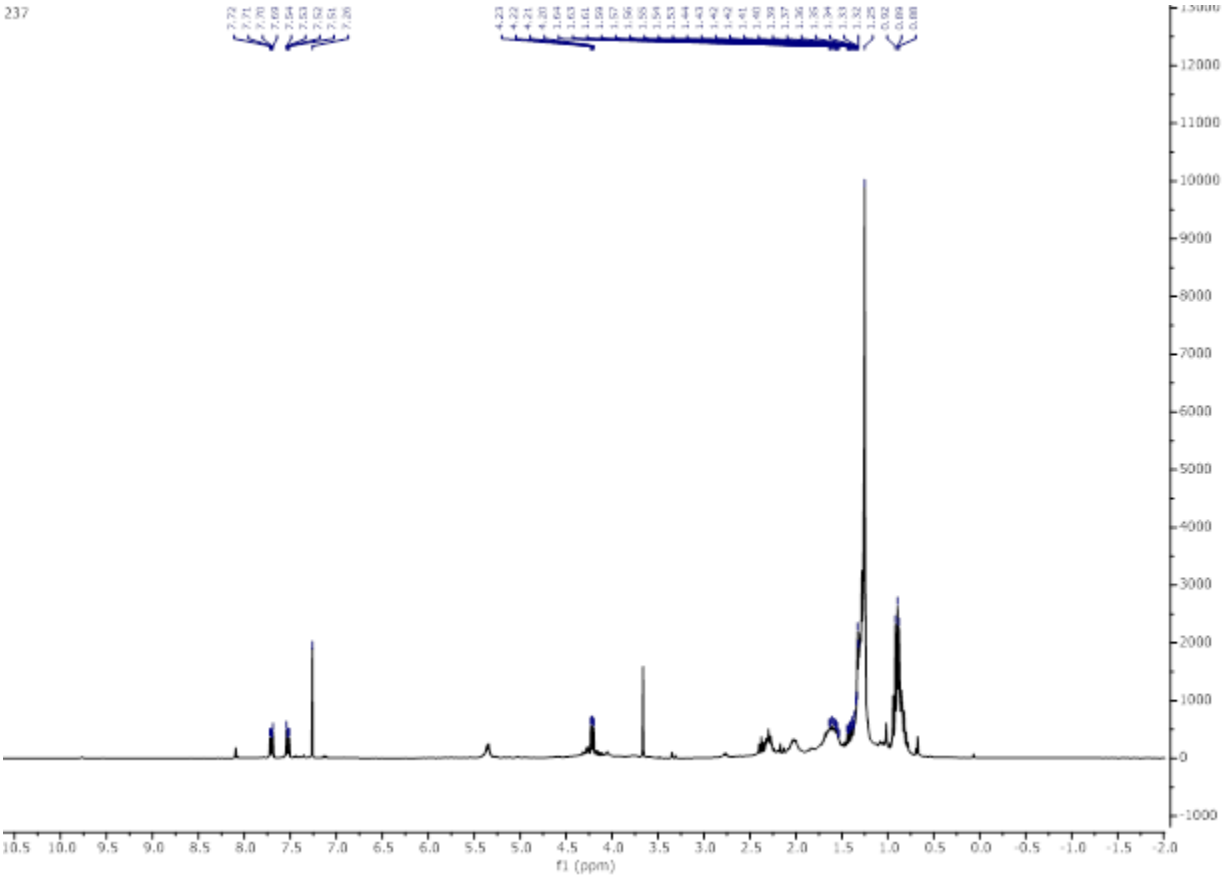

Appendix 15C: ^{13}C NMR spectrum of bis(2-ethylheptyl) phthalate (**250**), $CDC1_3$, 75 MHz

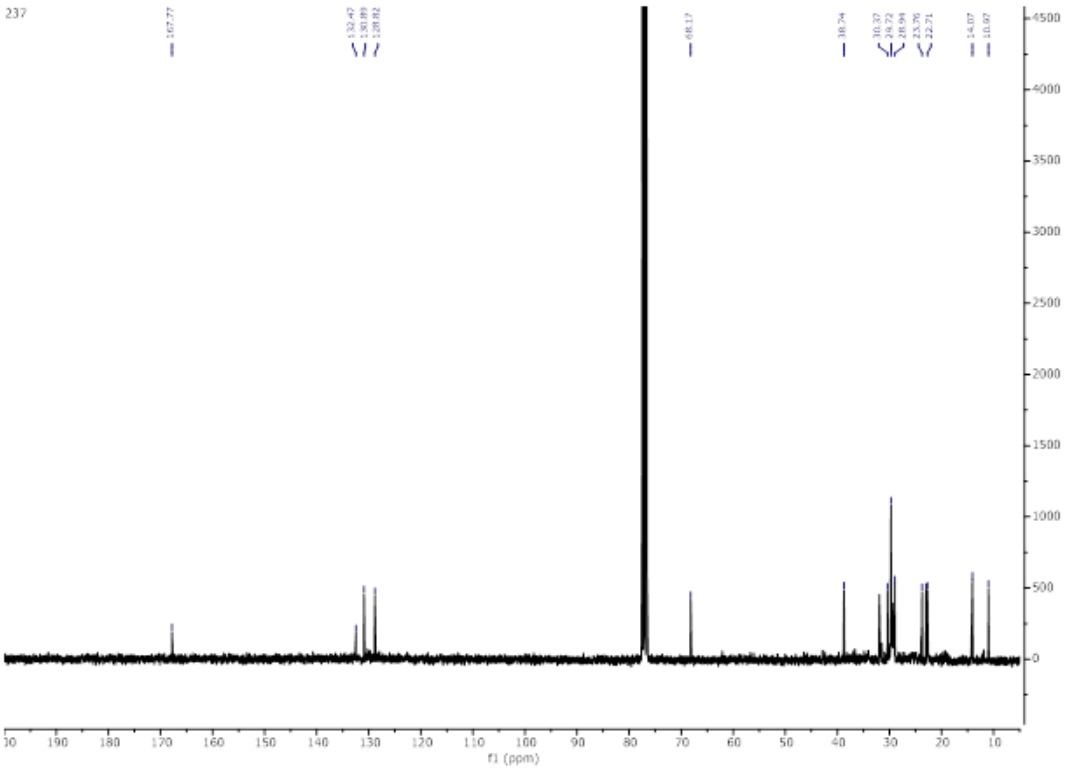

Appendix 15D: DEPT-135 spectrum of bis(2-ethylheptyl) phthalate (**250**), $CDC1_3$, 75 MHz

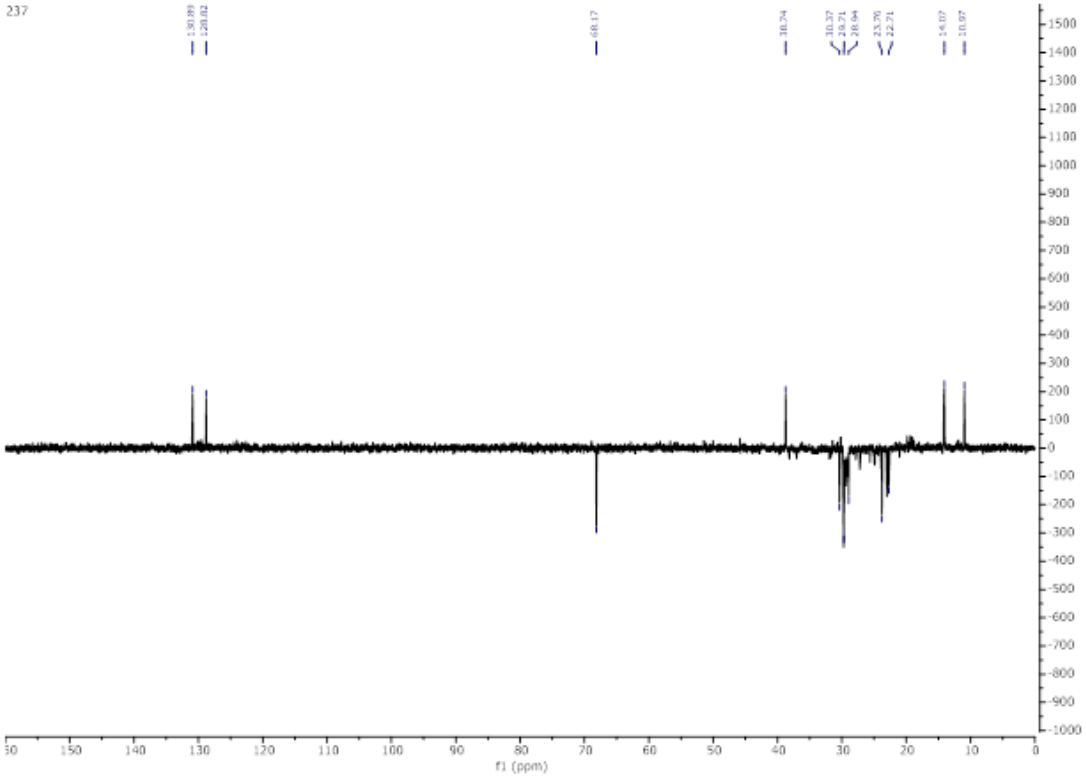

Appendix 15E: COSYspectrum of bis(2-ethylheptyl) phthalate (**250**)

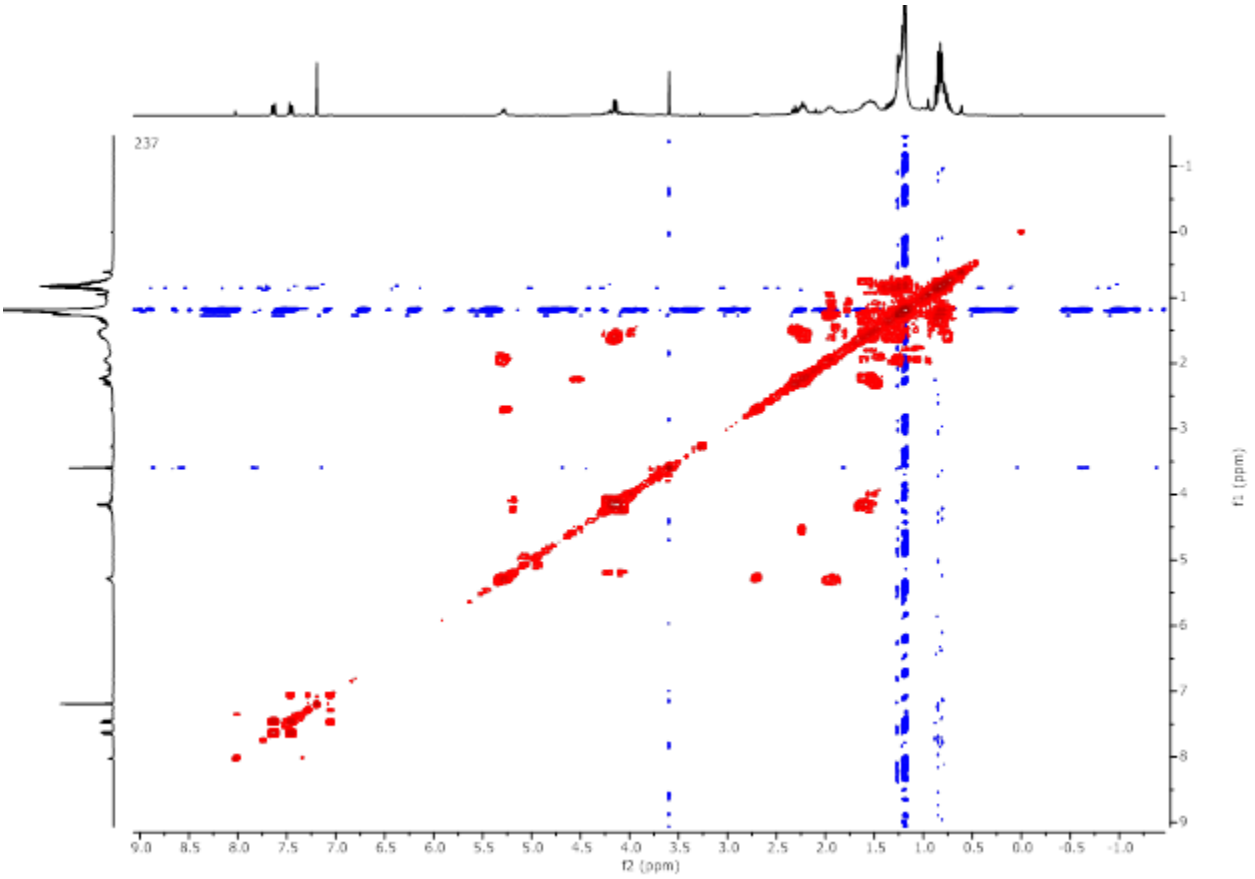

Appendix 15F:HSQC spectrum of bis(2-ethylheptyl) phthalate (**250**)

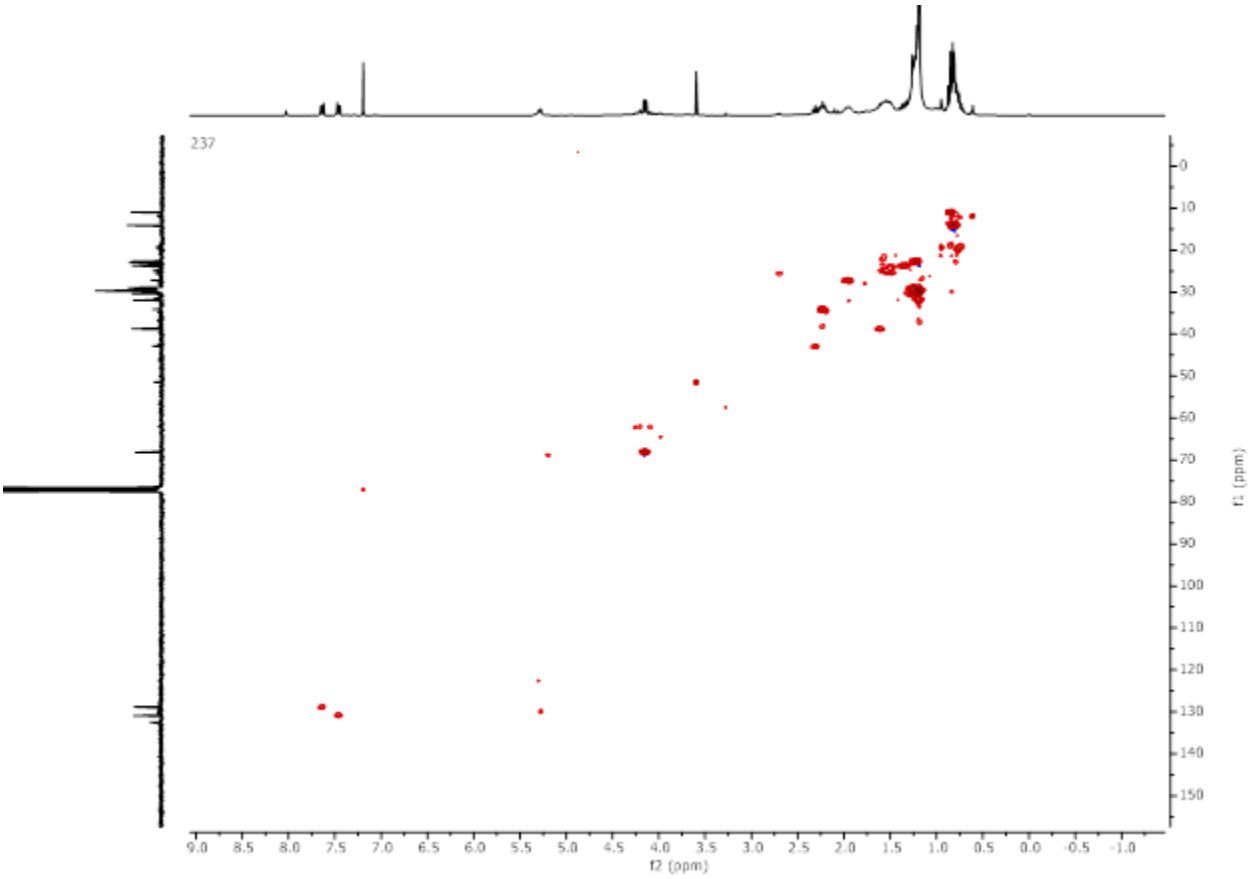

Appendix 15G: HMBC spectrum of bis(2-ethylheptyl) phthalate (**250**)

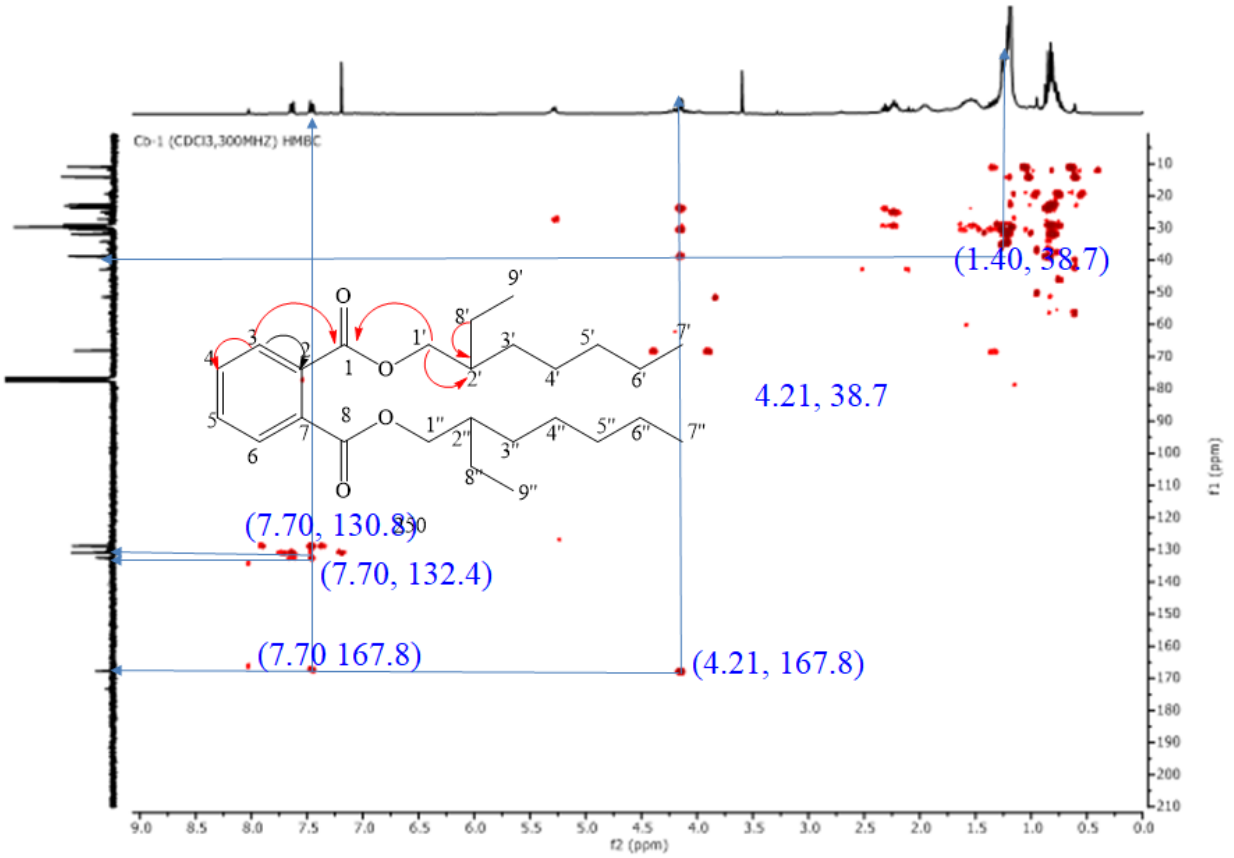

102

Appendix 16A: IR spectrum of lupeol (**98**)

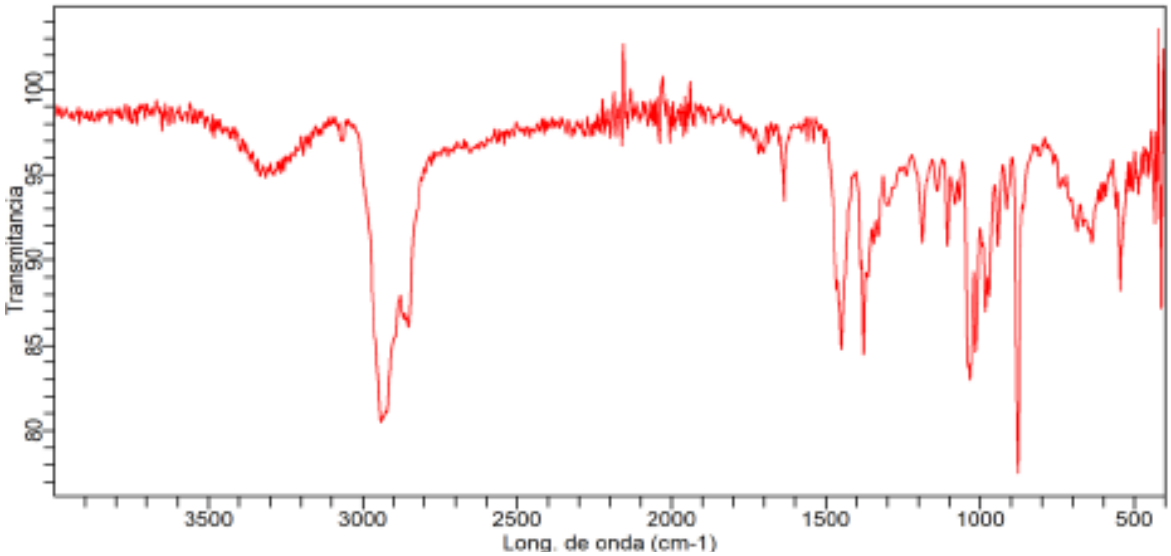

Appendix 16B: ^{1}H NMR spectrum of lupeol (**98**), $CDC1_3$, 300 MHz

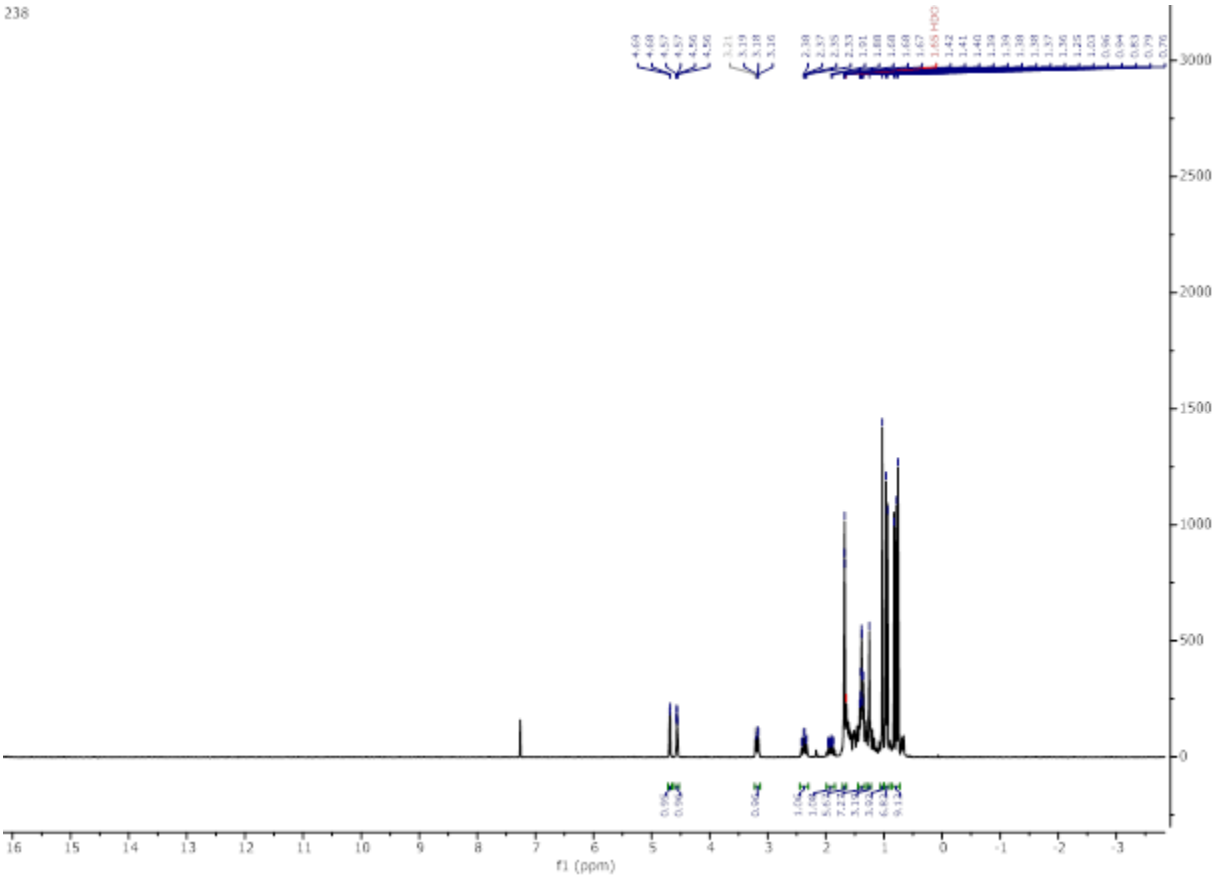

Appendix 16C: 13C NMR spectrum of lupeol (**98**), $CDC1_3$, 75 MHz

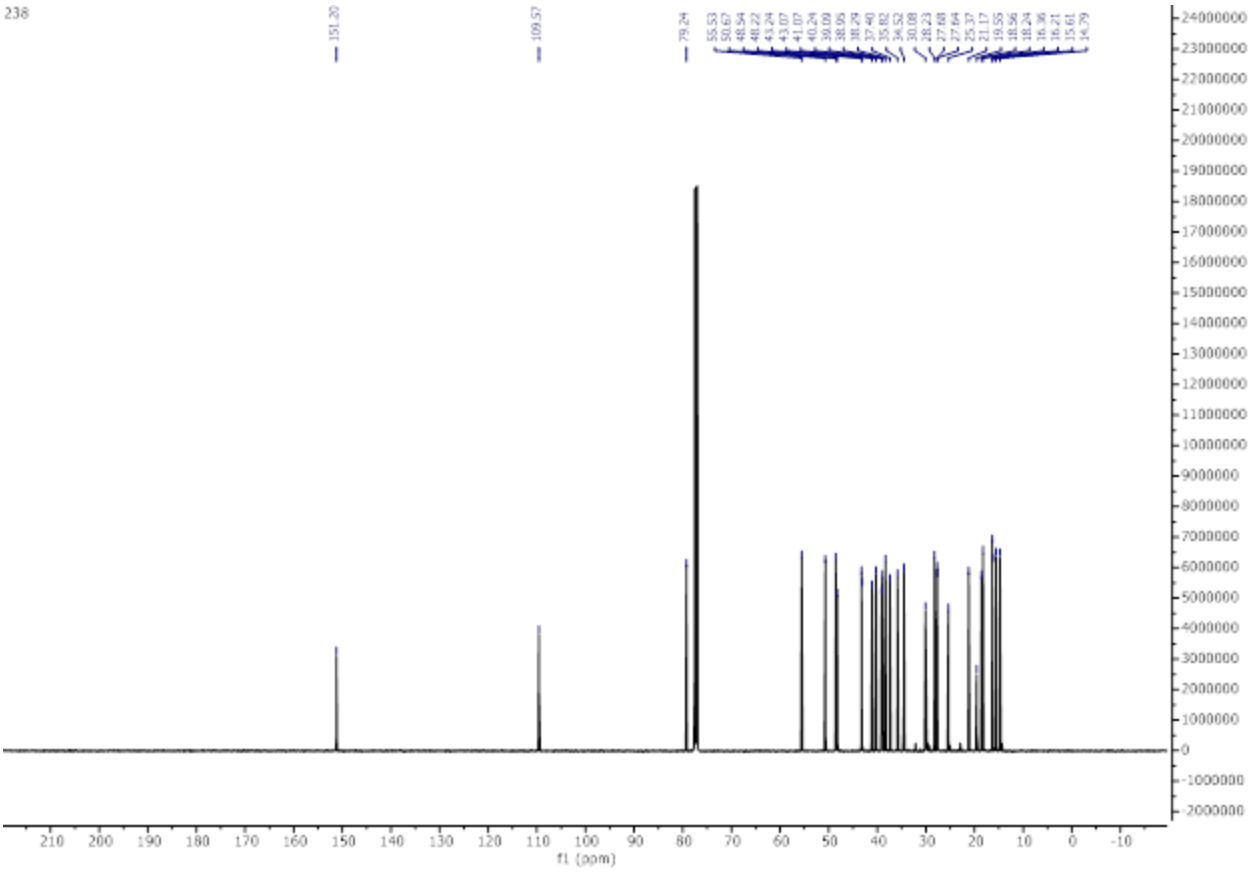

Appendix 16D: DEPT-135 spectrum of lupeol (**98**), $CDC1_3$, 75 MHz

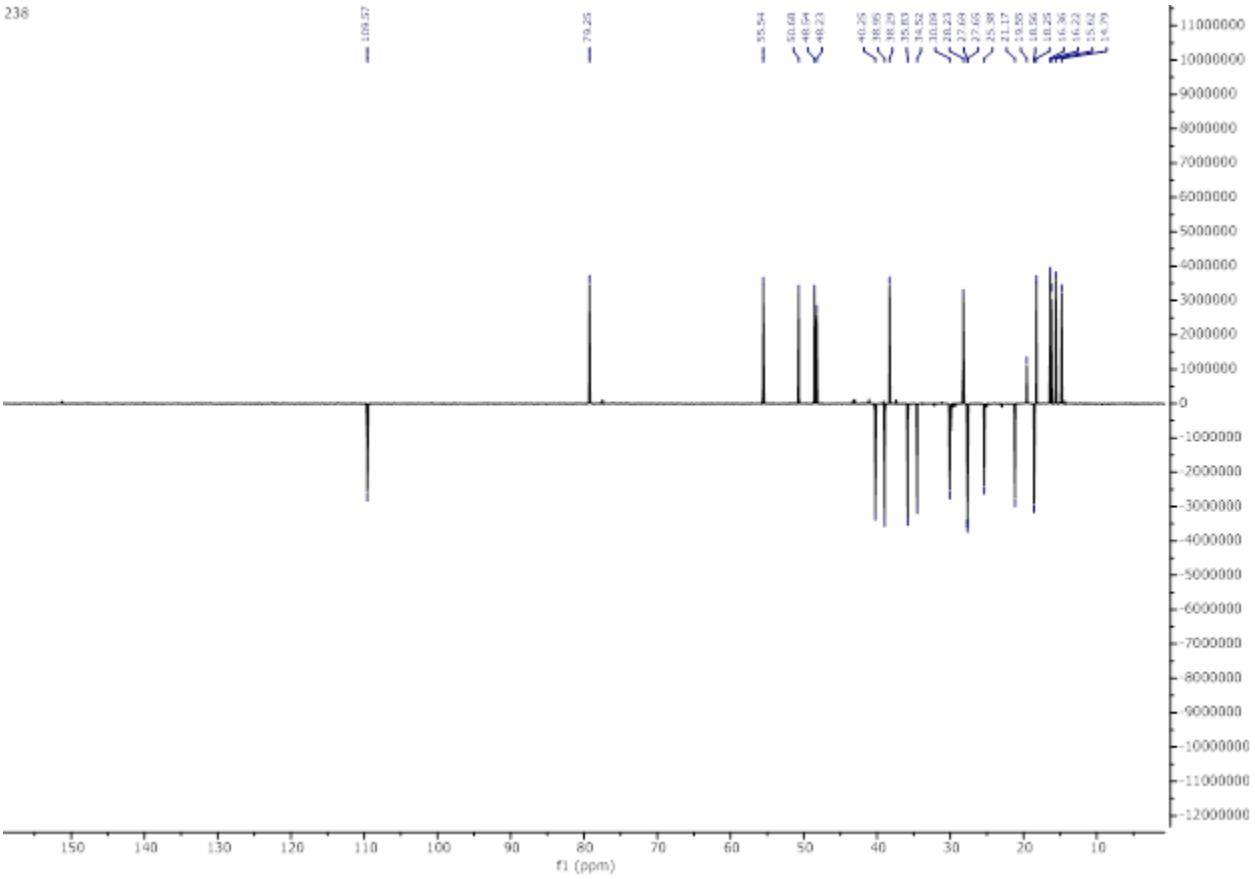

Appendix 17A: ^{1}H NMR spectrum of Linoleic acid fatty acid (**251**), $CDC1_3$, 300 MHz

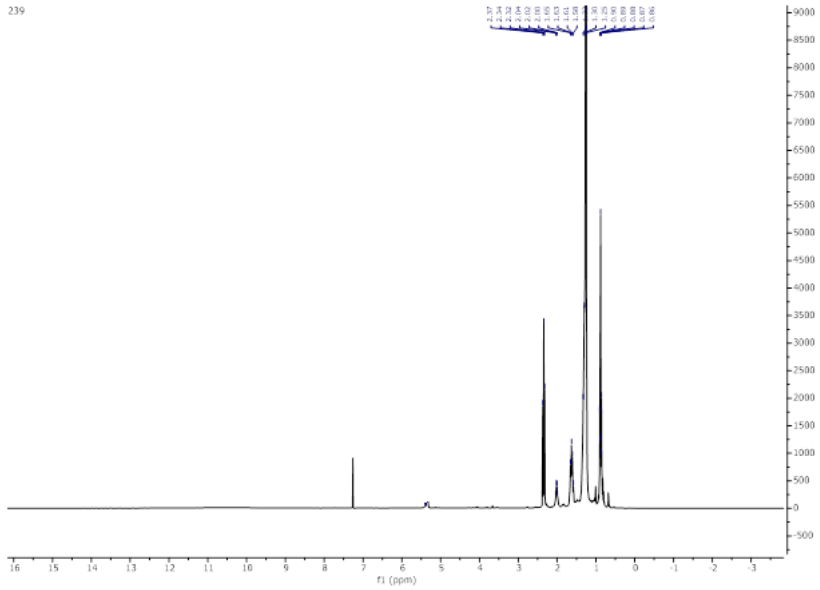

Appendix 17B: ^{13}C NMR spectrum of Linoleic acid fatty acid (**251**), $CDC1_3$, 75 MHz

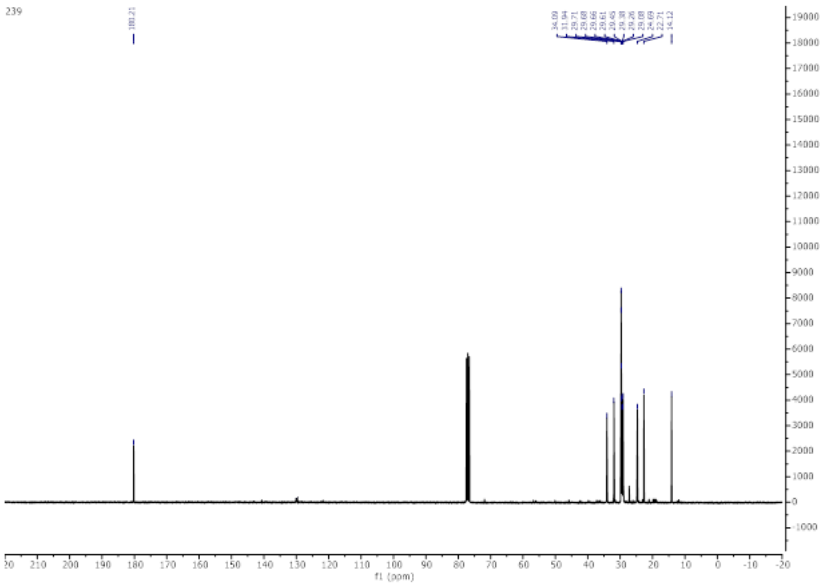

Appendix 17C: DEPT-135 spectrum of Linoleic acid fatty acid (**251**), $CDC1_3$, 75 MHz

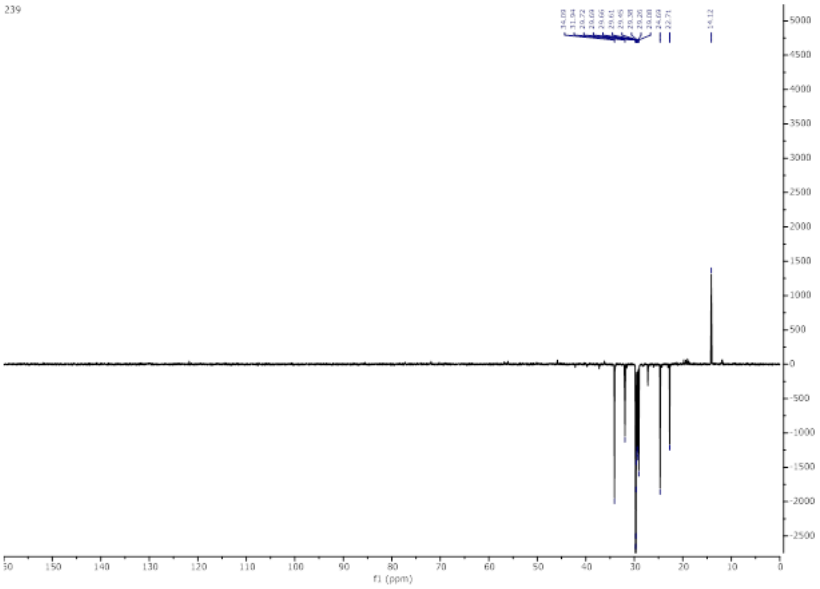

Appendix 18A: IR spectrum of suberosin derivative (**252**)

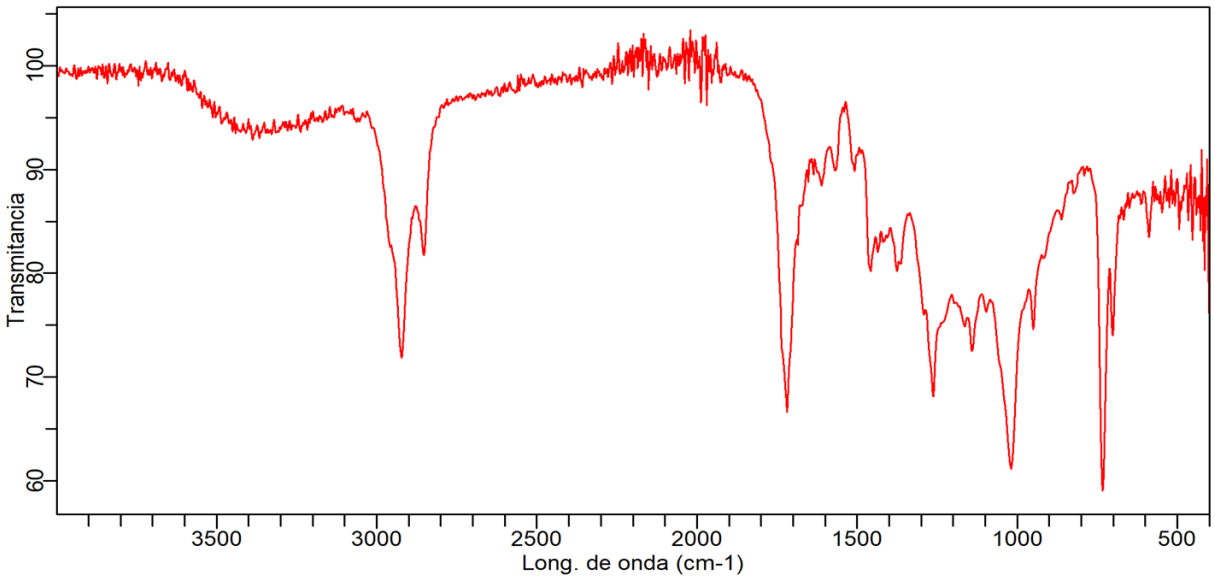

Appendix 18B: ^{1}H NMR spectrum of suberosin derivative (**252**), $CDC1_3$, 300 MHz

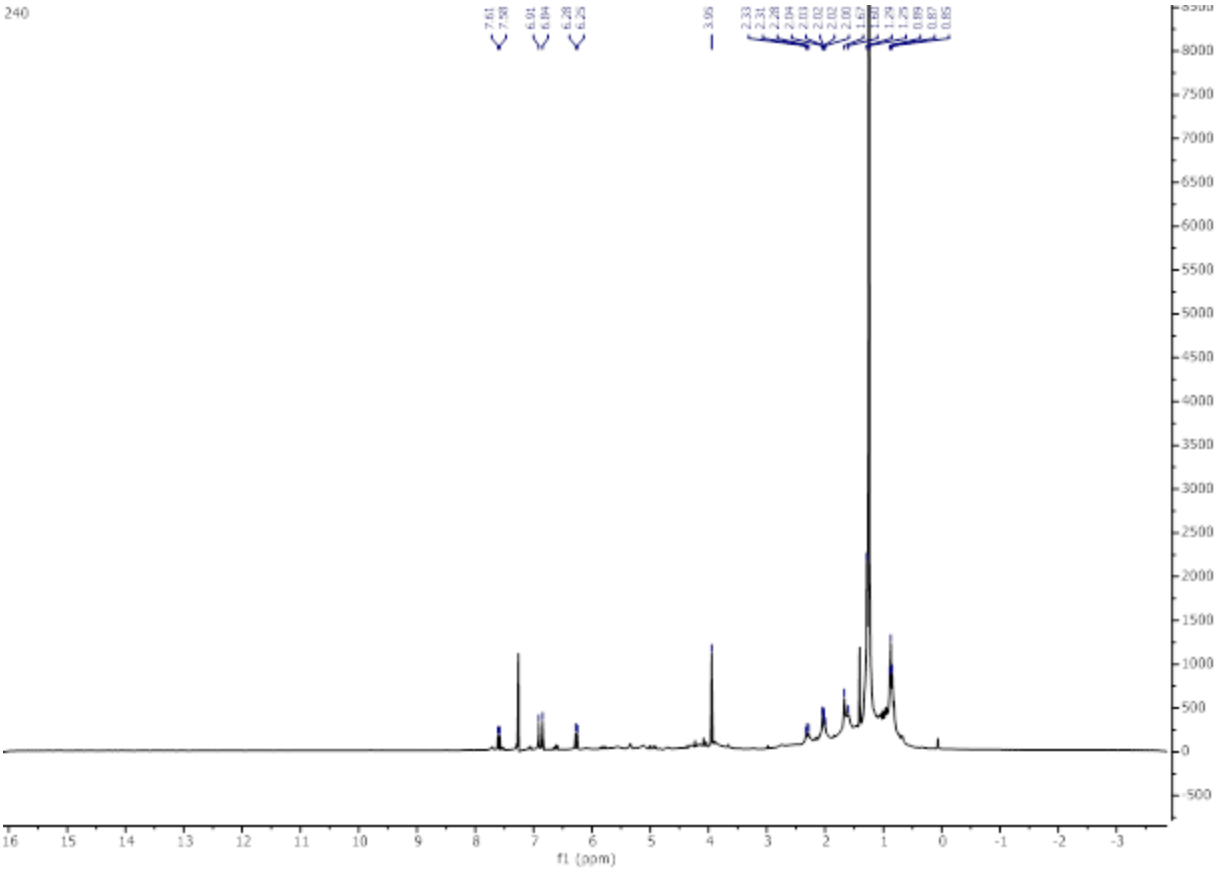

Appendix 18C: ^{13}C NMR spectrum of suberosin derivative (**252**), $CDC1_3$, 75 MHz

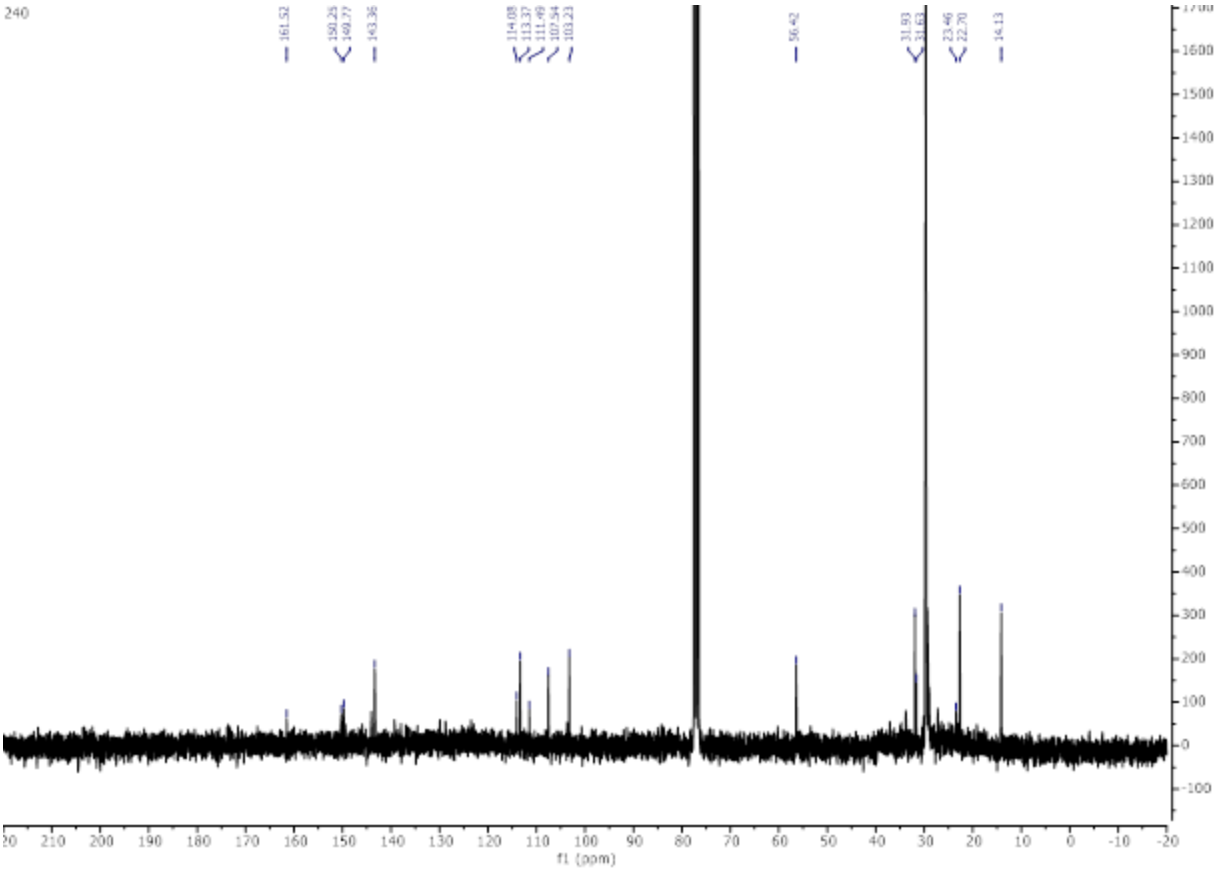

Appendix 18D: Dept-135 spectrum of suberosin derivative (**252**), $CDC1_3$, 75 MHz

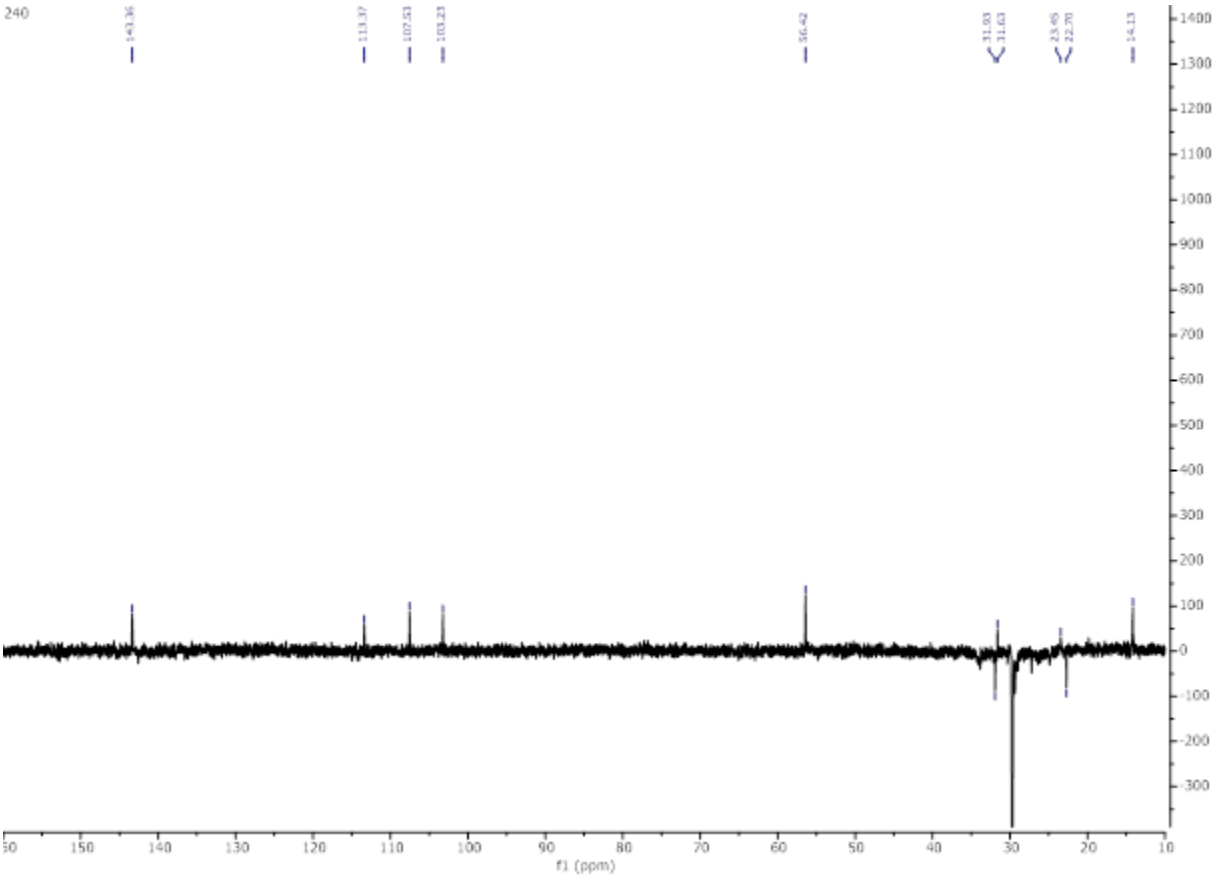

Appendix 19A: ^{1}H NMR spectrum of glycosylmethylamine derivative (**254**), $CDC1_3$, 300 MHz

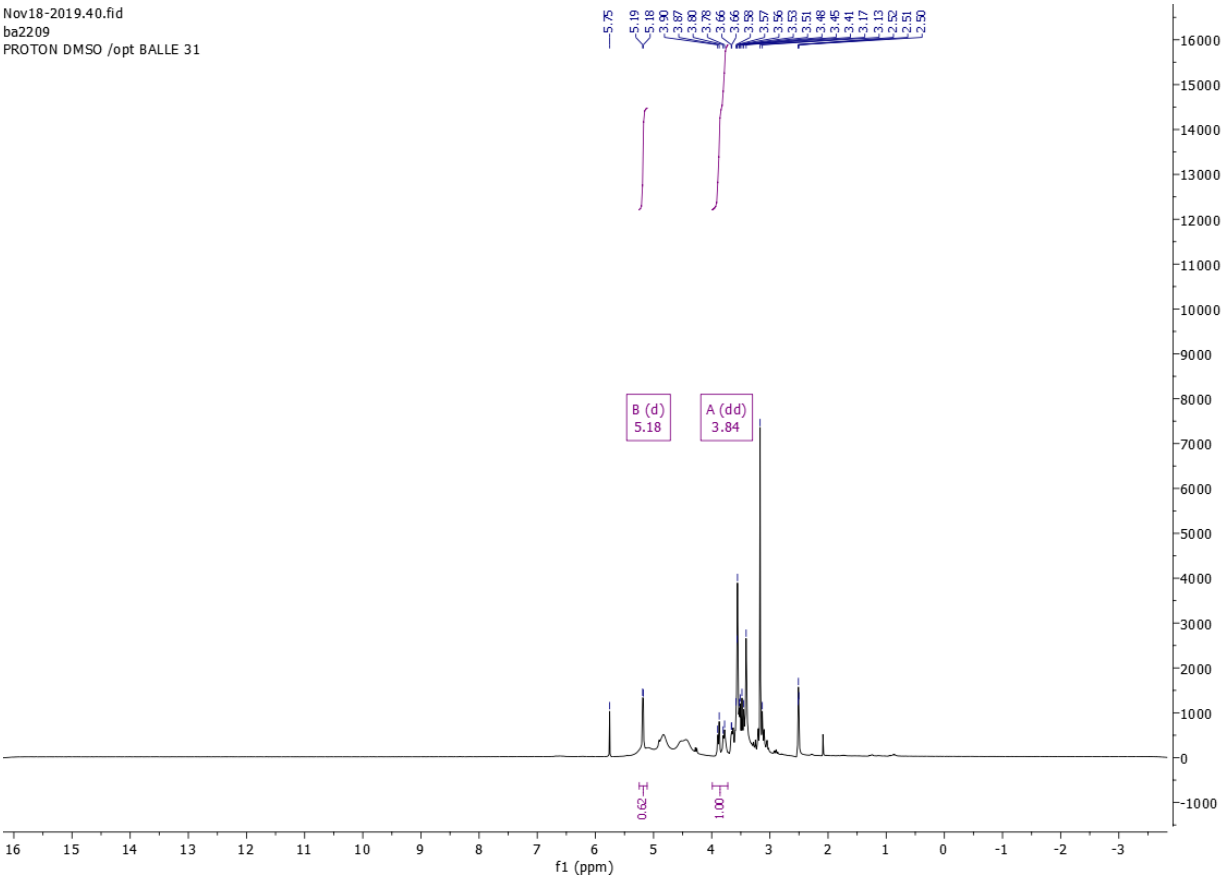

Appendix 19B: 13C NMR spectrum of glycosylmethylamine derivative (**254**), CDC13, 300 MHz

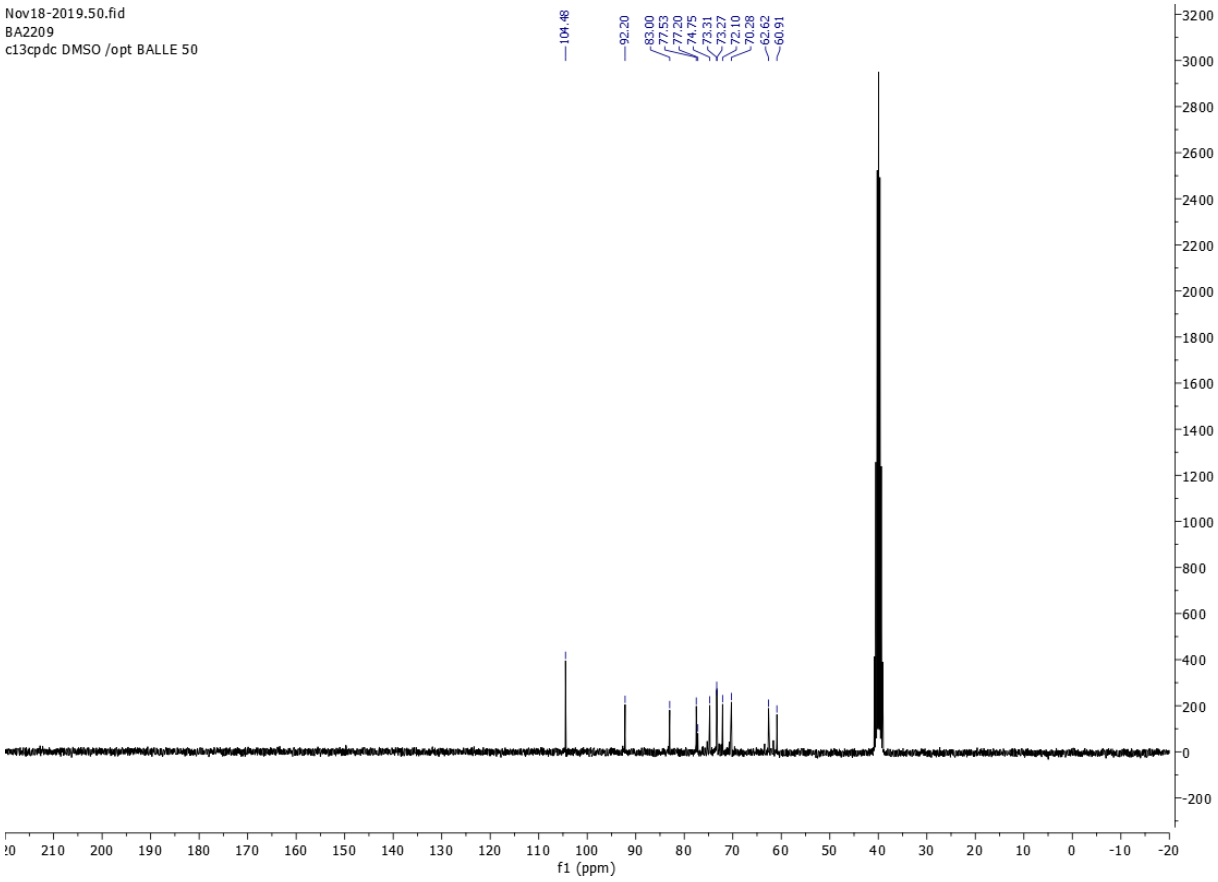

Appendix 19C: Dept-135 spectrum of glycosylmethylamine derivative (**254**), CDC13, 300 MHz

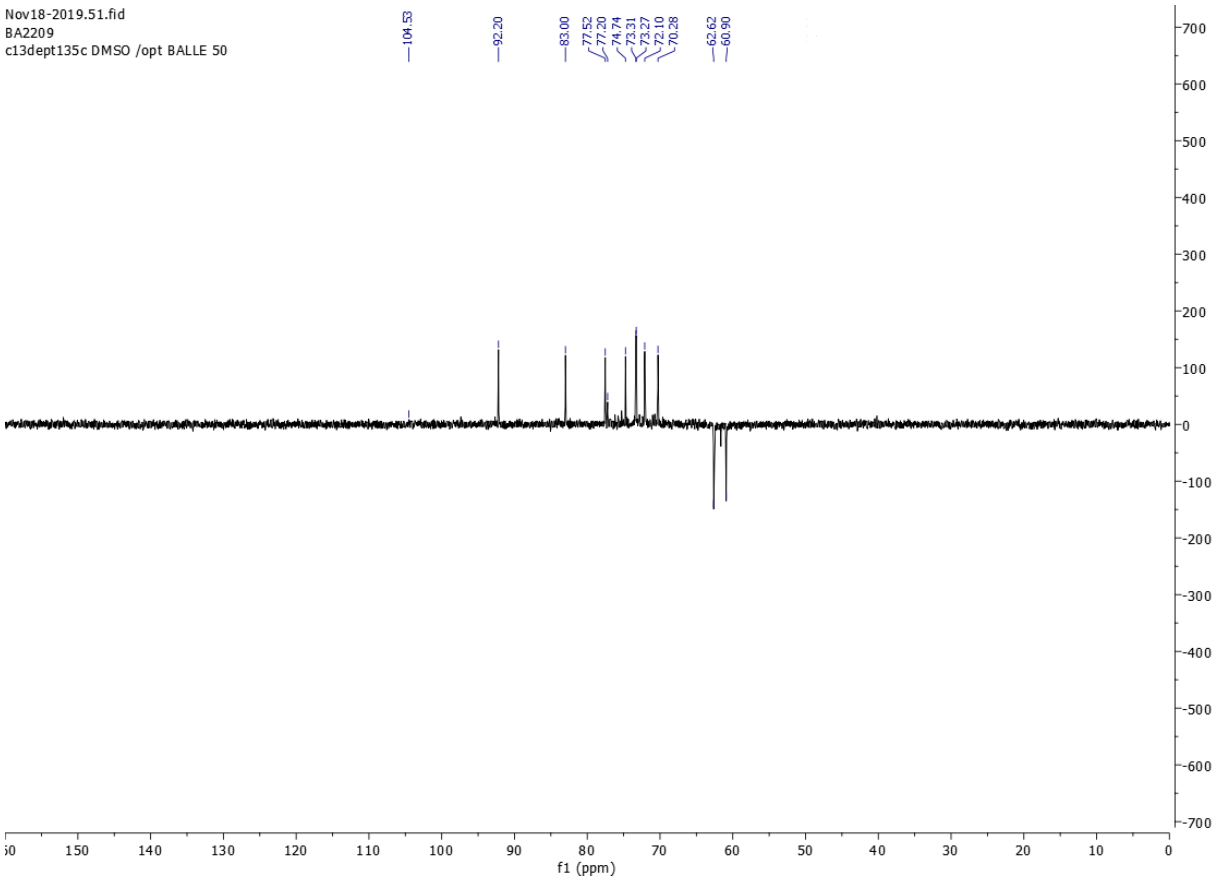

Appendix 20: GC/MS spectra of chemical constituent (**255**).

Compound Label	Name	RT	Algorithm
Cpd 9: 13,27-Cycloursan-3-one	**13,27-Cycloursan-3-one**	33.11	Find by Integration

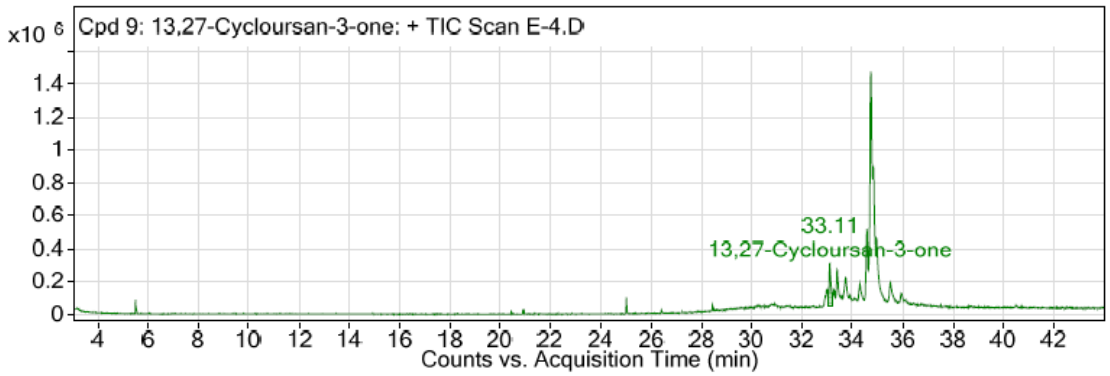

MS Spectrum

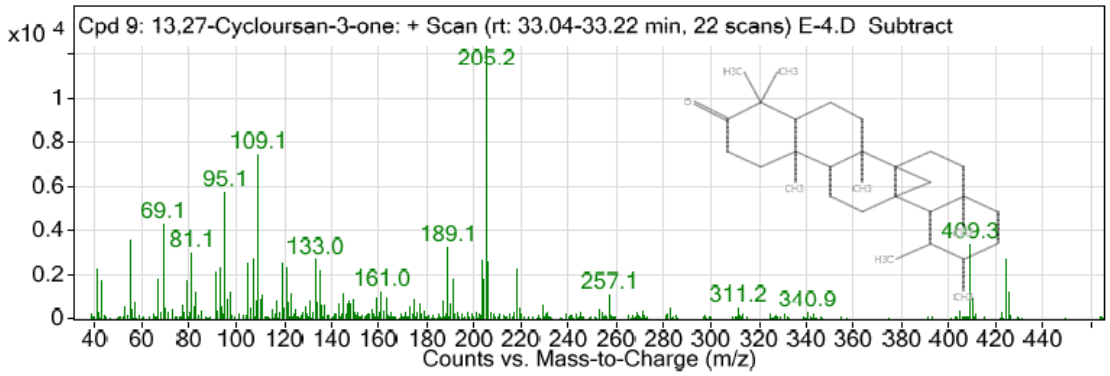

Appendix 21: GC/MS spectra of chemical constituent (**256**).

Compound Label	Name	RT	Algorithm
Cpd 11: 6a,14a-Methanopicene, perhydro-1,2,4a,6b,9,9,12a-heptamethyl-10-hydroxy-	**6a,14a-Methanopicene, perhydro-1,2,4a,6b,9,9,12a-**	33.39	Find by Integration

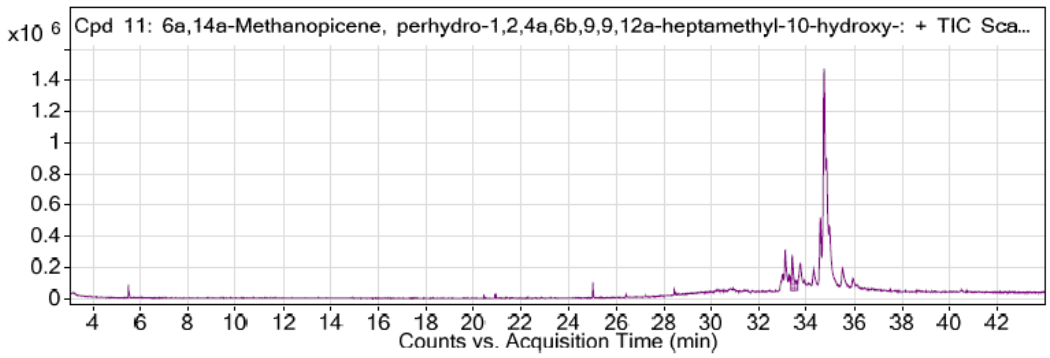

MS Spectrum

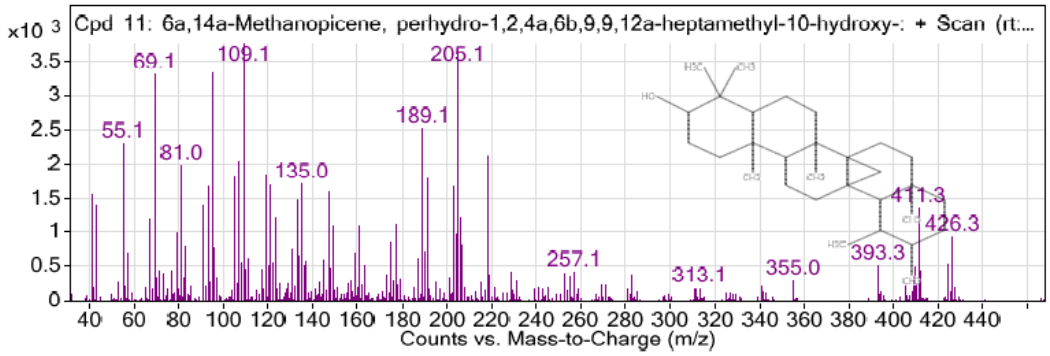

Appendix 22: GC/MS spectra of chemical constituent (**257**).

Compound Label	Name	RT	Algorithm
Cpd 16: 24-Methylenecycloartan-3-	**24-Methylenecycloartan-3-**	34.58	Find by Integration

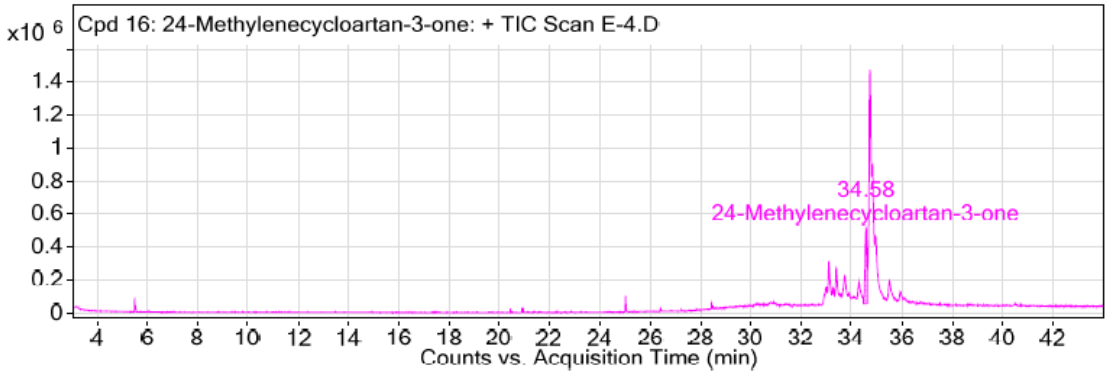

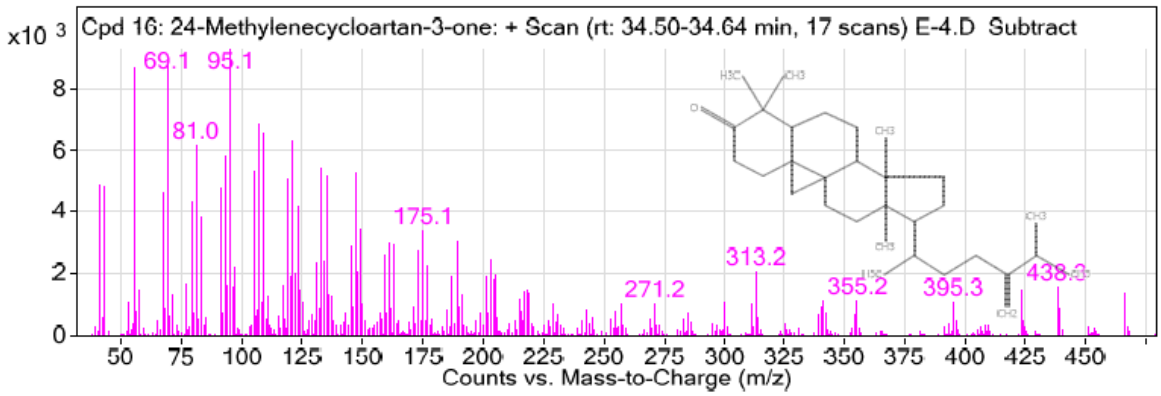

Appendix 23: GC/MS spectra of chemical constituent (**258**).

Compound Label	Name	RT	Algorithm
Cpd 17: Lup-20(29)-en-3-ol, acetate, (3.beta.)-	**Lup-20(29)-en-3-ol, acetate, (3.beta.)-**	34.73	Find by Integration

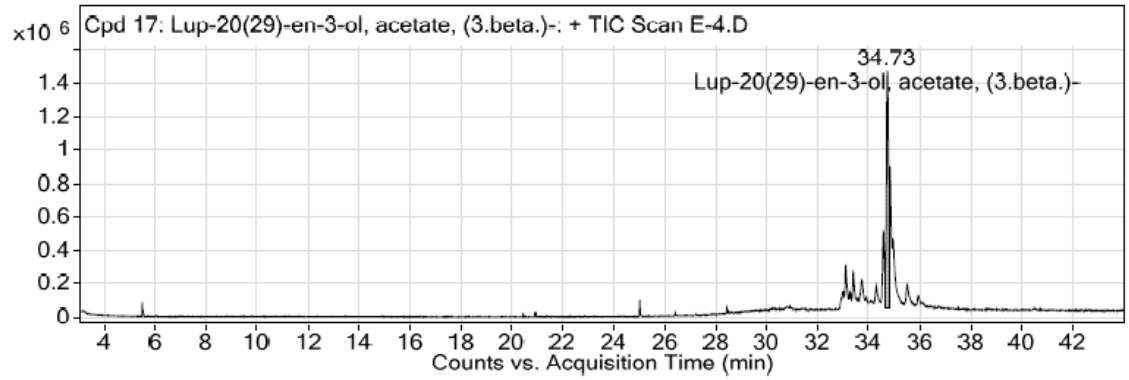

MS Spectrum

MS Zoomed Spectrum

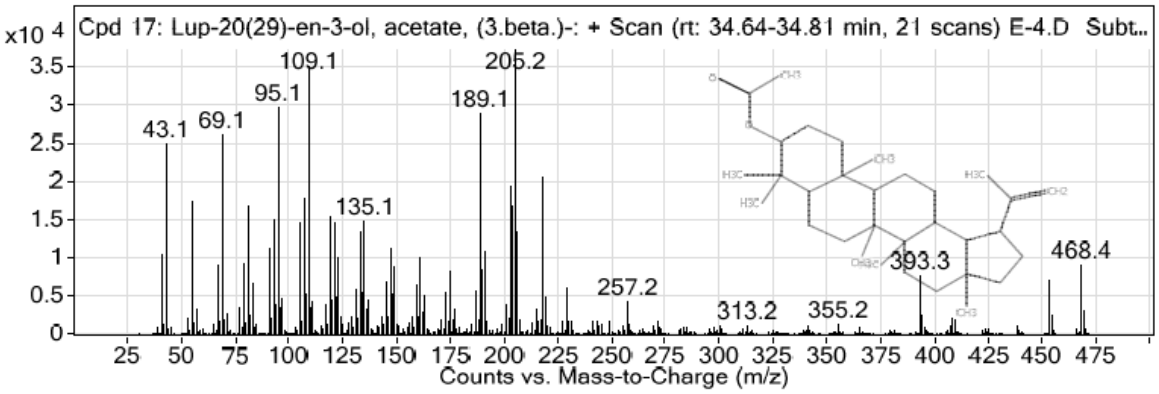

Appendix 24: GC/MS spectra of chemical constituent (**259**).

Compound Label	Name	RT	Algorithm
Cpd 18: 12-Oleanen-3-yl acetate, (3.alpha.)-	**12-Oleanen-3-yl acetate, (3.alpha.)-**	34.84	Find by Integration

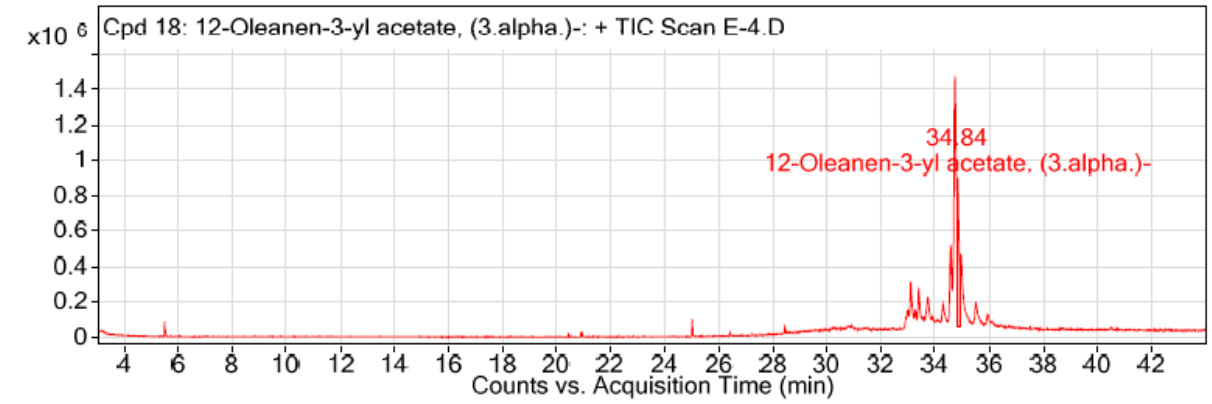

MS Spectrum

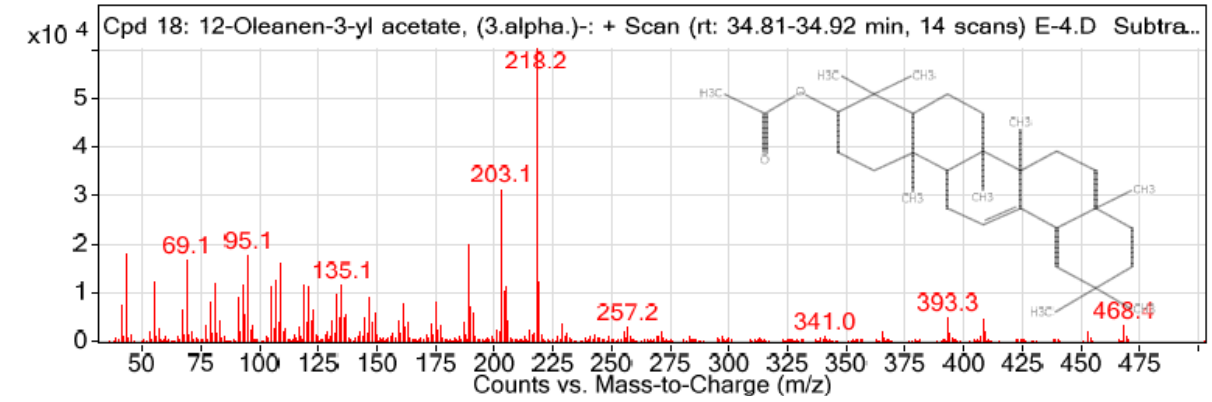

Appendix 25: GC/MS spectra of chemical constituent (**260**).

Compound Label	Name	RT	Algorithm
Cpd 19: Germanicol	**Germanicol**	34.96	Find by Integration

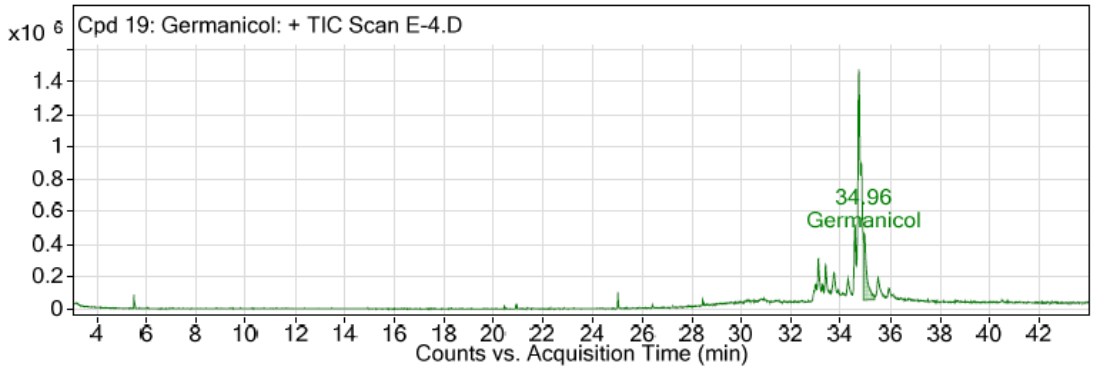

MS Spectrum

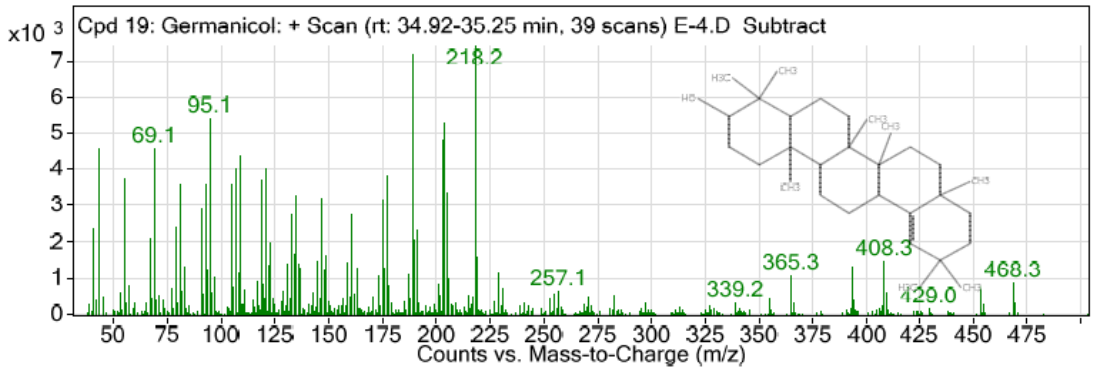

Appendix 26: Chromatogram for essential oil of *U. scheflerri*

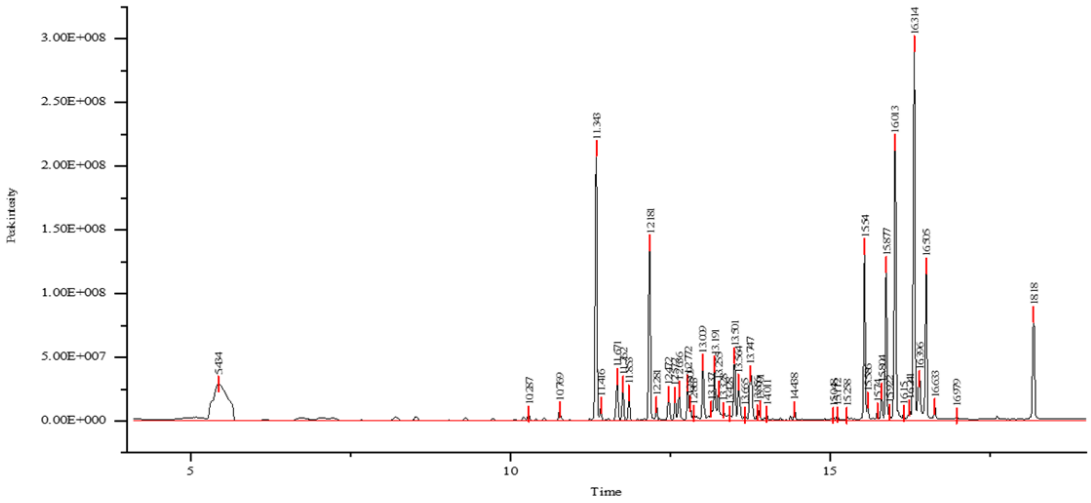

Figure 1. Chromatogram for essential oil of *U. Scheffleri*

Appendix 27: Chromatogram for essential oil of *Z. chalybeum*

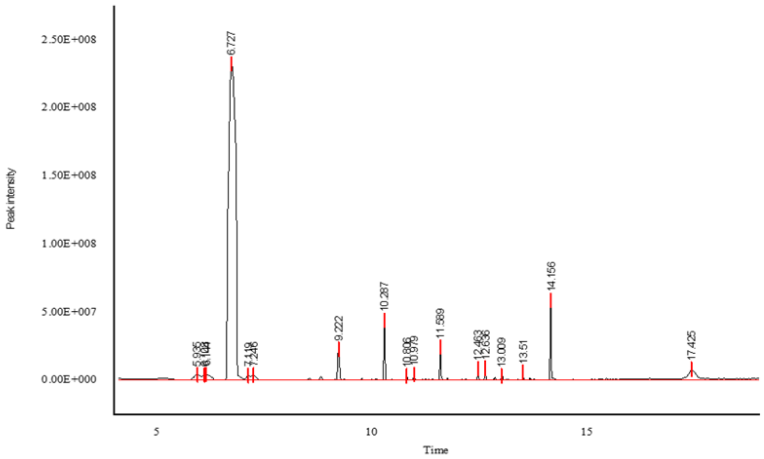

Figure 2. Chromatogram for essential oil of *Z. chalybeum*

Appendix 28: Chromatogram for essential oil of *V. dainelli*

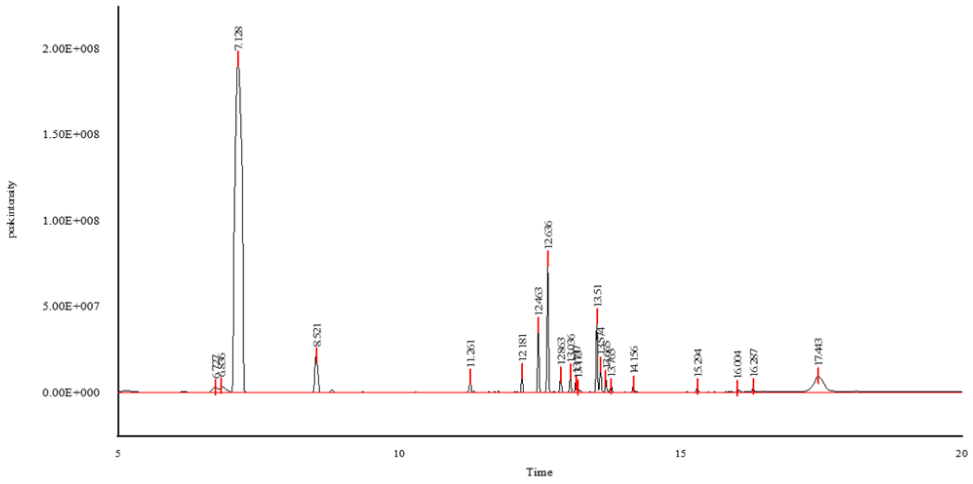

Figure 3. Chromatogram for essential oil of *V. dainelli*